

**TWIST1 SUPPRESSES APOPTOSIS AND MEDIATES THERAPEUTIC RESISTANCE
IN NON-SMALL CELL LUNG CANCER**

by

ZACHARY ALAN YOCHUM

B.S., UNIVERSITY OF NOTRE DAME, 2012

Submitted to the Graduate Faculty of
School of Medicine in partial fulfillment
of the requirements for the degree of
PhD in Molecular Pharmacology

University of Pittsburgh

2018

UNIVERSITY OF PITTSBURGH
SCHOOL OF MEDICINE

This dissertation was presented

by

Zachary Alan Yochum

It was defended on

May 25, 2018

and approved by

Donald DeFranco, Ph.D., Professor, Pharmacology and Chemical Biology

Steffi Oesterreich, Ph.D., Professor, Pharmacology and Chemical Biology

Lin Zhang, Ph.D., Professor, Pharmacology and Chemical Biology

James Herman, MD., Professor, Department of Medicine

Dissertation Advisor: Timothy Burns, MD., Ph.D., Assistant Professor, Pharmacology and

Chemical Biology

Copyright © by Zachary Alan Yochum

2018

TWIST1 SUPPRESSES APOPTOSIS AND MEDIATES THERAPEUTIC RESISTANCE IN NON-SMALL CELL LUNG CANCER

Zachary Alan Yochum, PhD

University of Pittsburgh, 2018

Patients with non-small cell lung cancer (NSCLC) are classified into molecular subgroups based on the presence of oncogenic drivers. Patients with targetable oncogenic drivers, such as mutant *EGFR*, have benefited from tyrosine kinase inhibitors (TKIs) targeting these oncogenes. However, *de-novo* and acquired resistance to TKIs limits their efficacy. Studies investigating mechanisms of resistance to TKIs in NSCLC have demonstrated that epithelial-mesenchymal transition (EMT) is associated with resistance. TWIST1 is an EMT-transcription factor that is required for oncogene-driven NSCLC. Utilizing a chemical-bioinformatic screen, we identified the harmala alkaloid, harmine, as a first-in-class TWIST1 inhibitor. Harmine inhibited multiple TWIST1 functions, promoted TWIST1 degradation, and had activity in oncogene driver-defined NSCLC cell lines. Additionally, harmine cytotoxicity required degradation of the TWIST1-E2A heterodimer. Harmine also had activity in murine models of *KRAS* mutant NSCLC. Following identification of this novel TWIST1 inhibitor, we explored TWIST1 as potential target to overcome EGFR TKI resistance in *EGFR* mutant NSCLC. We demonstrated that TWIST1 expression is sufficient to mediate resistance to EGFR TKIs *in vitro* and *in vivo*. Genetic and pharmacological inhibition of TWIST1 in EGFR TKI resistant *EGFR* mutant cells increased sensitivity to EGFR TKIs. TWIST1-mediated EGFR TKI resistance was due in part to TWIST1 suppression of transcription of the pro-apoptotic gene, *BCL2L1* (BIM), by directly binding to

BCL2L11 intronic regions and promoter. In MET-driven NSCLC, TWIST1 overexpression mediated resistance to MET TKIs. Targeting TWIST1 with harmine increased crizotinib sensitivity in *MET* altered NSCLC cells. We also demonstrated that hepatocyte growth factor (HGF), a known mediator of EGFR and MET TKI resistance, induced TWIST1 expression. Harmine treatment overcame HGF-mediated resistance to MET and EGFR TKIs in MET- and EGFR-driven NSCLC. We also explored the role of TWIST1 in mediating resistance to other targeted agents in NSCLC. We demonstrated that TWIST1 negatively regulates death receptor signaling by directly upregulating transcription of *CFLAR* (CFLIP), an inhibitor of death receptor 4 and 5. TWIST1 upregulation of cFLIP was associated with resistance to TRAIL-based agents in NSCLC. Overall, these studies demonstrate that targeting TWIST1 is viable therapeutic strategy to overcome resistance to TKIs and TRAIL-based therapies in NSCLC.

TABLE OF CONTENTS

PREFACE.....	XVII
1.0 INTRODUCTION.....	1
1.1 LUNG CANCER.....	1
1.1.1 Lung cancer histological and genetic subtypes	2
1.1.2 Lung cancer treatment modalities	5
1.1.2.1 Definitive local treatment: Surgery and Radiation.....	7
1.1.2.2 Chemotherapy	8
1.1.2.3 Immunotherapy.....	9
1.1.2.4 EGFR targeted therapy	11
1.1.2.5 ALK targeted therapy	14
1.1.2.6 MET targeted therapy	17
1.1.3 Driver independent resistance mechanisms to targeted therapies in lung cancer 21	
1.1.3.1 Bypass signaling pathway activation.....	21
1.1.3.2 HGF-MET Pathway Alterations.....	23
1.1.3.3 Histological Transformation	24
1.1.3.4 Epithelial-Mesenchymal Transition	25
1.2 APOPTOSIS AND CANCER.....	26

1.2.1	Apoptotic pathways	27
1.2.2	Aberrations in apoptotic pathways and proteins in cancer	30
1.2.3	Apoptosis and response to targeted therapy in lung cancer	32
1.3	TWIST1	33
1.3.1	TWIST1 and development.....	33
1.3.2	Regulation of TWIST1 expression	35
1.3.2.1	Transcriptional control of <i>TWIST1</i>	36
1.3.2.2	Post-transcriptional control of TWIST1.....	37
1.3.3	TWIST1 and cancer	39
1.3.3.1	EMT.....	40
1.3.3.2	Apoptosis.....	41
1.3.3.3	Senescence.....	42
1.3.3.4	Therapeutic resistance.....	43
2.0	IDENTIFICATION OF A FIRST-IN-CLASS TWIST1 INHIBITOR WITH ACTIVITY IN ONCOGENE-DRIVEN LUNG CANCER.....	45
2.1	ABSTRACT.....	45
2.2	INTRODUCTION	47
2.3	MATERIAL AND METHODS	49
2.3.1	Cell lines and reagents.....	49
2.3.2	Cell viability assays.....	49
2.3.3	SA- β -galactosidase staining	50
2.3.4	Colony formation assay	50
2.3.5	Quantitative RT-PCR.....	51

2.3.6	Immunoblot analysis	51
2.3.7	Connectivity MAP analysis.....	52
2.3.8	3D organoid assay.....	52
2.3.9	FGF2-branching experiments	52
2.3.10	Lentiviral shRNA and cDNA overexpression experiments	52
2.3.11	Pulse-Chase experiments	53
2.3.12	Quantification of caspase-3/7 activity.....	53
2.3.13	Luciferase promoter reporter assay	54
2.3.14	Transgenic Mice	54
2.3.15	Patient-derived xenograft experiments	54
2.3.16	Histology and immunohistochemistry	55
2.3.17	Statistics.....	55
2.4	RESULTS.....	56
2.4.1	Identification of novel TWIST1 inhibitors with a Connectivity MAP analysis	56
2.4.2	Harmine inhibits growth in oncogene driver-defined NSCLC cell lines and phenocopies loss of TWIST1.....	60
2.4.3	Harmine treatment results in TWIST1 protein degradation	68
2.4.4	TWIST1 and the E2A proteins reciprocally stabilize each other and harmine leads to degradation of both components of this dimer	73
2.4.5	The TWIST1/E2A heterodimer is critical for TWIST1 function and therapeutic response to harmine.....	79

2.4.6	Harmine has <i>in vivo</i> activity in both transgenic and patient-derived xenograft mouse models of <i>KRAS</i> mutant lung cancer.....	83
2.5	DISCUSSION.....	87
3.0	TARGETING THE EMT-TRANSCRIPTION FACTOR TWIST1 OVERCOMES RESISTANCE TO EGFR INHIBITORS IN <i>EGFR</i> MUTANT NON-SMALL CELL LUNG CANCER.....	90
3.1	ABSTRACT.....	90
3.2	INTRODUCTION	92
3.3	MATERIAL AND METHODS	94
3.3.1	Cell lines and reagents.....	94
3.3.2	Quantification of caspase-3/7 activity	95
3.3.3	Quantitative RT-PCR.....	95
3.3.4	Cell proliferation assays.....	96
3.3.5	Western blot and antibodies	96
3.3.6	Chromatin immunoprecipitation	96
3.3.7	Lentiviral shRNA and cDNA overexpression	97
3.3.8	Transgenic mice	97
3.3.9	Histology and immunohistochemistry	98
3.4	RESULTS	98
3.4.1	Genetic or pharmacologic inhibition of TWIST1 results in growth inhibition and apoptosis in <i>EGFR</i> mutant NSCLC	98
3.4.2	TWIST1 is necessary and sufficient for EGFR TKI resistance in a subset of <i>EGFR</i> mutant NSCLC cell lines.....	102

3.4.3	TWIST1 suppresses BIM expression.....	109
3.4.4	Creation and characterization of an autochthonous <i>EGFR</i> mutant <i>Twist1</i> overexpression lung tumor mouse model.....	113
3.4.5	<i>Twist1</i> expression induces erlotinib resistance <i>in vivo</i>	118
3.5	DISCUSSION.....	122
4.0	TWIST1 IS A KEY MEDIATOR OF HGF-MET DRIVEN RESISTANCE TO TARGETED THERAPIES IN <i>EGFR</i> MUTANT AND MET-DRIVEN LUNG CANCER	126
4.1	ABSTRACT.....	126
4.2	INTRODUCTION	128
4.3	METHODS.....	130
4.3.1	Cell lines and reagents.....	130
4.3.2	Cell proliferation assays.....	131
4.3.3	Western blot and antibodies	131
4.3.4	Lentiviral shRNA and cDNA overexpression	131
4.3.5	Pulse-Chase experiments	132
4.3.6	Xenograft experiments.....	132
4.3.7	Transgenic Mice.....	133
4.4	RESULTS.....	133
4.4.1	Pharmacologic inhibition of TWIST1 overcomes HGF-mediated resistance to MET and EGFR TKIs in <i>EGFR</i> mutant and <i>MET</i> amplified NSCLC	133
4.4.2	TWIST1 mediates resistance to MET TKIs in <i>MET</i> altered NSCLC	136

4.4.3	Twist1 cooperates with Hgf to promote tumorigenesis in a mouse model of Hgf-driven lung cancer	138
4.5	DISCUSSION.....	139
5.0	TWIST1 MEDIATES RESISTANCE TO TRAIL-BASED THERAPIES THROUGH DIRECT UPREGULATION OF C-FLIP.....	143
5.1	ABSTRACT.....	143
5.2	INTRODUCTION	144
5.3	METHODS.....	147
5.3.1	Cell lines and reagents.....	147
5.3.2	Cell proliferation assays	147
5.3.3	Western blot and antibodies	148
5.3.1	Luciferase reporter assay.....	148
5.3.2	Chromatin immunoprecipitation	148
5.3.3	Lentiviral shRNA and cDNA overexpression	149
5.4	RESULTS	149
5.4.1	Apoptosis following loss of TWIST1 expression requires both the intrinsic and extrinsic apoptotic pathways	149
5.4.2	TWIST1 directly upregulates cFLIP.....	155
5.4.3	TWIST1 mediates resistance to TRAIL-based therapies	160
5.5	DISCUSSION.....	163
6.0	CONCLUSIONS	166
	APPENDIX A	174
	BIBLIOGRAPHY.....	180

LIST OF TABLES

Table 1. List of primers used for SYBR Green qRT-PCR	174
Table 2. List of Primers used for Taqman qRT-PCR	175
Table 3. List of antibodies used for western blotting and immunohistochemistry	175
Table 4. Sequences for TWIST1/BCL2L11/TCF3 shRNA (5'-3') in pKLO.1	176
Table 5. ORFs obtained from Johns Hopkins University HiT Center	177
Table 6. Source of plasmids utilized.....	177
Table 7: ChIP Primers for <i>BCL2L11</i> Promoter.....	178
Table 8: ChIP Primers for <i>CFLAR</i> Promoter	179

LIST OF FIGURES

Figure 1: Distribution of histological subtypes of lung cancer.....	3
Figure 2: Targetable molecular drivers in NSCLC with adenocarcinoma and squamous histology	5
Figure 3: Treatment paradigm for patients with metastatic Non-Small Cell Lung Cancer	6
Figure 4: Mechanisms of resistance to EGFR and ALK TKIs in NSCLC	20
Figure 5: Intrinsic and extrinsic apoptotic pathways	28
Figure 6: Illustration of the TWIST1 protein and key domains.....	37
Figure 7: Connectivity MAP (CMAP) analysis identifies compounds which inhibit NSCLC proliferation, TWIST1-dependent dissemination and TWIST1-suppression of organoid branching	58
Figure 8: FGF2 treatment induces branching morphogenesis of primary epithelial cells in 3D culture	60
Figure 9: Harmine inhibits growth through the induction of oncogene-induced senescence (OIS) in oncogene driver-defined NSCLC cell lines	63
Figure 10: Basal expression levels of TWIST1 in <i>KRAS</i> mutant and <i>MET</i> amplified/mutant NSCLC cell lines	64

Figure 11: Harmine treatment induces Oncogene-Induced Senescence (OIS) in EGFR and MET mutant NSCLC cell lines	65
Figure 12: TWIST1 suppresses oncogene-induced apoptosis in MET amplified NSCLC	66
Figure 13: Harmine induces apoptosis in oncogene-driven NSCLC cell lines	67
Figure 14: Harmine treatment leads to TWIST1 protein degradation	70
Figure 15: Harmine treatment promotes TWIST1 degradation and decreases TWIST1 protein stability.....	72
Figure 16: The E2A proteins and TWIST1 reciprocally stabilize each other.....	76
Figure 17: Harmine leads to degradation of the E2A proteins which are required for suppression of OIS.....	77
Figure 18: Silencing of <i>E2A</i> induces apoptosis and phenocopies silencing of <i>TWIST1</i>	78
Figure 19: The TWIST1/E2A heterodimer is critical for TWIST1 function and therapeutic response to harmine	81
Figure 20: Overexpression of TWIST1 or its binding partner, E2A, rescues harmine induced growth inhibition.....	82
Figure 21: Harmine has activity in <i>Kras</i> ^{G12D} / <i>Twist1</i> mouse model of autochthonous lung adenocarcinoma	85
Figure 22: Treatment with harmine decrease tumor growth in a <i>KRAS</i> mutant Patient-Derived Xenograph (PDX) model and degrades <i>Twist1</i> and induces apoptosis in a transgenic mouse model of <i>Kras</i> mutant lung cancer.....	86
Figure 23: TWIST1 is required for <i>EGFR</i> mutant NSCLC.....	100
Figure 24: Inhibition of TWIST1 induces apoptosis in a subset of <i>EGFR</i> mutant NSCLC cell lines.....	101

Figure 25: TWIST1 overexpression is sufficient to mediate resistance to EGFR TKIs.....	104
Figure 26: TWIST1 overexpression suppresses EGFR TKI-induced apoptosis in <i>EGFR</i> mutant NSCLC cell lines	105
Figure 27: Inhibition of TWIST1 is sufficient to overcome EGFR TKI resistance	106
Figure 28: Inhibition of TWIST1 can overcome acquired resistance to erlotinib	108
Figure 29: TWIST1 suppresses BIM expression by directly suppressing its transcription	111
Figure 30: TWIST1 overexpression does not decrease BIM protein half-life.....	113
Figure 31: Generation and characterization of a novel Twist1 overexpressing, mutant EGFR autochthonous lung tumor mouse model	116
Figure 32: Twist1 overexpression <i>in vivo</i> is sufficient to cause erlotinib resistance.....	120
Figure 33: Characterization of Twist1-mediated erlotinib resistance <i>in vivo</i>	121
Figure 34: HGF treatment increases TWIST1 protein stability.....	135
Figure 35: Pharmacologic inhibition of TWIST1 overcomes HGF-mediated resistance to MET and EGFR TKIs in <i>EGFR</i> mutant and <i>MET</i> amplified NSCLC.....	135
Figure 36: TWIST1 modulates sensitivity to crizotinib in <i>MET</i> altered NSCLC.....	137
Figure 37: Harmine has activity in a PDX mouse model of <i>EGFR</i> mutant <i>MET</i> amplified lung cancer	137
Figure 38: Twist1 overexpression leads to increased tumor size in a mouse model of Hgf-driven lung cancer	139
Figure 39: Silencing of <i>TWIST</i> leads to apoptosis in NSCLC cell lines.....	151
Figure 40: Growth inhibition following genetic inhibition of <i>TWIST1</i> requires apoptosis	152
Figure 41: Overexpression of c-FLIPs or BCL-2 partially rescues apoptosis and growth inhibition following silencing of <i>TWIST1</i>	153

Figure 42: Knockdown of BIM partially rescues growth inhibition following pharmacologic and genetic inhibition of TWIST1	154
Figure 43: Modulation of TWIST1 expression results in altered expression of extrinsic apoptotic pathway members	158
Figure 44: The TWIST1 homodimer and heterodimer transactivates the <i>CFLAR</i> promoter	159
Figure 45: TWIST1 directly binds to the <i>CFLAR</i> promoter	160
Figure 46: TWIST1 mediates resistance to TRAIL-based therapies	162

PREFACE

I would like to thank Dr. Burns for his incredible mentorship during my time in graduate school. To members of the Burns and Stabile lab, specifically Lucia, Suman, Eric, Natalie, and Susheel, it has been a great experience working alongside all of you. I would also like to thank our collaborators Drs. Phuoc Tran, Jessica Cades, and Charles Rudin, who were instrumental in the mouse studies in Chapters 2-3. I thank my committee and Dr. Steinman for their helpful feedback and support over the past 4 years. To my friends, specifically Joe and Erik, our friendship means to the world to me. Finally, I would like to thank my parents. Without their support, sacrifice, and love, I would have never been able to complete this journey.

1.0 INTRODUCTION

1.1 LUNG CANCER

Lung cancer is the leading cause of cancer-related death in the United States and worldwide (1). In 2018, it is estimated that 234,030 patients will be diagnosed with lung cancer and approximately 154,050 deaths will occur due to lung cancer (2). While survival rates have marginally improved over the past few decades (1), 5-year survival rates for lung cancer patients remain a dismal 18% (2). 5-year survival rates for lung cancer patients diagnosed with local disease are 56%, however, only 15% of patients are diagnosed with local disease (1,2). For those patients diagnosed with metastatic disease, the 5-year survival rate is 5% (2). While targeted therapies and immunotherapies have improved outcomes for distinct subsets of patients with metastatic lung cancer, most systemic therapies remain marginally effective in the metastatic setting and few patients are cured in the metastatic setting.

There are numerous behavioral risk factors and environmental exposures that are known to increase lung cancer risk. The leading cause of lung cancer is cigarette smoking. It is estimated that approximately lung cancer deaths in 90% of men and 75-80% of women can be attributed to cigarette smoking (1). Smoking leads to lung cancer through exposure to polycyclic aromatic hydrocarbons and N-nitro compounds both of which are potent carcinogenic compounds found in cigarette smoke (1,3,4). The second leading cause of lung cancer is

exposure to radon (5). Occupational exposures to high levels of radon have been linked to increased risk of lung cancer (1,6). Radon is hypothesized to be carcinogenic when it is inhaled, as the decay of radon causes release of high energy α -particles in the lung (1,7,8). Occupational exposures account for approximately 5% of lung cancers, the most important of these exposures being asbestos. Studies have demonstrated that asbestos functions as carcinogen by promoting chronic inflammation in the lung (9).

1.1.1 Lung cancer histological and genetic subtypes

Lung cancer is not just a single disease but rather a collection of distinct neoplasms with distinct histologies, biologies and clinical outcomes (10). Lung cancer is classified by both histology and/or molecular drivers. Histologically, there are two main types of lung cancer: small cell lung cancer (SCLC) and non-small cell lung cancer (NSCLC). SCLC, which accounts for approximately 15% of all lung cancers, is a neuroendocrine tumor that is initially responsive to chemotherapy (11). However, resistance to chemotherapy inevitably occurs and median survival for patients with advanced disease is approximately one year (11). Beyond mutations in *TP53* (75-90%) and *RBI* (60-90%), few molecular drivers have been identified in SCLC and few patients with SCLC benefit from molecularly targeted therapies (11).

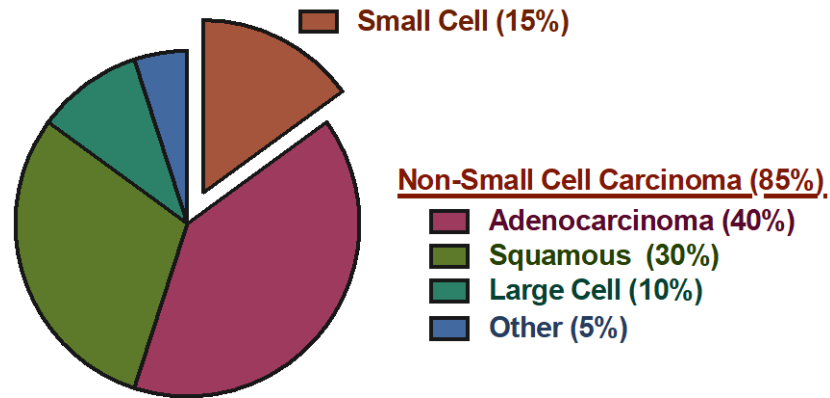


Figure 1: Distribution of histological subtypes of lung cancer

NSCLC accounts for approximately 85% of lung cancers and has multiple major histological subtypes including adenocarcinoma, squamous cell carcinoma, and large cell carcinoma (**Figure 1**). Studies investigating genomic alterations in NSCLC with adenocarcinoma histology have identified a number of potentially targetable molecular drivers (**Figure 2**) (12-14). These molecular drivers are actionable as they have targeted therapies that are FDA approved or in clinical trials. Currently, patients with mutations in *EGFR*, *ALK* translocations, *BRAF* mutations and *ROS1* translocations are treated with FDA approved targeted therapies (15). Other putative oncogenic drivers such as *MET* mutations/amplifications, *RET* translocations, *NTRK* translocations and *HER2* mutations have been identified and targeting these oncogenic drivers is currently being explored both pre-clinically and in clinical trials (15).

Importantly, *KRAS* mutations are found to be oncogenic drivers in approximately 25% of patients with NSCLC with adenocarcinoma histology. Attempts to inhibit this oncogenic driver both directly and indirectly have failed (16). Direct inhibition of mutant *KRAS* has proven to be difficult due to the affinity of mutant *KRAS* for GTP and limited availability of binding sites (17). However, covalent inhibitors have been recently identified that specifically inhibit the *G12C* mutant form of *KRAS* by covalently binding to the allosteric switch II pocket of the GDP

bound form of KRAS (18,19). These covalent inhibitors have pre-clinical activity in mutant *KRAS G12C*-driven cancers, however, resistance to these agents has already been observed pre-clinically and clinical efficacy of these compounds needs to be explored (18,19). Indirect strategies to target mutant *KRAS* have included interrupting key post-translational modifications and inhibiting key downstream pathways. For example, KRAS requires prenylation and subsequent localization to the cell membrane in order activate downstream signaling pathways and enzymes such as farnesyltransferase are important for this process (17). Use of farnesyltransferase inhibitors had promising preclinical efficacy but failed clinically. A potential reason for this poor clinical efficacy is that KRAS can be alternatively prenylated by enzymes such as geranylgeranyltransferase (17). In addition, salirasib (*S*-trans,trans-farnesylthiosalicylic acid), which is a small molecule farnesylcysteine mimetic that inhibits RAS function by interfering with RAS plasma membrane docking, also failed to have clinical efficacy in KRAS-driven tumors despite preclinical activity (17,20,21).

Targeting downstream effector pathways of KRAS has been largely unsuccessful as well. There have been efforts to target signaling molecules within the PI3K and MAPK signaling pathways, which are two key downstream effector pathways of KRAS. However, given the complexity of KRAS signaling and redundancy within the multiple signaling pathways that mutant *KRAS* activates, efforts to target individual signaling molecules, such as PI3K, BRAF, and MEK, have failed despite promising preclinical studies (17). Current efforts are aimed at determining if genetic subgroups within *KRAS* mutant tumors may respond to targeted therapy and if combinations of targeted agents may have superior outcomes in *KRAS* mutant tumors (17). Targeted therapies in NSCLC are discussed in detail in Section 1.1.2.

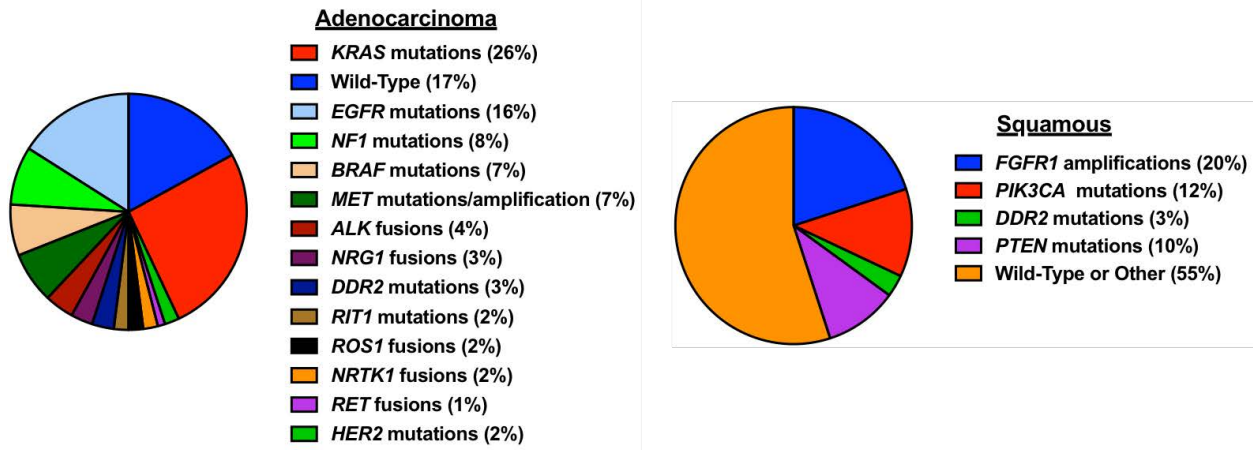


Figure 2: Targetable molecular drivers in NSCLC with adenocarcinoma and squamous histology

Within NSCLC with squamous histology, putative oncogenic drivers, specifically actionable oncogenic drivers, are less frequent compared to NSCLC with adenocarcinoma histology (**Figure 2**). Early efforts to determine genetic aberrations in NSCLC with squamous histology revealed frequent *TP53* mutations (81%) as well as mutations in *MLL2* (20%), *PI3K* (16%), *CDKN2A* (15%) (10,22). Unlike adenocarcinoma, NSCLC with squamous histology rarely has mutations in *EGFR* and *KRAS* (10). Potential actionable oncogenic drivers in patients with squamous histology include amplifications in *FGFR1*, mutations in *DDR2*, and *PIK3CA* mutations (**Figure 2**) (10,12,23). Clinical trials are currently investigating the efficacy of targeting of potential oncogenic drivers in NSCLC with squamous histology including a SWOG cooperative study called the LUNG-MAP study (24).

1.1.2 Lung cancer treatment modalities

Patients with NSCLC have a number of therapeutic options including: definitive surgery or radiation, chemotherapy, targeted therapy, or immunotherapy. Patients with early stage disease,

which is typically identified as an incidental finding on imaging (chest X-Ray or computed tomography (CT) scan) or on a screening CT scan for heavy smokers, are commonly candidates for definitive local treatment which includes surgery, radiation, and/or perioperative chemotherapy followed by surgery. Diagnosis of metastatic disease typically precludes patients from surgical intervention. Choice of first-line systemic therapy is contingent on the presence or absence of “targetable” molecular drivers. Those patients with actionable molecular drivers typically receive first-line targeted therapy. Those patients without targetable molecular drivers with tumors positive for Programmed death-ligand 1 (PD-L1) expression are offered immunotherapy. Chemotherapy with and without immunotherapy remains the mainstay of therapy for patients with advanced lung cancer that do not qualify for targeted agents or immunotherapies.

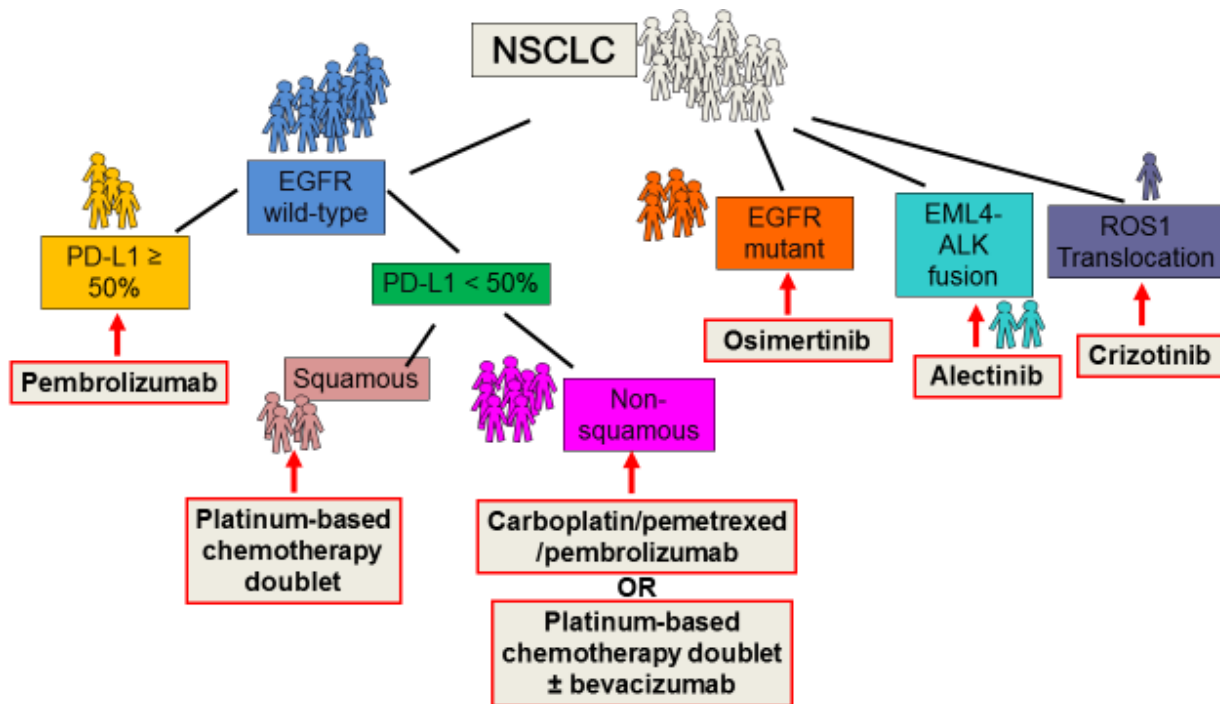


Figure 3: Treatment paradigm for patients with metastatic Non-Small Cell Lung Cancer

1.1.2.1 Definitive local treatment: Surgery and Radiation

The mainstay of treatment for patients with early stage NSCLC (Stage I-II) or a subset of locally advanced NSCLC (Stage IIIa) is surgical resection of the tumor (25,26). The types of surgical procedures recommended for NSCLC differ between stage and histological subtypes but segmentectomy or lobectomy is generally reported to have superior outcomes to wedge resections (26). Adjuvant or postoperative chemotherapy has been investigated extensively in patients with local disease. Currently, it is recommended that patients with Stage II-III disease post-resection receive a cisplatin-based chemotherapy regimen, given that chemotherapy for these patients provides an approximate 5% increase in 5-year survival (25,27). Additionally, chemotherapy may be considered for patients with Stage 1B disease as it has been shown to provide a small increase in survival (27). Several studies have also demonstrated that neoadjuvant therapy is equivalent to adjuvant therapy and is used by some centers across the country (28).

For those patients with Stage I-II local disease, who either do not qualify or refuse surgical resection, radiation therapy is recommended. For patients with Stage I disease, disease control rates for patients receiving high-dose stereotactic radiation therapy have disease control rates are between 85-90% (25,29-33). For patients with larger tumors (Stage II), conventional radiation is recommended rather than stereotactic radiation (25). However, outcomes for patients with inoperable Stage II disease receiving radiation therapy is worse than those that can receive surgery (34). Additionally, there is no evidence to support the addition of chemotherapy to radiation for Stage I-II.

For those patients with Stage III unresectable disease, 5- year survival is poor at 15-20% (33). The standard of care for these patients is definitive chemotherapy and radiotherapy (25,33).

Early studies demonstrated that the addition of sequential chemotherapy plus radiation provided a survival benefit to radiotherapy alone (35,36). Subsequent studies demonstrated concurrent chemotherapy plus radiation provided a greater survival advantage to sequential chemotherapy plus radiation (35,37). The most commonly used chemotherapy regimens include cisplatin-etoposide or carboplatin-paclitaxel (35,38). Cisplatin-based regimens have been shown to have better response versus carboplatin-based regimens, while cisplatin-based regimens have higher rates of side effects (35,38,39). Of note, there was preclinical evidence that resistance to chemotherapy and radiation therapy may occur through upregulation of PD-L1 expression within tumors (35,40,41). Based on this evidence, the recent PACIFIC trial (NCT02125461) investigated whether patients with unresectable Stage III disease previously treated with chemoradiation would benefit from the PD-L1 inhibitor, durvalumab. The results of the trial revealed that there was significant increase in progression free survival (PFS) for those patients that received the PD-L1 inhibitor, durvalumab (16.8 months) versus those that received placebo (5.6 months) with median survival not reached in the durvalumab group at the time of the publication (42). Additionally, the quality of life for those patients receiving durvalumab was not significantly different than those patients receiving placebo (43).

1.1.2.2 Chemotherapy

For those patients with advanced or metastatic NSCLC without a targetable molecular driver or elevated levels of PD-L1 expression (>50%), the standard of care treatment remains systemic chemotherapy with or without immunotherapy (**Figure 3**) (44). Currently, the recommended chemotherapy regimens include a platinum-based chemotherapy, such as cisplatin or carboplatin, plus another chemotherapy agent (44). Other chemotherapies that can be utilized include taxanes (docetaxel), antimetabolites such as gemcitabine and pemetrexed, and vinca

alkaloids such as vinorelbine. The current recommended platinum-based chemotherapy doublet therapy in non-squamous histologies is cisplatin plus pemetrexed as it provides a greater survival benefit compared to other regimens (**Figure 3**) (44-46). For patients with nonsquamous histology, the addition of a monoclonal antibody against vascular endothelial growth factor (VEGF) to chemotherapy results in increased survival and PFS (**Figure 3**) (44,47). Additionally, as discussed in Section 1.1.2.3, pembrolizumab plus chemotherapy (carboplatin and pemetrexed) is another option for patients with advanced NSCLC as this regimen was recently shown to be superior to chemotherapy alone in patients with advanced nonsquamous NSCLC (48). However, overall survival (OS) remains poor for patients without molecular drivers or PD-L1 expression, as systemic chemotherapies remain marginally beneficial (44).

1.1.2.3 Immunotherapy

For those patients with metastatic NSCLC in the absence of targetable molecular drivers, survival remains poor, with most patients who receive chemotherapy succumbing to the disease within a year (49-51). However, immunotherapies have emerged as a new class of agents for patients with advanced or metastatic NSCLC. Due to initial poor success of immunotherapies, lung cancer was largely considered to be nonimmunogenic (52). In lung cancer, specifically advanced lung cancer, there is an immunosuppressive tumor microenvironment that results from secretion of immunosuppressive cytokines, loss of antigen expression for major histocompatibility complex, decreased presence of intratumoral lymphocytes, and increased intratumoral T regulatory cells (52-56).

Current successful immunotherapies have focused on targeting checkpoint pathways that negatively regulate T cell activation. One such molecule is cytotoxic T-lymphocyte antigen-4 (CTLA-4), which functions as a T-cell checkpoint inhibitor. T-cells express a co-stimulatory

protein, CD28, which binds to CD80/86 proteins on antigen-presenting cells (APCs) and increases T-cell activation (52,57). CTLA-4 is also expressed on T-cells and binds to CD80/86 on APCs, resulting in suppression of T-cell activation (52,57). Interestingly, CTLA-4 binds with greater affinity to CD80/86 and the relative abundance of CTLA-4 versus CD28 determines whether a T-cell will proliferate or become anergic (57). Currently, ipilimumab, a monoclonal anti-CTLA antibody, has shown activity in solid tumors and is currently FDA approved for metastatic and unresectable melanoma but failed to show activity in combination with chemotherapy in NSCLC (57-59). Another pathway that has been the focus of immunotherapy is the programmed death-1 (PD-1) pathway. Programmed death-ligand 1 (PD-L1) is expressed on APCs and aberrantly expressed on tumor cells and binds to PD-1 which is expressed on the surface of T-cells (57). The binding of PD-L1 to PD-1 on T-cells results in decreased T-cells activation (57). There are a number of FDA approved monoclonal antibody therapies targeting PD-1 (Nivolumab and Pembrolizumab) and PD-L1 (Durvalumab and Atezolizumab) that have activity in both melanoma and NSCLC.

Currently, pembrolizumab is the first-line treatment for patients with metastatic NSCLC with $\geq 50\%$ of tumor cells positive for PD-L1 expression (**Figure 3**). This first-line designation was a result of the KEYNOTE-024 trial that demonstrated in patients with metastatic NSCLC and $\geq 50\%$ PD-L1 expression that pembrolizumab significantly increased overall survival and PFS compared to platinum-based chemotherapy (51,60). Additionally, pembrolizumab is approved as a first-line therapy for metastatic NSCLC patients (with and without PD-L1 expression) with nonsquamous histology in combination with chemotherapy, as a result of the KEYNOTE-021 and KEYNOTE-189 trials that demonstrated pembrolizumab plus chemotherapy resulted in superior response rates, PFS, and OS compared to chemotherapy alone

(Figure 3) (48,51,61). In the second-line setting, pembrolizumab is approved in the PD-L1 positive population while both nivolumab and atezolizumab are approved regardless of PD-L1 status as all three agents have shown superiority in overall response rates (ORR), PFS, and OS compared to docetaxel (51,62). Interestingly, the combination of CTLA-4 and PD-1 inhibitors in patients with metastatic melanoma has impressive activity and has demonstrated a marked survival benefit for these patients. In NSCLC, a recent Phase I trial demonstrated that the combination of ipilimumab and nivolumab resulted in a high response rate and durable responses in patients with advanced NSCLC (63). A recent study has suggested that this combination may be beneficial in the first-line setting in patients with high tumor mutational burden (64). Given the early success of combinations of immunotherapies, there are numerous trials investigating combination of CTLA-4 and PD-1/PD-L1 inhibitors in NSCLC as well as other novel immunotherapy agents.

1.1.2.4 EGFR targeted therapy

Epidermal growth factor receptor (EGFR) is a member of the ErbB family of receptor tyrosine kinases (RTKs) (65). EGFR can bind to multiple ligands including epidermal growth factor (EGF), amphiregulin, and transforming growth factor α (TGF α) (65). EGFR binding these ligands results in homodimerization or heterodimerization with other members of ErbB family of receptors (65). EGFR dimerization results in transphosphorylation of EGFR and provides docking sites for proteins involved in activation of downstream pathways including the PI3K-mTOR pathway, RAS/RAF/MEK pathway, and JAK-STAT pathway (65). These pathways regulate cell proliferation, angiogenesis, apoptosis, migration, and cell motility (10). Aberrations in EGFR signaling can result from protein overexpression, gene amplification, or mutations

within the receptor (66). These all can result in aberrant activation of EGFR and its downstream signaling pathways and can promote tumorigenesis.

In patients with NSCLC, the most frequent actionable EGFR aberrations are mutations within the tyrosine kinase domain (10). Mutations in the *EGFR* gene occur in approximately 30-50% of patients of East Asian descent and 15% of patients of non-East Asian descent (10,33). Of note, East Asian patients who are never smokers this proportion of *EGFR* mutations is greater than 50% (10). The majority of *EGFR* mutations (~90%) found in NSCLC patients are exon 19 deletions and *L858R* point mutations within exon 21 (10). Both mutations result in ligand-independent constitutively active receptors (67,68). Structural studies of *L858R* mutated *EGFR* have demonstrated that the *L858R* mutation prevents the activation loop of EGFR from adopting an inactive conformation resulting in a constitutively active protein (67). Interestingly, these *EGFR* mutations (exon 19 deletions and *L858R* mutations) are termed “sensitizing mutations” because these mutated receptors display an increased binding affinity for 1st generation EGFR TKIs such as erlotinib and gefinitib (67,69). Additionally, these sensitizing mutations display a reduced binding affinity for adenosine triphosphate (ATP) which may account for their increased sensitivity to competitive ATP inhibitors such as erlotinib and gefinitib (67,69).

EGFR TKIs were initially established as first-line therapy for patients with late stage (IIIb or IV) *EGFR* mutated NSCLC based on the results of the phase III Iressa Pan-Asia Study (IPASS) (70). This trial was the first to establish that the EGFR TKI, gefinitib, was superior to chemotherapy for patients with *EGFR* mutations. Patients with *EGFR* mutations, the majority (~90%) of whom had exon 19 deletions or *L858R* mutations, who received gefinitib displayed a significantly increased response rate, relative risk reduction, and PFS compared to patients that received chemotherapy (70). Interestingly, this study also demonstrated that in patients with

wild-type *EGFR* gefinitib resulted in worse clinical outcomes than chemotherapy (70). Since IPASS, there have been numerous phase III trials that have also demonstrated that EGFR TKIs are a superior first-line treatment for patients with *EGFR* mutations over chemotherapy (33,71-74).

A major hurdle for EGFR targeted therapy is acquired resistance. Resistance can occur through EGFR-dependent mechanisms (amplification or 2nd site mutations) or through EGFR-independent mechanisms or bypass signaling pathways which will be discussed in Section 1.1.3. The most frequent mechanism of resistance (~49%) is secondary to *T790M* mutations in *EGFR* (75). The *T790M* mutation introduces a hydrophobic, bulky methionine amino acid for the hydrophilic threonine into the ATP binding pocket of EGFR (76,77). Mutant *EGFR* with secondary *T790M* mutations retains affinity for gefinitib or erlotinib, however, this mutation significantly increases affinity of EGFR for ATP, thus reducing the potency of first generation EGFR TKIs (76,77). 3rd generation EGFR TKIs are irreversible inhibitors that covalently bind to cysteine 797 within the ATP binding pocket (77,78). As opposed to 2nd generation EGFR TKIs which inhibited both wild type and mutant *EGFR*, 3rd generation EGFR TKIs are more selective for mutant forms of *EGFR* (77,78). Previously, osimertinib had been established as the mainstay of treatment for patients with *EGFR* mutant NSCLC that had progressed on 1st generation EGFR TKIs (79-81). Recently, osimertinib was established as the first-line therapy for patients with *EGFR* mutant NSCLC (**Figure 3**). The recent Phase III FLAURA study, demonstrated that use of first-line osimertinib resulted in a significantly longer PFS (18.9 months) compared to FDA approved first-line EGFR TKIs (10.2 months) (82). Additionally, first-line osimertinib resulted in a significantly longer duration of response compared to 1st generation EGFR TKIs (17.2 months for osimertinib versus 8.5 months for erlotinib/gefitinib) (82). Similar to 1st generation

EGFR TKIs, acquired resistance to osimertinib has limited its long-term efficacy (82). Additional mutations in *EGFR* are the most common mechanisms of osimertinib resistance (83,84). Initial studies have demonstrated that approximately 25% of osimertinib resistant patients develop the *C797S* mutation, which prevents osimertinib from covalently binding to EGFR (83,84). Currently, there are efforts to develop fourth-generation EGFR TKIs to target the *C797S EGFR* mutation (85,86).

1.1.2.5 *ALK* targeted therapy

Anaplastic lymphoma kinase (ALK) is a receptor tyrosine kinase that is a member of the insulin receptor family (87). The function of wild type ALK is not fully understood, as it is rarely expressed postnatally in humans and mice (87). In mouse models, Alk has shown to play role in the development of the nervous system and following nervous system development Alk expression is drastically reduced (87). Additionally, mouse *Alk* knockout models develop normally except for minor behavioral abnormalities (87). However, in zebrafish models, Alk expression is required for survival and differentiation of neural progenitors in the developing central nervous system (88). There are case reports in humans in which germline mutations in *ALK* are associated with a neuroblastoma accompanied by encephalopathy and abnormal brainstem development (89). Interestingly, ALK was shown to play a role in cancer when *ALK* fusion genes with nucleophosmin (*NPM*) were identified in anaplastic large-cell lymphoma (ALCL) (87,90). The *NPM-ALK* fusion gene in ALCL results in constitutively active ALK protein that drives ALCL tumorigenesis (87,90). Recently, an *ALK* fusion gene with echinoderm microtubule-associated protein-like 4 (*EML4*) was identified in patients with NSCLC (87,90). Both *ALK* and *EML4* are located on chromosome 2 and the *EML4-ALK* fusion occurs via an inversion event at this chromosome (90). Since discovery of the *EML4-ALK* fusion, in patients

with NSCLC, a number of *EML4-ALK* variants have been identified, as well as, additional ALK fusions such as *KIF5B-ALK*, *TFG-ALK*, and *KLC1-ALK* (10). With the *EML4-ALK* fusion being the most common, *ALK* translocations have been identified in approximately 3-7% of NSCLC (87,90,91). Importantly, these *ALK* translocations appear to be mutually exclusive from other potential molecular drivers such as mutant *KRAS* or *EGFR* (92).

Despite having different fusion partners, all *ALK* translocations share a number of common characteristics. First, the fusion gene includes the full tyrosine kinase domain of *ALK* (90). Additionally, the promoter of the fusion gene originates from the fusion partner as the promoter of the *ALK* gene is inactive postnatally and is unable to drive transcription of the fusion gene (87,90). Lastly, the fusion gene includes an oligomerization domain from the fusion partner that is capable of inducing ligand-independent dimerization (90). Importantly, the *EML4-ALK* translocation in NSCLC has the aforementioned characteristics. In a number of pre-clinical models, *EML4-ALK* was confirmed as a potential oncogenic driver in lung cancer as its expression was sufficient for development of lung tumors (87). Additionally, in these models *EML4-ALK*-driven tumors were sensitive to *ALK* inhibition (87). Similar to *EGFR*, *ALK* promotes tumorigenesis via activating a number of downstream pathways that play important roles in regulating proliferation, apoptosis, angiogenesis and migration including the PI3K-mTOR pathway, RAS/RAF/MEK pathway, and JAK-STAT pathway (87).

Four years following identification of the *ALK* translocation in NSCLC, crizotinib was approved by the FDA for the treatment of *ALK*-driven NSCLC. Crizotinib is an *ALK* ATP competitive inhibitor that was originally developed as a *MET* inhibitor. Crizotinib eventually became a first-line therapy for *ALK* rearranged advanced NSCLC as a Phase III study (PROFILE 1014) demonstrated that patients that received crizotinib had a significantly longer PFS (10.9

months) compared to patients receiving chemotherapy (7.0 months) (93). However, similar to erlotinib/ gefitinib in *EGFR* mutant NSCLC, patients with ALK-driven NSCLC inevitably develop resistance to crizotinib. The most common mechanism of resistance are secondary aberrations in ALK. In approximately 20-36% of patients develop mutations within the tyrosine kinase domain of *ALK* that results in decreased sensitivity to crizotinib (92,94,95). The most common mutation secondary mutation in *ALK* is the “gatekeeper” *L1196M* mutation, which introduces a bulky methionine group into the active site and sterically hinders crizotinib from accessing the hydrophobic active site (87,96). Another common mutation is *G1269A* which near the N-terminus of the activation loop and introduces an alanine for a glycine. Substitution of an alanine for glycine sterically hinders crizotinib from accessing the active site of ALK (90,97). Interestingly, other secondary *ALK* mutations have been identified including the *C1156Y* mutation near the α C-Helix, which stabilize the active conformation of ALK and promotes increased ATP binding, thus decreasing the potency of crizotinib (87,97). Additionally, approximately 9% of patients develop *ALK* amplification as a mechanism of resistance to crizotinib (90,94). Interestingly, patients can have concurrent *ALK* mutations and amplifications as a mechanisms of resistance to crizotinib (90).

Interestingly, second generation ATP competitive inhibitors of ALK such as alectinib and ceritinib are potent ALK inhibitors that have activity against multiple *ALK* mutations including the *L1196M* “gatekeeper” mutation. Additionally, ceritinib has been shown to have activity in *EML4-ALK*-driven NSCLC with amplification of the *EML4-ALK* allele, suggesting that second generation ALK TKIs can overcome multiple mechanisms of resistance to crizotinib (97). Multiple Phase III trials have demonstrated that ceritinib was more efficacious than chemotherapy and was subsequently approved as first-line therapy for *ALK* rearranged NSCLC

in 2017 (87). However, crizotinib and ceritinib have limited activity in the central nervous system (CNS) given that they are both substrates for and removed from the CNS via the p-glycoprotein (87). The poor penetration into the CNS results in frequent brain recurrence for patients that have progressed on crizotinib. Alectinib has marked CNS penetrance as it is not a target of the p-glycoprotein and is highly effective in patients with CNS disease (98). The recent ALEX trial demonstrated that alectinib was more efficacious than crizotinib in ALK-driven NSCLC and resulted in fewer CNS recurrences than crizotinib (99). As a result, alectinib was approved as a first-line therapy for *ALK*-positive NSCLC and is the current standard of care treatment for *ALK*-positive NSCLC (**Figure 3**).

Over 50% of patients become resistant to alectinib and ceritinib via secondary mutations in *ALK*, the most common being the *G1202R* mutation which sterically blocks these second generation drugs from accessing the kinase domain (87). Lorlatinib, a third generation ALK inhibitor has efficacy against *G1202R ALK* mutation (87,100). A recent Phase I trial revealed that lorlatinib has efficacy in patients resistant to second generation drugs (101). Additionally, there is currently a Phase III trial comparing the efficacy of lorlatinib versus crizotinib (NCT03052608).

1.1.2.6 *MET* targeted therapy

The c-MET (MET) protein is a receptor tyrosine kinase which upon binding its only known ligand, hepatocyte growth factor (HGF), mediates tumor cell proliferation, epithelial-mesenchymal transition (EMT), motility, invasion and angiogenesis all of which contribute to its role in tumorigenesis (102). The MET signaling pathway is often dysregulated in lung cancer as a result of several mechanisms including MET or HGF protein overexpression, *MET* amplification and *MET* mutations (103). MET overexpression occurs in up to 61% of NSCLC

and is correlated with poor prognosis (104,105). Likewise, HGF overexpression is also linked to poor survival (106). HGF/MET receptor pathway alterations, such as *MET* amplification and mutations, specifically exon 14 skipping mutations which result in increased MET stability, have recently been recognized as potential targetable oncogenic drivers in NSCLC. *MET* amplification is found in approximately 5-6% of NSCLC tumors (107) and is associated with poor prognosis and mediastinal lymph node metastases (105,108). In both gastric adenocarcinoma and lung cancer, preclinical studies have demonstrated that *MET* amplification can predict response to MET TKIs (109-111). In multiple Phase I trials, patients with *MET* amplified advanced NSCLC had dramatic responses to MET TKIs (112,113). Additionally, the results of these trials suggest that patients with higher levels of *MET* amplification are more likely to respond to MET inhibition (112). Currently, there are numerous clinical trials such as NCT02750215, NCT00585195, and NCT02132598, further investigating the role of MET inhibitors in *MET* amplification NSCLC.

MET mutations have been identified in 3-8% of lung tumors (49,114). These mutations reside in the extracellular semaphorin domain as well as the intracellular juxtamembrane domain which affect ligand binding and receptor downregulation, respectively (104,115,116). In particular, *MET* Exon 14 skipping mutations have been investigated as potential drivers of NSCLC. Exon 14 contains the juxtamembrane domain of MET. Mutations around the splicing junction of Exon 14 cause aberrant splicing of the *MET* transcript and loss of Exon 14 (111,117). Importantly, the juxtamembrane domain contains a binding site for the E3 ubiquitin ligase, casitas B-lineage lymphoma (CBL) (111,117). Loss of this site (Y1003) results in increased MET half-life, protein stability and prolonged PI3K-AKT and MAPK pathway activation (117). Preclinical studies have demonstrated that *MET* Exon 14 skipping mutations were sufficient to

induce adenocarcinoma in mouse models, confer anchorage independent growth in cell lines, and markedly increase sensitivity to MET TKIs (117,118). Additionally, dramatic responses have been observed in patients with *MET* mutant tumors treated with the MET TKIs, crizotinib or capmatinib (117-120). Similar to EGFR and ALK TKIs in *EGFR* mutant and *ALK*-positive NSCLC, patients *MET* mutations inevitably develop resistance to MET TKIs. Initial studies investigating mechanisms of resistance to MET TKIs have identified secondary mutations in *MET* (117,121). Interestingly, these secondary mutations in *MET* prevent binding of type I MET TKIs, which preferentially bind active conformation of MET, such as crizotinib or capmatinib, but are still sensitive to type II MET TKIs, which bind to the inactivation form of MET, such as cabozantinib (121,122). A case report has demonstrated that a patient that developed resistance to type I MET TKIs responded to a type II MET TKI, cabozantinib (122).

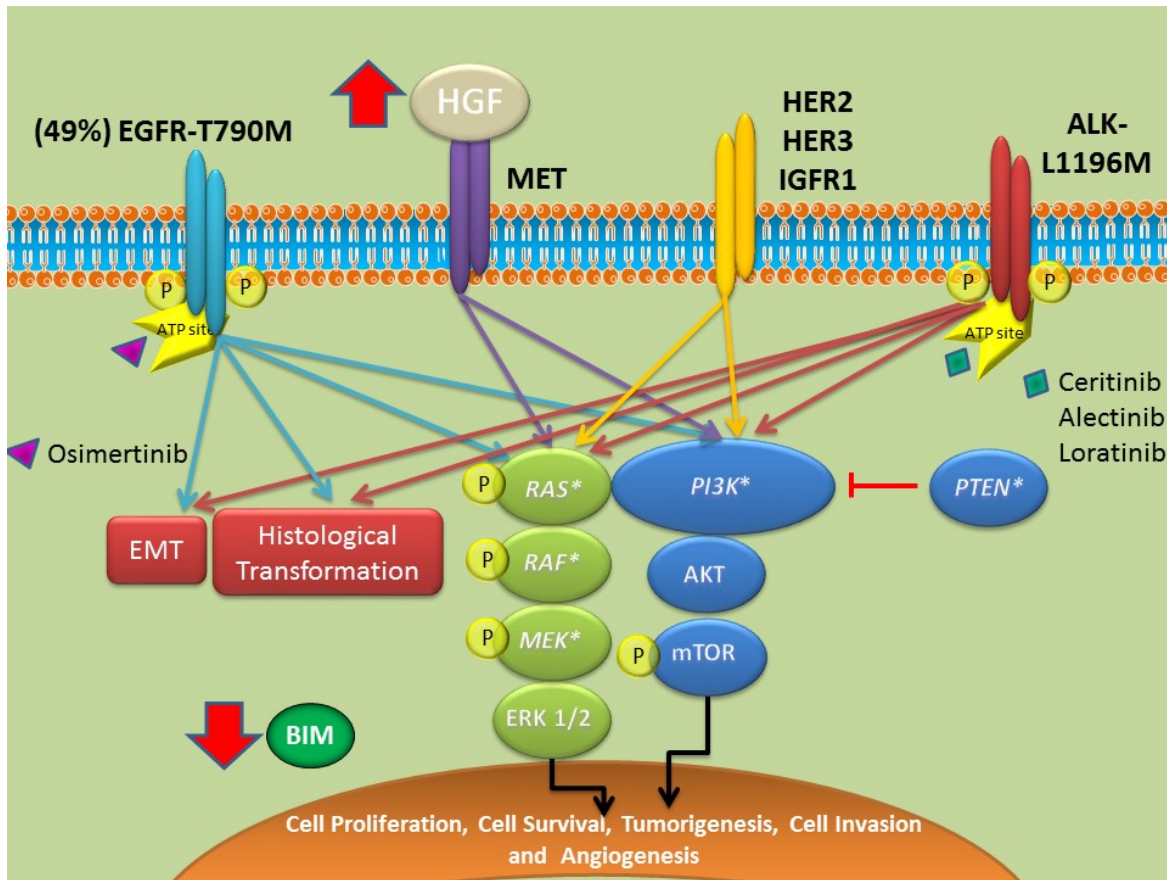


Figure 4: Mechanisms of resistance to EGFR and ALK TKIs in NSCLC

Despite impressive responses to EGFR and ALK TKIs, patients with EGFR- and ALK-driven NSCLC inevitably develop acquired resistance to these therapies. The most common mechanism of acquired resistance to EGFR and ALK TKIs are second site mutations within *EGFR* and *ALK*, respectively. These mutations, such as the *T790M EGFR* mutation and the *L1196 ALK* mutation, lead to TKI resistance by preventing drug binding or increasing affinity for ATP over the TKI. Alternatively, activation of bypass signaling pathways has been identified as a mechanism of resistance. Commonly, TKI resistant tumors increase activity of alternative receptor tyrosine kinases (RTKs) such as MET, HER2, HER3, and IGFR1, through genetic mutation/amplification or through increased expression of ligands, such as HGF for the MET receptor. Additionally, mutations in individual genes (*PIK3CA*, *PTEN*, *RAF*, *MEK*) within important signaling pathways can also confer TKI resistance. Independent of bypass signaling, epithelial-mesenchymal transition and histological transformation have been associated with resistance to EGFR and ALK TKIs. Decreased expression of the pro-apoptotic BCL-2 protein, BIM, and polymorphisms in the BIM gene, *BCL2L11*, have also been linked to resistance to TKIs in NSCLC. * denotes genes mutated in TKI resistant setting

1.1.3 Driver independent resistance mechanisms to targeted therapies in lung cancer

In molecularly defined subpopulations of patients with NSCLC, use of targeted therapies typically result in marked response rates and improved clinical outcomes (123). However, the efficacy of targeted therapies is significantly limited due to the frequency of *de-novo* resistance and the almost universality of acquired resistance in patients that initially response to these therapies (123). As mentioned in Sections 1.1.2.4-1.1.2.6, the most frequent mechanisms of acquired resistance are “on-target resistance” mechanisms such as secondary site mutations or gene amplification of the molecular target. Alternatively, patients can develop resistance to targeted therapies via mechanisms that are independent of the molecular driver. These mechanisms include activation of bypass signaling pathways, histological transformation, or EMT, all of which render the original tumor no longer dependent on the initial molecular driver.

1.1.3.1 Bypass signaling pathway activation

By directly inhibiting EGFR and ALK, EGFR and ALK TKIs suppress activity through key signaling pathways required for tumorigenesis. Patients with resistance to EGFR and ALK TKIs frequently have genetic aberrations or increased autocrine signaling that activates bypass signaling pathways required for tumor growth, proliferation, and survival (124,125). A common mechanism of resistance occurs via increased signaling through alternative receptor tyrosine kinases (RTKs) such as MET (discussed in the following Section), HER2, HER3, and IGF1R (**Figure 4**) (124,125). Activation of these RTKs can occur with gene amplification or mutations as found with *HER2* or *MET* or increased ligand expression as found with HER3 and IGF1R (124-128). While activation of alternative RTKs has been observed as a mechanism to 1st generation EGFR and ALK TKIs, these mechanisms appear to be relevant in resistance to later

generation TKIs as well, as patients with osimertinib and alectinib/ceritinib resistance commonly have aberrations in RTK signaling (124,125,129,130).

KRAS is a GTPase protein that activates numerous of signaling pathways such as RAF/MEK/ERK and PI3K/AKT/mTOR (131). Mutations in *KRAS* are oncogenic drivers in approximately 25% of NSCLC (131). While *KRAS* mutations are rarely seen in treatment naïve *EGFR* mutant or *ALK* translocation positive NSCLC, they have been observed in patients with acquired resistance to EGFR and ALK TKIs (**Figure 4**) (95,124,129,130,132,133). Importantly, in *EGFR* mutant NSCLC, *KRAS* mutations have been identified as a mechanism of resistance to osimertinib (129,130,132).

An additional mechanism of bypass signaling-mediated resistance to TKIs in NSCLC is mutations in individual signaling molecules within key mitogenic pathways. Two commonly mutated genes within the PI3K signaling pathway include, *PIK3CA* which is the gene that encodes the catalytically active subunit of the PI3K protein, and *PTEN* which is a negative regulator of PI3K signaling (**Figure 4**) (124). Activating mutations in *PIK3CA* and inactivating mutations in *PTEN* lead to aberrant activity of PI3K-AKT-mTOR signaling. *In vitro*, these mutations have been demonstrated to be sufficient to mediate resistance to TKIs (134). Interestingly, approximately 5% NSCLC patients with acquired resistance to erlotinib have *PIK3CA* mutations (75). *PIK3CA* mutations are also found in patients with acquired resistance to osimertinib and approximately 4% of patients with acquired resistance to alectinib (100,130). *PTEN* mutations have been identified in patients with both acquired and *de-novo* resistance to ALK and EGFR TKIs (135-137). Additionally, aberrations in the MAPK pathway have been identified in patients with acquired resistance. Specifically, activating mutations in *BRAF* and

MAP2K1 (gene encoding MEK1), which both lead to constitutive MAPK signaling, are seen in patients with acquired resistance to EGFR and ALK TKIs (**Figure 4**) (130,138,139).

1.1.3.2 HGF-MET Pathway Alterations

A frequent mechanism of resistance to targeted therapy in NSCLC is activation of the HGF-MET pathway. Activation of this signaling pathway serves as a bypass mechanism to targeted therapy as it results in activation of pathways such as MAPK and PI3K/AKT/mTOR, which are required for cell survival and proliferation in ALK- or EGFR-driven NSCLC (140,141). There are typically two aberrations of this pathway that are seen in resistance to targeted therapy: *MET* amplification and HGF overexpression (**Figure 4**). Importantly, these aberrations are seen across genetic subtypes of NSCLC in the resistance setting, which suggests that there is a conservation of HGF-MET function across genetic subtypes (141).

MET amplification promotes resistance to targeted therapy in lung cancer cells via HGF-independent activation of PI3K signaling by directly interacting with ERBB3 (142). *MET* amplification serves as mechanism of resistance in 5-20% of *EGFR* mutant patients that develop acquired resistance to erlotinib (75,142). Importantly, *MET* amplification has also been observed as a mediator of resistance to the third-generation EGFR TKI, osimertinib (143,144). In regards to ALK-driven NSCLC, *MET* amplification can mediate resistance to second generation ALK TKIs, alectinib and ceritinib (144,145). Additionally, there is clinical evidence that the MET/ALK TKI, crizotinib has activity in EGFR- and ALK-driven NSCLC with concurrent *MET* amplification (140,144,146). Currently, there are clinical trials investigating the efficacy of MET inhibitors in *EGFR* mutant NSCLC patients with MET-mediated resistance to EGFR inhibitors (140).

Similar to *MET* amplification, HGF overexpression promotes resistance to targeted therapies in lung cancer by reactivating MAPK and PI3K signaling (147,148). HGF overexpression can result in autocrine activation of MET signaling via direct release from cancer cells or paracrine activation of MET signaling via release from stromal cells, specifically fibroblasts (147). HGF overexpression has been observed as a mechanism of resistance to both EGFR and ALK TKIs (147-151). In *EGFR* mutant patients, HGF overexpression has been observed in as many as 60% of patients with resistance to erlotinib (151). HGF overexpression can also result in *de-novo* resistance to EGFR TKIs (149). In addition, HGF has been shown to mediate resistance to alectinib in ALK-driven NSCLC and use of crizotinib has been shown to overcome this HGF-mediated resistance (150).

1.1.3.3 Histological Transformation

A fundamental change in histology from NSCLC to SCLC is observed in patients with EGFR- and ALK-driven NSCLC resistant to EGFR and ALK TKIs, respectively (**Figure 4**) (141). In *EGFR* mutant NSCLC, this histological switch is observed in approximately 5-15% of patients resistant to 1st generation EGFR TKIs (152). Importantly, this transformation to SCLC has been observed following resistance to the 3rd generation TKI, osimertinib, which is currently the first-line treatment for patients with *EGFR* mutations (136). While histological transformation is more frequently observed in resistance to EGFR TKIs, it has also been identified as mechanism of resistance to ALK TKIs in NSCLC patients with *ALK* translocations (153,154). Mechanistic investigation into this histological change has revealed that these tumors both clinically and genetically resemble neuroendocrine SCLC. Clinically, these tumors grow rapidly, respond initially to chemotherapy, and invariably develop chemoresistance. Genetically, these tumors universally have genetic loss of *RBI*, which is a hallmark genetic event for patients with SCLC

(152). These tumors also have low or absent EGFR expression, potentially accounting for the fact that these tumors are no longer responsive to EGFR TKIs (152). Additionally, a hallmark of SCLC in pre-clinical studies is sensitivity to BCL-2 inhibition as approximately 65% of SCLC overexpress BCL-2 and a subset of these tumors are sensitive to BCL-2 inhibitors (155). Interestingly, *EGFR* mutant tumors that have undergone a switch to SCLC are sensitive to BCL-2 inhibition, providing a potential avenue to treat this mechanism of EGFR TKI resistance (152).

1.1.3.4 Epithelial-Mesenchymal Transition

Epithelial-mesenchymal transition (EMT) is a process in which epithelial cells transdifferentiate and adopt a mesenchymal phenotype (156,157). EMT results in loss of epithelial cell polarity and cell-cell interactions (156,157). In the setting of tumorigenesis, EMT is associated with cell invasion, migration, and metastasis (156,157). EMT can also lead to suppression of apoptosis and senescence (156,157). Interestingly, the presence of an EMT or mesenchymal phenotype has been observed in patients with acquired and *de-novo* resistance to targeted therapies in EGFR- and ALK-driven NSCLC (**Figure 4**) (75,100,158-161). In the acquired resistance setting, EMT, defined by morphology and changes in E-cadherin, Vimentin, or AXL expression, is seen in as many as 20% of patients resistant to EGFR TKIs and 40% of patients resistant to ALK TKIs (100,161). The mechanisms by which an EMT phenotype is associated with resistance to targeted therapies remains unclear. Previous studies have demonstrated that expression of EMT-transcription factors, ZEB1 and SNAI2, can lead to EGFR TKI resistance by suppressing EGFR TKI-induced apoptosis (160,162-164). Additionally, increased expression of AXL, SRC, TGF- β and IGF1R have been shown to lead to EMT and mediate resistance to TKIs in lung cancer (90,161,165-167). In *EGFR* mutant NSCLC, there are numerous clinical trials investigating if targeting these aforementioned upstream mediators of EMT can overcome *de-novo* and acquired

resistance to EGFR TKIs, however, EMT-transcription factors have not been targeted to date (141).

1.2 APOPTOSIS AND CANCER

Apoptosis is a form of programmed cell death that plays a pivotal role in development and homeostasis by removing unneeded or damaged cells (168,169). Apoptosis occurs in response to extracellular or intracellular stress signals that leads to cellular shrinkage, condensation of chromatin, fragmentation of DNA, plasma membrane blebbing, and formation of apoptotic bodies which are small vesicles that are subsequently engulfed by neighboring phagocytes (168,169). Unlike other forms of programmed cell death, apoptosis is unique in that it does not result in an inflammatory response (168).

There are two main pathways of apoptosis: intrinsic and extrinsic apoptosis. Mitochondrial or intrinsic apoptosis is activated in response to internal cell stress signaling, while the extrinsic apoptotic pathway is activated in response to death receptor signaling. The cellular mediators of apoptosis are caspases (cysteine aspartic-specific proteases). There are two forms of caspases: “initiator” and “executioner” caspases. In response to stress signals, initiator caspases (caspase-2, -8, -9, and -10) cleave and activate executioner caspases (caspase-3 or -7), which when activated cleaved a variety of cellular substrates such as cytoskeletal and nuclear proteins (170). Interestingly, aberrations in these apoptotic pathways and proteins within these pathways are an almost universal feature in cancers. The ability to suppress apoptosis in the presence of cellular stresses is a “hallmark of cancer” and the goal of most systemic therapies is to overcome this suppression of apoptosis (170,171).

1.2.1 Apoptotic pathways

Intrinsic apoptosis is a form of apoptosis that occurs in response to internal cellular stresses such as DNA damage, hypoxia, metabolic stress, withdrawal of growth factors, replicative stress, and microtubular/mitotic defects (169,170). The initiating step of intrinsic apoptosis is mitochondrial outer membrane permeabilization (MOMP). Members of the BCL-2 family of proteins regulate this fundamental step of intrinsic apoptosis (172). In response to apoptotic signals, BAX and BAK, which are pro-apoptotic effectors of the BCL-2 family of proteins, induce MOMP by oligomerizing and forming pores on the outer mitochondrial membrane. Anti-apoptotic members of the BCL-2 family, such as BCL-2, BCL-xL, MCL-1, and BCL-W, antagonize the function of BAX/BAK by directly binding to BAX/BAK and preventing their oligimerization (168). Anti-apoptotic BCL-2 family members are counteracted by pro-apoptotic BCL-2 family members, such as BIM, PUMA, BAD, which complex with anti-apoptotic BCL-2 proteins and free BAX/BAK (168). Pro-apoptotic members, such as BIM, BID, and PUMA, can also directly activate BAX/BAK and promote their oligimerization (169).

Once a pore is formed by BAX/BAK on the outer mitochondrial membrane, cytochrome c and second mitochondria-derived activator of caspases (SMAC) are released from the mitochondria into the cytosol. Once in the cytosol, cytochrome c complexes with adaptor protein apoptotic protease-activating factor 1 (APAF-1), procaspase-9, and ATP (172). This complex, referred to as the apoptosome, results in activation of caspase-9 (172). Activated caspase-9 then subsequently cleaves and activates the executioner caspases-3/7. In addition, upon release from the mitochondria SMAC promotes apoptosis by inhibiting X-linked inhibitor of apoptosis protein (XIAP), which is an inhibitor of caspase-3, -7, and -9.

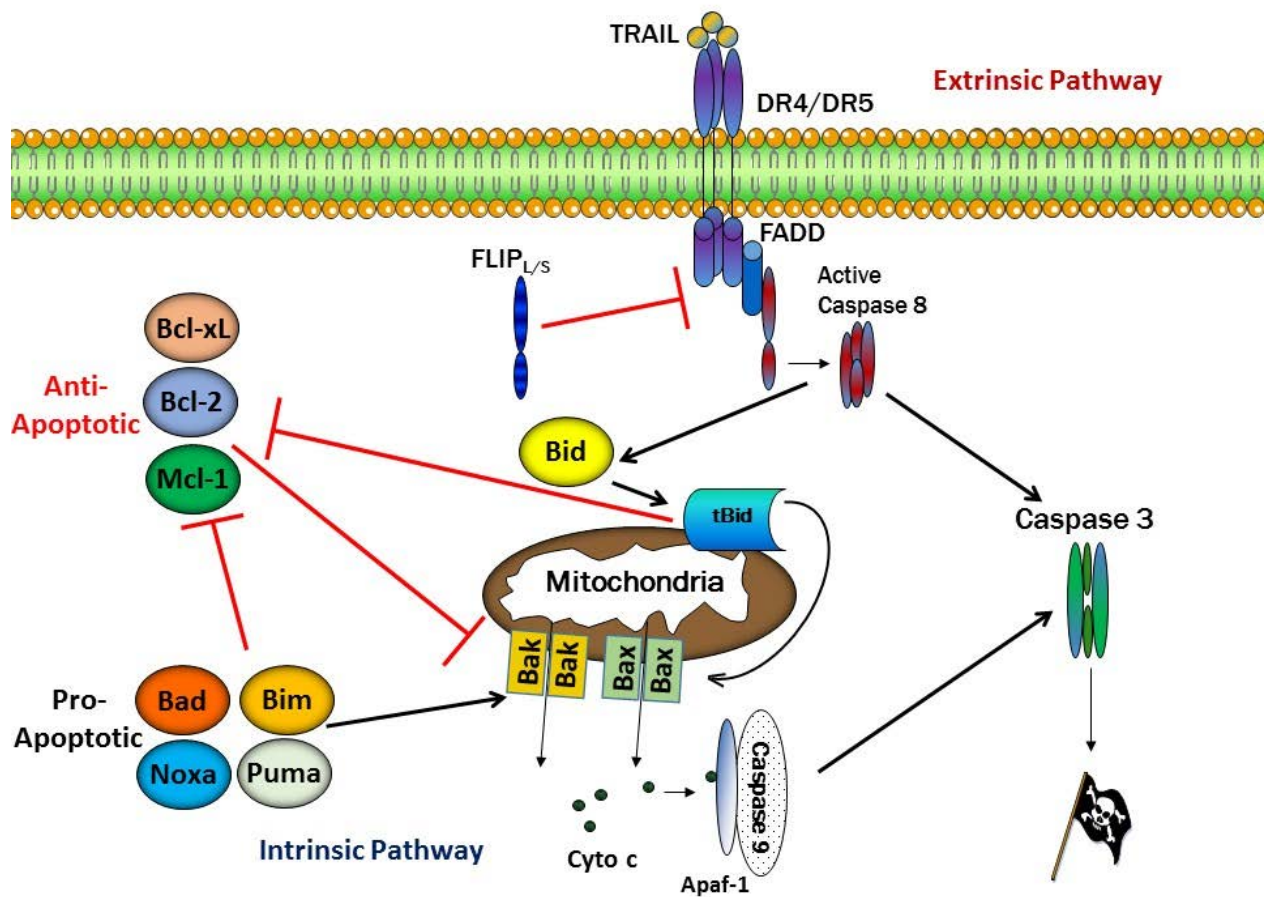


Figure 5: Intrinsic and extrinsic apoptotic pathways

Intrinsic or mitochondrial-mediated apoptosis is mediated by BAX/BAK oligomerization at the outer mitochondrial membrane (OMM). BAX/BAK form a pore on the OMM, which leads to cytochrome c release and subsequent caspase-9 activation. Caspase-9 then activates “executioner” caspases-3/7 which cleave a variety of cellular substrates that ultimately induce apoptosis. BAX/BAK activation is modulated by expression of anti-apoptotic and pro-apoptotic BCL-2 family members. During extrinsic apoptosis, death ligands bind to corresponding death receptors, which results in death receptor trimerization and recruitment of caspase-8. Once bound to death receptors in a complex called the DISC, caspase-8 is activated and subsequently activates downstream executioner caspases-3/7. Additionally, caspase-8 can activate intrinsic apoptotic by cleaving BID, which can translocate to the mitochondria and directly activate BAX/BAK and/or inhibit anti-apoptotic BCL-2 proteins. Extrinsic apoptosis is antagonized by cFLIP which is a negative regulator of caspase-8 activation at the DISC.

Extrinsic apoptosis is a form of apoptosis that involves activation of death receptors (TNFR1, FAS, DR4/5) via binding of cognate death ligands (FASL, TNF- α , TRAIL). Following binding death ligands, death receptors trimerize, which allows for formation of the essential mediator of extrinsic apoptosis, the death-inducing signaling complex (DISC) (173). At the DISC, Fas associated via death domain (FADD) binds to the trimerized death receptor via homotypic interactions between death domain (DD) regions of both proteins. Once bound to a death receptor, FADD undergoes a conformational change which exposes its death effector domain (DED). Procaspase-8 has two DED on its N-terminus. DED1 of procaspase-8 binds to the DED of TRADD, while DED2 of procaspase-8 interactions with DED1 of another procaspase-8 molecule (173-175). This DED interaction between procaspase-8 molecules results in oligomerization and procaspase-8 filament formation. After approximately six procaspase-8 molecules form a filament, procaspase-8 undergoes autoproteolytic cleavage, which results in activation of caspase-8 (173,175). In type I cells, activation of caspase-8 is sufficient to activate executioner caspases-3/7 and induce apoptosis. In type II cells, the presence of XIAP prevents caspase-8 from inducing apoptosis. In these cells in order to induce apoptosis, caspase-8 must cleave and activate the pro-apoptotic BCL-2 protein, BID, which results in BID translocation to the mitochondria and activation of mitochondria-mediated apoptosis.

FLICE-like inhibitory protein (cFLIP) is the major modulator of extrinsic apoptosis. There are two functional isoforms of cFLIP: cFLIP short (cFLIP_s) and cFLIP long (cFLIP_L). cFLIP_s is a truncated form of procaspase-8, which contains two DEDs and a truncated C-terminal domain (173). The short isoform of cFLIP blocks extrinsic apoptosis by blocking procaspase-8 filament formation (173). cFLIP_L resembles full length procaspase-8, however, lacks autocatalytic function of procaspase-8. Interestingly, the function of cFLIP_L is complex, as the

levels of cFLIP_L determine its regulation of apoptosis. At low levels, cFLIP_L promotes apoptosis by enhancing caspase-8 activation at the DISC, while at high levels cFLIP_L inhibits apoptosis by reducing procaspase-8 activity at the DISC (173). The exact mechanism by which cFLIP_L has these dichotomous function is not understood. The current paradigm is that at low levels, cFLIP_L heterodimerizes with procaspase-8 and promotes its activation, while at higher levels, cFLIP_L blocks procaspase-8 filament formation (173).

1.2.2 Aberrations in apoptotic pathways and proteins in cancer

Evasion of apoptosis despite high levels of both internal and external stress signaling is a hallmark of malignant cells (171). The main mechanisms by which cancer cells evade apoptosis is via modulating expression of apoptotic proteins within both the intrinsic and extrinsic pathway. Within the intrinsic apoptotic pathway, cancer cells evade apoptosis by increasing the expression of anti-apoptotic BCL-2 family proteins. Approximately one half of all hematological and solid malignancies, including lung cancers, overexpress BCL-2 (176). Additionally, many solid tumors, including lung and breast cancers, have gene amplification of *BCL-xL* or *MCL-1* (172). Increased expression of these proteins anti-apoptotic BCL-2 family members is associated with therapeutic resistance, poor prognosis, and tumor recurrence (172).

Another strategy employed by cancer cells to evade apoptosis is to decrease the expression of pro-apoptotic BCL-2 family members. One of the main mechanism by which cancer cells decrease pro-apoptotic protein expression is via genetic loss or mutation of *TP53*, which occurs in approximately 50% of cancers (172). Numerous pro-apoptotic genes, including *BAX*, *PUMA*, *NOXA*, and *APAF-1*, are upregulated by p53 (172). Subsequently, loss of p53 increases the threshold for mitochondrial mediated-apoptosis (172). Pro-apoptotic BCL-2

proteins are also subject to post-translational regulation. In cancers, these proteins are frequently phosphorylated and/or ubiquitinated which results in their inactivation and/or degradation. An example of this post-translational regulation of pro-apoptotic BCL-2 proteins is extracellular signal-regulated kinase (ERK)-mediated phosphorylation of BIM. This phosphorylation event leads to downregulation of BIM expression by increasing its ubiquitination and proteasomal degradation (172,177).

In addition to evading mitochondrial-mediated cell death, cancer cells frequently suppress death receptor signaling. One common mechanism that cancers evade extrinsic apoptosis is via mutations in death receptors. Several malignancies, including NSCLC, have mutations the death domains of *FAS* and *DR5*, which results in an impaired ability to activate caspase-8 at the DISC (178). Additionally, decoy death receptors are frequently overexpressed and/or amplified in cancers (178,179). These decoy receptors share homology with functional death receptors but typically lack a functional death domain, which allows decoy receptors to bind ligand without activating caspase-8 (180). The ability of cancer cells to undergo extrinsic apoptosis is influenced by the relative expression of functional death receptor versus decoy receptor.

The main regulator of death receptor signaling, cFLIP, is frequently overexpressed in solid tumors and v-FLIP_s serves as a viral oncogene in herpesviruses (179,181). cFLIP overexpression, both cFLIP_s and cFLIP_L, is associated with resistance to TRAIL-based therapies and chemotherapy as well as poor clinical prognosis (179,182-184). Another important mechanism by which cancers evade extrinsic apoptosis is via mutations in caspase-8 and epigenetic silencing of caspase-8 (179). Mutations in caspase-8 have been shown to not only

suppress death receptor-mediated cell death but can also confer therapeutic resistance and enhance tumorigenesis (185).

1.2.3 Apoptosis and response to targeted therapy in lung cancer

Apoptosis has been shown to be the main mechanism by which targeted therapies lead to tumor regression. (186). Robust apoptotic responses to targeted therapies have been linked to improved clinical outcomes (186). The main mediator of apoptosis in response to targeted therapies in oncogene-driven NSCLC, including *MET* amplified, *EGFR* mutant, and *EML4-ALK* positive NSCLC, and other oncogene-driven cancers is the pro-apoptotic protein, BIM (186-191). Previous studies have demonstrated that BIM expression predicts response to targeted therapies in *EGFR* mutant NSCLC and *HER* amplified breast cancers (186). Additionally, those *EGFR* mutant NSCLC patients with high levels of *BCL2L1* (gene encoding BIM) mRNA expression have increased response rates and PFS (186). Interestingly, a subset of patients have a polymorphism in the *BCL2L1* gene, which results in preferential splicing of exon 3 over exon 4, which contains the functional BH-3 domain (192). This splicing results in increased expression of a non-functional BIM protein (192). The *BCL2L1* polymorphism has been associated with decreased response, decreased PFS, and *de-novo* resistance to EGFR and ALK TKIs in *EGFR* mutant and ALK-driven NSCLC (**Figure 4**) (135,192,193).

Other BCL2- family members have been implicated in response to targeted therapies. The pro-apoptotic protein, PUMA, has been shown to be required for apoptotic responses to targeted therapies in oncogene-driven NSCLC and breast cancer (194). A previous study has demonstrated an impaired response to erlotinib in a *Puma* deficient mouse model of *Egfr* mutant NSCLC (194). Additionally, the anti-apoptotic protein, MCL-1, has been implicated in resistance

to targeted therapies in NSCLC. Previous studies have demonstrated that the EGFR TKIs, erlotinib and osimertinib, require MCL-1 degradation in order to induce apoptosis (191,195). Impaired MCL-1 degradation in these models is associated with resistance to EGFR TKIs (191,195).

1.3 TWIST1

TWIST1 is a basic-helix-loop-helix (bHLH) transcription factor that binds to canonical E-box response elements and regulates the expression of numerous target genes (196-198). Depending on the target gene, TWIST1 can activate gene transcription via recruiting coactivators such as p300 or inhibit gene transcription via inhibiting acetyl-transferases or recruiting histone deacetylases (198,199). TWIST1 expression is essential for proper development and organogenesis. As TWIST1 is rarely expressed post-natally, its physiological function in adults is not well understood (200,201). However, TWIST1 expression is frequently reactivated in cancers. TWIST1 promotes tumorigenesis by inducing EMT, invasion, and metastasis. Additionally, TWIST1 overexpression can lead to suppression of the failsafe programs of senescence and apoptosis. Given its pleotropic role in cancer and its restricted expression post-natally, TWIST1 is a potential therapeutic target in cancer.

1.3.1 TWIST1 and development

Twist1 was first identified in *Drosophila* as a gene required for ventral furrow development (198,202). During *Drosophila* development, *Twist1* is highly expressed in cells of the mesoderm

in early development and is essential for mesodermal specification and differentiation into distinct tissue types (203). Lack of Twist1 expression in *Drosophila* results in abnormal development (lack of a mesoderm and abnormal gastrulation) and death before completion of embryogenesis (203,204).

Similar to its function in *Drosophila*, Twist1 expression is essential for mesodermal-derived tissue differentiation in mice. Unlike *Drosophila* lacking *Twist1* expression, *Twist1*^{-/-} mice undergo normal gastrulation, but die at E10.5-11 due to lack of closure of the neural tube and marked defects in the cranial mesoderm, branchial arches, facial primordium, and limb bud (198). These defects suggest that Twist1 in vertebrates functions after mesodermal specification but remains important for mesodermal differentiation (198). Importantly, Twist1 is not required postnatally as mice with conditional *Twist1* knockout postnatally do not exhibit a phenotype (205).

Interestingly, TWIST1 can form both homodimers and heterodimers with the E2A proteins or HAND2. During development, Twist1 homodimers display distinct functions and often antagonist functions when compared to Twist1 heterodimers (198,206,207). The levels of Twist1 homodimers versus heterodimers are critically important in proper limb development and cranial suture formation and closure (198,206,207). The formation of Twist1 homodimers versus heterodimers is determined by the expression levels of other bHLH transcription factors and inhibitor helix loop helix proteins, such as the Id proteins (208). For example, expression of Id proteins, which resemble bHLH transcription factors without a functional DNA binding domain, promotes formation of Twist1 homodimers as the Id proteins avidly bind and sequester the E2A proteins (208). In addition, phosphorylation of Twist1 can influence the composition of Twist1 dimers (208). Specially, phosphorylation of Twist1 at threonine 125 and serine 127 favors the

formation of Twist1 homodimers and reduces formation of Twist1-E2A and Twist1-Hand2 heterodimers (208,209).

Twist1 haploinsufficiency in mice does not result in lethality, however, results in marked craniofacial abnormalities and polydactyl (198). In humans, *TWIST1* mutations lead to Saethre-Chotzen syndrome, which is characterized by craniofacial and limb defects similar to those found in *Twist1* haploinsufficient mice (198). Twist1 expression maintains chondrocyte and osteoblasts in an immature state. *Twist1* haploinsufficiency in mice or *TWIST1* mutations in humans results in premature osteoblastic differentiation and close of sutures (198). This premature osteoblastic differentiation has also been tied to alterations in Twist1 homodimer and Twist1-E2A heterodimer formation (198).

1.3.2 Regulation of TWIST1 expression

TWIST1 expression in adult humans is restricted to precursor cells in mesodermal tissues such as the heart, skeletal muscle, and placental (198,210). While the physiological role of TWIST1 in adult humans is not well understood, previous studies have demonstrated that TWIST1 is expressed in white and brown adipose tissue and may play a role in adaptive thermogenesis and energy homeostasis (198,200). As mentioned in Section 1.3, TWIST1 is frequently overexpressed in cancers including carcinomas, sarcomas, melanomas, and neuroblastomas (198). While TWIST1 overexpression via gene amplification is seen in approximately 20% of osteosarcomas, in most cancers it is likely that TWIST1 overexpression is the result of a confluence of aberrations in multiple signaling pathways (211,212). In both physiologic and pathologic settings, TWIST1 is regulated both at the transcriptional and post-transcriptional levels.

1.3.2.1 Transcriptional control of *TWIST1*

TWIST1 is regulated on the transcriptional level by a number of different signaling pathways and transcription factors. These pathways play a role in both the physiologic and pathologic transcriptional regulation of *TWIST1*. Firstly, previous studies have demonstrated that in the setting of hypoxia and HIF-1 α stabilization, *TWIST1* levels are increased (198). HIF-1 α was found to upregulate *TWIST1* transcription by directly binding to a hypoxia-response element in the *TWIST1* promoter region (198). STAT3 has also been shown to directly upregulate *TWIST1* transcription via direct binding of the *TWIST1* promoter (213,214). Interestingly, a previous study has demonstrated that in addition to direct upregulation of *TWIST1*, STAT3 can indirectly upregulate *TWIST1* mRNA via increasing HIF-1 α stabilization (215). Furthermore, *TWIST1* has been identified as direct target gene of NF-KB (213). In the setting of inflammation, specifically TNF- α -mediated inflammation, *TWIST1* expression is induced in a NF-KB-dependent manner (213,216). However, *TWIST1* has anti-inflammatory effects as it negatively regulates NF-KB activity by directly binding to RelA and inhibiting its ability to activate pro-inflammatory target genes (213,217). Lastly, the RAS and TGF- β signaling pathways have been shown to directly upregulate *TWIST1* expression via upregulation of the downstream transcription factors, Msh homeobox protein (MSX2) and high mobility group A2 (HMGA2), respectively (213,218,219). Interestingly, the promoter of *TWIST1* has been found to be highly methylated in some cancers. However, numerous studies have demonstrated that *TWIST1* promoter methylation does not correlate with *TWIST1* mRNA or protein expression (198,220,221).

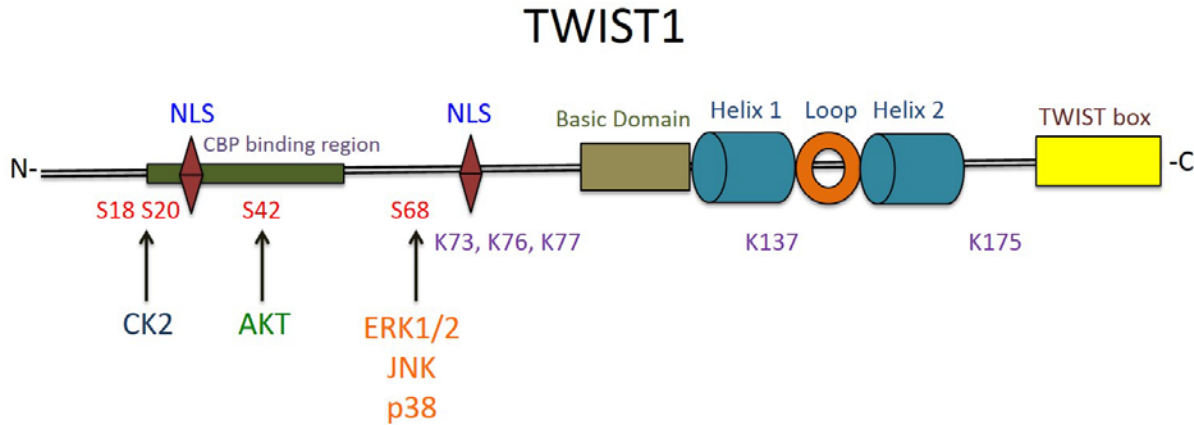


Figure 6: Illustration of the TWIST1 protein and key domains

TWIST1 function and stability is regulated by multiple post-translational modifications such as phosphorylation, ubiquitination, and acetylation. TWIST1 is phosphorylated by casein kinase 2 (CK2), AKT, and MAPKs (ERK1/2, JNK, and p38) at key residues (red) that regulate both TWIST1 function and stability. The TWIST1 box region is required not only for TWIST1 target gene regulation and interaction with other proteins such as p53 but also TWIST1 polyubiquitination and proteasomal degradation. TWIST1 is also regulated by polyubiquitination and acetylation at certain lysine residues (purple). K175, K137, K77, K76, and K73 have all been implicated in TWIST1 polyubiquitination, while K76 and K73 are acetylated. NLS=Nuclear Localization Signal, CBP=CREB binding protein.

1.3.2.2 Post-transcriptional control of TWIST1

Post-transcriptional control of TWIST1 is critically important for regulation of TWIST1 expression and function. One of the main post-translational modifications that effects TWIST1 expression and function is phosphorylation. Previous studies have demonstrated that multiple mitogen activated protein kinases (MAPKs), including p38, c-Jun N-terminal kinase (JNK), and extracellular signal-regulated kinase (ERK) can increase TWIST1 protein accumulation (203,213). MAPKs phosphorylate TWIST1 on serine 68 (S68), which increases TWIST1 by preventing TWIST1 ubiquitination and proteasomal degradation (**Figure 6**) (203,213). This phosphorylation event is required for TWIST1-mediated invasion and EMT in the setting of RAS activation and TGF- β /TGF- β receptor signaling (203,213). Similarly, casein kinase 2 (CK2) phosphorylation of TWIST1 on serine 18 and 20 results in increased protein stability and increased TWIST1-mediated motility (**Figure 6**) (213). Additionally, TWIST1 is phosphorylated

on serine 42 (S42) by AKT/protein kinase B (PKB) (**Figure 6**) (222). This phosphorylation event has been shown to be required for TWIST1-mediated metastasis in breast cancer models (222). Interestingly, studies have demonstrated that different isoforms of AKT have differential effects on TWIST1 stability and activity (213,223). AKT1 specifically has been shown to negatively regulate TWIST1 expression and EMT. AKT1/PKB phosphorylates TWIST1 on S42, T121, and S123, resulting in increased TrCP- β -mediated ubiquitination and proteasomal degradation of TWIST1 (**Figure 6**) (213,223). However, these negative regulatory effects are not seen with AKT2/3 (213,223). Beyond TrCP- β , additional other E3 ligases, such as F-box and leucine-rich repeat protein 14 (FBXL14), have been shown to negatively regulate TWIST1 expression (224). A previous study demonstrated the small molecule imipramine blue, can decrease TWIST1 expression by increasing FBXL14-mediated poly-ubiquitination of TWIST1 (224).

Specific domains of TWIST1 have been implicated in polyubiquitination and proteasomal degradation of TWIST1. The TWIST1 box is a domain of TWIST1 essential for its function in development and tumorigenesis, as it is required for target gene regulation and binding of other transcription factors such as Runx2 and p53 (**Figure 6**) (225-227). Despite the absence of lysines in the TWIST1 box, it is required for polyubiquitination and degradation of TWIST1 (228,229). Outside of the TWIST1 box, lysine 175 (K175) has been shown to be essential for TWIST1 polyubiquitination, as point mutations in *K175* increase TWIST1 stability and inhibit ubiquitination (**Figure 6**) (228). Other lysines such K73, 76, 77, and K137 have been implicated in polyubiquitination and stability of TWIST1 (**Figure 6**) (228).

A previous report has demonstrated that TWIST1 acetylation may be required for target gene induction. In basal-like breast cancer (BLBC), Tip60-mediated diacetylation of TWIST1 at lysines 73 and 76 was required for induction of *WNT5A* (**Figure 6**) (213,230). Diacetylated

TWIST1 binds to the bromodomain and extra terminal domain (BET) family member, BRD4 (213,230). The TWIST1-BRD4 complex binds to acetylated histones and subsequently recruits P-TEFb/RNA-POL II to the promoter of *WNT5A* (213,230). Disruption of TWIST1 acetylation in BLBC prevents *WNT5A* activation and suppresses EMT and invasion (213,230).

Independent of its post-translational modification, one of the most important factors in determining TWIST1 stability is expression of the helix-loop-helix ID proteins, which lack the ability to bind DNA but can avidly bind and sequester the E2A proteins, E12/47 (198,203). Studies have demonstrated that the TWIST1-E2A heterodimer is more stable than the TWIST1-TWIST1 homodimer (231). Increased expression of ID proteins can result in decreased TWIST1 stability by promoting TWIST1 homodimerization (231,232). In addition to the difference in stability between TWIST1 homo- and heterodimer, the different TWIST1 dimers induce distinct transcriptional target genes and distinct phenotypes (198,203).

1.3.3 TWIST1 and cancer

TWIST1 is overexpressed in a variety of cancers including breast, colon, pancreatic, prostate, head and neck, melanoma, and lung cancers (198). Overexpression of TWIST1 is associated with aggressive, high grade cancers, increased risk of metastasis, tumor recurrence and poor patient prognosis (213). We and others have demonstrated that TWIST1 is overexpressed in a significant fraction of NSCLC (198,233). Given its role as a pleiotropic gene regulator, TWIST1 mediates multiple phenotypes that promote tumorigenesis such as EMT, metastasis, and cancer stemness (198,213). Independent of its ability to induce EMT, TWIST1 also suppresses the failsafe programs of oncogene-induced senescence and apoptosis, a critical step in tumor progression

(234). In addition to promoting tumorigenesis, TWIST1 overexpression confers chemoresistance in many cancer types (213).

1.3.3.1 EMT

As mentioned in Section 1.1.3.3, EMT is a transdifferentiation process in which epithelial cells adopt a mesenchymal phenotype, loose cell-cell contacts, and polarity (156,157). Additionally, EMT is associated with invasion, migration, and cancer cell metastasis (156,157). As a EMT-transcription factor, TWIST1 activates a transcriptional network that leads to EMT changes. Previous studies have demonstrated that E-cadherin is a main mediator of epithelial cell phenotype and loss of E-cadherin expression is a pivotal event in the process of EMT (156,157). One mechanism by which TWIST1 induces EMT is via direct repression of E-cadherin expression (213,235). TWIST1 directly binds to E-boxes in the promoter of *CDH1* (E-cadherin gene) and represses transcriptional activity (213,235). TWIST1 can also indirectly inhibit E-cadherin expression by directly upregulating other EMT-transcription factors that repress *CDH1* promoter activity, such as SNAI2 (236). Additionally, TWIST1 has been shown to upregulate mesenchymal genes such as *CDH2* (gene encoding N-cadherin) (237). TWIST1 binds to an E-box in the *CDH2* promoter and increases mRNA *CDH2* expression (237).

Numerous studies have demonstrated that TWIST1-induced EMT is associated with its ability to promote metastasis. An early study investigating the role of Twist1 and metastasis demonstrated that expression of Twist1 decreased E-cadherin expression, increased expression of mesenchymal genes, and increased breast cancer cell motility (238). While knockout of *Twist1* in breast cancer cells suppressed their ability to form lung metastasis without affecting primary tumor growth (238). Additional studies in lung and head and neck cancers, demonstrated that knockdown of TWIST1 reversed EMT and suppressed metastasis (239). In patients,

TWIST1 expression is associated with EMT and distant metastasis (213). The pro-metastatic function of TWIST1 may be connected with its ability to promote invadopodia formation, migration, and invasion (213). Additionally, TWIST1-induced EMT is associated with acquisition of stem-cell like properties in cancer cells. TWIST1 confers stem-cell like properties by directly upregulating BMI-1, a polycomb-group protein that promotes EMT and stemness (213,240). However, other studies have demonstrated that TWIST1 expression can confer stem-cell like properties independently of EMT (213). Additional studies are needed to determine whether TWIST1-induced EMT is required for TWIST1-mediated phenotypes or is simply a marker of TWIST1 expression.

1.3.3.2 Apoptosis

TWIST1 was initially identified as an oncogene that could suppress MYC-induced apoptosis (198,241). One main mechanism by which TWIST1 suppresses apoptosis is via direct and indirect inhibition of p53. Initial studies revealed that the N-terminus of TWIST1 can directly bind to the C-terminus of p53 (227,242). This interaction inhibits not only p53 DNA binding but also key post-translational modifications of p53 important for p53 stability (227). TWIST1 expression also enhances MDM2-mediated degradation of p53 (227,242). Interestingly, the p53-TWIST1 interaction inhibits both proteins from activating known target genes (242). Other studies suggest that TWIST1 can inhibit p53 through indirect mechanisms. TWIST1 can suppress transcription of *TP53*, by directly binding and inhibiting a p53 transactivator, HOXA5 (213,243). TWIST1 also decreases transcription of *TP53* by downregulation of a p53-activator, p14^{ARF} (213,244). Additionally, TWIST1 can decrease p53 access to target genes by binding and inactivating histone acetyltransferase p300, which is required for opening of chromatin at p53

target genes (245). These mechanisms of indirect inhibition of p53 have been linked to the ability of TWIST1 to suppress DNA damage-induced apoptosis (246).

TWIST1 can also suppress apoptosis independent of p53. One p53-independent mechanism includes TWIST1 modulating the expression of BCL-2 family members. In NSCLC cell lines, inhibition of TWIST1 results in decreased MCL-1 protein expression (247). Additionally, TWIST1 expression can also decrease BAX expression and increase the BCL-2/BAX ratio (198). In oncogene-driver defined NSCLC cell lines, we have demonstrated that inhibition of TWIST1 results in apoptosis in p53 mutant NSCLC cell lines, suggesting that TWIST1 suppresses apoptosis in NSCLC independently of p53 (234). However, the mechanism(s) by which TWIST1 suppresses apoptosis and modulates expression of BCL-2 family members remains poor elucidated.

1.3.3.3 Senescence

A known barrier to oncogenic transformation is the failsafe program of oncogene-induced senescence (OIS), which is a form of irreversible cell arrest characterized by a flattened and enlarged cell body, condensed chromatin, and senescence-associated β -galactosidase activity (234). Oncogenic activation in early lesions can result in OIS and in order to progress into malignant lesions, pre-malignant lesions must overcome OIS (234). Activation of the p53 and/or RB pathways can lead to induction of OIS. TWIST1 has been shown to inhibit OIS in many cancers including breast, prostate, and lung cancers (198). In breast cancers, TWIST1 expression suppresses OIS following RAS and ERBB2 activation (248,249). TWIST1 suppresses OIS in breast cancer by inhibiting transcriptional activation of p21^{WAF1} and p16^{INK4A} and in prostate cancer via inhibition of p14^{ARF} (244,249). In NSCLC, TWIST1 cooperates with mutant *Kras* in murine models of lung cancer by suppressing OIS (233). Genetic inhibition of *TWIST1* in

oncogene driver-defined NSCLC including those tumors with *KRAS* mutations, *MET* amplification/mutants, and *EGFR* mutations, results in OIS (234). Interestingly, in NSCLC, OIS following genetic silencing of *TWIST1* does not require p53 and/or RB expression, suggesting that *TWIST1* regulates additional mediators of OIS outside the p53 and Rb-pathway (234).

1.3.3.4 Therapeutic resistance

Systemic chemotherapies remain an important treatment modality for cancers, especially in the advanced setting. However, chemoresistance remains a major barrier to long-term efficacy of chemotherapy. *TWIST1* has been identified as a mediator of chemoresistance in solid tumors including lung, breast, and prostate cancers (213). Given its role as a pleiotropic gene regulator, *TWIST1* can mediate chemoresistance through a variety of mechanisms (198).

One mechanism by which *TWIST1* mediates chemoresistance is by increasing expression of transport proteins. *TWIST1* can confer multi-drug resistance (MDR) to chemotherapies by directly upregulating ATP binding cassette transporters (ABC transporters), which directly efflux a variety of chemotherapeutic agents (213,250,251). In colon cancer cells, *TWIST1* mediates chemoresistance by directly upregulating the expression of *ABCB1* and *ABCC1* (251). In breast cancer, *TWIST1* increases promoter activity and expression of *ABCC4* and *ABCC5* (250). *TWIST1* also mediates chemoresistance in breast, bladder, and colon cancers by upregulating the ABC transporter, P-glycoprotein (P-gp) (213). Multiple pre-clinical studies have demonstrated that targeting *TWIST1* can reverse MDR by decreasing the expression of ABC transporters (213).

Additional mechanisms of *TWIST1*-mediated chemoresistance involve increasing expression of proteins within oncogenic signaling pathways and/or modulating apoptotic

proteins. In breast cancer, TWIST1 overexpression confers paclitaxel resistance by increasing AKT2 expression (252). TWIST1 binds to E-box binding sites within the *AKT2* promoter and directly upregulates *AKT2* expression (252). In head and neck cancer, TWIST1 mediates chemoresistance by directly increasing Jagged1 expression and activating Notch signaling (253). Jagged1/Notch signaling increases KLF4 activity, which confers chemoresistance by inducing a stem-cell like phenotype (253). TWIST1 is also a key mediator of NF-KB-mediated chemoresistance in prostate cancer (254). NF-KB directly upregulates TWIST1 in response to chemotherapy (254). In prostate cancer cells, TWIST1 suppresses chemotherapy-induced apoptosis by suppressing inhibitory phosphorylation of BCL-2 (254).

TWIST1 has also been linked to chemoresistance to SCLC and NSCLC (213,255). In NSCLC, TWIST1 mediates cisplatin resistance through multiple mechanisms. Inhibition of TWIST1 in NSCLC cell lines resistant to cisplatin, restored cisplatin sensitivity by decreasing MCL-1 expression by increasing AMP-activated protein kinases (AMPK)-mediated inhibition of mTOR and ribosome protein S6 kinase 1 (S6K1) (247). Another study demonstrated that inhibition of TWIST1 increases cisplatin sensitivity via increasing the BCL-2/BAX ratio and mitochondrial-mediated apoptosis (198). Recent studies have demonstrated that EMT-transcription factors including ZEB1, SNAI2, and TWIST1 may lead to resistance to targeted therapies in *EGFR* mutant NSCLC (160,162-164). Overall, these previous studies suggest that TWIST1 may mediate therapeutic resistance to multiple modalities of systemic therapies in lung cancer.

2.0 IDENTIFICATION OF A FIRST-IN-CLASS TWIST1 INHIBITOR WITH ACTIVITY IN ONCOGENE-DRIVEN LUNG CANCER

2.1 ABSTRACT

TWIST1, an epithelial-mesenchymal transition (EMT) transcription factor, is critical for oncogene-driven non-small cell lung cancer (NSCLC) tumorigenesis. Given the potential of TWIST1 as a therapeutic target, a chemical-bioinformatic approach using connectivity mapping (CMAP) analysis was used to identify TWIST1 inhibitors. Characterization of the top ranked candidates from the unbiased screen revealed that harmine, a harmala alkaloid, inhibited multiple TWIST1 functions including single-cell dissemination, suppression of normal branching in 3D epithelial culture, and proliferation of oncogene driver-defined NSCLC cells. Harmine treatment phenocopied genetic loss of *TWIST1* by inducing oncogene-induced senescence or apoptosis. Mechanistic investigation revealed that harmine targeted the TWIST1 pathway through its promotion of TWIST1 protein degradation. As dimerization is critical for TWIST1 function and stability, the effect of harmine on specific TWIST1 dimers was examined. TWIST1 and its dimer partners, the E2A proteins, which were found to be required for TWIST1-mediated functions, regulated the stability of the other heterodimeric partner post-translationally. Harmine preferentially promoted degradation of the TWIST1-E2A heterodimer compared to the TWIST1-TWIST1 homodimer and targeting the TWIST1-E2A heterodimer was required for harmine

cytotoxicity. Finally, harmine had activity in both transgenic and patient-derived xenograft (PDX) mouse models of *KRAS* mutant NSCLC. These studies identified harmine as a first-in-class TWIST1 inhibitor with marked antitumor activity in oncogene-driven NSCLC including *EGFR* mutant, *KRAS* mutant and *MET* altered NSCLC.

IMPLICATIONS: TWIST1 is required for oncogene-driven NSCLC tumorigenesis and EMT, thus harmine and its analogues/derivatives represent a novel therapeutic strategy to treat oncogene-driven NSCLC as well as other solid tumor malignancies.

Contributors to study: Zachary A. Yochum, ^{1-2*}, Jessica Cades, ^{3-5*}, Lucia Mazzacurati, ², Neil M. Neumann, ⁶, Susheel K. Khetarpal, ², Suman Chatterjee,², Hailun Wang,⁴, Myriam A. Attar, ², Eric H.-B. Huang, ², Sarah N. Chatley, ^{2#}, Katriana Nugent, ⁴, Ashwin Somasundaram, ², Johnathan A. Engh, ⁷, Andrew J. Ewald,⁶, Yoon-Jae Cho, ⁸, Charles M. Rudin, ⁹, Phuoc T. Tran,^{4-5, 10}, Timothy F. Burns¹⁻²

¹Department of Pharmacology and Chemical Biology, University of Pittsburgh, Pittsburgh, PA

²Department of Medicine, Division of Hematology-Oncology, University of Pittsburgh Cancer Institute, Pittsburgh, PA.

³Department of Pharmacology, Sidney Kimmel Comprehensive Cancer Center, Johns Hopkins University School of Medicine, Baltimore, MD.

⁴Department of Radiation Oncology and Molecular Radiation Sciences, Sidney Kimmel Comprehensive Cancer Center, Johns Hopkins University School of Medicine, Baltimore, MD, USA

⁵Department of Oncology, Sidney Kimmel Comprehensive Cancer Center, Johns Hopkins University School of Medicine, Baltimore, MD, USA

⁶Department of Cell Biology, Center for Cell Dynamics, Johns Hopkins University School of Medicine, Baltimore, MD.

⁷Department of Neurological Surgery University of Pittsburgh Medical Center, Pittsburgh, PA

⁸ Division of Pediatric Neurology, Oregon Health & Science University, Portland, OR.

⁹Department of Medicine, Thoracic Oncology Service, Memorial Sloan Kettering Cancer Center, New York, NY.

¹⁰Department of Urology, Johns Hopkins University School of Medicine, Baltimore, MD

This work is published in Molecular Cancer Research:

Yochum ZA*, Cades J*, Mazzacurati L, Neumann NM, Khetarpal SK, Chatterjee S, Wang H, Attar MA, Huang EH, Chatley SN, Nugent K, Somasundaram A, Engh JA, Ewald AJ, Cho YJ, Rudin CM, Tran PT, Burns TF. A First-in-Class TWIST1 Inhibitor with Activity in Oncogene-Driven Lung Cancer. *Mol Cancer Res.* 2017;15(12):1764-76. doi: 10.1158/1541-7786.MCR-17-0298. PubMed PMID: 28851812; PMCID: PMC5712248.

* -- denotes these authors contributed equally to the work

2.2 INTRODUCTION

As the leading cause of cancer deaths in the U.S. and worldwide, lung cancer remains a major public health problem. Recent advances in classifying non-small cell lung cancer (NSCLC) into molecularly-defined subgroups that respond to targeted therapies have shifted the treatment paradigm in NSCLC from standard chemotherapy to a personalized therapeutic approach. While initial response rates to these targeted therapies are high, resistance is all but inevitable (75,94,256). Additionally, patients with the most frequent molecular driver, mutant *KRAS*, lack effective targeted therapies (257). New strategies are needed to effectively and durably target oncogene-driven NSCLC.

Epithelial-mesenchymal transition (EMT) is a reversible biological process that allows for the transdifferentiation of epithelial cells to adopt a mesenchymal phenotype, resulting in an increase in motility and a loss of epithelial polarity (156). EMT-transcription factors (EMT-TF) such as the TWIST, SNAIL and ZEB proteins are drivers of the EMT transcriptional program. Expression of EMT-TFs and subsequent induction of EMT is associated with invasion, dissemination, metastasis, suppression of oncogene-induced senescence (OIS) and apoptosis, and promotion of a cancer stem cell phenotype (156,258). Additionally, induction of EMT and expression of EMT-TF have also been implicated in resistance to chemotherapy, radiation and targeted therapies (75,259,260). Developing molecules that can effectively inhibit the activity of EMT-TFs would have significant therapeutic implications given the diverse role of EMT-TFs in tumorigenesis, metastasis and therapeutic resistance.

We previously demonstrated that TWIST1 is required for tumorigenesis in NSCLC characterized by defined oncogenic drivers including *KRAS* mutant, *EGFR* mutant and *MET* amplified/mutant tumors (233,234). We have also demonstrated that Twist1 cooperates with mutant *Kras* to induce lung adenocarcinoma *in vivo* and that suppression of Twist1 expression can lead to OIS and oncogene-induced apoptosis (OIA) (233,234). TWIST1 has been shown to promote tumorigenesis in breast and prostate carcinomas through induction of EMT, invasion, and metastasis as well as suppression of OIS and apoptosis (214,238,239,249,252,254,261). While TWIST1 has been implicated in tumorigenesis through its ability to promote EMT and metastasis, we have demonstrated that TWIST1 in oncogene-driven NSCLC functions to primarily suppress OIS and OIA (233,234). Taken together, data from these previous studies suggests that pharmacological inhibition of TWIST1 may be a valuable therapeutic strategy across multiple solid tumors. In the current study, we identified and characterized harmine as the

first pharmacologic inhibitor of TWIST1 with significant antitumor activity in oncogene-driven lung cancer.

2.3 MATERIAL AND METHODS

2.3.1 Cell lines and reagents

All human non-small cell lung cancer cell lines, (A549, H460, H358, H23, H727, H23, Calu-1, Calu-6, PC-9, H1975, H3255, Hcc827, H1650, H1437, H596, H1648, and H1993) and embryonic kidney cell line HEK 293T were obtained from the American Type Culture Collection (ATCC) and grown in media as recommended by ATCC. Cell lines were authenticated using a short tandem repeat (STR) DNA profiling from the cell bank from which they were acquired. Cell lines were tested for mycoplasma every six months using MycoAlert Detection Kit (Lonza). Harmine (286044-1G) and cyclohexamide (C4859) was purchased from Sigma-Aldrich and Q-VD-oPH (A1901) was purchased from ApexBio Technology.

2.3.2 Cell viability assays

For all harmine experiments, NSCLC cell lines were seeded in 96 well plates at an appropriate cell density based on their optimal growth rates. Following a 24-hour incubation, cells were treated with harmine for 24, 48, and 72 hours. For all E2A knockdown and Twist1-E2A harmine rescue experiments, NSCLC cell lines were seeded in 96 well plates at an appropriate cell density and were infected with lentivirus for 24 hours. Following 24 hours of infection, lentivirus

was replaced with normal growth media or media with harmine. Cell viability was assessed at 24 and 48 hours following harmine treatment or at Day 4, 5 and 6 after lentiviral infection. Cell viability was assessed using CellTiter96® Aqueous One Solution Cell Proliferation Assay kit (Promega) or CellTiter-Glo (Promega) according to manufacturer's protocol. For all viability experiments, experimental treatment groups were performed in quadruplet and experiments were performed at least twice to ensure consistent results. All viability data was normalized to its appropriate non-treated control. IC₅₀ values were calculated using Prism V6 software.

2.3.3 SA-β-galactosidase staining

SA-β-galactosidase staining was performed as previously described utilizing the Senescence β-Galactosidase Staining Kit (Catalogue #9860) from Cell Signaling (234).

2.3.4 Colony formation assay

On day 4 or 6 after infection with the indicated shRNA lentiviruses, cells were plated in 12-well plates at a density of 5,000-10,000 cells/well. On day 12, the cells were stained with crystal violet (0.5% in 95% ethanol) as previously described (234). For all colony forming experiments, experimental treatment groups were performed in triplicate and experiments were repeated at least twice to ensure consistent results.

2.3.5 Quantitative RT-PCR

Total RNA was isolated from cells using the QIAprep RNeasy Kit (Qiagen) according to manufacturer's protocol. Using 1µg of RNA, cDNA was generated using the High-Capacity cDNA Reverse Transcription Kit (Applied Biosystems). 34 ng equivalents of cDNA were applied for amplification of the transcripts described below using an Applied Biosystems StepOne RT-PCR system (Perkin Elmer Applied Biosystems) for 40 cycles using the PowerUp™ SYBR® Green Master Mix (Perkin Elmer Applied Biosystems) or TaqMan® Universal PCR Master Mix (Perkin Elmer Applied Biosystems) according to manufacturer's protocol. Taqman was used for determining baseline *TWIST1* and *TCF3* mRNA levels in Figure 14B, while SYBR Green was used in Figure 16E. Following amplification, data was analyzed using the Applied Biosystems StepOne Real-Time PCR Software (Perkin Elmer Applied Biosystems). For each sample, the RNA levels of genes of interest were standardized using a housekeeping gene (18s) within that sample. The level of the gene of interest was normalized to the expression of that gene from the appropriate comparator sample. Primer list is available in Table 1-2 (Appendix A).

2.3.6 Immunoblot analysis

After treatment with harmine or infection with lentivirus, cells were lysed and protein was quantified, prepared, and western blots were performed as previously described (234). Table 3 (Appendix A) contains details of primary antibodies used. The antigen-antibody complexes were visualized by chemiluminescence (ECL and ECL-plus reagent by GE Healthcare). Western blot experiments were performed at least twice unless otherwise stated.

2.3.7 Connectivity MAP analysis

A gene signature after silencing of TWIST1 was generated based on our previous published data (234) and used to query against publically available gene expression profiles for a panel of drugs (<http://www.broad.mit.edu/cmap>). Connectivity analysis was performed as previously described (262).

2.3.8 3D organoid assay

Generation of the 3D organoid system, activation of TWIST1, and subsequent analysis of dissemination and branching was performed as previously described (263). Mammary organoids were isolated from the previously described, *CMV::rtTA;TRE-Twist1* mice (233,263).

2.3.9 FGF2-branching experiments

Generation of the 3D organoid system, treatment with FGF2, and subsequent analysis of mammary epithelial organoid branching was performed as previously described (263).

2.3.10 Lentiviral shRNA and cDNA overexpression experiments

293T cells were seeded (4×10^6 cells) in T-25 flasks and lentiviral particles were generated using a four-plasmid system and infected as according to the TRC Library Production and Performance Protocols, RNAi Consortium, Broad Institute (264), and as previously described (234). A full list

of constructs used is available in Tables 4-6 (Appendix A). The sequence of these constructs and any primers used are available upon request.

2.3.11 Pulse-Chase experiments

For harmine pulse-chase experiments, PC9 TRE3G-TWIST1 cells were treated with doxycycline (500 ng/ml) for 24 hours and subsequently treated with doxycycline (500ng/ml) and harmine (10 μ M) or vehicle (DMSO) for an additional 48 hours. Cells were then treated with cyclohexamide (50 μ g/ml) and harvested at the indicated time points. For E2A pulse-chase experiments, PC9 TRE3G-TWIST1 and H1975 TRE3G-TWIST1 cells were treated with doxycycline (500 ng/ml) for 24 hours and 72 hours, respectively. Cells were then treated with cyclohexamide (25 μ g/ml) and harvested at the indicated time points.

2.3.12 Quantification of caspase-3/7 activity

For quantification of caspase-3/7 activity, NSCLC cells were seeded in T-25 flask at an optimal cell density based on growth rate and treated with harmine or infected with lentivirus (shTCF3 or shScram). After treatment period, cells were harvested and washed once with phosphate buffered saline (PBS). CellEvent® Caspase-3/7 Green Detection Reagent was added to cells at a concentration of 500nM and incubated at 37°C for 25 min. Following incubation, SYTOX™ AADvanced™ stain was added at a concentration of 1 μ M and incubated for 5 min. at 37°C. A total of 50,000 events per replicate were analyzed using Accuri C6 Cytometer (BD Biosciences) and corresponding Accuri C6 software.

2.3.13 Luciferase promoter reporter assay

Luciferase promoter reporter assays were performed as previously described (265). Cell extracts were prepared 48 hours after transfection in passive lysis buffer, and the reporter activity was measured using the Dual-Luciferase Reporter Assay System (Promega).

2.3.14 Transgenic Mice

All mice were housed in pathogen free facilities and all experimental procedures were approved by the Institutional Animal Care and Use Committee of The Johns Hopkins University. Inducible *Twist1/Kras^{G12D}* transgenic mice in the FVB/N inbred background were of the genotype: *CCSP-rtTA/tetO-Kras^{G12D}/Twist1-tetO-luc* (CRT). All the mice were weaned 3–4 weeks of age and then placed on doxycycline at 4–6 weeks of age. The CRT mice treated had similar levels of tumor burden per CT. Micro-CT imaging and quantification of tumor burden was performed as previously described (233). For *in vivo* experiments, harmine was dissolved in normal saline by heating and sonication. The mice received 10 mg/kg harmine or saline via intraperitoneal injection daily, 5 days a week for 3 weeks.

2.3.15 Patient-derived xenograft experiments

All mice were maintained in pathogen-free animal facilities and experiments were conducted under an approved Institutional Animal Care and Use Committee protocol at the University of Pittsburgh (Pittsburgh, PA). For the PDX experiments, we used a *KRAS* mutant PDX established from the brain metastasis (BM012-15 M3VF) of a patient with *KRAS* mutant (G12C mutation)

lung cancer. 2 mm² tumor tissues cut with sterile blade were implanted subcutaneously into 6-8 week old Athymic Nude Mice [Crl:NU (NCR)-F] (Charles Rivers). Once reaching ≥ 150 mm³, animals were randomized into 2 arms and i.v. dosed with saline, or harmine (10 mg/kg) via intraperitoneal injection daily, 5 days a week for 16 days. Tumor sizes [$1/2(\text{length} \times \text{width}^2)$] were measured by digital caliper twice a week until they reached ~ 2000 mm³. When this size was reached, animals were sacrificed and tumors were collected for further analysis.

2.3.16 Histology and immunohistochemistry

Histology and immunohistochemistry and were performed as previously described (266). Primary antibodies were used at the following dilutions: Ki-67 at 1:2000 and cleaved caspase-3 at 1:500.

2.3.17 Statistics

Student's t-test was performed where indicated. For dissemination experiments (Figure 7C-J), data did not follow a normal distribution, therefore non-parametric comparison testing was performed (Kruskal-Wallis). For the PDX experiment, a Student t-test was performed on the finalized tumor volumes between the harmine and vehicle treated groups.

2.4 RESULTS

2.4.1 Identification of novel TWIST1 inhibitors with a Connectivity MAP analysis

Transcription factors, such as TWIST1, have long been considered a potential therapeutic target for cancer, given their essential role in modulating transcriptional networks that drive tumorigenesis. Beyond therapies targeting ligand-activated nuclear receptors, such as selective estrogen receptor modulators (SERMS) targeting the estrogen receptor, effective small molecule therapies that inhibit the majority of transcription factors without ligand binding pockets remain elusive (267). Therefore, the identification of inhibitors of oncogenic EMT-transcription factors would be a significant advance in cancer therapeutics and potentially lead to therapies which would not only inhibit tumor growth but metastatic potential as well. Connectivity mapping (CMAP) is a tool that compares gene signature changes associated with biological manipulation or disease to corresponding changes produced by potential drugs (262). In order to identify potential TWIST1 targeting chemical compounds, we utilized our previously published *TWIST1* knockdown expression profile (234) as the query signature for CMAP analysis. CMAP analysis generated a rank list of the 6100 compounds based on statistical correlation between changes in global gene expression signature induced by drug versus that induced by *TWIST1* knockdown (**Figure 7A, Data Supplement 1**). We selected eight of the top thirty ranked compounds based on a review of the literature suggesting that these compounds inhibited pathways important in tumorigenesis or anti-cancer activity. These compounds were evaluated for their respective cytotoxic activity *in vitro* in *KRAS* mutant NSCLC cell lines (**Figure 7A**). Of these compounds, only four demonstrated anti-proliferative effects in NSCLC (**Figure 7B**). To identify inhibitors of TWIST1 that suppress TWIST1-dependent processes that are independent of proliferation

such as single-cell dissemination, we utilized our previously published 3D organoid assay with primary breast epithelial cells derived from our doxycycline inducible *CMV:rtTA;TRE-Twist1* mouse model (233,263). We have previously shown that expression of Twist1 inhibits normal branching morphogenesis and leads to rapid and widespread dissemination of primary breast epithelial cells from the 3D organoid (**Figure 7C**) which can be reversed by removing doxycycline from the medium (263). We therefore examined whether selected candidate compounds could inhibit the Twist1-dependent dissemination in this model. Remarkably, all of seven compounds tested resulted in a significant decrease in Twist1-mediated dissemination (**Figure 7D-J**) compared to the vehicle control (**Figure 7C**). In this 3D organoid system, FGF2 treatment induces normal branching morphogenesis of primary breast epithelial cells (**Figure 8A-C**) (263). We next examined the ability of these compounds to restore FGF2-induced branching which we have previously shown is inhibited by Twist1 expression in this model (263). Two compounds, meteneprost and the harmala alkaloid, harmine were able to restore FGF2-induced branching in a dose dependent manner (**Figure 7D, 7H**) compared to the vehicle control (**Figure 7C**). Interestingly, three harmine analogues were in the top 80 compounds identified in the CMAP analysis, with two of the compounds being in the top 40 (**Data Supplement 1**). Previous studies have reported that harmine and its analogues have marked antitumor activity (268-270). While two compounds screened, harmine and meteneprost, inhibited TWIST1-dependent single epithelial cell dissemination and TWIST1-suppression of epithelial organoid branching (**Figure 7D, 7H**), harmine was the only compound screened that inhibited growth in lung cancer cell lines as well as the aforementioned TWIST1-dependent functions in our mammary 3D organoid system. Given these factors, we decided to further characterize the biological activities of harmine as a TWIST1 inhibitor.

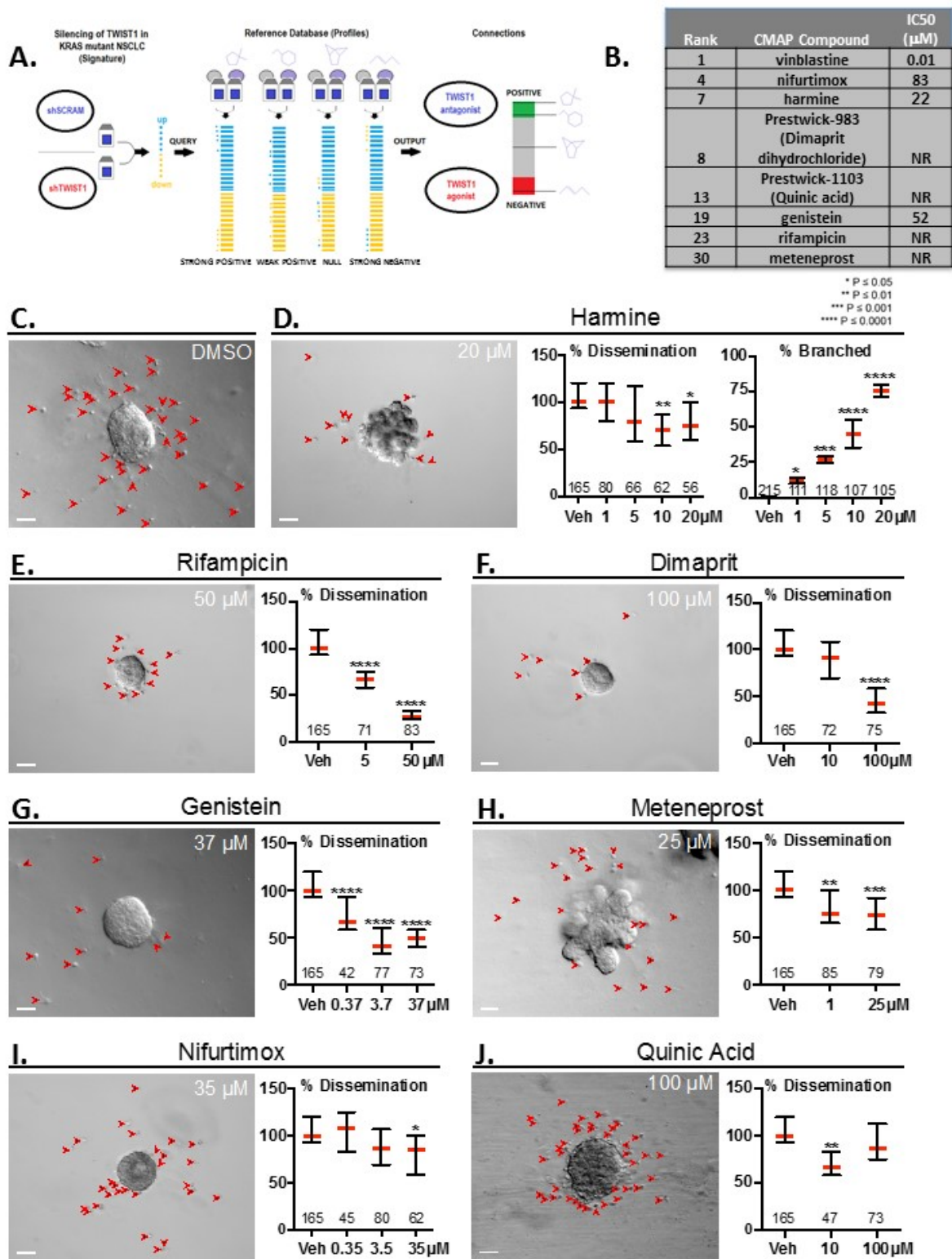


Figure 7: Connectivity MAP (CMAP) analysis identifies compounds which inhibit NSCLC proliferation, TWIST1-dependent dissemination and TWIST1-suppression of organoid branching

(A) CMAP Analysis Schematic. A gene signature for *TWIST1* knockdown was utilized to query the Connectivity Map (Broad Institute). (B) Chart depicting eight of the top 30 ranked compounds which were selected for further analysis. IC_{50} was determined in two *KRAS* mutant NSCLC cell lines (A549 and H460) at 72 hours using MTS assays. (C) *TWIST1* induction with doxycycline results in profound dissemination of cells and prevents branching (DMSO, upper left panel). Primary *Twist1* inducible breast epithelial cells are implanted as organoids in 3D culture. Red arrowheads indicate disseminated cells. (D-J) Candidate compounds inhibit *Twist1*-induced 3D dissemination and/or restore FGF2-induced branching of primary breast epithelial cells *in vitro*. Values within the graph indicate the number of organoids quantified per treatment condition. Dissemination data is normalized to the median of each experimental replicate. Error bars, 95% Confidence Intervals. Treatment with small molecules listed at the indicated doses induced statistically significant (Kruskal-Wallis test, $P < .05$) reductions in dissemination. (D) Branching data is presented as mean of each experimental replicate. See Figure 8A-C for representative images of unbranched versus branched organoids. Error bars, \pm SD. Treatment with harmine at the indicated doses induced statistically significant (One-way ANOVA, $P < .05$) increases in branching. Scale bar, 50 μ m.

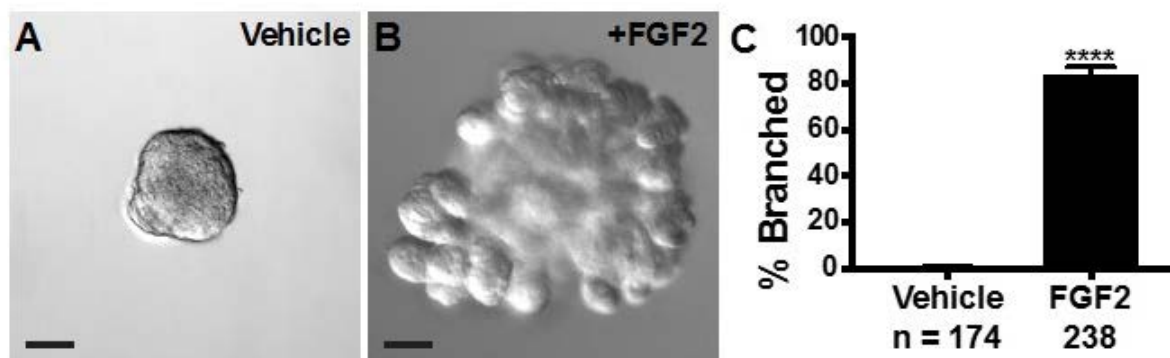


Figure 8: FGF2 treatment induces branching morphogenesis of primary epithelial cells in 3D culture

(A-B) Representative images demonstrating a mammary organoid in 3D culture in the absence (unbranched) or presence (branched) of FGF2. (C) FGF2 treatment results in a significant increase in mammary organoid branching. Mammary epithelial organoids were embedded in Matrigel and treated with 2.5 nM FGF2 (bFGF) or Vehicle (D-PBS) (n=174 for vehicle and n=238 for FGF2). Branched organoids were counted as 3 or more branches per organoid. Data represent mean \pm SD. *, $p < .05$, 2-tailed Student's t-test.

2.4.2 Harmine inhibits growth in oncogene driver-defined NSCLC cell lines and phenocopies loss of TWIST1

Harmine was originally identified as an active β -carbolin alkaloid found in the herb *Peganum harmala* (*P. harmala*), which has long been used in traditional medicine as a sedative and for treating conditions like hypertension and depression (271). Studies investigating the activity of harmine and other active β -carbolins found in *P. harmala* in the nervous system have demonstrated that these compounds inhibit monoamine oxidase-A (271). Additionally, in traditional medicine, *P. harmala* has been used to treat malignancy. Previous studies have demonstrated that harmine has antitumor activity, which has been linked to its ability to inhibit DYRK1A, topoisomerase I, and suppress homologous recombination (272-276). However, the mechanism(s) by which harmine inhibits tumor growth remain poorly described and its activity in lung cancer has not been explored. Here, we first characterized the growth inhibitory effects of

harmine (**Figure 9A**) across a panel of oncogene driver-defined NSCLC lines which we had previously reported as dependent on TWIST1 expression (234). Similar to genetic silencing of *TWIST1*, we found harmine treatment to be cytotoxic across the panel of oncogene driver-defined NSCLC lines (*KRAS* mutant, *MET* amplified/mutant, and *EGFR* mutant) (**Figure 9B**). While harmine was more potent in cell lines with high TWIST1 levels (**Figure 9B**), harmine also had activity in cell lines with low TWIST1 expression (**Figure 10**) (277). Additionally, harmine had activity in NSCLC cell lines with primarily epithelial or mesenchymal phenotypes, suggesting that the activity of harmine is independent of EMT status (277-279). We had previously demonstrated that inhibition of TWIST1 leads to oncogene-induced senescence (OIS) in *KRAS* mutant NSCLC lines (233). Similar to silencing of *TWIST1*, treatment of the *KRAS* mutant NSCLC lines A549, H460, and H358 with harmine induced changes characteristic of OIS, including positive Senescence-Associated Beta-galactosidase (SA- β -Gal) staining and induction of p21 and p27 (**Figure 9C**). We also found that harmine treatment induced OIS in NSCLC cell lines with *EGFR* and *MET* mutations (**Figure 11A-B**). While an increase in SA- β -Gal staining was observed in both *EGFR* and *MET* mutant NSCLC cells lines, an increase in p21/p27 expression was only observed in the *EGFR* mutant cell line. Importantly, we have previously demonstrated that OIS following genetic inhibition of *TWIST1* does not require p21 or p27 (234).

We have also previously shown that TWIST1 is required for suppression of OIA in a subset of *KRAS* mutant lung cancer cells including Calu-6 and H23 (234). We expanded upon these studies and demonstrated that knockdown of TWIST in the *MET* amplified NSCLC cell line, H1648, results in growth inhibition and in induction of apoptosis (**Figure 12A**). Of note, H1648 cells have high levels of TWIST1 and therefore may be more dependent on TWIST1 for

survival (**Figure 10**). Consistent with a TWIST1-suppressive effect, after harmine treatment, we observed a significant induction of apoptosis, in a dose-dependent manner in all three cell lines (**Figure 12B, 13A**). Of note, in the H1648 cell line, a more robust apoptotic response was observed following harmine treatment as compared to genetic inhibition of *TWIST1*. Given that rapid apoptosis occurs in this cell line, the increased apoptotic response observed with harmine could be due to the fact that apoptosis was analyzed at an earlier timepoint in the harmine treatment group than the TWIST1 knockdown group. The growth inhibition by harmine in these cells was dependent on apoptosis as co-treatment with the pan caspase inhibitor, Q-VD-oPH, prevented the cytotoxic effects of harmine (**Figure 13B**). Furthermore, BCL-2 overexpression partially prevented harmine-induced apoptosis, suggesting that the intrinsic apoptotic pathway is required for the growth inhibitory effects of harmine in these lines (**Figure 13C**).

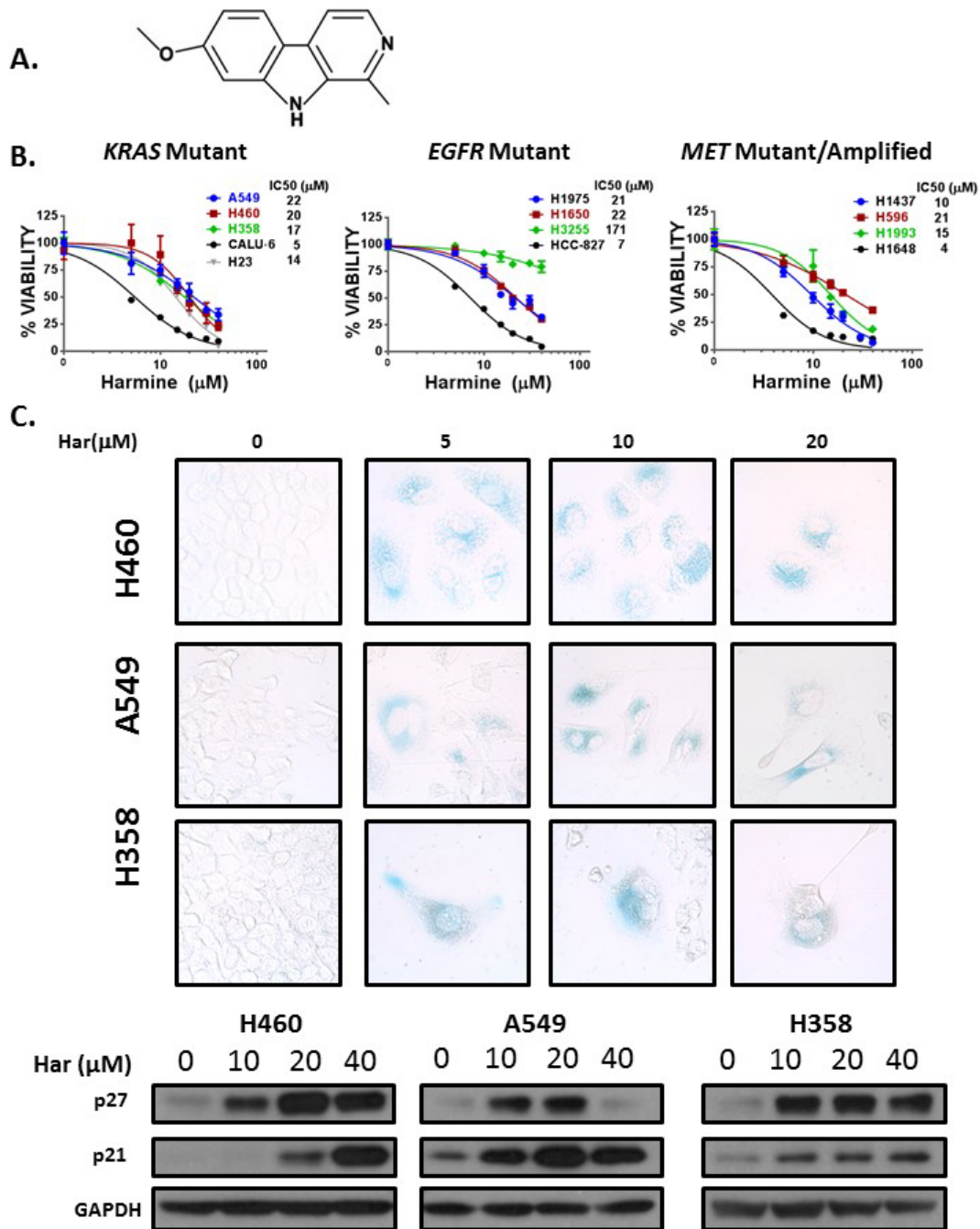


Figure 9: Harmine inhibits growth through the induction of oncogene-induced senescence (OIS) in oncogene driver-defined NSCLC cell lines

(A) Chemical structure of the harmala alkaloid, harmine. (B) MTS assays demonstrating growth inhibition in the indicated *KRAS* mutant, *EGFR* mutant, and *MET* mutant/amplified NSCLC cells following harmine treatment at 72 hours. Data represent mean \pm SD (n=4 technical replicates). (C) UPPER: Senescence-Associated Beta-galactosidase (SA- β -Gal) staining demonstrating that harmine (Har) treatment leads to oncogene-induced senescence (OIS) in *KRAS* mutant NSCLC cell lines. Cells were treated at the indicated doses for 72 hours and stained 7 days following treatment. Images were obtained with bright field objective at 40X magnification. LOWER: Western blot demonstrating a marked increase in p21 and p27 expression 48 hours after harmine treatment at the indicated doses.

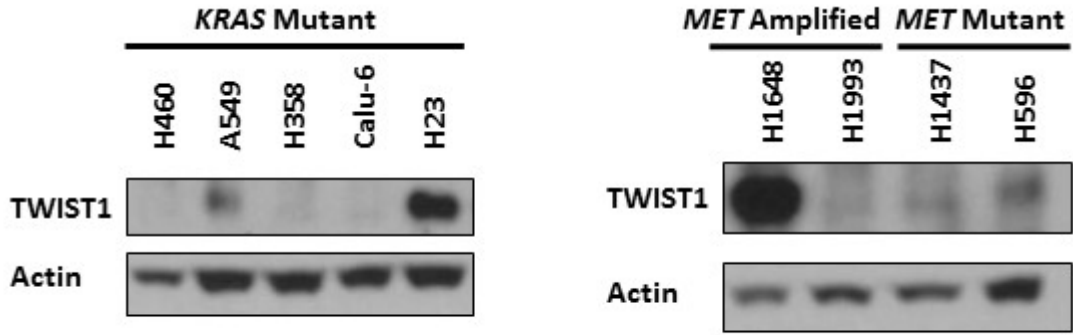


Figure 10: Basal expression levels of TWIST1 in *KRAS* mutant and *MET* amplified/mutant NSCLC cell lines
 Western blot demonstrating baseline levels of TWIST1 in *KRAS* mutant and *MET* altered NSCLC cell lines.

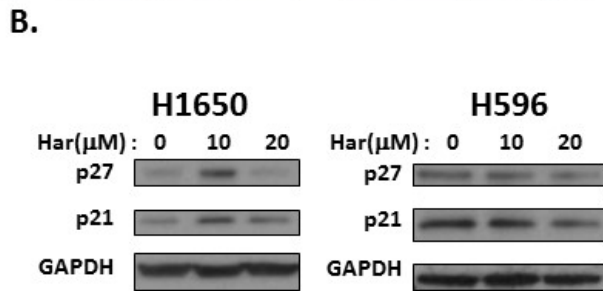
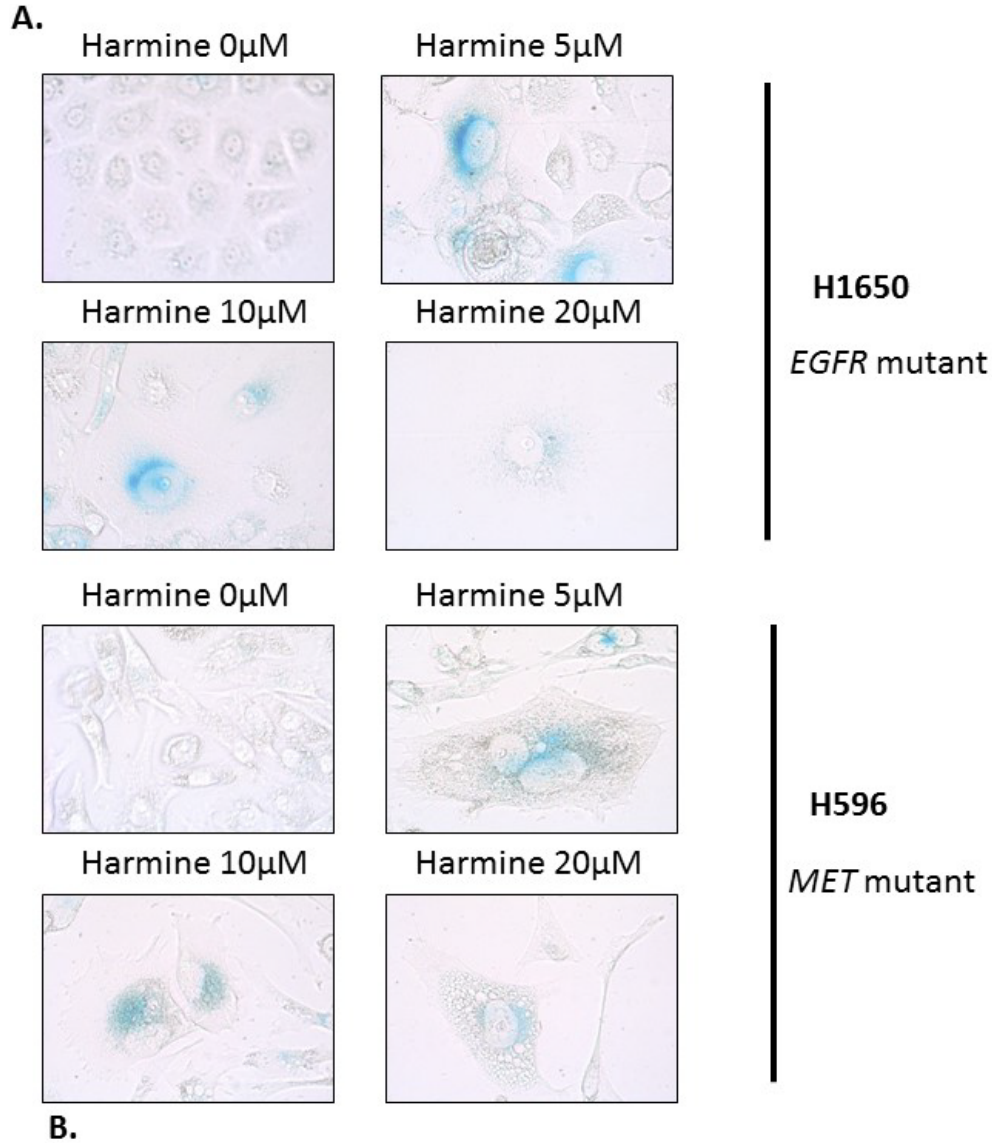
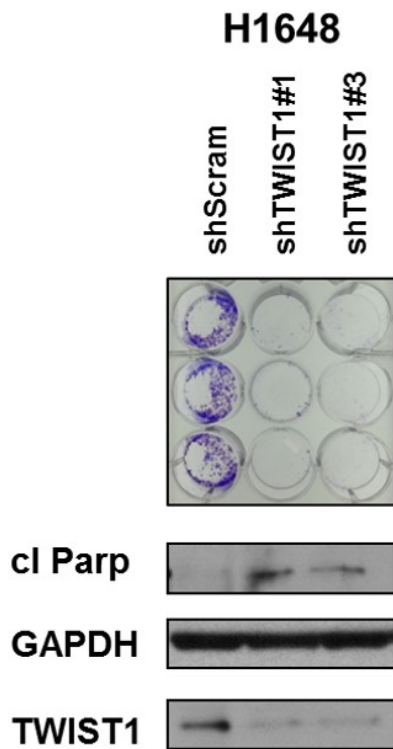


Figure 11: Harmine treatment induces Oncogene-Induced Senescence (OIS) in EGFR and MET mutant NSCLC cell lines

(A) Senescence-Associated Beta-galactosidase (SA- β -Gal) staining demonstrating that harmine treatment leads to OIS in *EGFR* mutant and *MET* mutant cell lines, H1650 and H596. Cells were treated with the indicated doses of harmine for 72 hours and stained 7 days following harmine treatment. Images were obtained with bright field objective at 40X magnification. (B) Western blot demonstrating that harmine treatment leads to increased p27 and/or p21 expression in a cell line specific manner, as induction of p21 and p27 was observed in H1650 cells but not H596 cells. Cells were treated with the indicated doses of harmine for 48 hours.

A. MET AMPLIFIED



B.

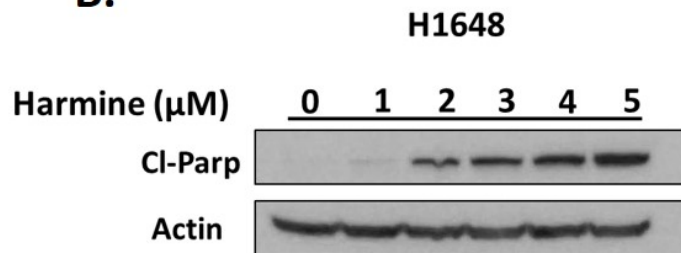


Figure 12: TWIST1 suppresses oncogene-induced apoptosis in MET amplified NSCLC

(A) Silencing of *TWIST1* with two distinct shRNAs resulted in growth inhibition and apoptosis in a *MET* amplified cell line (H1648) as shown by colony formation assay (UPPER) and western blot (LOWER). H1648 cells were harvested 10 days following lentiviral infection for colony formation assay and 4 days following lentiviral infection for western blot analysis. (B) Western blot demonstrating an increase in cleaved PARP, a maker of apoptosis, following harmine treatment. H1648 cells were treated with the indicated doses of harmine for 48 hours and harvested for western analysis.

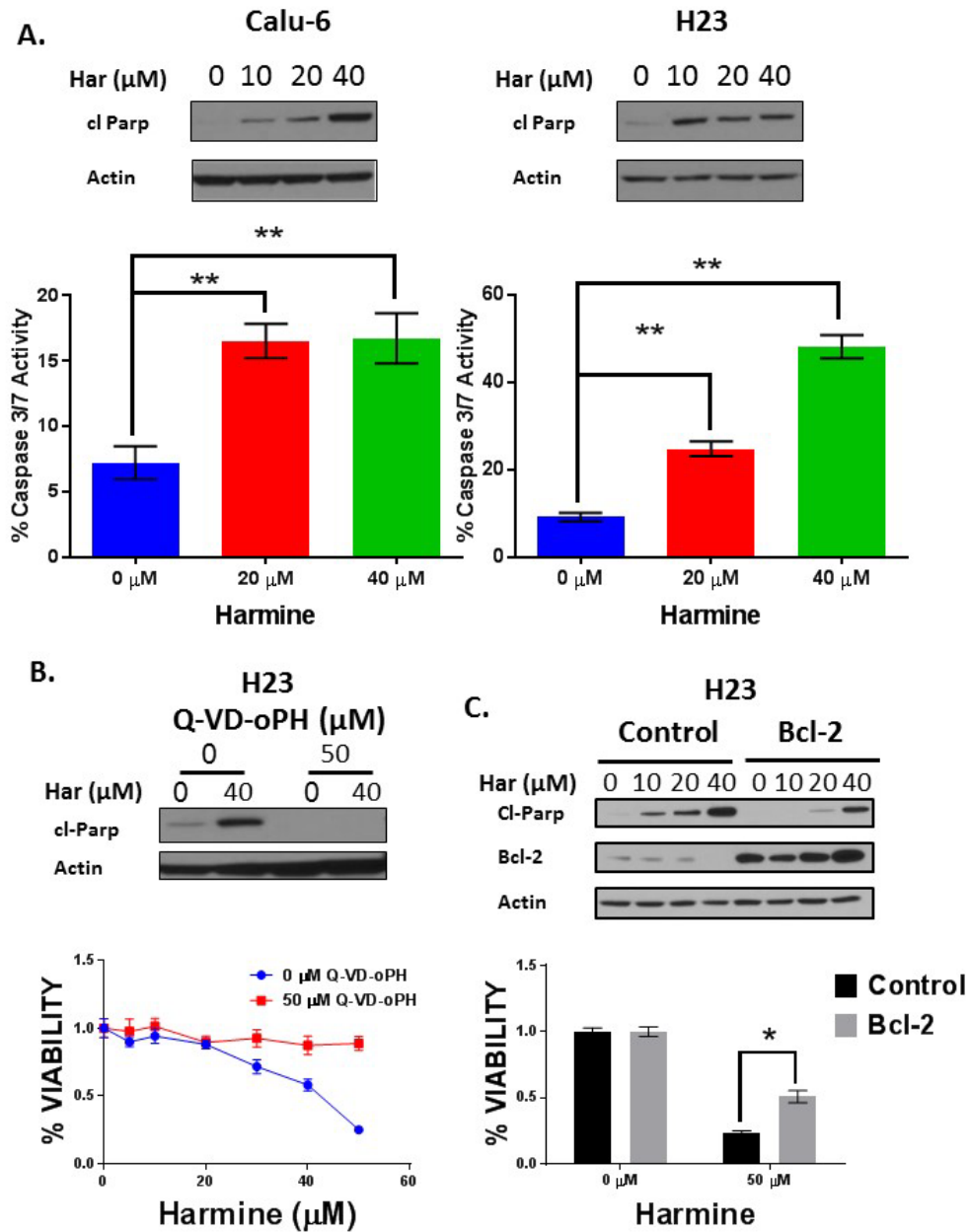


Figure 13: Harmine induces apoptosis in oncogene-driven NSCLC cell lines

A) UPPER: Western blot demonstrating PARP cleavage 48 hours after harmine treatment at the indicated doses of harmine in two *KRAS* mutant cell lines (Calu-6 and H23). LOWER: Active Caspase 3/7 staining demonstrating the induction of apoptosis after harmine treatment at the indicated doses. Calu-6 cells were treated for 36 hours while H23 cells were treated for 24 hours. Data represent mean \pm SD (n=3 biological replicates). **, p<.01, 2-tailed Student's t-test. **(B)** UPPER: Western blot demonstrated that co-treatment with pan-caspase inhibitor Q-VD-oPH prevents harmine-induced apoptosis. LOWER: MTS proliferation assay demonstrating that growth inhibition following harmine treatment can be prevented by treatment with Q-VD-oPH, a pan caspase inhibitor. Cells were pre-treated with Q-VD-oPH for 4 hours and were subsequently co-treated with Q-VD-oPH and harmine for 24 hours. Data represent mean \pm SD (n=4 technical replicates). **(C)** UPPER: Western Blot demonstrating that BCL-2 overexpression prevents PARP cleavage 24 hours following harmine treatment at the indicated doses. LOWER: MTS proliferation assay demonstrating that growth inhibition following harmine treatment can be partially prevented by BCL-2 overexpression. Data represent mean \pm SD (n=4 technical replicates). *, p<.05, 2-tailed Student's t-test.

2.4.3 Harmine treatment results in TWIST1 protein degradation

Previous studies have demonstrated that modulation of TWIST1 protein stability is a critical regulatory mechanism of TWIST1 function (231,280-282). To determine whether harmine directly targets TWIST1 or the TWIST1 pathway, we first examined the effect of harmine on TWIST1 protein stability. Harmine treatment reduced the levels of TWIST1 protein in a dose and time dependent manner as shown by western blotting and this was accompanied by a reciprocal induction of p21 (**Figure 14A, 15A**), a known TWIST1 repressed transcriptional target gene (242,283). The effect of harmine on TWIST1 expression appears to occur through a post-translational mechanism as harmine treatment did not decrease *TWIST1* mRNA levels (**Figure 14B**) but did decrease the half-life of the TWIST1 protein (**Figure 14C, Figure 15B**).

In addition to harmine, several other harmala alkaloid compounds were identified in our CMAP analysis. To determine if particular structural features of harmala alkaloids were important for the induction of TWIST1 degradation, we selected three related compounds that differed from harmine in key structural positions (**Figure 14D**, left panel). We were interested in both the 7-methoxy structural moiety which has previously been shown to effect cytotoxicity and neurotoxicity and the saturation level of the pyridine ring, which has been demonstrated to affect the biological activity of beta-carbolines (268-270,284). Of note, harmine and harmaline have a methoxy group, whereas harmol and harmalol have hydroxyl groups at the position R7. Conversely, harmine and harmol contain pyridine rings with three versus two double bonds found in harmaline and harmalol. The compounds (harmine and harmol) which contained pyridine rings with three double bonds exhibited the most cytotoxicity suggesting that this

feature was critical for tumor growth inhibition and TWIST1 degradation (**Figure 14D-E**). However, the presence of a methoxy or hydroxyl group, at the position R7 did not correlate with increased cytotoxicity and the ability to degrade TWIST1. Notably, the relative potency of these compound directly correlated with their ability to lead to TWIST1 degradation (**Figure 14D-E**).

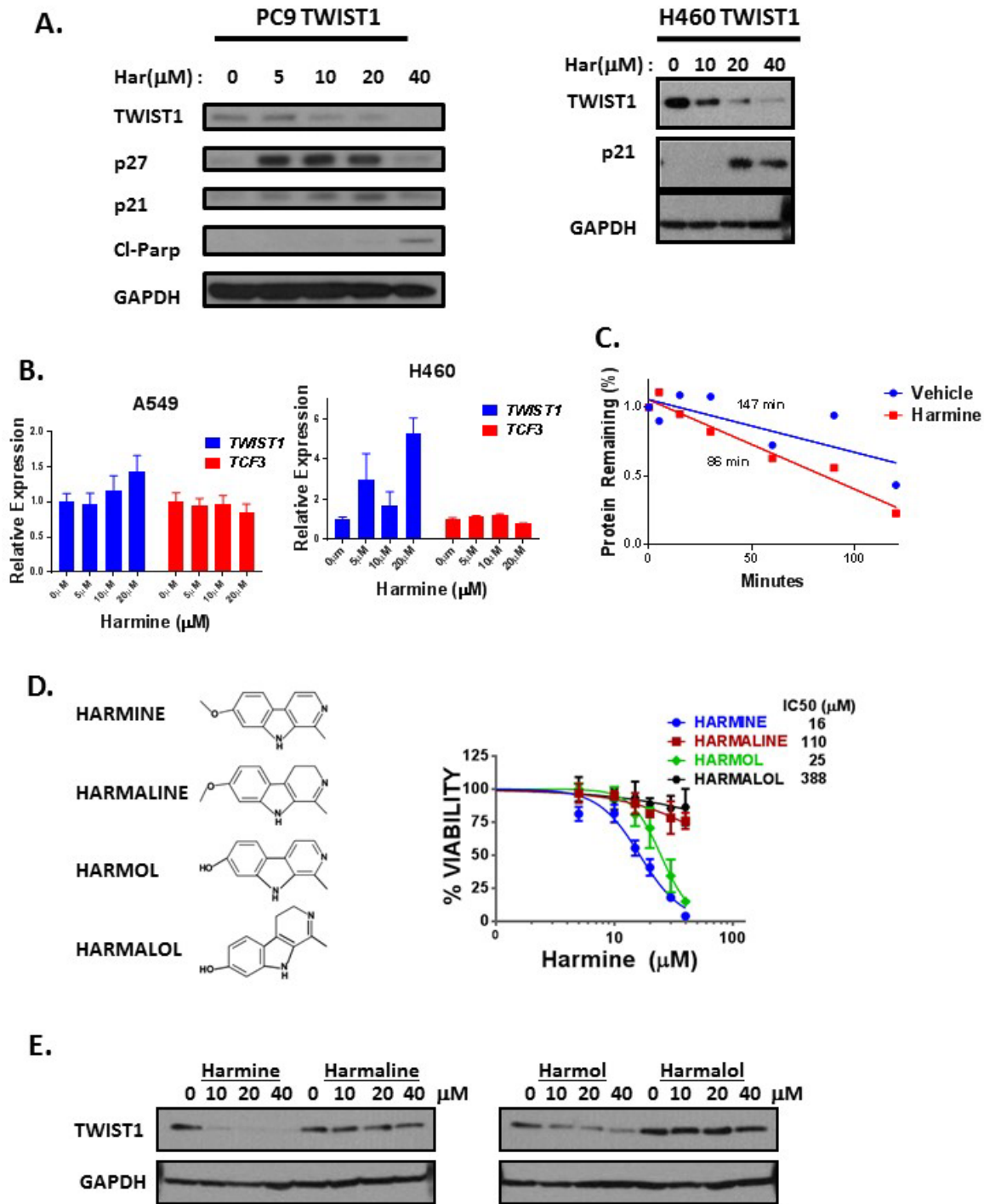


Figure 14: Harmine treatment leads to TWIST1 protein degradation

(A) LEFT: Western blot demonstrating 72 hours of harmine treatment promotes TWIST1 degradation and subsequent oncogene-induced senescence (p27 and/or p21) and apoptosis (Cl-Parp) in a dose-dependent manner in the *EGFR* mutant NSCLC cell line, PC-9. RIGHT: Western blot demonstrating reduction of exogenous TWIST1 protein expression as well as induction of p21 after 72 hours of harmine treatment in the *KRAS* mutant NSCLC cell line, H460. (B) Quantitative RT-PCR analysis of *TWIST1* and *TCF3* mRNA transcripts following 72 hours of harmine treatment in A549 and H460 cells which failed to detect a decrease in mRNA levels of *TWIST1* or *TCF3*. All harmine treatment groups are normalized to untreated group. Data represent mean \pm SD (n=3 technical

replicates). (C) Harmine treatment decreases the half-life of TWIST1 protein. Protein concentration was quantified using densitometry and protein half-lives were estimated using linear regression analysis. (D) LEFT: Chemical structures of Harmala Alkaloid compounds identified as potential TWIST1 inhibitors from CMAP analysis. RIGHT: MTS assays demonstrating growth inhibition of a H460 TWIST1 NSCLC cell line in a dose dependent manner following treatment with indicated harmala alkaloids at 72 hours. Data represent mean \pm SD (n=4 technical replicates). (E) Western blot demonstrating reduction of exogenous TWIST1 protein expression by harmine and harmol in H460 TWIST1 overexpressing cells 72 hours after treatment with the indicated doses.

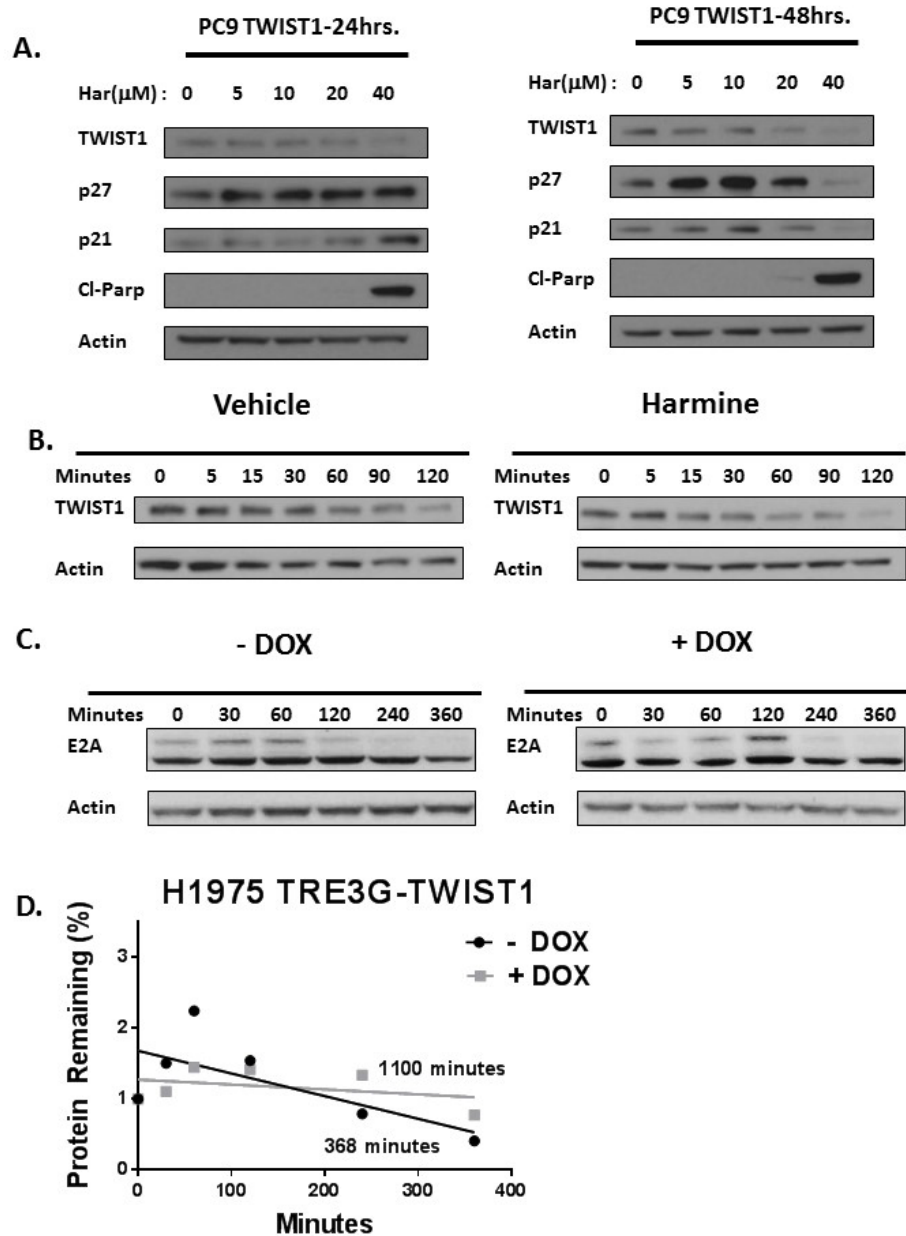


Figure 15: Harmine treatment promotes TWIST1 degradation and decreases TWIST1 protein stability

(A) Western blots demonstrating harmine treatment promotes TWIST1 degradation and subsequent oncogene-induced senescence (p27 and/or p21) and apoptosis (Cl-PARP) in a dose and time dependent manner. PC9 TRE3G-TWIST1 cells were treated with doxycycline (500 ng/ml) for 24 hours and subsequently treated with doxycycline and the indicated doses of harmine. Cells were harvested at 24 and 48 hours following harmine treatment. (B) Western blot demonstrating that harmine treatment decreases the half-life of TWIST1 protein. PC9 TRE3G-TWIST1 cells were treated with doxycycline (500 ng/ml) for 24 hours, subsequently treated with doxycycline (500 ng/ml) and harmine (10 μ M) or vehicle (DMSO) for an additional 48 hours. Cells were then treated with cyclohexamide (50 mg/ml) and harvested at the indicated time points. (C) Western blot demonstrating that TWIST1 overexpression increases the half-life of the E2A proteins. PC9 TRE3G-TWIST1 cells were treated with doxycycline (500 ng/ml) for 24 hours. Cells were then treated with cyclohexamide (25 μ g/ml) and harvested at the indicated time points. (D) TWIST1 overexpression in H1975 TRE3G-TWIST1 cells increases the half-life of E2A proteins. Protein concentration was quantified using densitometry and protein half-lives were estimated using linear regression analysis.

2.4.4 TWIST1 and the E2A proteins reciprocally stabilize each other and harmine leads to degradation of both components of this dimer

The TWIST1 protein forms both homo- and hetero-dimers and its functions are dependent on its respective dimer partner (208). We and others have previously shown that heterodimerization with the proteins encoded by the *TCF3* gene, here after referred to as the E2A proteins (E12 and E47), are critical for TWIST1 function in tumorigenesis and EMT (248,265,285) and TWIST1 protein stability in osteoblasts (231). Therefore, we decided to examine the role of the E2A proteins in regulating both TWIST1 protein stability in NSCLC and response to harmine. To examine the effect of modulating the levels of TWIST1 and E2A proteins on the stability of the other dimer partner, we knocked down and overexpressed each of the proteins and examined the effect on the protein level of its dimer partner. Silencing of *TCF3* in the *KRAS* mutant NSCLC cell line A549 induced modest downregulation of TWIST1 (**Figure 16A**) and conversely overexpression of the E12 or E47 induced upregulation of TWIST1 (**Figure 16B**). In both *KRAS* mutant (A549, H460), MET-amplified (H1648, H1993) NSCLC cell lines, silencing of *TWIST1* induced downregulation of E2A proteins (**Figure 16C**). Conversely, overexpression of TWIST1 in *KRAS* mutant H460 cells and an *EGFR* mutant NSCLC cell line (PC9) increased E2A protein expression (**Figure 16D**). To explore the mechanism of TWIST1 regulation of E2A, we analyzed *TCF3* mRNA levels following TWIST1 overexpression. We found that in H460 and PC9 cell lines, TWIST1 overexpression does not result in a marked increase in *TCF3* mRNA levels, and in fact decreases *TCF3* mRNA levels in PC9 cells, suggesting that it is unlikely that TWIST1 regulates *TCF3* transcriptionally. Also, we found that TWIST1 overexpression in multiple cell

lines leads to an increase in E2A protein half-life (**Figure 15C-D, Figure 16E**). These results suggest that TWIST1 regulates expression of the E2A proteins post-translationally.

Given the ability of the E2A proteins and TWIST1 to reciprocally stabilize each other, we examined the effect of harmine on the E2A proteins. Treatment with harmine resulted in a dose-dependent decrease of E2A protein expression in both *KRAS* mutant and *MET*-mutant/amplified NSCLC cell lines (**Figure 17A**). This decrease in E2A protein expression also appears to be post-transcriptional as harmine treatment does not decrease *TCF3* RNA levels (**Figure 17B**). To further characterize the potential role of the E2A proteins in TWIST1-mediated lung tumorigenesis, we silenced *TCF3* in *KRAS* mutant NSCLC cell lines. Silencing of *TCF3* also resulted in OIS, phenocopying silencing of *TWIST1*. Similar to our previously published results (233,234), both growth inhibition in colony formation assays and OIS as evidenced by increased SA- β -Gal staining and p21/p27 levels were observed with silencing of *TCF3* (**Figure 17B**). Of note, an increase in p21 expression was not observed following silencing of *TCF3* in A549 cells. Similarly, in A549 cells, we have previously observed that p21 expression is not increased following knockdown of TWIST1. Importantly, we have also demonstrated that OIS following genetic inhibition of *TWIST1* does not require p21 expression (234).

As discussed above, TWIST1 is required for suppression of OIA in a subset of lung cancer cells and we wanted to examine whether we could observe a similar phenotype after silencing of *TCF3* (234). Genetic silencing of *TCF3* in the *KRAS* mutant cell lines, Calu-6 and H23, resulted in significant growth inhibition and a corresponding increase in apoptosis (**Figure 18A-C**) phenocopying our previous studies with silencing of *TWIST1* (234) and studies above with harmine (**Figure 12-13**). Furthermore, we demonstrated that the growth inhibition after

silencing of *TCF3* was dependent on apoptosis as pre-treatment with the pan caspase inhibitor, Q-VD-oPh rescued cell viability (**Figure 18C**).

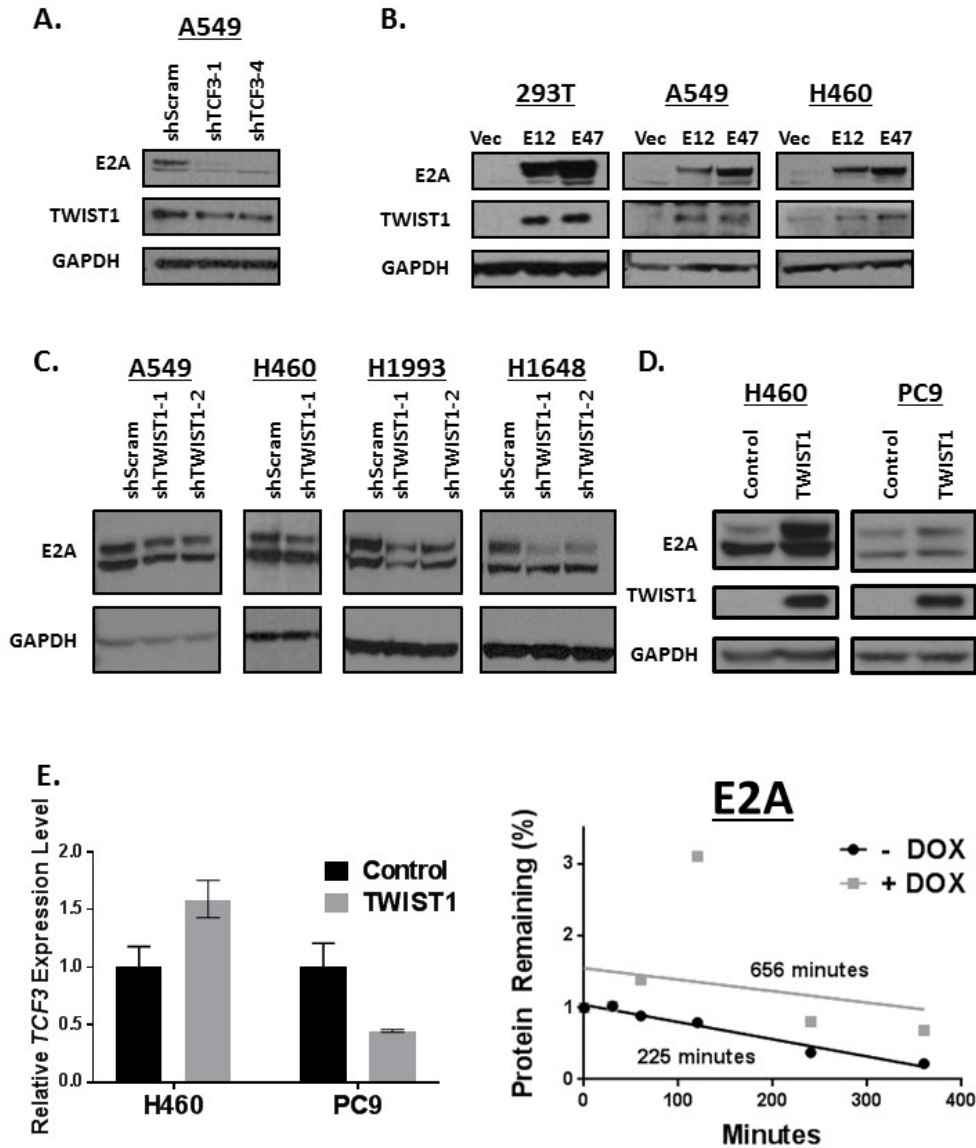


Figure 16: The E2A proteins and TWIST1 reciprocally stabilize each other

(A) Silencing of *TCF3* leads to downregulation of TWIST1 in the *KRAS* mutant NSCLC cell line, A549. Cells were infected with the indicated shRNAs and were harvested for western blot analysis 96 hours following infection. (B) Overexpression of the E2A proteins, E12 or E47 induces upregulation of TWIST1 in 293T cells as well as in *KRAS* mutant NSCLC cells (A549, H460). 293T cells were harvested 72 hours following transfection. Experiments in A549 and H460 were performed in stable E12 or E47 overexpressing cell lines. (C) Silencing of *TWIST1* induces downregulation of E2A proteins in *KRAS* mutant (A549, H460) as well as in *MET* amplified (H1648, H1993) NSCLC cell lines. Cells were infected with the indicated shRNAs and were harvested for western blot analysis 96 hours following infection. (D) Overexpression of TWIST1 induces the E2A proteins in *KRAS* mutant NSCLC cells (H460) and *EGFR* mutant NSCLC cells (PC-9). H460 cells were harvested once stable cell lines were established. PC9 TRE3G-TWIST1 cells were harvested following 500 ng/ml treatment of doxycycline for 24 hours. (E) LEFT: TWIST1 induction of E2A proteins is not accompanied by a robust upregulation of *TCF3* mRNA in *KRAS* mutant (H460) and *EGFR* mutant NSCLC cells (PC-9). All TWIST1 overexpressing groups are normalized to untreated group (n=3 technical replicates). Data represent mean \pm SD. RIGHT: TWIST1 overexpression increases the half-life of E2A proteins. Protein concentration was quantified using densitometry and protein half-lives were estimated using linear regression analysis.

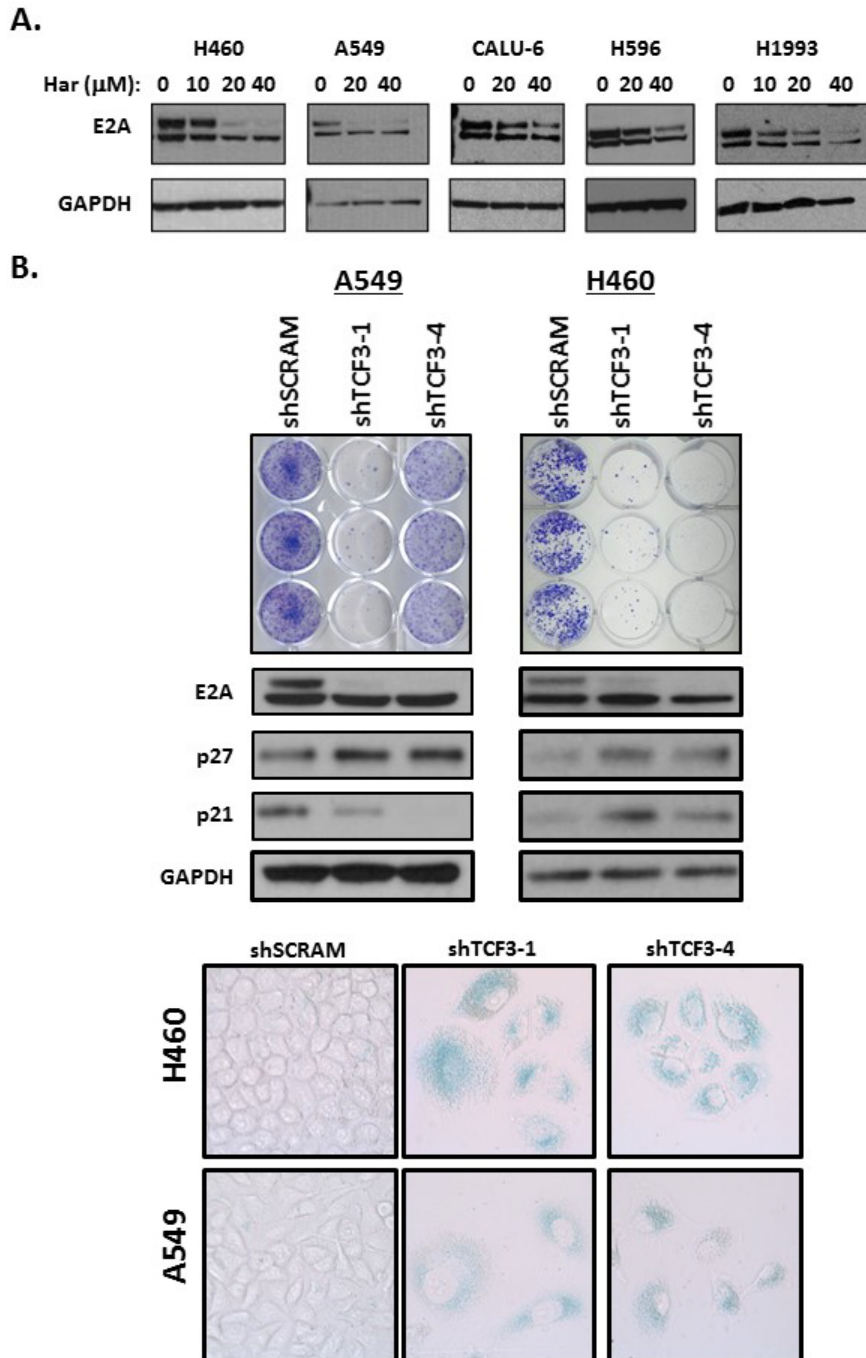


Figure 17: Harmine leads to degradation of the E2A proteins which are required for suppression of OIS

(A) Western blot demonstrating dose-dependent downregulation of E2A proteins in *KRAS* mutant (H460, A549 and Calu-6) and *MET* mutant/amplified (H596 and H1993) NSCLC cell lines following 72 hours of harmine treatment. (B) UPPER: shRNA silencing of *TCF3* in *KRAS* mutant NSCLC cell lines (A549 and H460) leads to growth inhibition as demonstrated in triplicates of crystal violet staining. MIDDLE/LOWER: shRNA silencing of *TCF3* induces OIS as shown by western blot demonstrating a marked increase in p21 and/or p27 expression and positive SA- β -Gal staining (LOWER). For western blotting, cells were infected with the indicated shRNAs for 96 hours and harvested. For SA- β -Gal staining cells were infected with the indicated shRNAs and stained for 10 days following infection. Images were obtained with bright field objective at 40X magnification.

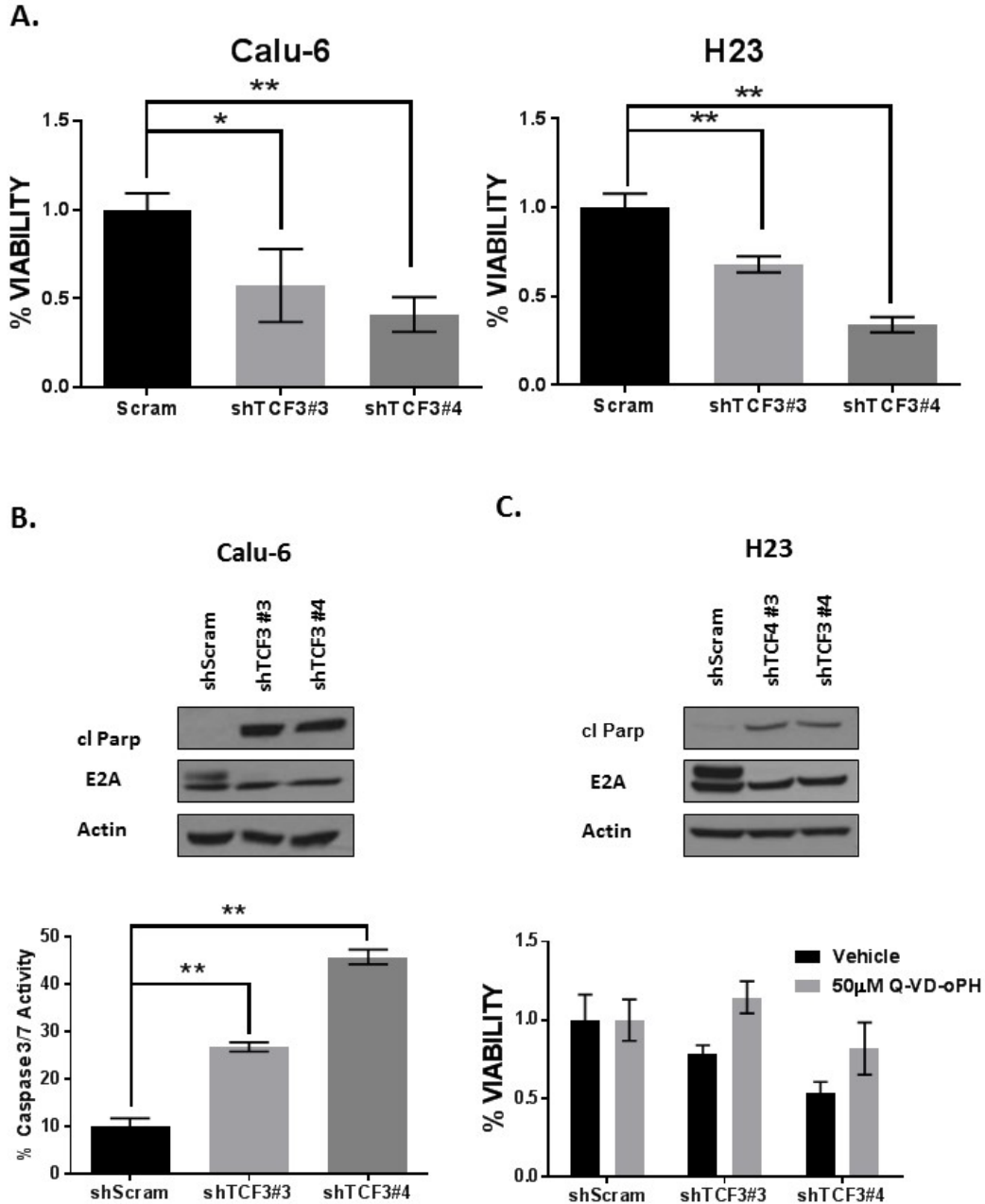


Figure 18: Silencing of *E2A* induces apoptosis and phenocopies silencing of *TWIST1*

(A) *TCF3* knockdown inhibits growth in *KRAS* mutant NSCLC cell lines. Calu-6 and H23 were infected with control shRNA (shSCRAM) or shRNA targeting *TCF3* (shTCF3 #3, #4) for 6 days before cell viability was measured using Cell-Titer Glo. % Viability is normalized to shScram control. Data represent mean \pm SD (n=4 technical replicates). *, p<.05, **, p<.01, 2-tailed Student's t-test. (B) UPPER: Western blot showing PARP cleavage 72 hours after silencing of *TCF3* in Calu-6 cells. LOWER: Active Caspase 3/7 staining demonstrating the induction of apoptosis after *TCF3* knockdown in Calu-6 cells. Cells were infected with shSCRAM, shTCF3#3, or shTCF3#4 for 72 hours and stained for active caspase 3/7. Data represent mean \pm SD (n=3 biological replicates). **, p<.01, 2-tailed Student's t-test. (C) UPPER: Western blot showing PARP cleavage 72 hours after silencing *TCF3* in H23 cells. LOWER: Pre-treatment with pan-caspase inhibitor prevents growth inhibition following *TCF3* knockdown. H23 cells were pre-treated with Q-VD-oPH for 4 hours and subsequently infected with control shRNA (shSCRAM) or shRNA targeting *TCF3* (shTCF3 #3, #4) for 4 days before cell viability was measured using Cell-Titer Glo. % Viability is normalized to shScram control. Data represent mean \pm SD (n=4 technical replicates).

2.4.5 The TWIST1/E2A heterodimer is critical for TWIST1 function and therapeutic response to harmine

The exact mechanism of how TWIST1 and E2A interact to promote lung tumorigenesis is unknown; however we propose two potential mechanisms for the cooperation between TWIST1 and the E2A proteins, E12 or E47, to promote their neoplastic phenotypes. In the first scenario (dimerization), the TWIST1-E12 heterodimer is directly required for the transcriptional activity of TWIST1 and induces tumorigenesis (**Figure 19A**). The second scenario (sequestration) suggests that E12/E47-mediated sequestration of Ids (Inhibitor of DNA-binding proteins) leads to TWIST1 transcriptional activity through allowing increased TWIST1 homodimer formation (**Figure 19A**). In order to determine which mechanism is important for TWIST1 transcriptional activity, we first performed a luciferase assay utilizing the promoters of SNAI2 and YBX1, known transcriptional targets of TWIST1 (286,287). As expected, increased induction of SNAI2 and YBX1 promoter activity was seen in cells transiently overexpressing Twist1. To determine the transcriptional function of the TWIST1 homo- and heterodimeric proteins, we expressed Twist1 tethered Twist1, Twist1 tethered E12 and Twist1 tethered E47 fusion proteins in these luciferase assays (288,289). The Twist1-E12 and Twist1-E47 had significantly increased transcriptional activity compared to the Twist1-Twist1 homodimer or Twist1 alone (**Figure 19B**). Since the Twist1-E2A heterodimers appeared to be the most potent inducer of transcription and harmine led to degradation of both TWIST1 and the E2A proteins we examined the relative effect of harmine on stability of the TWIST1 homo and heterodimers. We observed that harmine was most effective against the Twist1-E12 heterodimer following harmine treatment (**Figure 19C**). Further supporting a role for the TWIST1 heterodimer in TWIST1 function and therapeutic response, overexpression of TWIST1 or the E2A proteins, E12 and

E47, were able to rescue the harmine-induced growth inhibition in the *KRAS* mutant NSCLC cell lines A549 and H460 (**Figure 20A-C**). Furthermore, overexpression of the Twist1-E12 heterodimer similarly lead to a rescue of harmine-induced cytotoxicity, while overexpression of the Twist1-Twist1 heterodimer failed to lead to such rescue at most doses of harmine (**Figure 19D**). Together these data support the model that the E2A proteins are necessary for TWIST1 functions and that degradation of TWIST1-E2A heterodimer is critical for harmine-induced cytotoxicity.

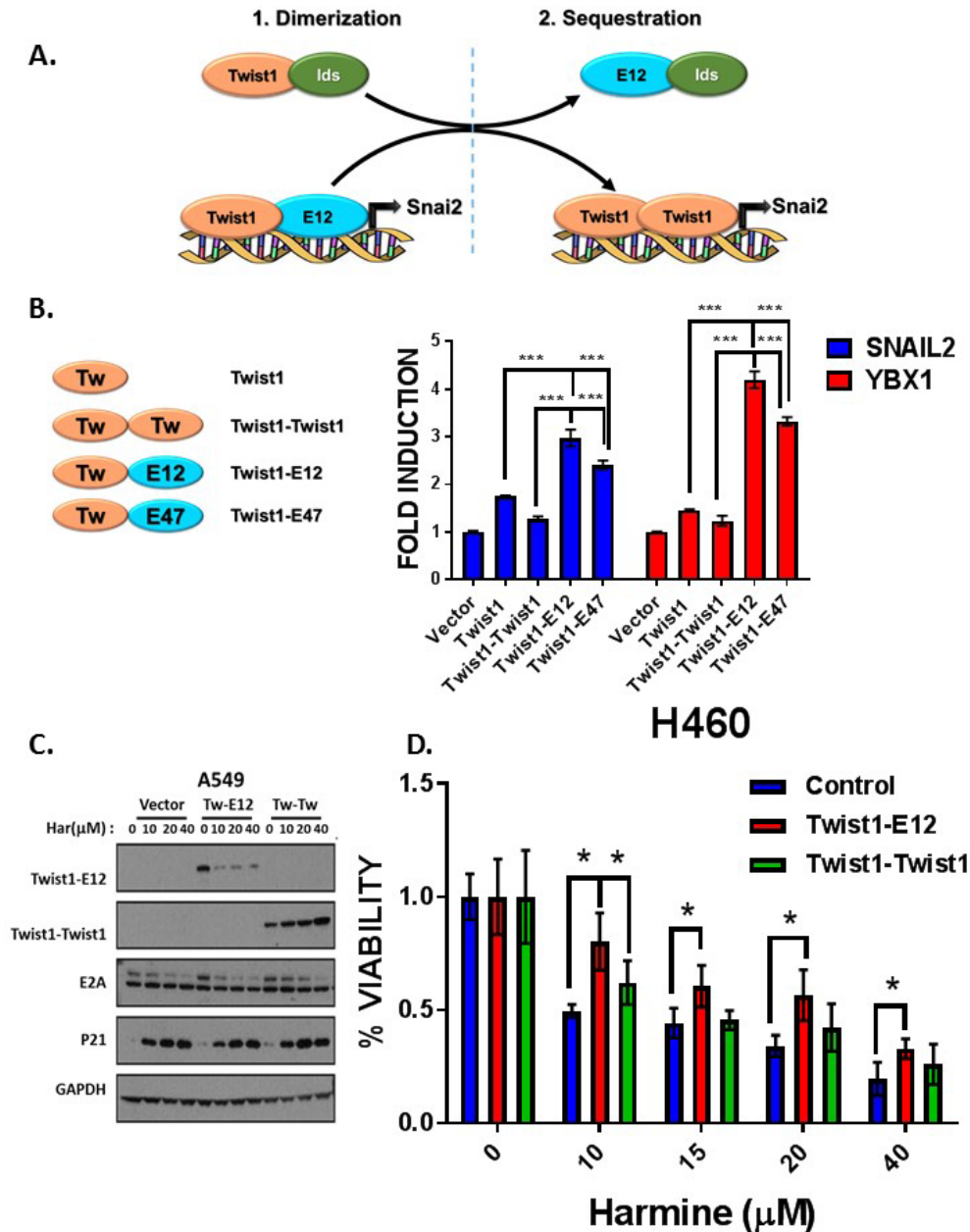


Figure 19: The TWIST1/E2A heterodimer is critical for TWIST1 function and therapeutic response to harmine

(A) Proposed model of potential mechanism(s) of TWIST1/E2A cooperation in tumorigenesis. (B) Luciferase assay showing increased induction of *SNAIL2* and *YBX1* promoter activity in cells transiently overexpressing either Twist1 alone, Twist1-Twist1 homodimer, or Twist1-E12 heterodimer compared to the reporter activity with the vector alone (fold induction = 1) after 48 hours. All luciferase values were normalized to the corresponding renilla luciferase value in each well. Differences were statistically different for each loci for Twist1-E12 or Twist1-E47 versus Twist1 or Twist1-Twist1, ***, $p < 0.0005$, 2-tailed Student's t-test. (C) Western blot demonstrating preferential downregulation of the Twist1-E12 heterodimer in A549 *KRAS* mutant cell line following 48-hour treatment with harmine at the indicated doses. (D) Representative Cell-Titer Glo assay demonstrating that overexpression of Twist1-E12 heterodimer rescues harmine-induced growth inhibition in a *KRAS* mutant NSCLC cell line (H460), while the Twist1-Twist1 homodimer fails to prevent harmine-induced cytotoxicity. Data represent mean \pm SD (n=4 technical replicates). *, $p < .05$, 2-tailed Student's t-test.

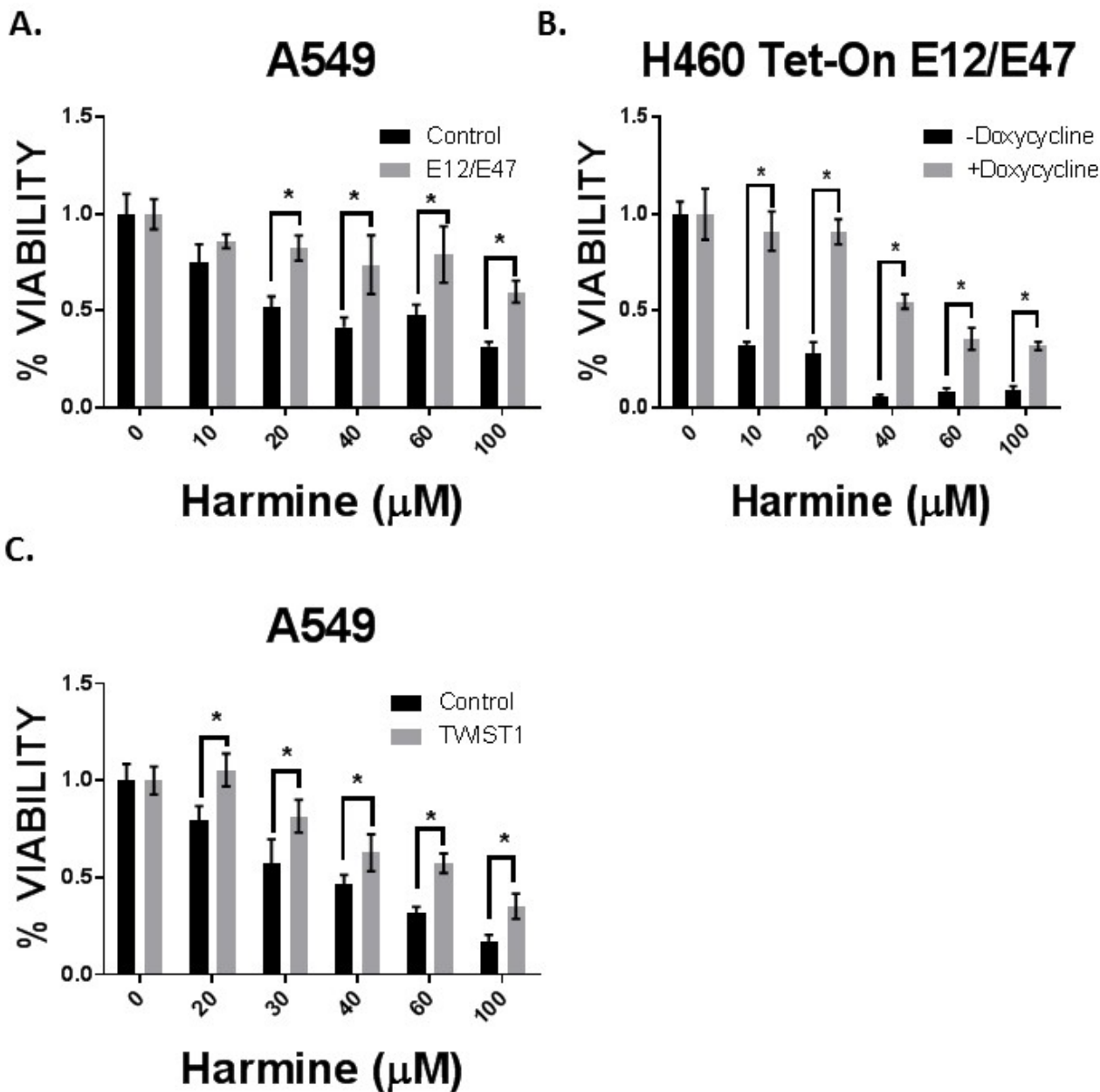


Figure 20: Overexpression of TWIST1 or its binding partner, E2A, rescues harmine induced growth inhibition

(A) MTS assays demonstrating that constitutively or inducibly (B) overexpressing both E12 and E47 partially rescues harmine induced growth inhibition 24 hours following harmine treatment in *KRAS* mutant NSCLC cell lines (A549 and H460). % Viability is normalized to untreated control. Data represent mean \pm SD (n=4 technical replicates). *, p<.05, 2-tailed Student's t-test. (C) Constitutively overexpressing TWIST1 partially rescues harmine induced growth inhibition following 24 hours of harmine treatment. Viability was measured by Cell-Titer Glo assay and percent viability was normalized to untreated control. Data represent mean \pm SD (n=4 technical replicates). *, p<.05, 2-tailed Student's t-test.

2.4.6 Harmine has *in vivo* activity in both transgenic and patient-derived xenograft mouse models of *KRAS* mutant lung cancer

Having observed *in vitro* activity in *KRAS* mutant NSCLC cell lines, we wanted to determine whether harmine would have *in vivo* efficacy in a *Kras*^{G12D}/*Twist1* mouse model of autochthonous lung adenocarcinoma. We treated the *CCSP-rtTA/tetO-Kras*^{G12D}/*Twist1-tetO7-luc* (CRT) mice, which overexpress mutant *Kras* and *Twist1* predominantly in the type II cells of the mouse lung and form lung adenocarcinoma by 15 weeks (233), with harmine for 3 weeks and measured index lung tumor volumes in mice at baseline and weekly with serial micro-computed tomography (microCT). Micro-CT images, comparing tumor volume at baseline and at the end of treatment, revealed that treatment with harmine decreased tumor volume growth (**Figure 21A**). Of note, the antitumor activity of harmine in our *Kras*/*Twist1* transgenic was similar to the tumor stasis seen in the same mice following genetic suppression of *Twist1* expression as we have previously published (233) Additionally, harmine significantly inhibited tumor growth in a patient-derived xenograft (PDX) mouse model of *KRAS* mutant lung cancer (**Figure 22A**). Treatment of the animals with harmine resulted in no change in body weight (data not shown) and no observable toxicity, which was assessed by changes in appetite, activity, coloration, waste elimination, and responsiveness.

We then examined the potential mechanisms of growth inhibition after harmine treatment *in vivo*. We first examined whether a decrease in proliferation was responsible for the observed growth inhibition, however, we observed no significant difference in proliferation rate as measured by Ki-67 staining after harmine treatment (**Figure 21C**). We next examined whether increased apoptosis contributed to the growth inhibitory effects of harmine and we did observe increased apoptosis as measured by cleaved caspase 3 and cleaved PARP with harmine (**Figure**

21B-C, Figure 22B). Most notably, harmine treatment led to marked decrease in Twist1 protein in the mouse lung tumors (**Figure 21C, Figure 22B**). Thus, harmine has cytotoxic effects *in vivo* on *Kras* mutant, *Twist1* overexpressing lung adenocarcinoma, which are accompanied by Twist1 degradation.

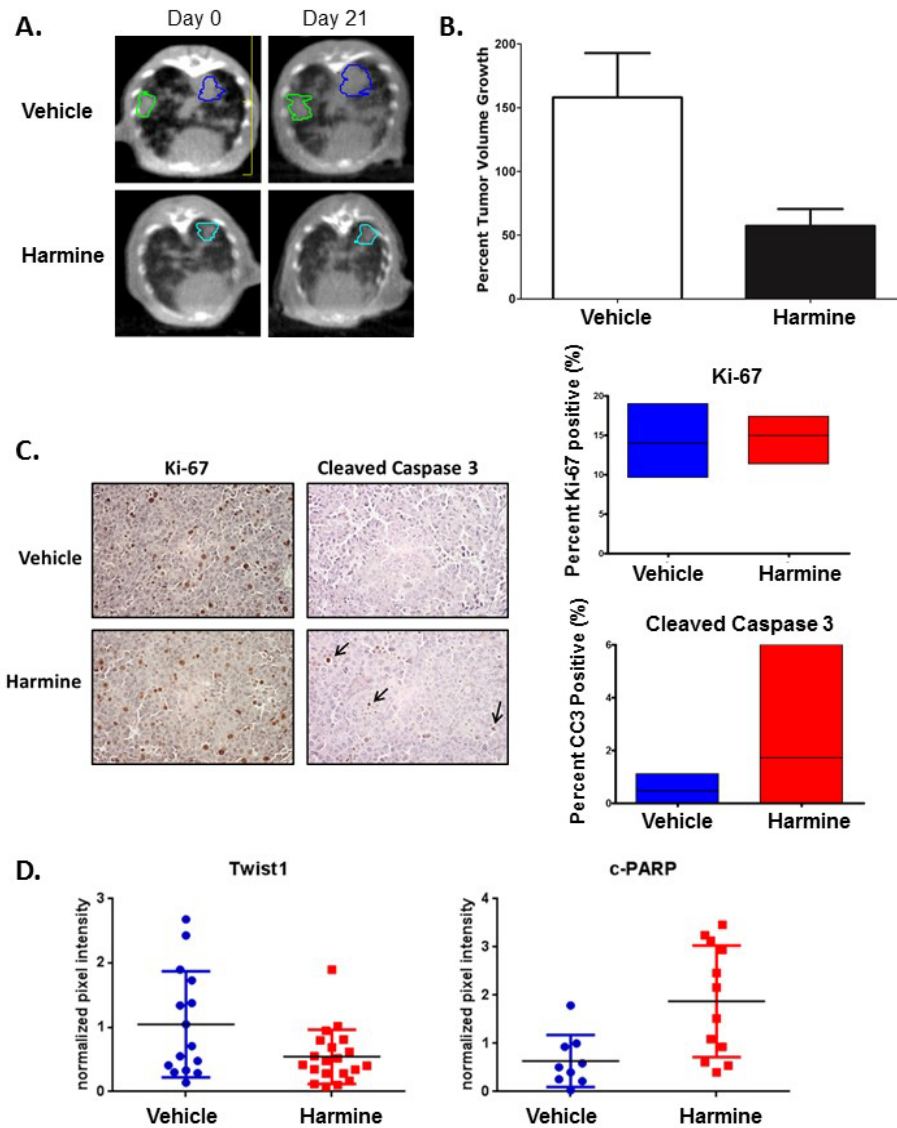


Figure 21: Harmine has activity in *Kras*^{G12D}/*Twist1* mouse model of autochthonous lung adenocarcinoma

(A) Representative microCT images of autochthonous lung tumors showing decreased lung tumor growth 3 weeks following treatment with harmine versus vehicle in the *CCSP-rtTA/tetO-KrasG12D/Twist1-tetO7-luc* (CRT) mice. Contoured lung tumors represent index lesions followed serially for tumor volume quantification. (B) Lung tumor volumes were quantified at baseline and weekly with serial micro-computed tomography (microCT) in the same CRT mice. MicroCT images were reviewed by a board certified radiation oncologist on multiple index tumors in a blinded fashion (n=18 tumors for vehicle from 6 mice and n=16 from 5 mice for harmine). Difference was statistically different using a Mann-Whitney test, P=0.0025. Volumes were normalized to the starting volume, t= 0 before harmine treatment, and percent tumor volume growth was then calculated by (normalized tumor vol. X 100%) - 100%. (C) LEFT: Treatment with harmine results in similar proliferation levels as measured by Ki-67 staining, but increased apoptosis as measured by cleaved caspase 3 staining indicated by black arrows. RIGHT: Quantification and comparison of Ki-67 staining (n=12 tumors for vehicle and n=15 for harmine) (p= 0.3621) and cleaved caspase 3 IHC (n=12 tumors for vehicle and n=16 for harmine) (p= 0.0453). (D) Quantification of Twist1 and cleaved PARP protein levels in vehicle and harmine treated animals at 3 weeks. Proteins were normalized to luciferase protein levels to control for possible differences in tumor burden. Differences were statistically significant (using Student's T-Test) for Twist1 (n=15 tumors for vehicle and n=20 tumors for harmine), P < 0.04 and c-PARP (n=9 tumors for vehicle and n=12 tumors for harmine), P < 0.005 respectively.

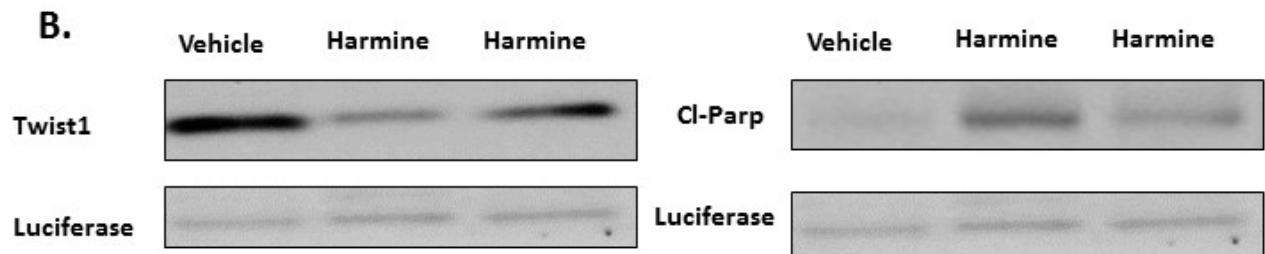
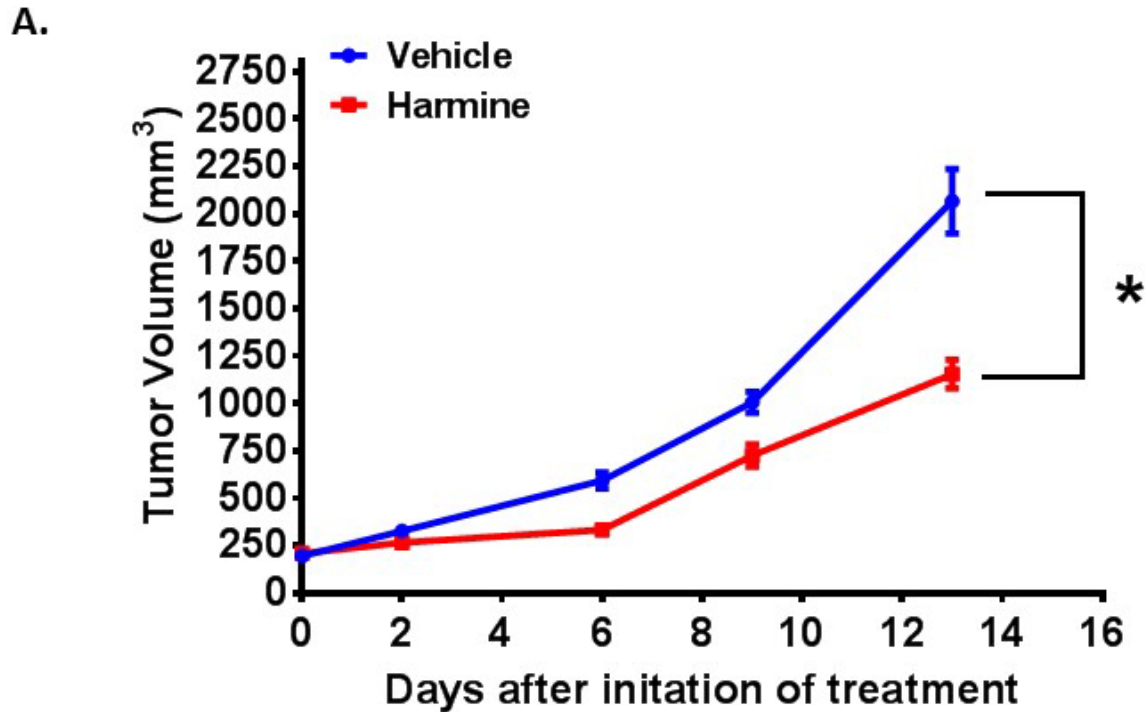


Figure 22: Treatment with harmine decrease tumor growth in a *KRAS* mutant Patient-Derived Xenograph (PDX) model and degrades Twist1 and induces apoptosis in a transgenic mouse model of *Kras* mutant lung cancer

(A) Tumor growth is decreased after 13 days of harmine treatment in the *KRAS* mutant (G12C) PDX model (BM012). Tumor size was monitored twice a week until tumors were approximately 2000 mm³. N = 7 mice in vehicle, and 5 in harmine arms in PDX model. Data represent mean \pm SEM. *, p<.05, 2-tailed Student's t-test. (B) Representative westerns from *CCSP-rtTA/tetO-KrasG12D/Twist1-tetO7-luc* (CRT) murine tumors demonstrating that harmine leads to decreased Twist1 and increased Cl-Parp expression. Tumors were harvested from CRT mice treated with vehicle or harmine for three weeks. Proteins were normalized to luciferase protein levels to control for possible differences in tumor burden.

2.5 DISCUSSION

Using a Connectivity MAP chemical-bioinformatic analysis, we identified multiple compounds that recapitulated the genetic signature of *TWIST1* knockdown. We subsequently assayed seven of the top ranked candidates from this screen for their ability to inhibit multiple *TWIST1*-mediated *in vitro* phenotypes that included single-cell dissemination and suppression of FGF2-dependent branching of mammary epithelial cells in a 3D organoid system. All seven compounds tested were able to inhibit *TWIST1*-mediated dissemination, while the harmala alkaloid compound, harmine, was also able to restore FGF2-dependent mammary epithelial cell branching. We chose to further characterize harmine and demonstrated that it had significant growth inhibitory activity in multiple oncogene-driven NSCLC cell lines. We demonstrated that harmine not only leads to *TWIST1* degradation but also phenocopied the loss of *TWIST1* by inducing either OIS or OIA in previously defined subsets of NSCLC cell lines. Remarkably, in our mouse model of *Kras* mutant, *Twist1* overexpressing lung cancer, harmine had significant antitumor activity, no overt toxicity, and led to decreased expression of *Twist1* protein *in vivo*.

These studies also revealed that *TWIST1* and its binding partners, the E2A proteins, reciprocally regulate the stability of each other. In addition, we demonstrated that genetic silencing of *TCF3* in part phenocopies the loss of *TWIST1*, with loss of *TCF3* expression reactivating latent senescence and apoptotic programs. Our data also suggests that the *TWIST1*-E2A heterodimer, rather than the *TWIST1*-*TWIST1* homodimer, is critical for the transcriptional activation of *TWIST1* target genes important for tumorigenesis. Interestingly, the *TWIST1*-E12 heterodimer has been previously shown to be critical for the ability of *TWIST1* to cooperate with *RAS* to promote mammary tumorigenesis and suppress senescence (248). In addition, the metastatic ability of *TWIST1* in prostate cancer cells requires the ability of *TWIST1* to

heterodimerize with the E2A proteins (265). Our data demonstrated that harmine preferentially induces degradation of the TWIST1-E2A heterodimer rather than the TWIST1-TWIST1 homodimer and degradation of the heterodimer is required for the cytotoxic effects of harmine. Future studies will be aimed at determining the mechanism(s) by which harmine leads to TWIST1 degradation, specifically the TWIST1-E2A heterodimer.

Although harmine was not associated with overt toxicity in our *in vivo* model, harmine has been found to have potentially dose-limiting neurotoxicity in humans (269,276). Previous structure-activity studies have determined that harmine derivatives with substituents at position-2 and -9 can modulate the cytotoxic effects of harmine, while the addition of a bulky substituent at the -7 position can ameliorate the neurotoxicity associated with harmine (268-270,276). Although micromolar range doses were required for harmine-mediated cytotoxicity *in vitro*, it should be noted that we were able to achieve doses *in vivo* that both inhibited tumor growth and promoted TWIST1 degradation without noticeable side effects. Current efforts in our laboratory are ongoing to identify harmine analogues or related compounds that allow for more potent inhibition of TWIST1 transcriptional activity without associated neurotoxicity. Harmine readily crosses the blood brain barrier (BBB) given its small size and hydrophobicity. One strategy we are currently exploring is to limit the neurotoxicity of harmine is via limiting the permeability of harmine across the BBB through the addition of bulky hydrophilic substituents.

In summary, we identified harmine as a first-in-class inhibitor of TWIST1 with broad cytotoxic activity in the three major classes of oncogene-driven NSCLC, *EGFR* mutant, *KRAS* mutant, and *c-MET* amplified/mutant. Given that we have previously established the requirement of TWIST1 for tumorigenesis in oncogene-driven lung cancer with these genetic backgrounds (234), using harmine derivatives may be a viable therapeutic option to treat oncogene-driven

NSCLC both in the treatment-naïve and acquired resistance setting. In addition, as TWIST1 is rarely expressed post-natally (200,201), pharmacological inhibition of TWIST1 may be associated with minimal side-effects. TWIST1 has been implicated in oncogenesis, EMT, metastasis, therapeutic resistance, and tumor stem cell maintenance, across multiple solid tumors including head and neck, lung, breast, and prostate cancers (222,224,247,265,290,291). The use of harmine and potential analogues has far-reaching therapeutic implications given the diverse roles of TWIST1 in tumorigenesis, metastasis, and therapeutic response. For this reason, we are currently screening harmine derivatives that allow for more potent, specific inhibition of TWIST1, which we can bring to the clinic.

3.0 TARGETING THE EMT-TRANSCRIPTION FACTOR TWIST1 OVERCOMES RESISTANCE TO EGFR INHIBITORS IN *EGFR* MUTANT NON-SMALL CELL LUNG CANCER

3.1 ABSTRACT

Patients with *EGFR* mutant non-small cell lung cancer (NSCLC) have significantly benefited from the use of EGFR tyrosine kinase inhibitors (TKIs). However, long-term efficacy of these therapies is limited due to *de novo* resistance (~30%) as well as acquired resistance. Epithelial-mesenchymal transition transcription factors (EMT-TFs), have been identified as drivers of EMT-mediated resistance to EGFR TKIs, however, strategies to target EMT-TFs are lacking. As the third-generation EGFR TKI, osimertinib, has now been adopted in the first-line setting, the frequency of *T790M* mutations will significantly decrease in the acquired resistance setting. Previously less common mechanisms of acquired resistance to 1st generation EGFR TKIs including EMT are now being observed at an increased frequency after osimertinib. Importantly, there are no other FDA approved targeted therapies after progression on osimertinib. Here, we investigated a novel strategy to overcome EGFR TKI resistance through targeting the EMT-TF, TWIST1, in *EGFR* mutant NSCLC. We demonstrated that genetic silencing of *TWIST1* or treatment with the TWIST1 inhibitor, harmine, resulted in growth inhibition and apoptosis in *EGFR* mutant NSCLC. TWIST1 overexpression resulted in erlotinib and osimertinib resistance

in *EGFR* mutant NSCLC cells. Conversely, genetic and pharmacological inhibition of TWIST1 in *EGFR* TKI resistant *EGFR* mutant cells increased sensitivity to *EGFR* TKIs. TWIST1-mediated *EGFR* TKI resistance was due in part to TWIST1 suppression of transcription of the pro-apoptotic BH3-only gene, *BCL2L11* (BIM), by directly binding to *BCL2L11* intronic regions and promoter. As such, pan-BCL2 inhibitor treatment overcame TWIST1-mediated *EGFR* TKI resistance and was more effective in the setting of TWIST1 overexpression. Finally, in a mouse model of autochthonous *EGFR* mutant lung cancer, Twist1 overexpression resulted in erlotinib resistance and suppression of erlotinib-induced apoptosis. These studies establish TWIST1 as a driver of resistance to *EGFR* TKIs and provide rationale for use of TWIST1 inhibitors or BCL2 inhibitors as means to overcome EMT-mediated resistance to *EGFR* TKIs.

Contributors to study: Zachary A. Yochum^{1-2*}, Jessica Cades^{3-5*}, Hailun Wang^{4*}, Suman Chatterjee², Brian W. Simons⁷, James P. O'Brien², Susheel K. Khetarpal², Ghali Lemtiri-Chlieh⁴, Kayla V. Myers², Eric H.-B. Huang², Charles M. Rudin⁶, Phuoc T. Tran^{4-5,7#}, Timothy F. Burns^{1-2#}

* -- denotes these authors contributed equally to the work

-- denotes co-corresponding authors

¹Department of Pharmacology and Chemical Biology, University of Pittsburgh, Pittsburgh, PA

²Department of Medicine, Division of Hematology-Oncology, UPMC Hillman Cancer Center, Pittsburgh, PA.

³Department of Pharmacology, Sidney Kimmel Comprehensive Cancer Center, Johns Hopkins University School of Medicine, Baltimore, MD.

⁴Department of Radiation Oncology and Molecular Radiation Sciences, Sidney Kimmel Comprehensive Cancer Center, Johns Hopkins University School of Medicine, Baltimore, MD, USA

⁵Department of Oncology, Sidney Kimmel Comprehensive Cancer Center, Johns Hopkins University School of Medicine, Baltimore, MD, USA

⁶Department of Medicine, Thoracic Oncology Service, Memorial Sloan Kettering Cancer Center, New York, NY.

⁷Department of Urology, Johns Hopkins University School of Medicine, Baltimore, MD

This work is currently under review for publication:

Yochum, Z.A.*, Cades, J.*, Wang J*, Chatterjee S, Simons BW, O'Brien JP, Khetarpal S.K., Lemtiri-Chlieh G, Christie I, Myers KV, Huang EH, Rudin CM, Tran PT, Burns TF. Targeting the EMT-transcription factor TWIST1 overcomes resistance to EGFR inhibitors in EGFR-mutant non-small cell lung cancer.

* -- denotes these authors contributed equally to the work

3.2 INTRODUCTION

Lung cancer is the leading cause of cancer related death in the United States and worldwide. Despite a 15% five-year survival rate, there have been improvements in the treatment of subsets of non-small cell lung cancer (NSCLC) patients with known targetable molecular drivers such as mutations in *EGFR*, *BRAF* and *MET*, and translocations involving *ALK*, *ROS1*, *RET* and *NTRK1/2* (33,107,114). Previous studies have demonstrated that patients with *EGFR* mutant tumors (~15%) can have a marked response to EGFR tyrosine kinase inhibitors (TKIs). While approximately 70% of patients demonstrate responses to such therapies, long-term efficacy of these therapies is limited due to the inevitability of acquired resistance and frequent

de-novo resistance (~30%) (70,292,293). Efforts to identify drivers of acquired resistance to first generation EGFR TKIs have revealed multiple mechanisms of resistance including *T790M* gatekeeper *EGFR* mutations (~49%), *MET* amplification (~5%), conversion to small-cell lung cancer (~14%), and *PIK3CA* mutations (~5%) (75).

In as many as 20% of patients, epithelial-mesenchymal transition (EMT) or a mesenchymal phenotype is observed at time of resistance to EGFR TKIs including third generation inhibitors, such as osimertinib (75,160,161,294). EMT is a reversible process of transdifferentiation in which epithelial cells lose their polarity and cell-cell interactions and adopt a mesenchymal phenotype (156,157). This process is associated with a variety of pro-tumorigenic functions such as with increased invasion, metastasis, and suppression of failsafe programs of apoptosis and senescence (156,157). Interestingly, the presence of an EMT or mesenchymal phenotype is associated with both *de-novo* as well as acquired resistance to EGFR TKIs (75,295-297). Previous studies have demonstrated that upregulation of AXL, TFG- β , and IGF1R signaling axes are drivers of EMT-mediated acquired resistance to EGFR TKIs (161,165-167). Recent studies have implicated EMT-transcription factors (EMT-TFs), which are drivers of global transcriptional changes that lead to EMT, in resistance to targeted therapies in *EGFR* mutant NSCLC (163). Specifically, upregulation of the EMT-TFs, SNAI2 and ZEB1, have been shown to can confer resistance to EGFR TKIs (162,164,298). However, the mechanism(s) by which these EMT-TFs mediate resistance and therapeutic strategies to target these EMT-TFs have been lacking.

We have previously demonstrated that the EMT-TF, TWIST1, is required for oncogene-driven NSCLC (Chapter 2) (234). In multiple oncogene-driver dependent settings, including tumors with *EGFR* mutations, TWIST1 functions to suppress oncogene-induced senescence and

apoptosis (232,234,299). In addition to suppressing failsafe programs, TWIST1 has also been shown to promote EMT, metastasis, and therapeutic resistance (238,249,252,254). We have also identified a first-in-class inhibitor of TWIST1, harmine that has marked antitumor activity in oncogene-driven NSCLC including *EGFR* mutant NSCLC (232). In the current study, we demonstrated genetic and pharmacological inhibition of TWIST1 resulted in growth inhibition and apoptosis in *EGFR* mutant NSCLC cell lines, including cells with acquired resistance *T790M* mutations. We also identified TWIST1 as a driver of resistance to EGFR TKIs in EGFR TKI naïve *EGFR* mutant NSCLC cell lines as well as in EGFR TKI acquired resistant cell lines with *T790M* mutations. We further demonstrated that TWIST1 induces EGFR TKI resistance in a transgenic mouse model of autochthonous *EGFR* mutant lung cancer. We have identified that one mechanism by which TWIST1 mediates resistance is through suppression of EGFR TKI-induced apoptosis by directly binding to the promoter and intronic regions of the pro-apoptotic BH3-only gene, *BCL2L11* (BIM) and repressing *BCL2L11* transcription. Additionally, we demonstrated that TWIST1-mediated EGFR TKI resistance can be overcome with either a BCL-2/BCL-XL inhibitor, or the TWIST1 inhibitor harmine, suggesting that targeting TWIST1 in the clinic may be a viable option to overcome EMT-mediated resistance to EGFR TKIs.

3.3 MATERIAL AND METHODS

3.3.1 Cell lines and reagents

PC9, H1975, H1650, Hcc4006, Hcc4011, Hcc2935, Hcc827, H3255, and embryonic kidney cell line HEK 293T were acquired from the American Type Culture Collection (ATCC) and were

cultured in the recommended ATCC media. Hcc827R2 and 11-18 cells were obtained from Dr. Christine Lovly (Vanderbilt University) and cultured in the recommended media. The identity of the aforementioned cell lines was verified by autosomal STR (short tandem repeat) profiling done at University of Arizona Genetics Core (UAGC). Cell lines were tested for mycoplasma every six months using MycoAlert Detection Kit (Lonza). Osimertinib and erlotinib were purchased from Selleck Chemicals (Houston, TX). Harmine was purchased from Sigma-Aldrich (St. Louis, MS). ABT-737 was purchased from ApexBio Technology (Houston, TX).

3.3.2 Quantification of caspase-3/7 activity

Cells were seeded at appropriate density in 25-cm² plates and incubated for 24 hours. Following incubation, cells were treated with harmine at 0, 20, 40 μ M for 48 hours. Apoptosis was analyzed as previously described in Chapter 2.3.12.

3.3.3 Quantitative RT-PCR

RNA isolation, cDNA generation, and cDNA amplification using PowerUpTM SYBR[®] Green Master Mix (Perkin Elmer Applied Biosystems) and TaqMan[®] Universal PCR Master Mix (Perkin Elmer Applied Biosystems) were carried out as previously described in Chapter 2.3.5. Primer list is available in Table 1-2 (Appendix A).

3.3.4 Cell proliferation assays

For all viability experiments, cells were seeded at an appropriate density in 96 well plates and incubated for 24 hours. Cells were subsequently treated with a range of doses of the appropriate inhibitor for 72 hours. Viability was determined using the CellTiter96® Aqueous One Solution Cell Proliferation Assay kit (Promega) or Cell-Titer Glo 2.0 Assay (Promega) according to manufacturer's protocol. Data was analyzed as previously described in Chapter 2.3.2. All experiments were performed at least twice to ensure consistent results.

3.3.5 Western blot and antibodies

Following appropriate treatment, cells were harvested and lysed and subsequent protein was quantified and western blotting was performed as previously described (234). All information on antibodies is included in Table 3 (Appendix A). Western blot experiments were performed at least twice unless otherwise stated.

3.3.6 Chromatin immunoprecipitation

H1975 TRE3G-TWIST1 cells were seeded in 15cm dishes and incubated for 24 hours. Cells were treated with 50ng/ml of doxycycline. Following 24 hours of doxycycline treatment, cells were harvested and Chromatin Immunoprecipitation (ChIP) was performed using SimpleChIP Enzymatic Chromatin IP Kit (Cell Signaling Technology) according to manufacturer's recommendations. ChIP primers that were used are included in Table 7 (Appendix A). For ChIP,

2 μ g of ChIP-grade TWIST1 antibody (Abcam, Ab5087) and 2 μ g Mouse IgG, Whole Molecule Control (Thermo Scientific, 31903) were used.

3.3.7 Lentiviral shRNA and cDNA overexpression

293T cells were seeded at a density of 4 X 10⁶ in 25-cm² flasks. Following a 24 hour incubation period, cells were transfected to generate lentivirus using a four -plasmid system according to the TRC Library Production and Performance protocols, RNAi Consortium, Broad Institute (264) and as previously described (234). A complete list of the constructs used is in Supplementary Tables 4-6 (Appendix A) and sequences of these constructs and primers used are available upon request.

3.3.8 Transgenic mice

Mice were housed in groups of no more than five per cage with free access to food and water, under controlled light/dark cycles, in facilities with regulated temperature and humidity. Mice were randomly assigned to different experimental groups.

Inducible *EGFR*^{L858R} and *Twist1/EGFR*^{L858R} transgenic mice in the FVB/N inbred background were of the genotype: *CCSP-rtTA/tetO-EGFR*^{L858R} (CE) or *CCSP-rtTA/tetO-EGFR*^{L858R}/*Twist1-tetO-luc* (CET). The *tetO-EGFR*^{L858R} mice were obtained from Dr. Katerina Politi (Yale University). All the mice were weaned at 3–4 weeks of age and then placed on doxycycline (DOX) drinking water at 4–8 weeks of age as previously described (299,300). After three weeks of DOX treatment, mice were randomized to vehicle and erlotinib treatment groups after

ensuring similar levels of tumor burden with micro-CT. Micro-CT imaging and quantification of tumor burden was performed as previously described (299). Erlotinib was purchased from Selleckchem (Houston, TX). For *in vivo* experiments, erlotinib was dissolved into a slurry in 0.5% methylcellulose. The mice received 50 mg/kg erlotinib or vehicle via oral gavage 6 days a week for 3 weeks.

3.3.9 Histology and immunohistochemistry

Tissues were fixed and subsequent histology and immunohistochemistry was performed as previously described (301). For immunohistochemistry, the primary antibodies were used at the following concentrations: Twist1 at 1:200, vimentin and E-cadherin at 1:400; cleaved caspase 3 at 1:500, and Ki-67 at 1:2000.

3.4 RESULTS

3.4.1 Genetic or pharmacologic inhibition of TWIST1 results in growth inhibition and apoptosis in *EGFR* mutant NSCLC

We previously observed that TWIST1 expression is required for tumorigenesis in oncogene-driven NSCLC as inhibition of *TWIST1*, in oncogene driver-defined NSCLC cell lines, results in activation of latent senescence and/or apoptotic programs (232,234,299). To more comprehensively test the role of TWIST1 in *EGFR* mutant lung cancers, we infected a panel of *EGFR* mutant lines with shRNAs targeting *TWIST1* or with scrambled control shRNA.

Silencing of *TWIST1* results in growth inhibition in the majority of lines screened (**Figure 23**). We have previously identified and characterized a novel *TWIST1* inhibitor, harmine that had antitumor activity in oncogene driver-defined NSCLCs, inhibited multiple *TWIST1*-dependent functions, and induced degradation of *TWIST1* (232). Similar to our previous findings in a limited number of *EGFR* mutant cell lines, harmine markedly inhibited growth across the large panel of *EGFR* mutant NSCLC cell lines, including *EGFR* TKI resistant lines, similar to the effects seen following silencing of *TWIST1* (**Figure 23**). While we have previously observed that genetic and pharmacological inhibition of *TWIST1* primarily results in oncogene-induced senescence (OIS) (232,234,299), there was a subset of cell lines that appeared more dependent on *TWIST1* expression for survival and underwent apoptosis following inhibition of *TWIST1* (232,234). We identified a subset of *EGFR* mutant cell lines (H1975 and PC9) that underwent apoptosis following knockdown of *TWIST1* and harmine treatment (**Figure 24A-B**). PC9 cells have an *EGFR* TKI sensitizing *EGFR* exon 19 deletion ($\Delta E746-A750$) and H1975 cells have both *EGFR* TKI sensitizing *L858R* mutation and an acquired resistance *T790M* mutation, suggesting that targeting *TWIST1* may be an effective therapeutic target for *EGFR* mutant disease in both the *EGFR* TKI naïve and *EGFR* TKI acquired resistance setting. Of note, genetic and pharmacologic inhibition of *TWIST1* (**Figure 23-24**) was also effective in the setting of *T790M* independent resistance such as in the *EGFR* TKI resistant cell line H1650 (137).

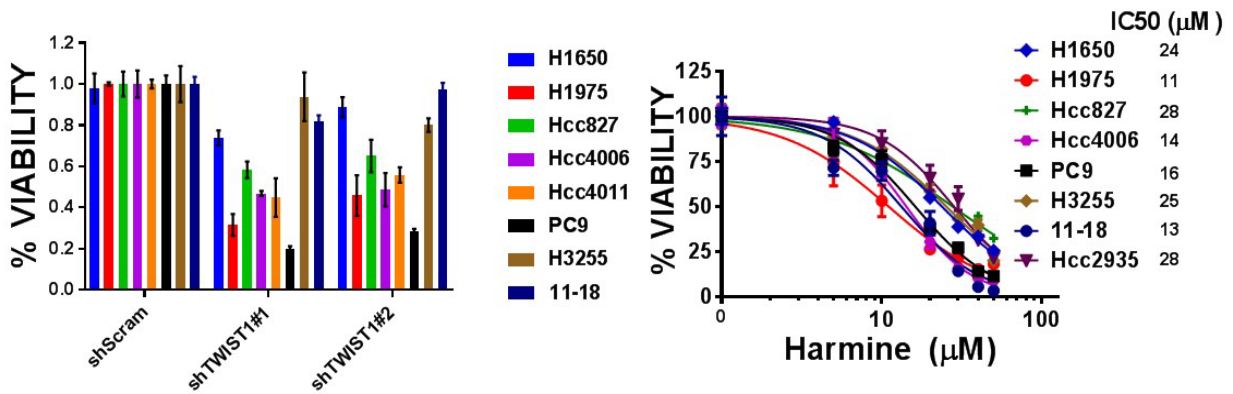
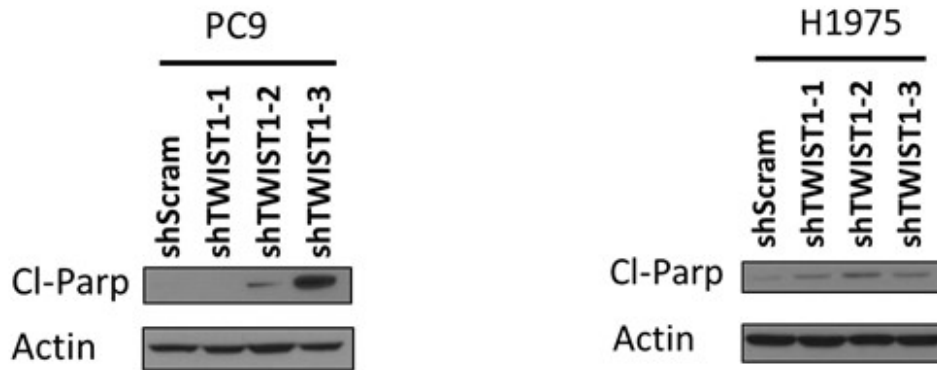


Figure 23: TWIST1 is required for *EGFR* mutant NSCLC

LEFT: Cell-Titer Glo assays demonstrating that knockdown of TWIST1 results in growth inhibition in a panel of *EGFR* mutant NSCLC cell lines. Cells were infected with shScram or shRNA targeting *TWIST1* (shTWIST1 #1, #2) for 6 days. Viability data was normalized to shScram control. Data represent mean \pm SD (n=4 technical replicates). Differences were statistically significant for each cell line for shScram versus shTWIST1#1 or shTWIST1#2, except for H1650 shScram versus shTWIST1#2, H3255 shScram versus shTWIST1#1, and 11-18 shScram versus shTWIST1#1/2, $p < .01$, 2-tailed Student's t-test. RIGHT: MTS assays demonstrating that harmine has activity in a panel of *EGFR* mutant NSCLC cells. Cells were treated with harmine for 72 hours. Data represent mean \pm SD (n=4 technical replicates).

A.



B.

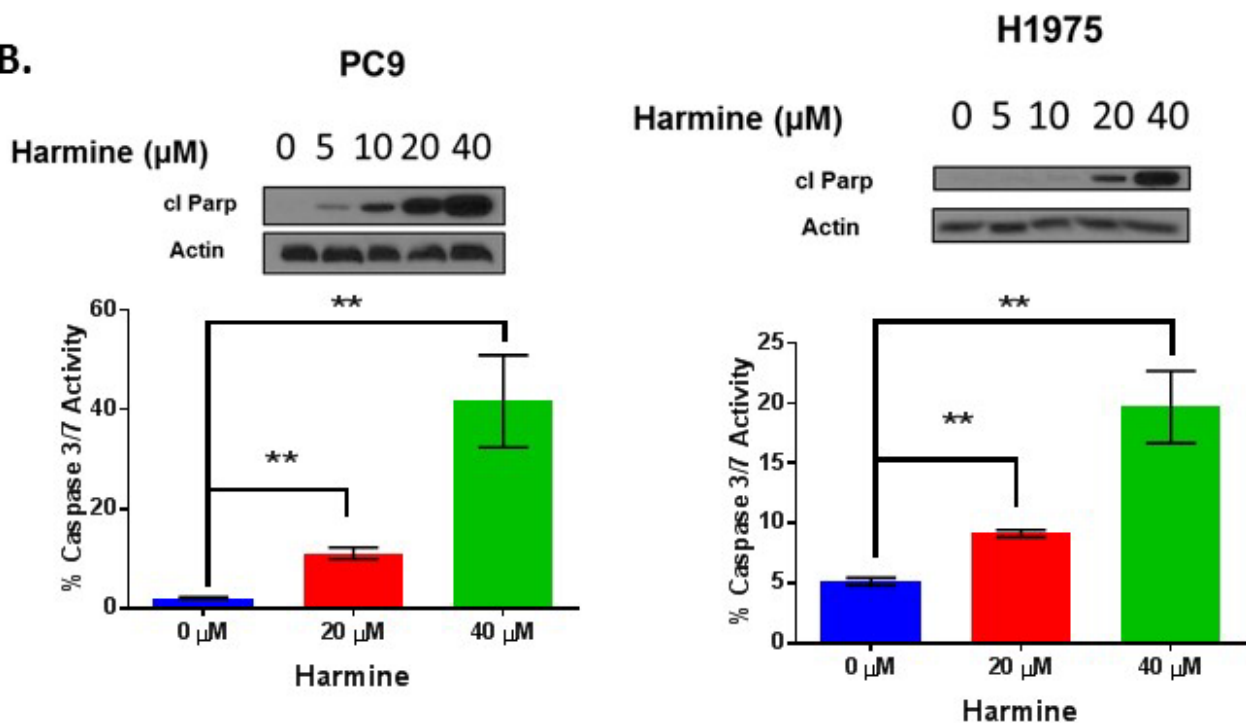


Figure 24: Inhibition of TWIST1 induces apoptosis in a subset of *EGFR* mutant NSCLC cell lines

(A) Western blot demonstrating that knockdown of TWIST1 induces apoptosis in PC9 cells with EGFR TKI sensitizing *EGFR* exon 19 deletion (*ΔE746-A750*) and H1975 cells with both EGFR TKI sensitizing *L858R* mutation and an acquired resistance *T790M* mutation. Cells were infected with shScram and shRNA targeting *TWIST1* (shTWIST1 #1-3) for 72 hours (PC9) or 6 days (H1975) and harvested for Western blot analysis. (B) UPPER: Western blots demonstrating that harmine treatment results in PARP cleavage in PC9 and H1975 cells. Cells were treated with harmine for 48 hours and harvested for Western blot analysis. LOWER: Active Caspase 3-7 staining demonstrating induction of apoptosis in PC9 and H1975 following 48 hours of harmine treatment. Data represents mean \pm SD (n=3 biological replicates). **, p<.01, 2-tailed Student's t-test.

3.4.2 TWIST1 is necessary and sufficient for EGFR TKI resistance in a subset of *EGFR* mutant NSCLC cell lines

Recent evidence has suggested that EMT-TFs mediate resistance to EGFR targeted therapy in lung cancer (162,164,298,302). TWIST1 has been implicated in chemoresistance in lung cancer and other cancer types (247,254,303,304). Given the requirement of TWIST1 for *EGFR* mutant NSCLC and its role in suppressing OIS and apoptosis in NSCLC, we investigated whether enforced TWIST1 expression would be sufficient to cause resistance to EGFR TKIs, using a panel of doxycycline inducible TWIST1 overexpressing *EGFR* mutant NSCLC cell lines. TWIST1 overexpression in these lines was sufficient to cause resistance to both 1st and 3rd generation EGFR TKIs (**Figure 25A-B**). Additionally, we observed that TWIST1-mediated resistance was associated with suppression of EGFR TKI-induced apoptosis in cells with and without the *T790M EGFR* gatekeeper mutation (**Figure 26**).

To investigate the requirement of TWIST1 for erlotinib resistance, we first assessed relative expression of TWIST1 in a panel of *EGFR* mutant TKI sensitive and resistant cell lines. We identified an *EGFR* mutant cell line, H1650 that had increased levels of TWIST1 mRNA and protein (**Figure 27A**). Interestingly, this cell line demonstrates *de-novo* resistance to EGFR TKIs (137). We found that genetic silencing of *TWIST1* increases sensitivity of this cell line to erlotinib (**Figure 27B**). We observed a similar increase of sensitivity to erlotinib when used in combination with our small molecule TWIST1 inhibitor, harmine (**Figure 27C**). This increase in erlotinib sensitivity corresponded to increased apoptosis and BIM expression with decreased TWIST1 expression following harmine and erlotinib co-treatment (**Figure 27C**). We also investigated the role of TWIST1 in mediating resistance in an *EGFR* mutant NSCLC cell line (HCC827R2) with acquired resistance to erlotinib (139). Although TWIST1 was not increased in

the resistant cell line compared to the parental cell line, we observed that this cell line maintained a requirement for TWIST1 expression and that targeting TWIST1 in these cells increased sensitivity to erlotinib (**Figure 28**). These observations indicate that inhibiting TWIST1 may be a viable target in erlotinib resistance settings in which TWIST1 is expressed.

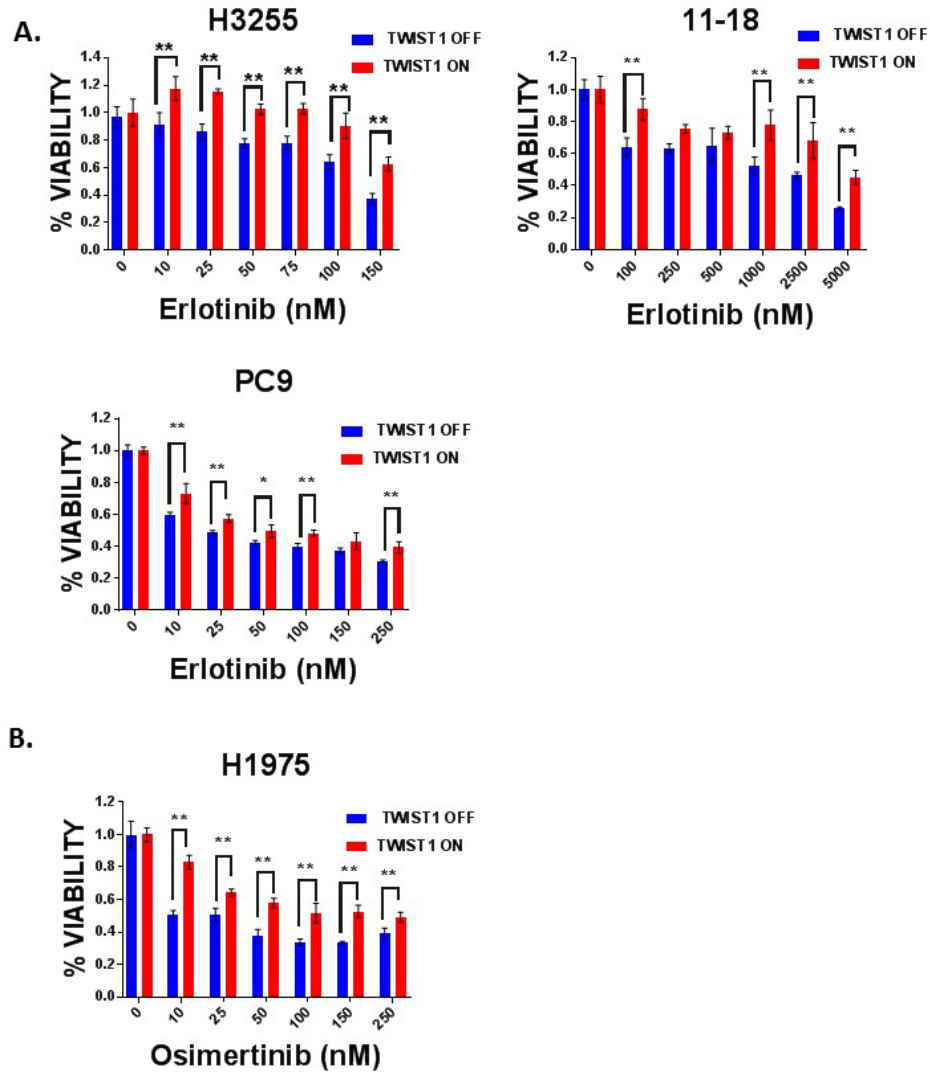


Figure 25: TWIST1 overexpression is sufficient to mediate resistance to EGFR TKIs

(A) UPPER: MTS or Cell-Titer Glo assays demonstrating that TWIST1 overexpression results in decreased response to erlotinib. H3255 TRE3G-TWIST1 (UPPER LEFT), 11-18 TRE3G-TWIST1 (UPPER RIGHT), and PC9 TRE3G-TWIST1 (LOWER) were pre-treated with doxycycline for 72 hours and then treated with doxycycline and erlotinib for 72 hours. Data represent mean \pm SD (n=4 technical replicates). *, P<.05, **, P<.01, 2-way ANOVA, followed by Tukey's Test. (B) MTS assay demonstrate that TWIST1 overexpression decreases response to osimertinib. H1975 TRE3G-TWIST1 were pre-treated with doxycycline for 72 hours prior to a 72-hour treatment with osimertinib. Data represent mean \pm SD (n=4 technical replicates). *, P<.05, **, P<.01, 2-way ANOVA, followed by Tukey's Test.

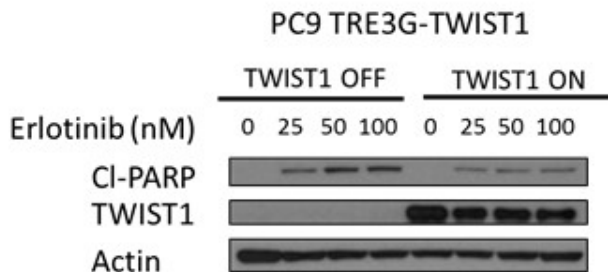
A.**B.**

Figure 26: TWIST1 overexpression suppresses EGFR TKI-induced apoptosis in *EGFR* mutant NSCLC cell lines

(A) Western blot demonstrating that TWIST1 overexpression decreases erlotinib-induced apoptosis as measured by PARP cleavage. PC9 TRE3G-TWIST1 cells were pre-treated with doxycycline (1000ng/ml) for 72 hours prior to a 48-hour treatment with erlotinib. (B) Western blot demonstrating that TWIST1 overexpression decreases osimertinib-induced apoptosis as measured by PARP cleavage. H1975 TRE3G-TWIST1 cells were pre-treated with doxycycline (50g/ml) for 72 hours prior to a 48-hour treatment with osimertinib.

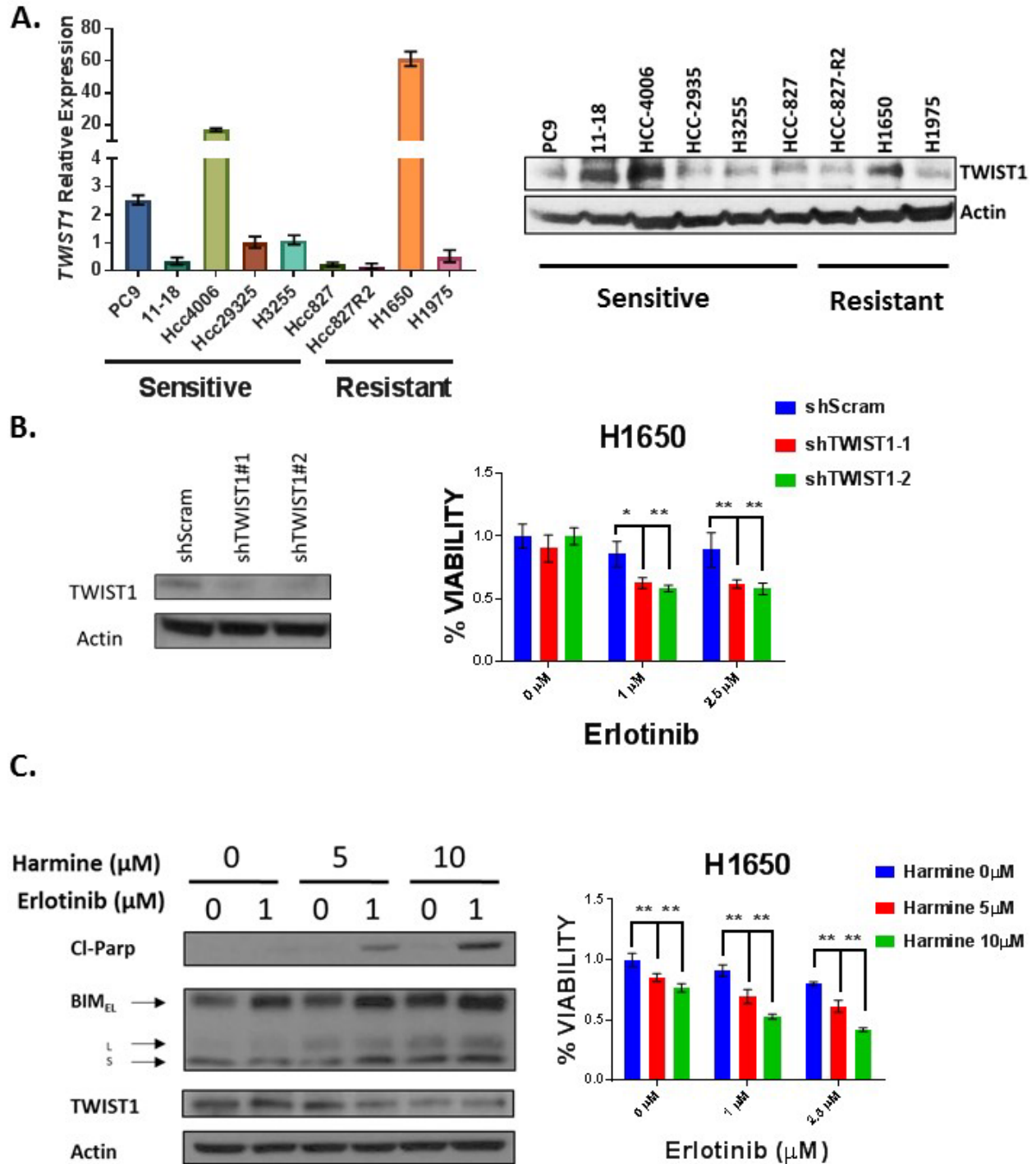
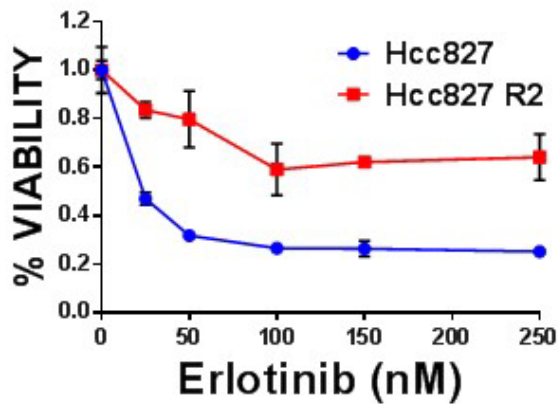


Figure 27: Inhibition of TWIST1 is sufficient to overcome EGFR TKI resistance

A) Quantitative RT-PCR demonstrating baseline *TWIST1* mRNA (LEFT) and protein (RIGHT) levels in a panel of erlotinib sensitive and resistant *EGFR* mutant NSCLC cells. RT-PCR was normalized to Hcc2935 *TWIST1* mRNA levels. Data represent mean \pm SD (n=3 technical replicates). (B) LEFT: Western blot demonstrating shRNA targeting *TWIST1* decreases *TWIST1* levels. The erlotinib resistant cell line, H1650 was infected with the indicated shRNA and harvested six days following infection for Western analysis. RIGHT: MTS assay demonstrating that knockdown of *TWIST1* in H1650 cells can re-sensitize cells to erlotinib. H1650 cells which harbor both *EGFR* and *PTEN* mutations, were infected with the indicated shRNAs for 48 hours and subsequently treated with erlotinib for 72

hours. Data represent mean \pm SD (n=4 technical replicates). *, P<.05, **, P<.01, 2-way ANOVA, followed by Tukey's Test. (C) LEFT: Western blot demonstrating that the combination of harmine and erlotinib results in increased apoptosis as measured by PARP cleavage as well as BIM expression, and decreased TWIST1 expression. H1650 cells were treated with the indicated doses of harmine and erlotinib for 48 hours and harvested for Western analysis. RIGHT: MTS assay demonstrating that harmine treatment increases H1650 cell sensitivity to erlotinib. Cells were treated with the indicated doses of harmine and erlotinib for 48 hours. Data represent mean \pm SD (n=4 technical replicates). *, P<.05, **, P<.01, 2-way ANOVA, followed by Tukey's Test.

A.



B.

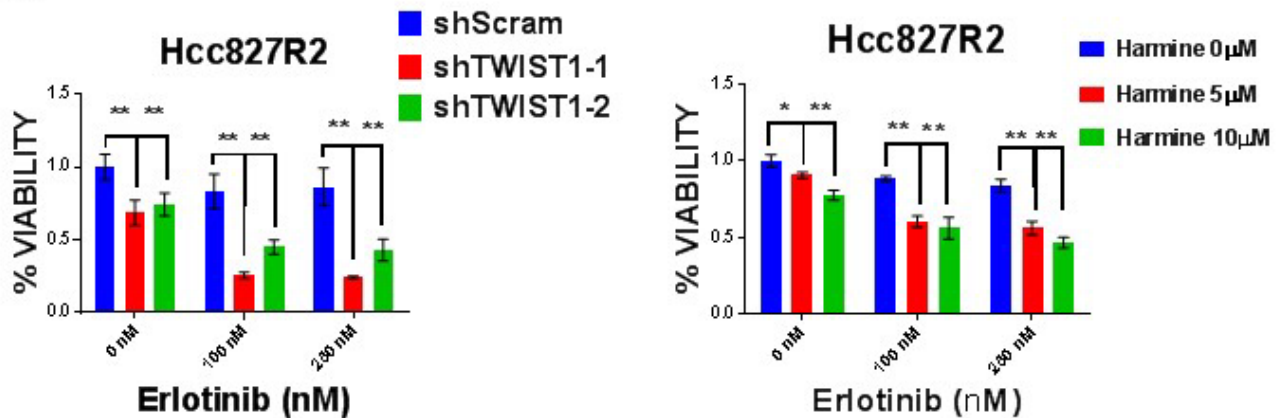


Figure 28: Inhibition of TWIST1 can overcome acquired resistance to erlotinib

(A) MTS assay demonstrating that Hcc827R2 cells, that harbor both an *EGFR* mutation and *MET* amplification are resistant to erlotinib. Cells were treated at the indicated doses of erlotinib for 72 hours. Data represent mean \pm SD (n=4 technical replicates). (B) LEFT: MTS assay demonstrating that knockdown of TWIST1 in Hcc827R2 cells can resensitize cells to erlotinib. Hcc827R2 cells were infected with the indicated shRNAs for 48hrs, and subsequently treated with erlotinib for 72hrs. Data represent mean \pm SD (n=4 technical replicates). RIGHT: MTS assay demonstrating that harmine treatment can partially resensitize Hcc827R2 cells to erlotinib. Hcc827R2 cells were treated for 48 hours with the indicated doses of harmine and erlotinib. Data represent mean \pm SD (n=4 technical replicates). Data represent mean \pm SD (n=4 technical replicates). 2-tailed Student's t-test. *, P<.05, **, P<.01.

3.4.3 TWIST1 suppresses BIM expression

Previous studies have established that response to oncogene targeted therapies requires BIM expression and loss of BIM expression is associated with EGFR TKI resistance in patients (139,186,190,191,305). BIM expression is regulated both transcriptionally and post-translationally (306). We investigated whether TWIST1 could regulate BIM expression in *EGFR* mutant NSCLC cell lines. We found that knockdown of TWIST1 resulted in increased *BCL2L1* (BIM gene) mRNA and protein expression of BIM (**Figure 29A**). In the cell lines in which TWIST1 was sufficient to mediate erlotinib resistance, we demonstrated that TWIST1 overexpression resulted in suppression of mRNA and protein expression of BIM (**Figure 29B-C**). To evaluate whether TWIST1 decreased BIM expression through a post-translational mechanism, we performed a pulse-chase experiment and demonstrated that TWIST1 did not decrease BIM half-life, suggesting that TWIST1 negative regulation of BIM expression is primarily at the mRNA level (**Figure 30**). To explore whether TWIST1 was directly repressing the transcription of *BCL2L1*, we performed TWIST1 ChIP on the promoter region and intron 1 which contained multiple E-box binding sites (CANNTG), the putative consensus binding site for TWIST1. We also performed TWIST1 ChIP on a putative TWIST1 binding site contained within the *BCL2L1* genomic region in intron 12 previously identified on a global TWIST1 ChIP analysis (285). We identified that TWIST1 bound to one site upstream of the transcriptional start site (BS1) and a site in intron 12 (BS5) (**Figure 29D**). Interestingly, in the regions flanking the E-boxes found at the BS1 and BS5 sites, there are predicted binding sites for nuclear factor-1 (NF-1), while these predicted sites are not found at the other E-box sites investigated. Although no previous studies have implicated NF-1 in TWIST1 target gene regulation, NF-1 has been implicated in tumorigenesis through its ability to regulate chromatin structure and DNA

accessibility (307). TWIST1 binding specifically to these sites may be influenced by the presence of other transcription factors, such as NF-1. Overall, these studies establish BIM as a novel target gene of TWIST1.

While others have previously established the requirement of BIM for response to EGFR TKIs (186,190,191,305), we confirmed that in H1975 cells that BIM expression was required for response to osimertinib (**Figure 29E**). As BIM is required for EGFR TKI-induced apoptosis (186,190), we examined whether inhibition of anti-apoptotic BCL2 family members with the BCL-2/BCL-XL inhibitor (ABT-737) would be effective in TWIST1 overexpressing *EGFR* mutant NSCLC. We observed that BCL2/BCLXL inhibitor (ABT-737) was able to overcome TWIST1-mediated resistance to osimertinib in H1975 TWIST1 overexpression cells (TWIST1-ON) but did not affect osimertinib sensitivity in the absence of TWIST1 (TWIST-OFF) (**Figure 29F**). These data suggest that TWIST1-mediated resistance may be overcome through use of BH3 mimetics and that these therapies may be more effective in TWIST1 overexpressing *EGFR* mutant NSCLC cells.

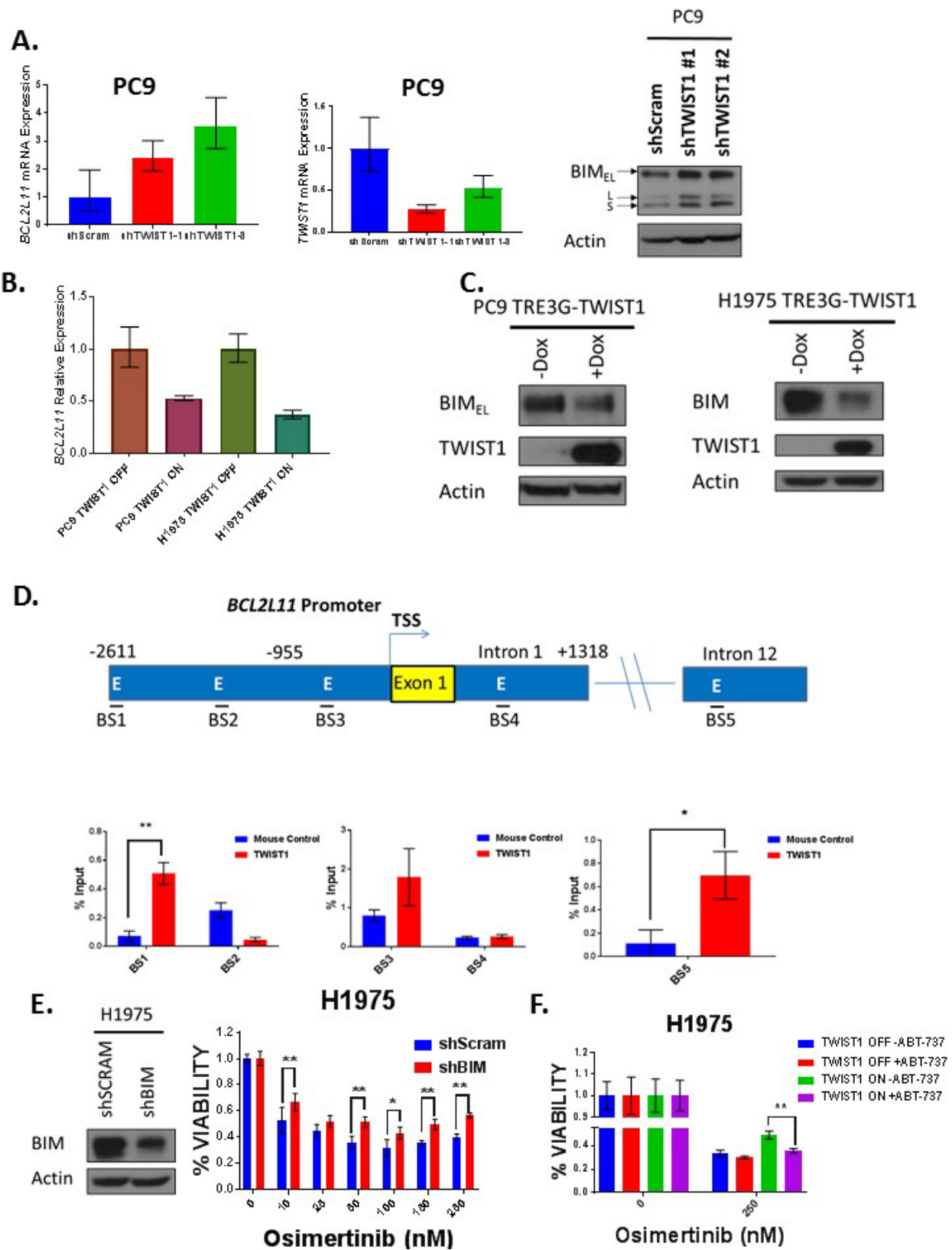


Figure 29: TWIST1 suppresses BIM expression by directly suppressing its transcription

(A) LEFT: Quantitative RT-PCR (qRT-PCR) demonstrating increased *BCL2L11* mRNA levels following knockdown of TWIST1. PC9 cells were infected with the indicated shRNA for 24 hours. Data represent mean \pm SD (n=3 technical replicates). RIGHT: Western blot demonstrating that knockdown of TWIST1 increased BIM protein levels. PC9 cells were infected with the indicated shRNA for 72 hours. **(B)** qRT-PCR demonstrating that TWIST1 overexpression decreased *BCL2L11* mRNA levels. PC9 TRE3G-TWIST1 cells and H1975 TRE3G-TWIST1 were treated with doxycycline for 24 hours. Data represent mean \pm SD (n=3 technical replicates). **(C)** Western blot demonstrating that TWIST1 overexpression decreased BIM protein levels. PC9 TRE3G-TWIST1 cells and H1975 TRE3G-TWIST1 were treated with doxycycline for 72 hours. **(D)** ChIP assay demonstrating TWIST1 binding to promoter and intronic regions of *BCL2L11*. UPPER: Model demonstrating E-box sites within the *BCL2L11* promoter, Intron 1, and Intron 12 that were interrogated for TWIST1 binding. LOWER: qRT-PCR demonstrating that TWIST1 is enriched at multiple sites within the *BCL2L11* promoter and intronic regions. Data represent mean \pm SD (n=3 technical replicates). *, P<.05, **, P<.01. 2-tailed Student's t-test. **(E)** LEFT: Western blot demonstrating that shRNA targeting BIM decreased BIM expression. RIGHT: MTS assay demonstrating decreased response to osimertinib following knockdown of BIM in H1975 cells. H1975 cells that stably express shScram or shBIM were treated with osimertinib for 72 hours. Data represent mean \pm SD (n=4 technical replicates). *, P<.05, **, P<.01, 2-way ANOVA, followed by Tukey's Test. **(F)** MTS assay demonstrating that TWIST1-mediated resistance to osimertinib can be overcome with ABT-737. H1975 TRE3G-TWIST1 cells were pre-treated with doxycycline for 72 hours and then co-treated with osimertinib and ABT-737 (1 μ M) \pm doxycycline for 72 hours. Data represent mean \pm SD (n=4 technical replicates). **, P<.01, 2-way ANOVA, followed by Tukey's Test.

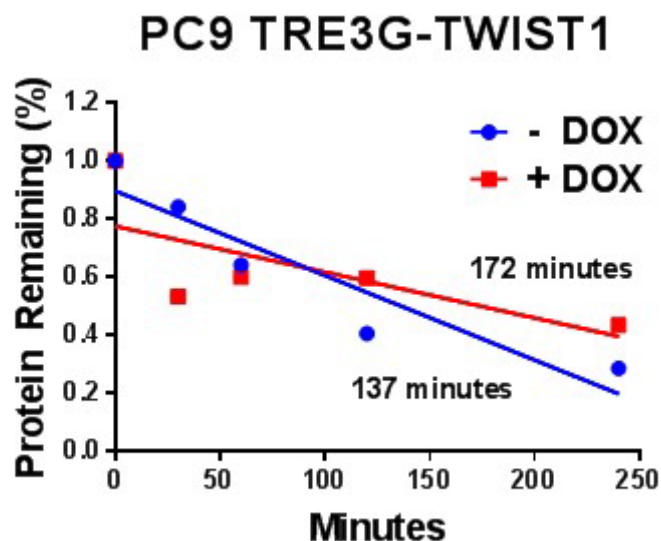


Figure 30: TWIST1 overexpression does not decrease BIM protein half-life

TWIST1 overexpression in PC9 TRE3G-TWIST1 cells does not marked alter BIM protein half-life. PC9 TRE3G-TWIST1 cells were treated for 72 hours with doxycycline (500ng/ml). Cells were then treated with cyclohexamide (50 mg/ml) and harvested at the indicated time points. Media without doxycycline was used as a control. Protein levels were determine using Image J densitometry and BIM protein half-life for –DOX and + DOX groups was estimated using linear regression analysis.

3.4.4 Creation and characterization of an autochthonous *EGFR* mutant *Twist1*

overexpression lung tumor mouse model

We previously demonstrated that *Twist1* could cooperate with mutant *Kras* for lung tumorigenesis and that genetic or pharmacologic inhibition of *Twist1* in this model inhibited growth of these lung tumors (232,234,299). To investigate whether EMT and *Twist1* could impart erlotinib resistance to *EGFR* mutant NSCLCs *in vivo* we made use of transgenic *EGFR^{L858R}* and *Twist1* inducible mouse models (299,300). Both of these strains are well established doxycycline inducible lung specific transgenic mouse models: *CCSP-rtTA/tetO-EGFR^{L858R}* (CE), expressing human *EGFR^{L858R}* and *CCSP-rtTA/Twist1-tetO7-luc* (CT), expressing mouse *Twist1*. We crossed these two lines to create triple transgenic mice, *CCSP-*

rtTA/tetO-EGFR^{L858R}/Twist1-tetO7-luc (CET) (**Figure 31A**). Cohorts of CE and CET mice, aged 4-8 weeks, were administered doxycycline in the drinking water to turn on the transgenes. After 4 weeks, a point by which CE mice were reported to develop lung tumors (300), mice were sacrificed and necropsies performed. Upon comparison of H&E lung sections from CE and CET mice by a veterinary pathologist, both genotypes resulted in similarly diffuse adenocarcinoma growth in both lungs, as had been previously published for the CE model (300), but CET tumors were more anaplastic as the tumors had larger, more irregularly shaped nuclei (**Figure 31B**). We had previously shown that Twist1 expression accelerates mutant *Kras* tumorigenesis (299), but after 4 weeks on doxycycline, tumor burden was similar between CE and CET mice as shown by pathologic assessment of lung tumor burden (0 meaning no hyperplasia and 5 meaning >75% of the lung was affected) and microCT (**Figure 31B-C**). Thus, TWIST1 expression did not appear to have a primary effect on tumor proliferation rate, but rather resulted in a more aggressive or anaplastic appearance in the CET tumors.

To further characterize the novel CET mouse model, we looked at levels of epithelial and mesenchymal markers. We immunostained lung sections from both CE and CET mice with antibodies for E-cadherin, an epithelial marker, and vimentin, a mesenchymal marker. There was no distinguishable difference in levels of either marker between CE and CET mice (**Figure 31D**). We also did not observe any increased metastasis in the CET mice. In other contexts, Twist1 has been shown to impact the proliferation rate of tumor cells as well as apoptosis levels (234,308). We next examined the levels of proliferation through immunohistochemistry with an antibody for Ki-67 and apoptosis with an antibody for cleaved caspase 3. The overexpression of Twist1 in CET mice in fact modestly decreased proliferation rates, as measured by Ki-67 IHC, in

comparison to CE mice (**Figure 31E**). There was no significant effect on apoptosis with Twist1 expression (**Figure 31F**).

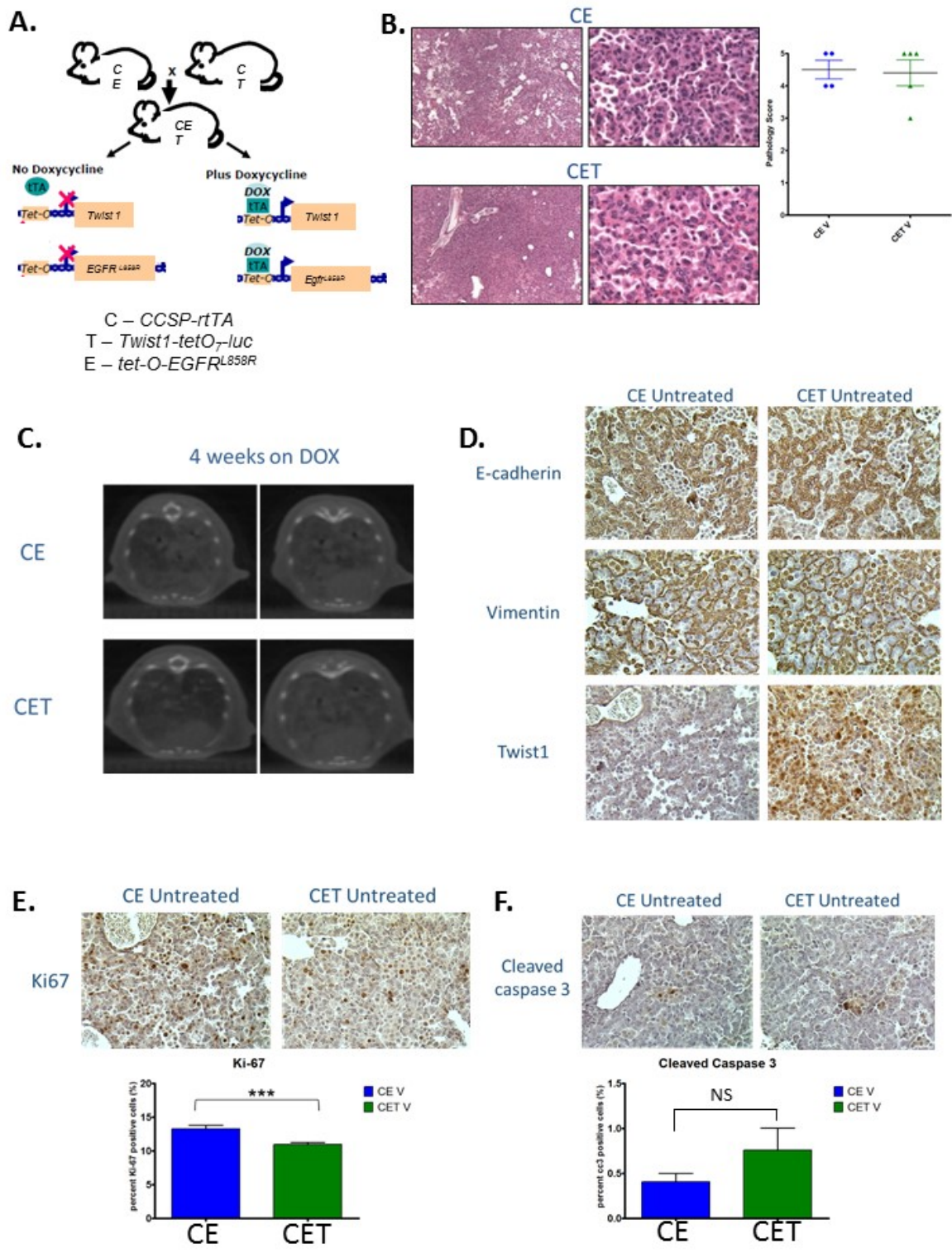


Figure 31: Generation and characterization of a novel Twist1 overexpressing, mutant EGFR autochthonous lung tumor mouse model

(A) Crosses (CE×CT) to produce *CCSP-rtTA/EGFR^{L858R}/Twist1-tetO₇-luc* (CET) mice. (B) UPPER: H&E images from lung tissue of CE and CET mice. CET histology was more anaplastic with larger, more irregular nuclei.

Lesions in both genotypes are more diffuse rather than discrete tumors. Black bars equal 500 and 50 μm . LOWER: Comparison of tumor burden, as percent of lung affected, between CE and CET untreated mice. Mice were on doxycycline for 4 weeks then sacrificed. **(C)** CT images from CE (upper) and CET (lower) mice on doxycycline for 4 weeks. As evidenced from the images, varying levels of tumor burden can be seen within a genotype, however the level is comparable between genotypes. CT images are non-invasive and based on density; the denser areas, like bone, appear white, while the air space is black. The mice are lying on their stomach with noses pointed forward. **(D)** Similar levels of E-cadherin and vimentin staining in CE and CET mice, with CET mice expressing Twist. **(E)** Decreased proliferation in CET mice compared to CE mice as determined by Ki-67 staining. Differences were statistically significant using Student t-test, ***, $P < 0.0005$. **(F)** Similar levels of apoptosis in CE and CET mice using cleaved caspase 3 IHC. For C-E, $n=4$ mice per genotype. 2-tailed Student's t-test, $P = \text{NS}$.

3.4.5 *Twist1* expression induces erlotinib resistance *in vivo*

After characterizing the novel CET mouse model in the absence of drug treatment, we investigated whether *Twist1* expression could induce resistance to the EGFR TKI erlotinib *in vivo*. As previously described, upon administration of erlotinib to CE mice, most lung tumors regress, with a distribution of objective responses including disease stabilization, partial response, and complete response (300). In order to compare CE and CET mice tumor responses and overall survival, all mice were put on doxycycline, to turn on transgene expression and allowed to develop tumors for 3 weeks. Both CE and CET mice had similar levels of tumor burden prior to the start of treatment. At that time point, treatment day 0, all mice were scanned by microCT and this scan was used as the baseline. The mice were treated for 3 weeks with erlotinib and scanned by microCT each week (**Figure 32A**). When baseline scans were compared to scans from after 3 weeks of erlotinib treatment, tumor regression was clearly visible in CE mice, while CET mice showed an increase in tumor burden (**Figure 32B**). All scans were assessed and tumor burden graded on a scale of 0 (no tumor visible) to 5 (lungs completely filled with tumor). Based on the tumor burden change from the beginning to the end of treatment, a majority of CE mice demonstrated no disease progression with erlotinib, with no progression including complete and partial responses as well as stable disease. Conversely, over half of the CET mice had tumor progression over the three weeks of treatment (**Figure 32C**). When examining erlotinib treatment responses based on degree of lung tumor regression, two-thirds of CE mice showed lung tumor regression, while only a quarter of CET mouse lung tumors regressed (**Figure 32C**). After the 3 weeks of treatment, mice were monitored for weight loss, lethargy and other signs indicating a need for euthanasia. CET mice median overall survival time from the beginning of treatment was 6.8 weeks, while CE mice lived a median of 8.7 weeks

(**Figure 32D**). Importantly, we have demonstrated that Twist1 expression does not lead to an increased tumor burden in the *EGFR* mutant background so an increased tumor burden cannot explain this decrease in overall survival (**Figure 32D**). These data support that expression of Twist1 in CET mice induces resistance to erlotinib as shown by increased lung tumor burden and decreased overall survival time following treatment with erlotinib.

To confirm the tumor burden differences seen by microCT, a cohort of CE and CET mice were treated with erlotinib for 1 week followed by euthanasia for macroscopic and histologic tumor assessment. While partial and complete responses were seen in CE mice, only partial and no responses occurred in the CET mice (**Figure 33A**). Tumor burden as assessed on H&E slides by a veterinary pathologist between CE and CET mice treated with erlotinib demonstrated an early trend towards CET mice having greater tumor burden at 1 week (**Figure 33A**).

We then examined the mechanism of Twist1-mediated resistance. Since Twist1 is one of the key mediators of EMT, the tumors in the CET mice could be undergoing this phenotypic change. However, staining for E-cadherin and vimentin showed no change with Twist1 expression, with or without erlotinib treatment (**Figure 33B**). Additionally, there was no significant difference between proliferation levels in CE and CET mice following erlotinib treatment (**Figure 33C**). Interestingly, when the amount of apoptosis was assessed through staining for cleaved caspase 3, the levels of apoptosis were decreased in CET erlotinib treated lung tumors compared to CE erlotinib treated lung tumors (**Figure 33C**). These data suggest that while EMT status and the level of proliferation is unchanged following erlotinib treatment, Twist1 expression inhibits apoptosis in *EGFR* mutant lung tumors following erlotinib treatment.

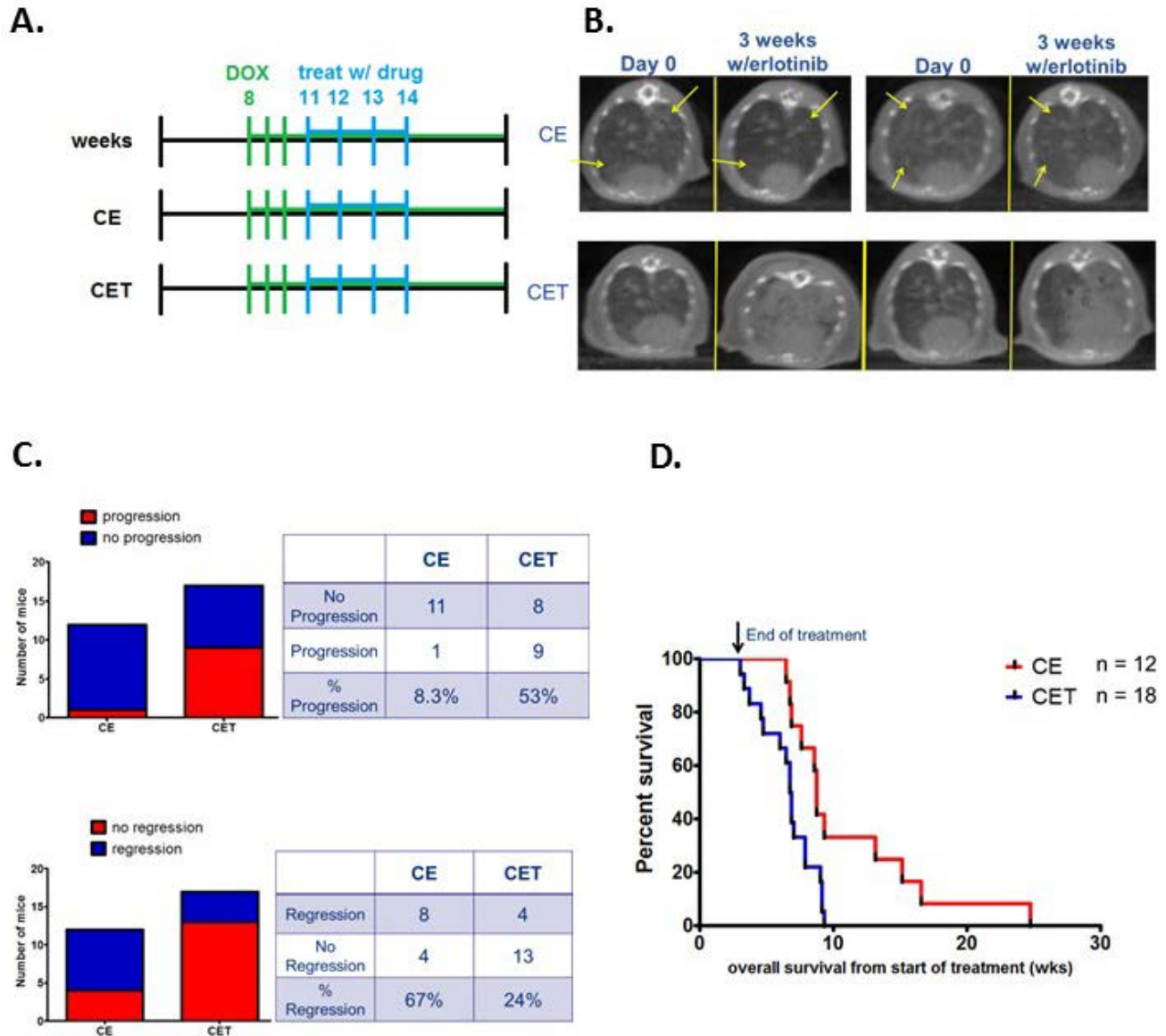


Figure 32: Twist1 overexpression *in vivo* is sufficient to cause erlotinib resistance

(A) Treatment schema for CE and CET mice erlotinib treatment. Mice were started on doxycycline, inducing *EGFR^{L858R}* and *Twist1* transgene expression, at 8 weeks of age and allowed to develop tumors for 3 weeks prior to erlotinib treatment. Mice were scanned at the beginning of treatment, week 11, and each week thereafter until the end of treatment. Mice are treated with 50 mg/kg erlotinib by oral gavage 6 days a week for 3 weeks (weeks 11-14). (B) Representative CT images from baseline and after 3 weeks of erlotinib treatment for CE and CET mice. CE mice show a decrease in tumor burden at the end of treatment compared to day 0. CET mice show a drastic increase in tumor burden despite 3 weeks of treatment. (C) Tumor burden, as visualized by CT image, was graded on a scale of 0 (no tumor) to 5 (lungs filled with tumor) at day 0 and the end of treatment. No progression was considered a complete or partial response as well as stable disease. Only 1 CE mouse demonstrated disease progression, while over half of the CET mice progressed despite erlotinib treatment. Regression was a decrease in tumor burden grade at 3 weeks compared to baseline. Two-thirds of CE mice regressed, while only one quarter of CET mice showed regression. (D) Kaplan-Meier overall survival from beginning of treatment. Median survival for CE mice was 8.7 weeks, for CET mice was 6.8 weeks. Difference in survival was statistically significant using the Mantel Cox test, $P=0.0073$.

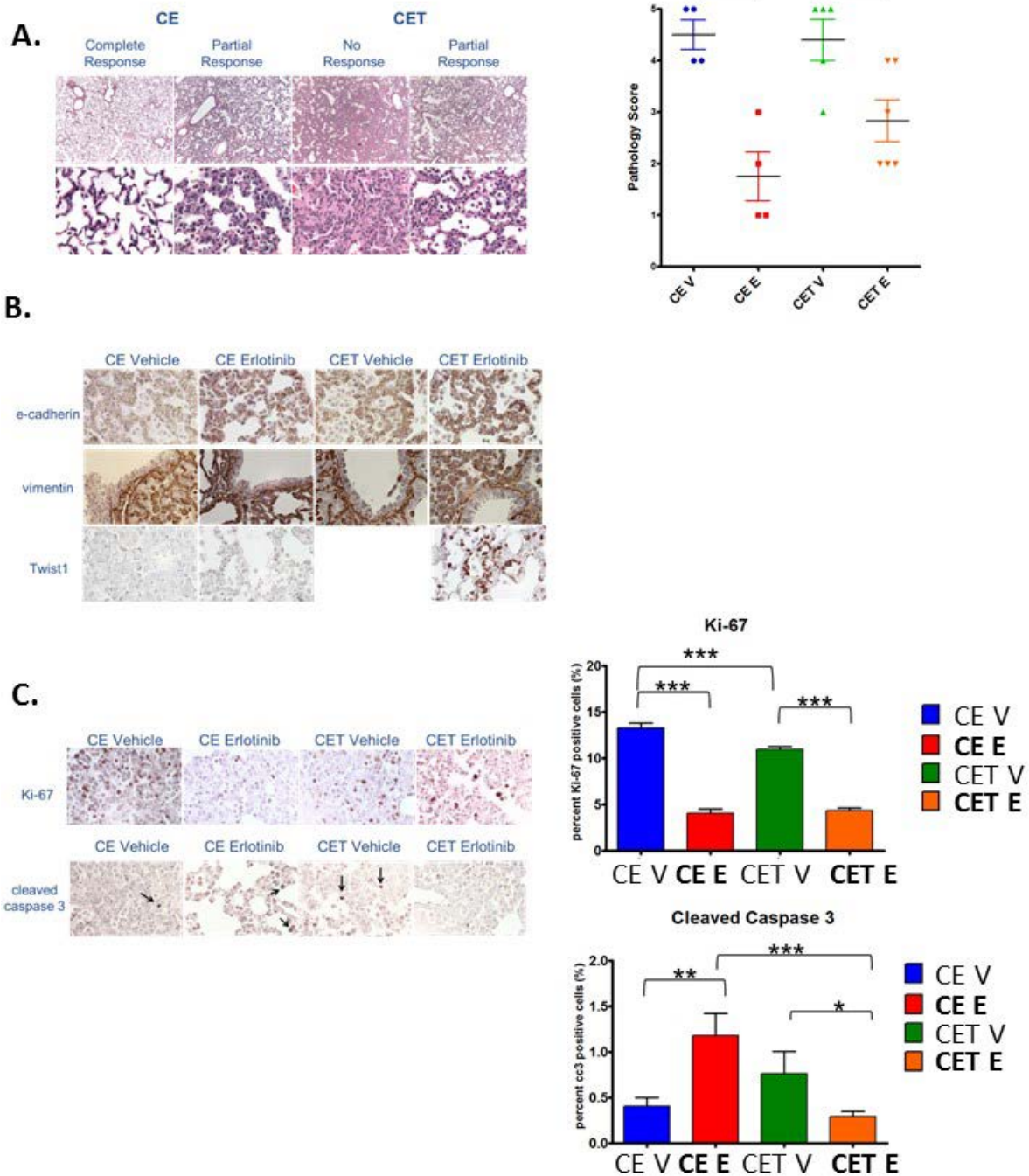


Figure 33: Characterization of Twist1-mediated erlotinib resistance *in vivo*

A) LEFT: H&E images showing comparison of responses seen in CE and CET mice after 7 days of erlotinib treatment. Black bars equal 500 (top) and 50 (bottom) μm . RIGHT: Pathology scores indicating tumor burden as percent of total lung affected. **(B)** Similar levels of E-cadherin and vimentin staining in CE and CET mice with and without erlotinib treatment, with CET mice expressing Twist1. **(C)** LEFT: Representative images of Ki-67 and cleaved caspase 3 staining and quantification (RIGHT) of staining showing a decrease in proliferation to similar levels with erlotinib treatment in both CE and CET mice and a decrease in apoptosis in CET compared to CE mice following erlotinib treatment. Differences were statistically significant using Student t-test, * $p < 0.05$, ** $p < 0.005$, *** $p < 0.0005$.

3.5 DISCUSSION

We have previously demonstrated that TWIST1 expression is required for oncogene-driven tumorigenesis and that loss of TWIST1 expression results in activation of latent senescence and/or apoptotic programs. Here, we demonstrated that both genetic silencing and pharmacological inhibition of TWIST1 results in growth inhibition in a large panel of *EGFR* mutant cell lines. Additionally, we identified that in a subset of *EGFR* mutant cell lines inhibition of TWIST1 results in induction of apoptosis. Of note, targeting TWIST1 resulted in growth inhibition in cells with *EGFR* TKI sensitizing mutations and acquired resistance *T790M* mutations, suggesting that targeting TWIST1 may be a viable option in *EGFR* mutant NSCLC both in the treatment naïve and acquired resistance settings.

Recently, others have demonstrated that EMT-TFs, specifically ZEB1 and SLUG (SNAI2), can contribute to resistance to EGFR TKIs (163,166,298). Hwang et. al have recently shown that TWIST1 overexpression is sufficient to cause EGFR TKI resistance in a single erlotinib sensitive cell line in long term assays and that VGF regulates TWIST1 (302). Here, we significantly expand upon these studies by demonstrating that TWIST1 overexpression is sufficient to cause resistance to EGFR TKIs, in multiple *EGFR* mutant cell lines with and without *T790M* mutations. We also establish that Twist1 overexpression promotes erlotinib resistance *in vivo*, using a mouse model of autochthonous *EGFR* mutant Twist1 overexpressing lung cancer. In both *EGFR* mutant NSCLC cell lines and our mouse model of *EGFR* mutant lung cancer, Twist1 overexpression was associated with suppression of EGFR TKI-induced apoptosis.

Importantly, as the third-generation EGFR TKI, osimertinib, has now been adopted in the first-line setting (82), the frequency of *T790M* mutations will likely significantly decrease in the

acquired resistance setting (82,130). Previously uncommon mechanisms of resistance have already been observed at increased frequency after osimertinib including *MET* and *HER2* amplifications, *KRAS* mutations, additional second site *EGFR* mutations, EMT and SCLC transformation (83,130,132,136,143,309-312). Of note, there are no other FDA approved targeted agents following progression on osimertinib (130). Thus, there is clearly a need for the development of novel targeted agents to prevent and overcome EGFR TKI resistance.

Our study is the first to establish that TWIST1 expression is required for resistance in *EGFR* mutant cells that demonstrate *de-novo* or acquired resistance to EGFR TKIs. Importantly, our study demonstrates that therapeutic targeting of an EMT-TF, is able to restore sensitivity to erlotinib in *EGFR* mutant NSCLC cells that are resistant to EGFR TKIs. Our findings suggest that use of small molecule compounds that inhibit TWIST1 may be a viable option to overcome *de-novo* and acquired resistance to EGFR TKIs in lung cancer. Harmine is an active β -carbolin alkaloid found in the herb *Peganum harmala* used in traditional medicine in Central Asia and the Middle East (271). However, in mouse model systems and in humans, the efficacy of harmine may be limited due to neurotoxic side effects, such as tremors (271,313). We have identified analogues of harmine that are potentially more potent inhibitors of TWIST1 without the neurotoxicity associated with harmine and are currently performing further preclinical evaluation of these compounds.

Others have previously demonstrated that BIM expression is required for response to EGFR TKIs (186,190,191,305). Additionally, BIM polymorphisms which result in decreased expression of functional BIM protein, are associated with resistance to EGFR TKIs (192,247,314). Here, we establish that TWIST1 suppresses BIM expression through direct binding at both the promoter and intronic regions. Future studies while be aimed at determining

the mechanism(s) by which TWIST1 suppresses BIM expression. Specifically, we will be investigating if TWIST1 binding at the *BCL2L1* promoter results in recruitment of histone deacetylases and/or co-repressors. Additionally, given that there are predicted binding sites for specific transcription factors, such as NF-1, found specifically at the E-box sites in which TWIST1 binds, we will also be investigating if binding of other transcription factors and/or cofactors influences TWIST1 binding to specific E-boxes within the *BCL2L1* promoter.

Overall, these data suggest that one of the mechanisms by which TWIST1 mediates EGFR TKI resistance is through inhibition of EGFR TKI-induced apoptosis by suppressing BIM expression. Interestingly, we demonstrated that TWIST1-mediated resistance can be overcome with use of BCL2/BCLxL inhibitors. BCL2/BCLxL inhibitors, such as ABT-263 are in clinical trials, and our data suggest that use of these inhibitors may provide rapid means to overcome TWIST1-mediated resistance in the clinic. While we established that one mechanism by which TWIST1 can mediate resistance is through suppression of apoptosis, TWIST1 has been previously shown to suppress senescence in both oncogene-driven NSCLC and breast cancer (234,248,299). We are currently exploring whether TWIST1-mediated suppression of senescence is another mechanism by which TWIST1 promotes EGFR TKI resistance. Of note, a recent study demonstrated that TWIST1 can mediate resistance to 3rd generation EGFR TKIs through upregulation of the EMT-TF, ZEB1 (160). This study established that ZEB1 can also directly suppress *BCL2L1* transcription (160). This study and our current study suggests that there are potentially multiple mechanisms by which TWIST1 can promote EGFR TKI resistance and multiple mechanisms by which TWIST1 can suppress BIM expression.

In summary, we demonstrated that genetic and pharmacological inhibition of TWIST1 results in growth inhibition in *EGFR* mutant NSCLC. In a subset of cell lines, including cell lines

with acquired resistance *T790M* mutations, inhibition of TWIST1 is associated with the induction of apoptosis. Additionally, we established that TWIST1 is both sufficient and, in some lines, required for EGFR TKI resistance in *EGFR* mutant NSCLC both *in vitro* and *in vivo*. We demonstrated that one of the mechanisms by which TWIST1 mediates resistance is through suppression of apoptosis via suppression of BIM expression. We also demonstrated that use of a TWIST1 inhibitor, harmine, was able to overcome both *de-novo* and acquired resistance to EGFR TKIs. Of note, targeting TWIST1 may be associated with minimal side effect because it is rarely expressed post-natally (200,201). Our data suggests that targeting TWIST1 may be option to overcome EGFR TKI resistance in *EGFR* mutant NSCLCs both in the *de-novo* and acquired resistance settings.

4.0 TWIST1 IS A KEY MEDIATOR OF HGF-MET DRIVEN RESISTANCE TO TARGETED THERAPIES IN *EGFR* MUTANT AND MET-DRIVEN LUNG CANCER

4.1 ABSTRACT

The c-Met (MET) receptor and its ligand, hepatocyte growth factor (HGF) are frequently altered in non-small cell lung cancer (NSCLC). Aberrations in the MET/HGF pathway have emerged as a targetable oncogenic driver, as patients with *MET* amplification and/or mutations have marked responses to the MET tyrosine kinase inhibitor (TKI), crizotinib. However, long-term efficacy of MET TKIs is limited as acquired resistance is inevitable and almost half of patients with *MET* alterations fail to respond to MET TKIs. *MET* amplification and HGF overexpression have also been identified as mechanisms of resistance to MET and EGFR TKIs in *MET* altered and *EGFR* mutant NSCLC, respectively. However, the mechanism(s) by which the HGF-MET pathway causes resistance are poorly understood. We previously established that the EMT-transcription factor, TWIST1, is required for *EGFR* mutant and MET-driven NSCLC. Here, we investigated the requirement of TWIST1 in HGF-mediated resistance to MET and EGFR TKIs and the role of TWIST1 in *de-novo* and acquired resistance to MET TKIs. We found that HGF treatment induced EMT in NSCLC cell lines and increased TWIST1 protein expression through a post-translational mechanism. We demonstrated that targeting TWIST1 pharmacologically with the TWIST1 inhibitor, harmine, overcame HGF-mediated resistance to

both MET and EGFR TKIs in MET- and EGFR-driven NSCLC. This suggests that TWIST1 is required for HGF-mediated resistance to targeted therapies. We also found that TWIST1 overexpression was sufficient to cause resistance to MET TKIs. In MET-driven NSCLC cell lines that express TWIST1 and are resistant to targeted therapies, we demonstrated that harmine treatment resensitized cells to MET TKIs. To investigate the role of Twist1 overexpression in Hgf-driven lung cancer, we utilized a *CCSP-Hgf* (CH) mouse model that constitutively overexpresses Hgf in the lung and develops crizotinib sensitive tumors following treatment with the tobacco carcinogen, nicotine-derived nitrosamine ketone (NNK). We demonstrated that Hgf and Twist1 overexpressing CTH (*CCSP-rtTA/Twist1-tetO-luc/CCSP-Hgf*) mice developed significantly larger tumors in response to NNK as compared to CH mice. These studies suggest that targeting TWIST1 may be an effective therapeutic strategy to overcome HGF-MET-driven resistance in *EGFR* mutant NSCLC as well as MET TKI resistance in MET-driven NSCLC.

Contributors to study: Yochum, ZA¹⁻², Chatterjee, S¹, Huang EH¹, Maurer, DM¹, Attar, MA¹, Dacic, S³, Stabile, LP², Burns, TF¹⁻²

¹Department of Medicine, Division of Hematology-Oncology, Hillman Cancer Center, University of Pittsburgh, Pittsburgh, PA.

²Department of Pharmacology and Chemical Biology, University of Pittsburgh, Pittsburgh, PA

³Department of Pathology, University of Pittsburgh Medical Center, Pittsburgh, PA, USA

4.2 INTRODUCTION

The receptor tyrosine kinase c-MET (MET) and its only known ligand, hepatocyte growth factor (HGF) have been implicated in tumorigenesis as MET/HGF signaling can promote epithelial-mesenchymal transition (EMT), proliferation, invasion, motility, and angiogenesis (102). Currently, the treatment paradigm around non-small cell lung cancer (NSCLC) revolves around classifying patient into subgroups based on histology and known or putative molecular drivers. Aberrations in the MET/HGF pathway, specifically *MET* amplifications and *MET* mutations, have emerged as a targetable molecular driver. The most common *MET* mutations in NSCLC are *MET* exon 14 skipping mutations, which lead to increased stability of MET by impairing ubiquitination and proteasomal degradation (111,117). Approximately 8-14% of NSCLC patients harbor *MET* amplifications/mutations and patients with these *MET* alterations have demonstrated marked responses to MET tyrosine kinase inhibitors such as crizotinib or capmatinib (107,112-114,117-120). However, long-term clinical efficacy of MET TKIs remains limited in NSCLC due the frequency of *de-novo* resistance (~50%) and the inevitability of acquired resistance (112,113,117,121). Additionally, mechanisms of resistance to MET TKIs in *MET* altered NSCLC remain poorly understood.

MET amplification and overexpression of the MET ligand, HGF have been associated with poor patient prognosis and decreased survival in NSCLC (104-106). Additionally, both aberrations have been identified as drivers of resistance to EGFR and MET TKIs in EGFR- and MET-driven NSCLC, respectively. *MET* amplification drives resistance in approximately 5-20% of patients with *EGFR* mutant NSCLC resistant to 1st generation EGFR TKIs, such as gefinitib or erlotinib (75,142). Additionally, *MET* amplification can also mediate resistance to osimertinib, the 3rd generation EGFR TKI which has activity against the *T790M* mutation and is currently the

first-line therapy for *EGFR* mutant patients (143,144). HGF overexpression has also been identified as a mediator of resistance to both MET and EGFR TKIs in NSCLC. HGF overexpression has been observed in patients with *de-novo* and acquired resistance to EGFR TKIs (149,151). Additionally, in MET-driven gastric cancer and NSCLC, HGF overexpression leads to resistance to multiple MET inhibitors, including MET TKIs and MET targeted monoclonal antibodies (315). Studies have revealed that both *MET* amplification and HGF overexpression may mediate resistance by activating bypass signaling, specifically reactivating PI3K and MAPK signaling (147). However, the specific downstream mediators of MET/HGF-driven resistance remain poorly elucidated.

The EMT-transcription factor, TWIST1, is overexpressed in approximately 40% of NSCLC and is associated with a more aggressive tumor phenotype, increased risk of metastasis, and worsened patient prognosis (198,233,316). We have previously demonstrated that TWIST1 expression is required for oncogene-driven NSCLC, including tumors with *EGFR* mutations and *MET* amplification/mutations (232,234). Genetic and pharmacological inhibition of TWIST1 in both EGFR- and MET-driven NSCLC results in oncogene-induced senescence (OIS) and in a subset of cells, apoptosis (232,234). Additionally, in Chapter 3, we have demonstrated that TWIST1 is both sufficient and required for EGFR TKIs resistance. In the current study, we explored the role of TWIST1 in HGF-driven resistance to both MET and EGFR TKIs in *MET* altered and *EGFR* mutant NSCLC, respectively, and in *de-novo* and acquired resistance to MET TKIs in *MET* altered NSCLC. We demonstrated that HGF treatment resulted in increased TWIST1 expression by increasing TWIST1 protein stability. Additionally, pharmacologic inhibition of TWIST1 was able to overcome HGF-mediated resistance to MET and EGFR TKIs. We demonstrated that TWIST1 overexpression was sufficient to cause decreased sensitivity to

the MET TKI, crizotinib. Additionally, targeting TWIST1 with our novel TWIST1 inhibitor, harmine, increased crizotinib sensitivity in MET-driven NSCLC cell lines. Of note, harmine had single agent activity in a patient-derived xenograft mouse model of *EGFR* mutant *MET* amplified NSCLC. In our transgenic mouse model of Hgf-driven NSCLC, we demonstrated that in response to the tobacco carcinogen, nicotine-derived nitrosamine ketone, mice that expressed Twist1 and Hgf developed larger tumors when compared to mice that expressed Hgf alone. Our studies demonstrate that TWIST1 is a potential therapeutic target to overcome resistance to MET and EGFR TKIs, in the presence and absence of HGF overexpression.

4.3 METHODS

4.3.1 Cell lines and reagents

H23, H1648, Hcc827, H596, H1993, H1437 and embryonic kidney cell line HEK 293T were acquired from the American Type Culture Collection (ATCC) and were cultured in the recommended ATCC media. 11-18 cells were obtained from Dr. Christine Lovly (Vanderbilt University) and cultured in the recommended media. The identity of the aforementioned cell lines was verified by autosomal STR (short tandem repeat) profiling done at University of Arizona Genetics Core (UAGC). Cell lines were tested for mycoplasma every six months using MycoAlert Detection Kit (Lonza). Recombinant Human HGF (294-HGN-005/CF 5 µg) was purchased from R&D Systems (Minneapolis, MN). Harmine (286044-1G) and cyclohexamide (C4859) was purchased from Sigma-Aldrich (St. Louis, MS). Crizotinib (S1068) was purchased from Selleck Chemicals (Houston, TX). 4-(Methylnitrosoamino)-1-(3-pyridyl)-1-butanone

(NNK) (M325750) was purchased from Toronto Research Chemicals (Toronto, ON) and was dissolved in 0.9% saline.

4.3.2 Cell proliferation assays

For all viability experiments, cells were seeded at an appropriate density in 96 well plates and incubated for 24 hours. Cells were subsequently treated with a range of doses of the appropriate inhibitor for the indicated timepoints. Viability was determined using the CellTiter96® Aqueous One Solution Cell Proliferation Assay kit (Promega) or Cell-Titer Glo 2.0 Assay (Promega) according to manufacturer's protocol. Data was analyzed as previously described in Chapter 2.3.2.

4.3.3 Western blot and antibodies

Following appropriate treatment, cells were harvested and lysed and subsequent protein was quantified and western blotting was performed as previously described (234). All information on antibodies is included in Table 3 (Appendix A). Western blot experiments were performed at least twice unless otherwise stated.

4.3.4 Lentiviral shRNA and cDNA overexpression

293T cells were seeded at a density of 4×10^6 in 25-cm² flasks. Following a 24-hour incubation period, cells were transfected to generate lentivirus using a four -plasmid system according to the

TRC Library Production and Performance protocols, RNAi Consortium, Broad Institute (264) and as previously described (234). A complete list of the constructs used is in Supplementary Tables 4-6 (Appendix A) and sequences of these constructs and primers used are available upon request.

4.3.5 Pulse-Chase experiments

For harmine pulse-chase experiments, H23 cells were treated with HGF (50 µg/ml) or vehicle for 48 hours. Cells were then treated with cyclohexamide (50 µg/ml) and harvested at the indicated time points. Data analysis was carried out as previously described in Chapter 2.3.11.

4.3.6 Xenograft experiments

All mice were maintained in pathogen-free animal facilities and experiments were conducted under an approved Institutional Animal Care and Use Committee protocol at the University of Pittsburgh (Pittsburgh, PA). For the patient-derived xenograft (PDX) experiments, we used a *EGFR* mutant *MET* amplified PDX established from the lung mass (MSK-LX29) of a patient with *EGFR* mutant (*L858R* mutation) *MET* amplified lung cancer (317). Tissue implantation, harmine treatment, and tumor measurement/analysis were carried out as previously described in Chapter 2.3.15.

4.3.7 Transgenic Mice

All mice were maintained in pathogen-free animal facilities and experiments were conducted under an approved Institutional Animal Care and Use Committee protocol at the University of Pittsburgh (Pittsburgh, PA). Constitutive Hgf and inducible Twist1 transgenic mice in the FVB/N inbred background were of the genotype: **CTH** (CCSP-rtTA/*Twist1-tetO-luc*/*CCSP-Hgf*). All the mice were weaned at 3–4 weeks of age and then placed on doxycycline containing chow or control chow at 6 weeks of age. At week 8, all mice received NNK i.p. injections twice per week (3mg per i.p. injection) for 5 weeks (6mg/week). Following NNK treatment, mice were observed for 17 weeks and then harvested for tumor analysis. Lungs tumors were analyzed by formalin inflation of the lungs and gross examination using a dissection microscope and Motic Image software to count and measure surface tumors.

4.4 RESULTS

4.4.1 Pharmacologic inhibition of TWIST1 overcomes HGF-mediated resistance to MET and EGFR TKIs in *EGFR* mutant and *MET* amplified NSCLC

HGF overexpression has been linked to EMT in cancer and resistance to EGFR and MET TKIs in EGFR- and MET-driven NSCLC, respectively (149,151,315,318-320). Additionally, HGF levels may be a key determinate of sensitivity or resistance to EGFR TKIs in treatment naïve *EGFR* mutant patients, as HGF is frequently overexpressed in patients with *de-novo* resistance to EGFR TKIs (149,151). Upregulation of TWIST1 has been associated with HGF-mediated EMT

(321,322). In breast cancer and melanoma, HGF increases TWIST1 expression and activity, potentially through increased AKT and ERK phosphorylation of TWIST1 (321,322). HGF treatment has also been linked to increased *TWIST1* mRNA expression (323). However, the mechanisms and downstream mediators of HGF-driven resistance to targeted therapies in NSCLC remain poorly understood. In the current study, we first examined whether HGF could induce EMT and increase TWIST1 expression in NSCLC. We found that HGF treatment in NSCLC cell lines leads to EMT and induces TWIST1 expression (**Figure 34A-B**). We demonstrated that HGF treatment markedly increases the protein half-life of TWIST1 (**Figure 34C**), suggesting that HGF increases TWIST1 expression via a post-translational mechanism(s). Given that HGF increased TWIST1 expression in NSCLC cell lines, we explored whether targeting TWIST1 can overcome HGF-mediated resistance to TKIs in *MET* amplified and *EGFR* mutant NSCLC cell lines. As seen in other studies (149,151,315), HGF treatment led to resistance to both EGFR TKI and MET TKIs in EGFR- and MET-driven NSCLC, respectively (**Figure 35A-B**). Interestingly, treatment with harmine was able to overcome HGF-mediated TKI resistance in both *EGFR* mutant and *MET* amplified NSCLC (**Figure 35A-B**). These studies suggest targeting TWIST1 pharmacologically may be a viable option to overcome HGF-driven resistance to MET and EGFR TKIs in NSCLC.

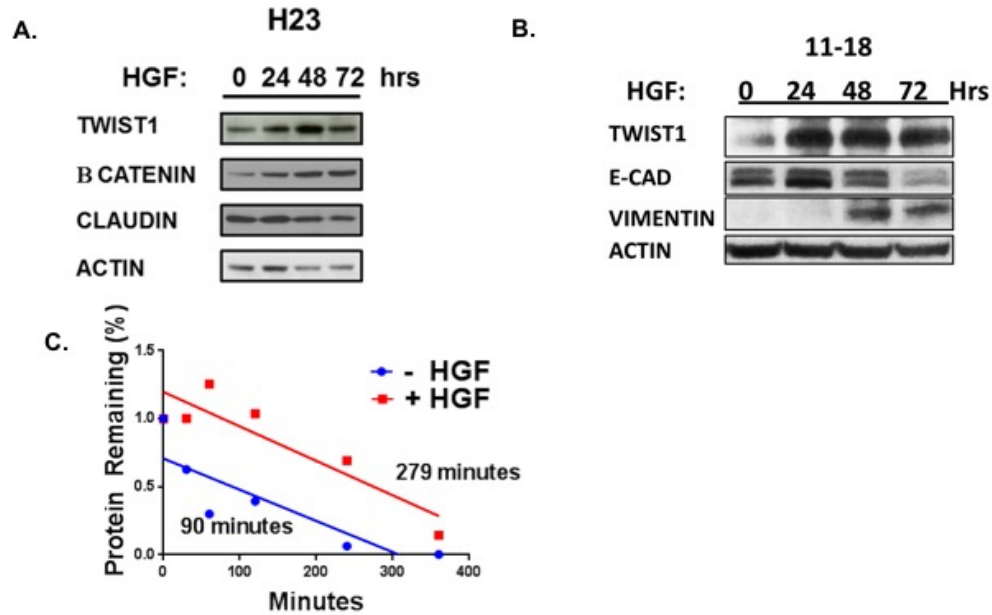


Figure 34: HGF treatment increases TWIST1 protein stability

(A-B) Induction of TWIST1 and markers of EMT (decreasing claudin or E-cadherin, increasing vimentin or β -catenin) in a *KRAS* mutant (A) and *EGFR* mutant (B) NSCLC cell lines after HGF treatment. (C) HGF treatment increases the half-life of TWIST1 protein. Protein concentration was quantified using densitometry and protein half-lives were determined using linear regression analysis.

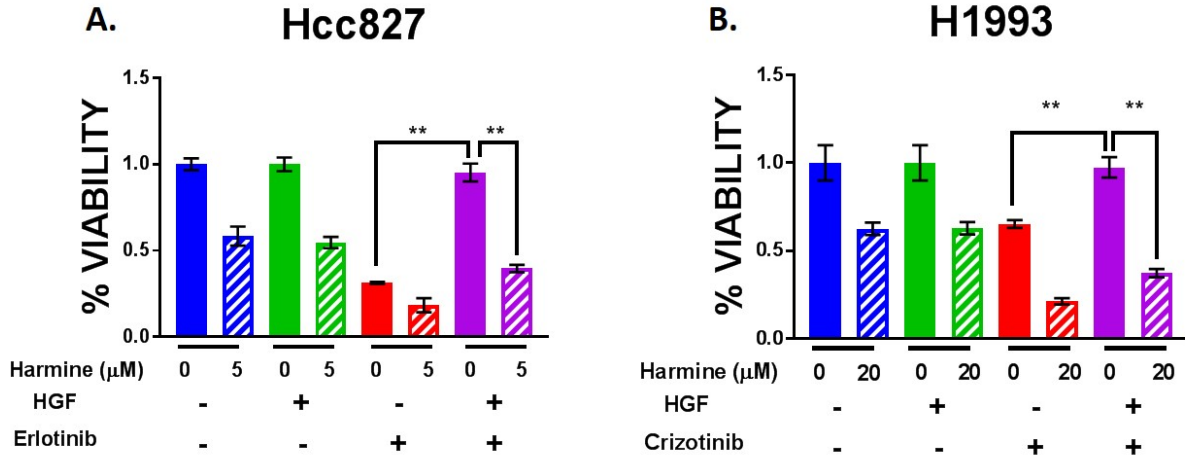


Figure 35: Pharmacologic inhibition of TWIST1 overcomes HGF-mediated resistance to MET and EGFR TKIs in *EGFR* mutant and *MET* amplified NSCLC

(A-B) MTS assay demonstrating that in *EGFR* mutant, Hcc827 (A), and *MET* amplified, H1993 (B), NSCLC cell lines that harmine overcomes HGF-mediated resistance to EGFR and MET targeted therapy. Cells were co-treated with the indicated doses of harmine, HGF (50ng/ml), erlotinib (100nM), and/or crizotinib (100nM) for 72 hours, and then harvested for MTS analysis. Data represent mean \pm SD (n=4 technical replicates). **, p<.01, 2-tailed Student's t-test

4.4.2 TWIST1 mediates resistance to MET TKIs in *MET* altered NSCLC

In Chapter 3, we demonstrated that TWIST1 is both sufficient and required for resistance in *EGFR* mutant NSCLC. While we demonstrated in this study that TWIST1 expression is required for HGF-mediated resistance to TKIs in *EGFR*- and *MET*-driven NSCLC (**Figure 35**), we also explored the role of TWIST1 in *MET* TKIs resistance in the absence of HGF overexpression. We found that TWIST1 overexpression decreased crizotinib sensitivity in a *MET* amplified NSCLC cell line (**Figure 36A**). Additionally, we demonstrated that harmine treatment increases crizotinib sensitivity in both *MET* amplified and mutant crizotinib resistant NSCLC cell lines that express TWIST1 (**Figure 36B-C**). We also explored the *in vivo* efficacy of harmine in a patient-derived xenograft (PDX) mouse model of *EGFR* mutant *MET* amplified NSCLC. In this PDX model, harmine significantly inhibited tumor growth as a single agent (**Figure 37**), which suggests that targeting TWIST1 may be viable therapeutic option in patients with *EGFR* mutations that develop *MET* amplification as a mechanism of acquired resistance to *EGFR* TKIs. Additionally, these studies also suggest that targeting TWIST1 may be a viable strategy to overcome *MET* TKI resistance in *MET* altered NSCLC.

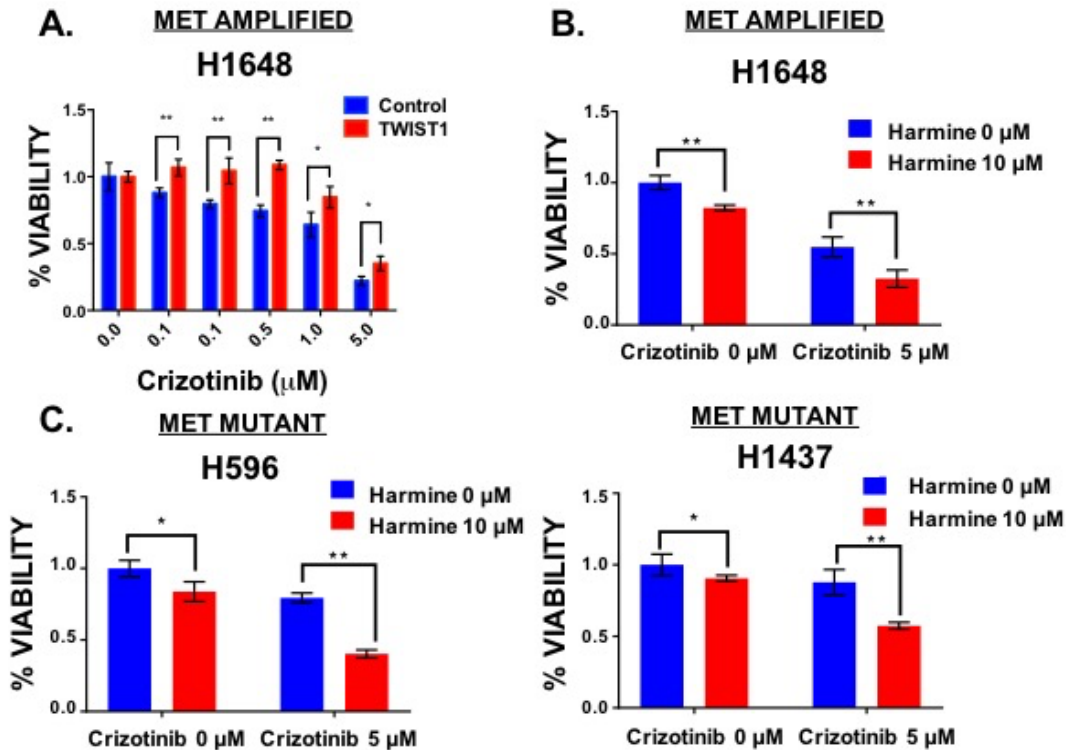


Figure 36: TWIST1 modulates sensitivity to crizotinib in *MET* altered NSCLC

(A) Cell-Titer Glo (CTG) assay demonstrating that TWIST1 overexpression decreases response to crizotinib in *MET* amplified H1648 cells. H1648 cells were infected with a TWIST1 overexpressing vector or a control vector. 72 hours following lentiviral infection, H1648 cells were treated with crizotinib for 24 hours and then harvested for CTG analysis. (B-C) MTS assay demonstrating that harmine increases sensitivity to crizotinib in *MET* mutant (B) and *MET* amplified (C) NSCLC cell lines. *MET* altered NSCLC cells were treated for the indicated doses of harmine and crizotinib for 48 hours or 72 hours and then harvested for MTS analysis. Data represent mean \pm SD (n=4 technical replicates). **, p<.01, 2-tailed Student's t-test

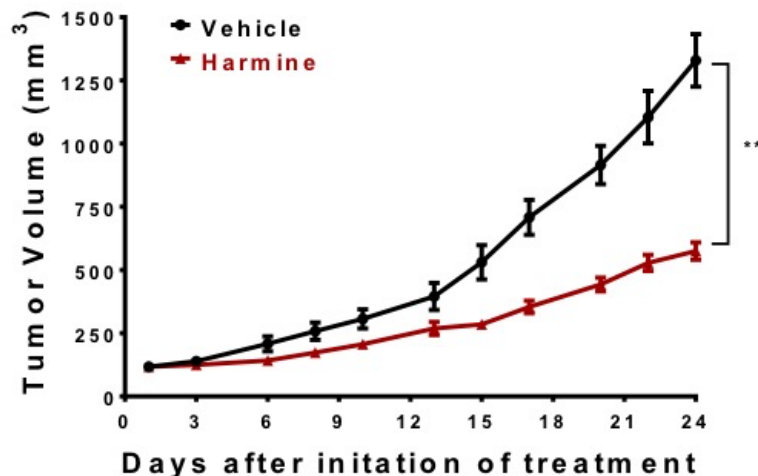


Figure 37: Harmine has activity in a PDX mouse model of *EGFR* mutant *MET* amplified lung cancer

Tumor growth is decreased after 24 days of harmine treatment in a *EGFR* mutant *MET* amplified PDX model (MSK-LX29). Tumor size was monitored twice a week until tumors were approximately 2000 mm³. N = 7 mice in vehicle arm, and n=5 mice in harmine arm. Data represent mean \pm SEM. **, p<.01, 2-tailed Student's t-test.

4.4.3 Twist1 cooperates with Hgf to promote tumorigenesis in a mouse model of Hgf-driven lung cancer

We have previously demonstrated that Twist1 cooperates with mutant *Kras in vivo* to accelerate tumorigenesis (233). Twist1 expression in our transgenic mouse models of *Kras* mutant NSCLC functions to suppress OIS and promote the transformation of lung adenomas to adenocarcinomas (233). In the current study, we next examined whether Twist1 cooperates with Hgf in our carcinogen-induced model of Hgf-driven lung cancer (324,325). *CCSP-Hgf* (CH) mice that constitutively overexpress Hgf in the lung, develop an increased number of tumors in response to the tobacco carcinogen, Nicotine-derived nitrosamine ketone (NNK) (324,325). Interestingly, in the CH model, NNK-induced tumors are sensitive to the MET TKI, crizotinib (324,325). To elucidate the role of TWIST1 in Hgf-driven tumorigenesis, we generated CTH (*CCSP-rtTA/Twist1-tetO-luc/CCSP-Hgf*) mice that both constitutively overexpress Hgf and doxycycline inducibly overexpress Twist1 in the lung by crossing our previously characterized CH and *CCSP-rtTA/Twist1-tetO-luc* (CT) mice (233,324,325) (**Figure 38A**). Following exposure to NNK, the number of tumors in the CHT animals was not significantly different in the presence or absence of Twist1 expression. However, we observed a 57% increase in tumor size in the presence of doxycycline (Twist ON) in the CTH animals when compared to the CHT animals that did not receive doxycycline (Twist OFF) (**Figure 38B**). These data suggest that Twist1 expression may cooperate with Hgf to promote tumorigenesis in the setting of carcinogen-induced lung cancer.

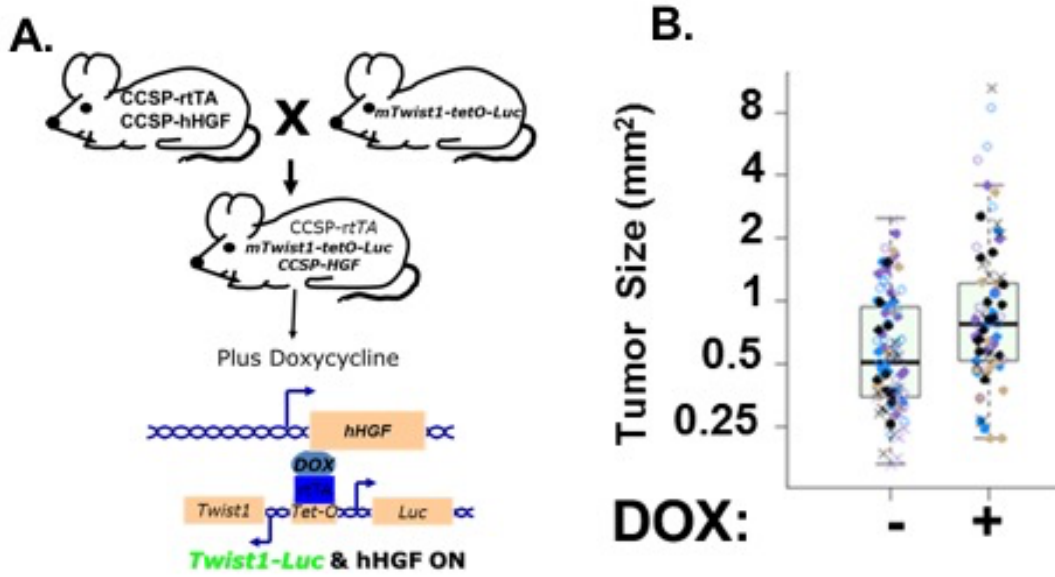


Figure 38: Twist1 overexpression leads to increased tumor size in a mouse model of Hgf-driven lung cancer
(A) Schema representing the creation of $CCSP-rtTA/Twist1-tetO-luc/CCSP-Hgf$ (CHT) by crossing $CCSP-Hgf$ (CH) mice with $CCSP-rtTA/Twist1-tetO-luc$ (CT). CHT mice constitutively overexpress HGF and doxycycline inducibly express Twist1. **(B)** TWIST1 overexpression leads to increased tumor size in a NNK-induced $CCSP-rtTA/Twist1-tetO-luc/CCSP-Hgf$ (CTH) lung cancer model in the presence of doxycycline. Tumor size was log₂ transformed. A single linear mixed effects was fitted to estimate group differences in tumor size, with a random intercept to accommodate multiple tumors per animal. On average tumor size in the CHT+NNK+DOX group was 57% greater than for CHT+NNK (95% CI 19%-108% greater), $p=0.0015$.

4.5 DISCUSSION

Our study is the first to demonstrate that HGF treatment leads to increased TWIST1 expression in NSCLC. We also demonstrate that HGF likely increases TWIST1 expression through a post-translational mechanism, as HGF treatment significantly increases TWIST1 protein half-life. Previous studies have demonstrated that TWIST1 can be regulated post-translationally by ERK and AKT phosphorylation. The major regulators of TWIST1 protein half-life are mitogen activated kinases (MAPKs). Phosphorylation of TWIST1 on serine 68 (S68) of TWIST1 by MAPKs such as p38, JNK, and ERK1/2 leads to increased protein stability by inhibiting its ubiquitination and proteasomal degradation (203). Interestingly, we have evidence that TWIST1

can increase ERK phosphorylation (data not shown), suggesting that there may be a positive feedback loop between ERK1/2 and TWIST1. We have observed an increase ERK phosphorylation 72 hours following TWIST1 overexpression. Currently, we are investigating the kinetics of this potential feedback loop between ERK and TWIST1. Additionally, AKT2 phosphorylation of TWIST1 is required for TWIST1-mediated metastasis in breast cancer (222). Previous studies have demonstrated that HGF/MET signaling leads to increased ERK and AKT activity (147). Future experiments will be aimed at determining if ERK and/or AKT phosphorylation of TWIST1 is required for HGF-mediated induction of TWIST1. Additionally, if ERK and/or AKT phosphorylation of TWIST1 is required for HGF induction of TWIST1, we will determine if treatment with ERK and/or AKT inhibitors is able to prevent TWIST1 induction following HGF-treatment. We also demonstrated that harmine treatment can overcome HGF-mediated resistance to EGFR and MET TKIs in *EGFR* mutant and *MET* amplified NSCLC, respectively. Currently, we are following up the aforementioned harmine experiments with genetic approaches to inhibit TWIST1 to ensure that TWIST1 inhibition by harmine is the main mechanism by which harmine overcomes HGF-mediated TKI resistance.

Our study also demonstrated that TWIST1 expression is sufficient to cause resistance to MET TKIs and that targeting TWIST1 with harmine increases crizotinib sensitivity in *MET* altered NSCLC cell lines. In Chapter 3, we demonstrated that TWIST1 direct suppression of *BCL2L11* (gene encoding BIM) transcription is critically important for TWIST1-mediated resistance EGFR TKIs in *EGFR* mutant NSCLC. Currently, we are exploring if TWIST1-suppression of apoptosis plays a role in TWIST1-mediated resistance to MET TKIs in the presence and absence of HGF. We are also examining if TWIST1 negatively regulates BIM expression in *MET* altered NSCLC. TWIST1 negative regulation of BIM in MET-driven NSCLC

also has implications in HGF-mediated resistance to MET and EGFR TKIs, as HGF suppression of BIM has been previously shown to be required for HGF-mediated resistance to targeted therapies in melanoma (326). If TWIST1 suppresses BIM-mediated apoptosis in response to MET TKIs, we will determine if use of BCL-2/BCL-xL inhibitors, such as navitoclax which is currently in clinical trials, is able to overcome TWIST1-mediated MET TKI resistance. Developing pharmacological strategies to overcome TWIST1-mediated resistance has important implications for not only patients with MET-driven NSCLC resistant to MET TKIs but also *EGFR* mutant patients with *MET* amplification as a mechanism of acquired resistance to EGFR TKIs, such as osimertinib.

In our mouse model of Hgf-driven tobacco carcinogen-induced lung cancer, we demonstrated that Twist1 expression leads to increased tumor size, suggesting that Twist1 may cooperate with Hgf *in vivo* to promote tumorigenesis. We are currently examining the mechanisms by which Twist1 promotes Hgf-mediated tumorigenesis and increases tumor size. Given that we previously demonstrated that Twist1 suppresses oncogene-induced senescence (OIS) in transgenic models of *Kras* mutant lung cancer, we are specifically investigating if Twist1 suppresses failsafe programs of OIS and/or apoptosis in our mouse model of Hgf-driven lung cancer. Importantly, *CCSP-Hgf* (CH) mice that constitutively overexpress Hgf in the lung develop tumors that are sensitive to the MET TKI, crizotinib (147,324,325). Utilizing our CHT mice that constitutively overexpress Hgf and doxycycline inducibly overexpression Twist1, we are investigating whether Twist1 overexpression leads to crizotinib resistance. Additionally, if Twist1 expression is sufficient to mediate crizotinib resistance in this model, we will explore if targeting TWIST1 with harmine is able to overcome Twist1-mediated crizotinib resistance.

In summary, we demonstrated that HGF treatment in NSCLC cells led to EMT and increased TWIST1 expression. TWIST1 induction following HGF treatment most likely occurs through a post-translational mechanism, as HGF significantly increased TWIST1 protein half-life. Targeting TWIST1 with harmine was able to overcome HGF-mediated resistance to MET and EGFR TKIs in *MET* amplified and *EGFR* mutant NSCLC cell lines. TWIST1 overexpression was also sufficient to decrease crizotinib sensitivity in a *MET* amplified NSCLC cell line. Additionally, harmine treatment increased crizotinib sensitivity in *MET* altered crizotinib resistant NSCLC cells that express TWIST1 and had single agent activity in a PDX mouse model of *EGFR* mutant *MET* amplified NSCLC. In our mouse model of Hgf-driven lung cancer, we demonstrated that Twist1 expression led to increased tumor size. Overall, our results suggest that TWIST1 is a potential therapeutic target to overcome EGFR and MET TKI resistance in the presence and absence of HGF overexpression.

5.0 TWIST1 MEDIATES RESISTANCE TO TRAIL-BASED THERAPIES THROUGH DIRECT UPREGULATION OF C-FLIP

5.1 ABSTRACT

TNF-related apoptosis inducing ligand (TRAIL) is a death ligand that binds death receptor 4 (DR4) and death receptor 5 (DR5) and activates extrinsic apoptosis. TRAIL is a promising therapeutic option as it can selectively induce apoptosis in cancer cells, while sparing normal cells. However, TRAIL has limited clinical efficacy due to the frequency of *de-novo* resistance and acquired resistance. Interestingly, a novel TRAIL-inducing small molecule TIC10/ONC201 has efficacy in solid tumors, however, mechanisms of resistance to TIC10/ONC201 have already been identified. In non-small cell lung cancer (NSCLC), epithelial-mesenchymal transition (EMT) has been associated with resistance to TRAIL. We have previously demonstrated that the EMT-transcription factor TWIST1 is required for oncogene-driven NSCLC, suppresses both oncogene-induced senescence (OIS) and apoptosis, and mediates resistance to targeted therapies in NSCLC. In this study, we investigated the role of TWIST1 in mediating resistance to TRAIL-based therapies. We found that TWIST1 overexpression suppressed both intrinsic- and extrinsic-mediated apoptosis in NSCLC cells. By genetically inhibiting *TWIST1* and overexpressing TWIST1, we demonstrated that TWIST1 positively regulates expression of cFLIP, a negative regulator of DR4/5 signaling, and negatively regulates expression of BID, a pro-apoptotic protein

that mediates crosstalk between intrinsic and extrinsic apoptosis. TWIST1 induced cFLIP expression through a direct transcriptional mechanism as we found that TWIST1 directly bound to the *CFLAR* (gene encoding cFLIP) promoter in ChIP assays and induced luciferase expression in a *CFLAR* promoter reporter construct. We also demonstrated that TWIST1 overexpression was sufficient to cause resistance to both recombinant TRAIL and TIC10. TWIST1 expression was required for TRAIL resistance as knockdown of TWIST1 in a TRAIL-resistance NSCLC cell line resulted in increased sensitivity to TRAIL. These studies demonstrate TWIST1 mediates resistance to TRAIL-based therapies by upregulating of its novel target gene, cFLIP.

Contributors to study: Zachary A. Yochum¹⁻², Susheel K. Khetarpal², Timothy F. Burns¹⁻²

¹Department of Pharmacology and Chemical Biology, University of Pittsburgh, Pittsburgh, PA

²Department of Medicine, Division of Hematology-Oncology, UPMC Hillman Cancer Center, Pittsburgh, PA.

Manuscript in preparation.

5.2 INTRODUCTION

TNF-related apoptosis inducing ligand (TRAIL) is a death ligand that induces extrinsic apoptosis by activating death receptor 4 (DR4) and death receptor 5 (DR5) signaling (173). Binding of TRAIL to DR4/5 results in receptor trimerization and recruitment of Fas associated via death domain (FADD) (173). Procaspase-8 subsequently binds to FADD, forming a death

receptor-FADD-caspase-8 complex referred to as the death inducing signaling complex (DISC) (173). At the DISC, procaspase-8 is cleaved into its active form, which induces apoptosis by activating executioner caspases-3/7 (173). Additionally, caspase-8 can activate intrinsic apoptosis by cleaving BID, a pro-apoptotic BCL-2 protein that translocates to the mitochondria. At the mitochondria, BID can induce apoptosis by directly activating BAX/BAK or inhibiting anti-apoptotic BCL-2 proteins.

Preclinical studies have demonstrated TRAIL can selectively induce apoptosis in cancer cells, while sparing normal cells (327). Despite promising preclinical evidence for the potential efficacy of recombinant TRAIL and TRAIL receptor agonists, these TRAIL-based therapies have largely failed clinically (328). *De-novo* and acquired resistance to TRAIL-based therapies have limited their clinical efficacy in solid tumors (329). Several mechanisms of resistance to TRAIL-based therapies have been identified and typically involve modulation of proteins within the extrinsic apoptotic pathway (168,327,329). One mechanism is upregulation of FLICE-inhibitor protein (cFLIP), which blocks caspase-8 activation at the DISC (330). Alternatively, cancers can decrease caspase-8 expression (331). Aberrations in DR4/5 can also cause resistance to TRAIL. Cancers frequently decrease DR4/5 transport to the plasma membrane or harbor mutations in DR4/5 that result in impaired caspase-8 activation at the DISC (178,327,332). Interestingly, Type II cells require BID cleavage by caspase-8 in order to undergo apoptosis. In Type II cells, resistance to TRAIL can be mediated by increasing expression of anti-apoptotic proteins such as BCL-2, MCL-1, and BCL-xL (327,329,333). New TRAIL-based therapies have shown activity in cancers resistant to recombinant TRAIL (328,334). Of note, TIC10/ONC201, a first-in-class small molecule that induces TRAIL and DR5 expression, has marked activity *in vivo* and *in vitro* activity in solid tumors, including lung cancer (334). TIC10 inhibits both ERK

and AKT, which results in FOXO3A translocation to the nucleus and increased TRAIL and DR5 transcription (334). The activity of TIC10 requires TRAIL/DR5 signaling (334).

Patients with non-small cell lung cancer (NSCLC) are currently classified based on histology and molecular driver. Some subsets of patients with targetable molecular drivers like those patients with *EGFR* mutation or *ALK* translocations demonstrate marked clinical benefit from therapies targeting these molecular drivers (10). However, most patients do not have a targetable oncogenic molecular driver and the most frequent driver, mutant *KRAS*, is not targetable (10). There is a significant need for novel agents to durably treat oncogene-driven NSCLC.

While there is a subset of non-small cell lung cancer (NSCLC) that are sensitive to TRAIL and TRAIL-based therapies, most NSCLC are resistant to these therapies (335,336). Interestingly, epithelial-mesenchymal transition (EMT) has been associated with TRAIL resistance in NSCLC (337). Our group and others have previously demonstrated that the EMT-transcription factor, TWIST1, is required for oncogene-driven NSCLC and can confer chemoresistance and resistance to targeted therapies in NSCLC (160,198,232,234). In the current study, we investigated the role of TWIST1 in mediating resistance to recombinant TRAIL and TRAIL-based therapies. We found that apoptosis is required for growth inhibition following genetic inhibition of *TWIST1*. TWIST1 suppresses apoptosis through transcriptional regulation of both intrinsic and extrinsic pathway members. Interestingly, TWIST1 modulates multiple proteins within extrinsic apoptotic pathway, including cFLIP. TWIST1 regulates cFLIP expression by increasing transcriptional activity at the *CFLAR* (gene encoding cFLIP) promoter and directly binding to multiple E-box binding sites with the *CFLAR* promoter. Additionally, overexpression of TWIST1 leads to TRAIL resistance, while TWIST1 inhibition increases

TRAIL sensitivity. TWIST1 also suppresses apoptosis in response to the novel TRAIL-inducing therapy, TIC10/ONC201.

5.3 METHODS

5.3.1 Cell lines and reagents

PC9, H460, Calu-6, H23 and embryonic kidney cell line HEK 293T were acquired from the American Type Culture Collection (ATCC) and were cultured in the recommended ATCC media. The identity of the aforementioned cell lines was verified by autosomal STR (short tandem repeat) profiling done at University of Arizona Genetics Core (UAGC). Cell lines were tested for mycoplasma every six months using MycoAlert Detection Kit (Lonza). Recombinant TRAIL was purchased from PeproTech (Rocky Hill, NJ). Harmine was purchased from Sigma-Aldrich (St. Louis, MS). TIC10/ONC201 was obtained from Oncoceutics (Philadelphia, PA).

5.3.2 Cell proliferation assays

For all viability experiments, cells were seeded at an appropriate density in 96 well plates and incubated for 24 hours. Cells were subsequently treated with a range of doses of the appropriate inhibitor for the indicated timepoints. Viability was determined using the CellTiter96® Aqueous One Solution Cell Proliferation Assay kit (Promega) or Cell-Titer Glo 2.0 Assay (Promega) according to manufacturer's protocol. Data was analyzed as previously described in Chapter 2.3.2.

5.3.3 Western blot and antibodies

Following appropriate treatment, cells were harvested and lysed and subsequent protein was quantified and western blotting was performed as previously described (234). All information on antibodies is included in Table 3 (Appendix A). Western blot experiments were performed at least twice unless otherwise stated.

5.3.1 Luciferase reporter assay

Luciferase promoter reporter assays were performed as previously described (265). Cell extracts were prepared 48 hours after transfection in passive lysis buffer, and the reporter activity was measured using the Dual-Luciferase Reporter Assay System (Promega). Full length, PR4, PR5 CFLAR constructs were a gift from Wafik El-Diery (Addgene plasmid #16016, 19129, and 19130). R281 and R201 fragments were amplified from full length CFLAR construct. R281, R201, and pGL3 were digested with Kpn and HindIII. Subsequently, R281 and R201 were cloned into pPGL3 using T4 DNA ligase. R281 and R201 pGL3 constructs were all sequence verified.

5.3.2 Chromatin immunoprecipitation

PC9 TRE3G-TWIST1 cells were seeded in 15cm dishes and incubated for 24 hours. Cells were treated with 1000ng/ml of doxycycline. Following 24 hours of doxycycline treatment, cells were harvested and Chromatin Immunoprecipitation (ChIP) was performed using SimpleChIP

Enzymatic Chromatin IP Kit (Cell Signaling Technology) according to manufacturer's recommendations. ChIP primers that were used are included in Table 8 (Appendix A). For ChIP, 2µg of ChIP-grade TWIST1 antibody (Abcam, Ab5087) and 2µg Mouse IgG, Whole Molecule Control (Thermo Scientific, 31903) were used.

5.3.3 Lentiviral shRNA and cDNA overexpression

293T cells were seeded at a density of 4×10^6 in 25-cm² flasks. Following a 24 hour incubation period, cells were transfected to generate lentivirus using a four -plasmid system according to the TRC Library Production and Performance protocols, RNAi Consortium, Broad Institute (264) and as previously described (234). A complete list of the constructs used is in Supplementary Tables 4-6 (Appendix A) and sequences of these constructs and primers used are available upon request. A pCR3-cFLIP_S plasmid was obtained from Dr. Shi-Yong Sun (Emory University) and the insert was cloned into the pDONOR plasmid. Using gateway cloning cFLIP_S was then cloned into pLENTI6 destination plasmid.

5.4 RESULTS

5.4.1 Apoptosis following loss of TWIST1 expression requires both the intrinsic and extrinsic apoptotic pathways

We have previously demonstrated that TWIST1 expression is required for oncogene-driven NSCLC including those tumors with *KRAS* mutations, *EGFR* mutations, and *MET*

mutations/amplifications (232-234). Loss of TWIST1 expression results in growth inhibition, typically due to induction of oncogene induced senescence (OIS) (232-234). However, there are a subset of NSCLC cell lines that may be more dependent on TWIST1 expression for survival and undergo apoptosis following loss of TWIST1 expression (**Figures 12, 24 and 39**). We investigated the mechanisms by which TWIST1 suppresses apoptosis in NSCLC. We first demonstrated that apoptosis is required for growth inhibition following genetic inhibition of *TWIST1* as use of a pan-caspase inhibitor rescues growth inhibition following TWIST1 knockdown (**Figure 40**). In order to better understand the requirement of the intrinsic apoptotic pathways following loss of TWIST1 expression, we overexpressed BCL-2, an inhibitor of intrinsic apoptosis, or genetically silenced *BCL2L1*, a pro-apoptotic gene involved in promoting intrinsic apoptosis that we demonstrated in Chapter 3.4.3 is negatively regulated by TWIST1. We demonstrated that BCL-2 overexpression or BIM knockdown partially suppressed apoptosis and growth inhibition following genetic inhibition of *TWIST1* in Calu-6 cells, a *KRAS* mutant NSCLC cell line that undergoes apoptosis following knockdown of TWIST1 (**Figure 41 and Figure 42A-B**). In addition, knockdown of BIM decreased the cytotoxicity of harmine, a TWIST1 inhibitor (**Figure 42C**). To explore the role of the extrinsic pathway, we overexpressed cFLIPs, an inhibitor of extrinsic apoptosis, in Calu-6 cells. We demonstrated that cFLIPs overexpression partially rescued apoptosis and growth inhibition, following genetic inhibition of *TWIST1* (**Figure 41C**). The rescue observed with cFLIPs overexpression was less robust than that seen with BCL-2 overexpression, which suggests that the intrinsic pathway is the dominant pathway in Calu-6 cells. Alternatively, Calu-6 cells may be type II cells in which death receptor activity is not sufficient to activate executioner caspases, but rather activates intrinsic apoptosis

by cleaving the pro-apoptotic protein BID. Overall, these data suggest that TWIST1 suppresses both intrinsic and extrinsic-mediated apoptosis.

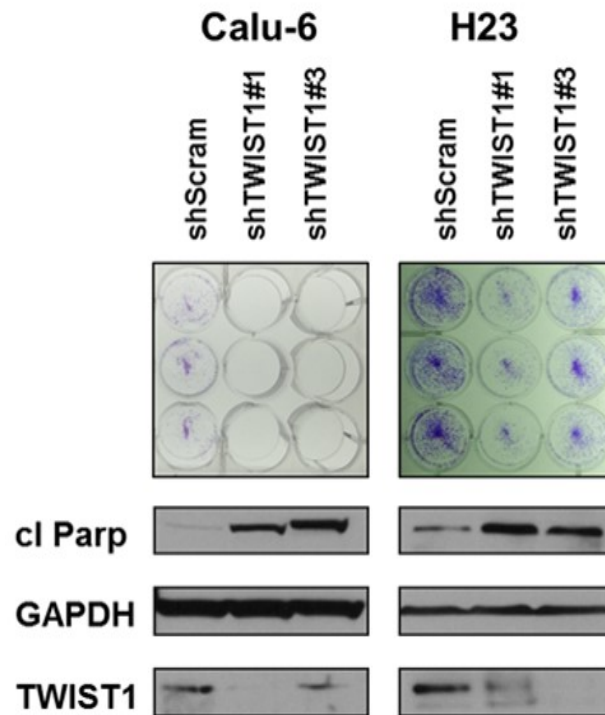


Figure 39: Silencing of *TWIST* leads to apoptosis in NSCLC cell lines

UPPER: Silencing of *TWIST1* with two different shRNAs (shTWIST1#1 and shTWIST1#3) resulted in growth inhibition of *KRAS* mutant (H23 and Calu-6) NSCLC cell lines, as shown by representative triplicates of crystal violet staining. LOWER: Western blot demonstrating an increase in cleaved PARP, a marker of apoptosis, 4 days following shRNA infection.

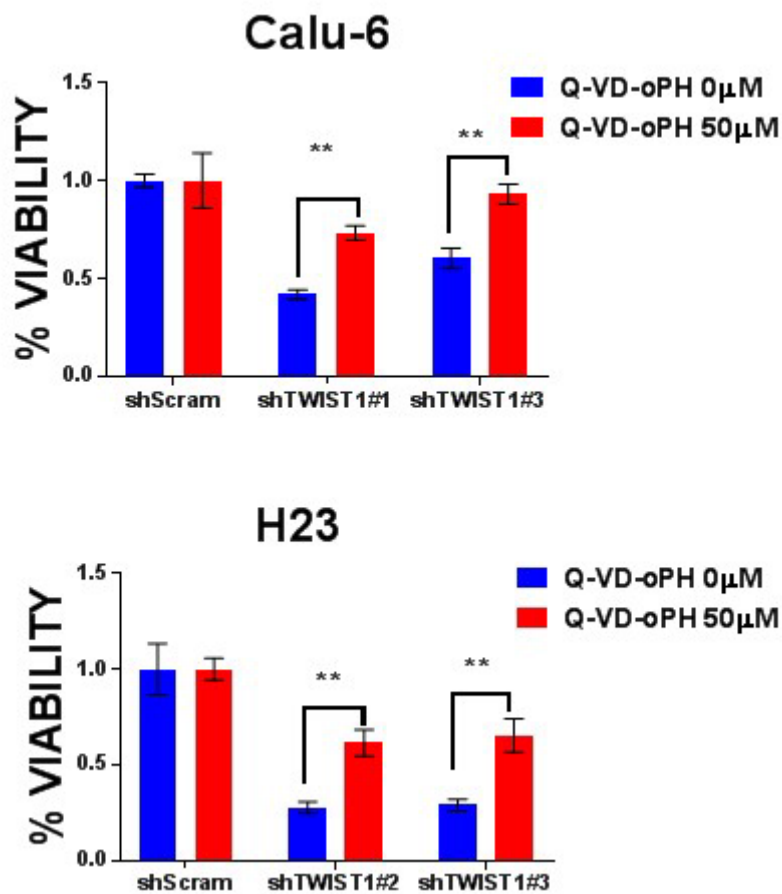


Figure 40: Growth inhibition following genetic inhibition of *TWIST1* requires apoptosis

Cell-Titer Glo proliferation assay demonstrating that growth inhibition following *TWIST1* knockdown can be prevented by treatment with Q-VD-oPH, a pan caspase inhibitor. Cells were pre-treated with Q-VD-oPH at the indicated uM concentrations (DMSO was used as control) for 3 hours and were subsequently infected with the indicated shRNA for 4 days (Calu-6) or 5 days (H23). Data represent mean \pm SD (n=4 technical replicates). **, p<.01, 2-tailed Student's t-test

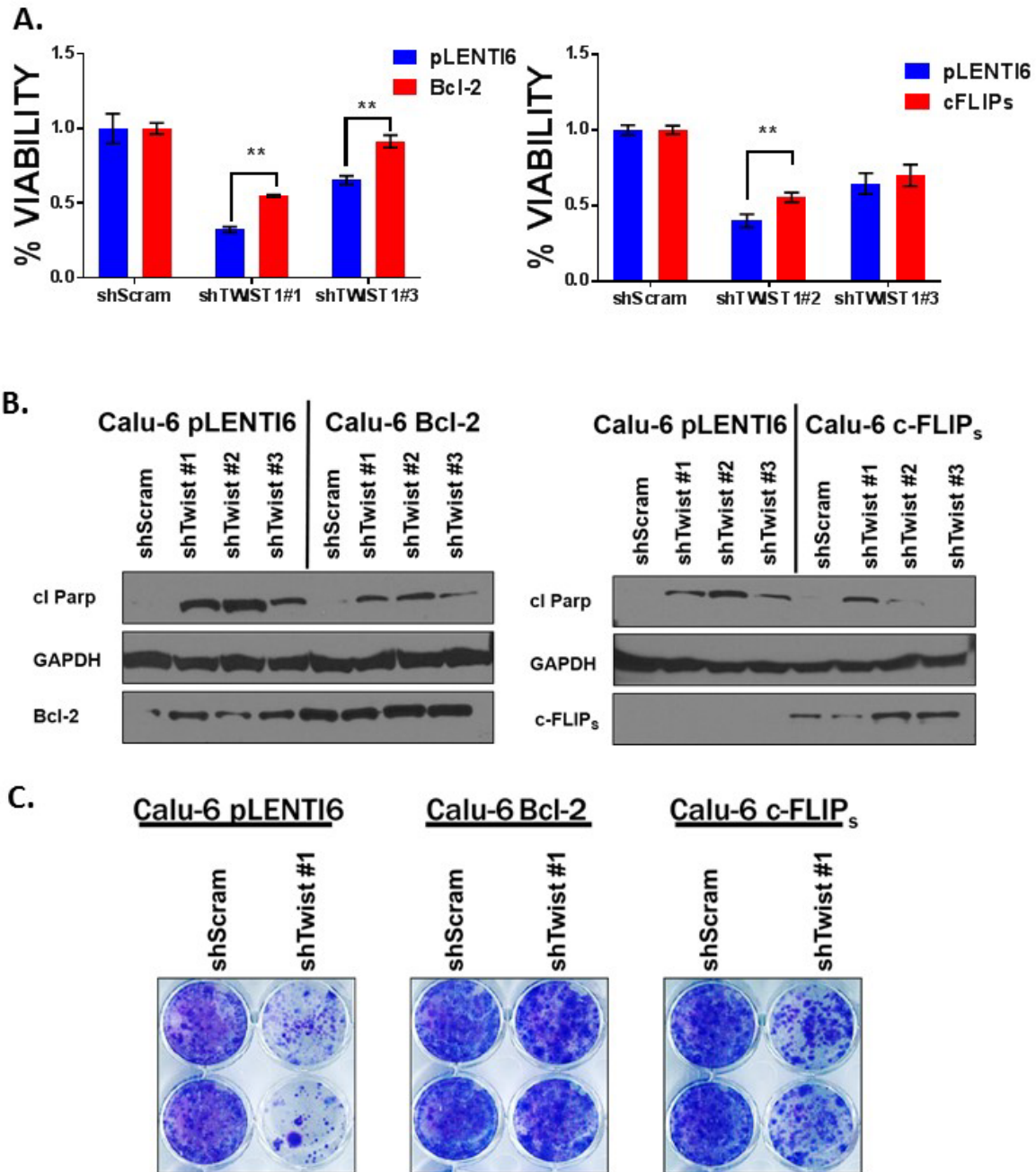


Figure 41: Overexpression of c-FLIP_s or BCL-2 partially rescues apoptosis and growth inhibition following silencing of *TWIST1*.

(A) Cell-Titer Glo proliferation assay demonstrating that overexpressing c-FLIP_s or Bcl-2 can partially rescue growth inhibition following silencing of *TWIST1*. Calu-6 cells that stably overexpress c-FLIP_s, Bcl-2, or empty vector were infected with the indicated shRNA for 96 hours. Data represent mean \pm SD (n=4 technical replicates). **, p<.01, 2-tailed Student's t-test (B) Western blot demonstrating that overexpressing of c-FLIP_s or Bcl-2 can partially prevent PARP cleavage following silencing of *TWIST1*. Calu-6 cells that stably overexpress c-FLIP_s or Bcl-2 were infected with the indicated shRNA for 72 hours and then harvested for Western blot analysis (cells transfected with empty vector, pLENTI6, were used as control). (C) Overexpression of Bcl-2 or c-FLIP_s results in partial rescue of long-term growth inhibition following silencing of *TWIST1*, as shown by duplicates of crystal violet staining 24 days following plating (28 days following *TWIST1* knockdown).

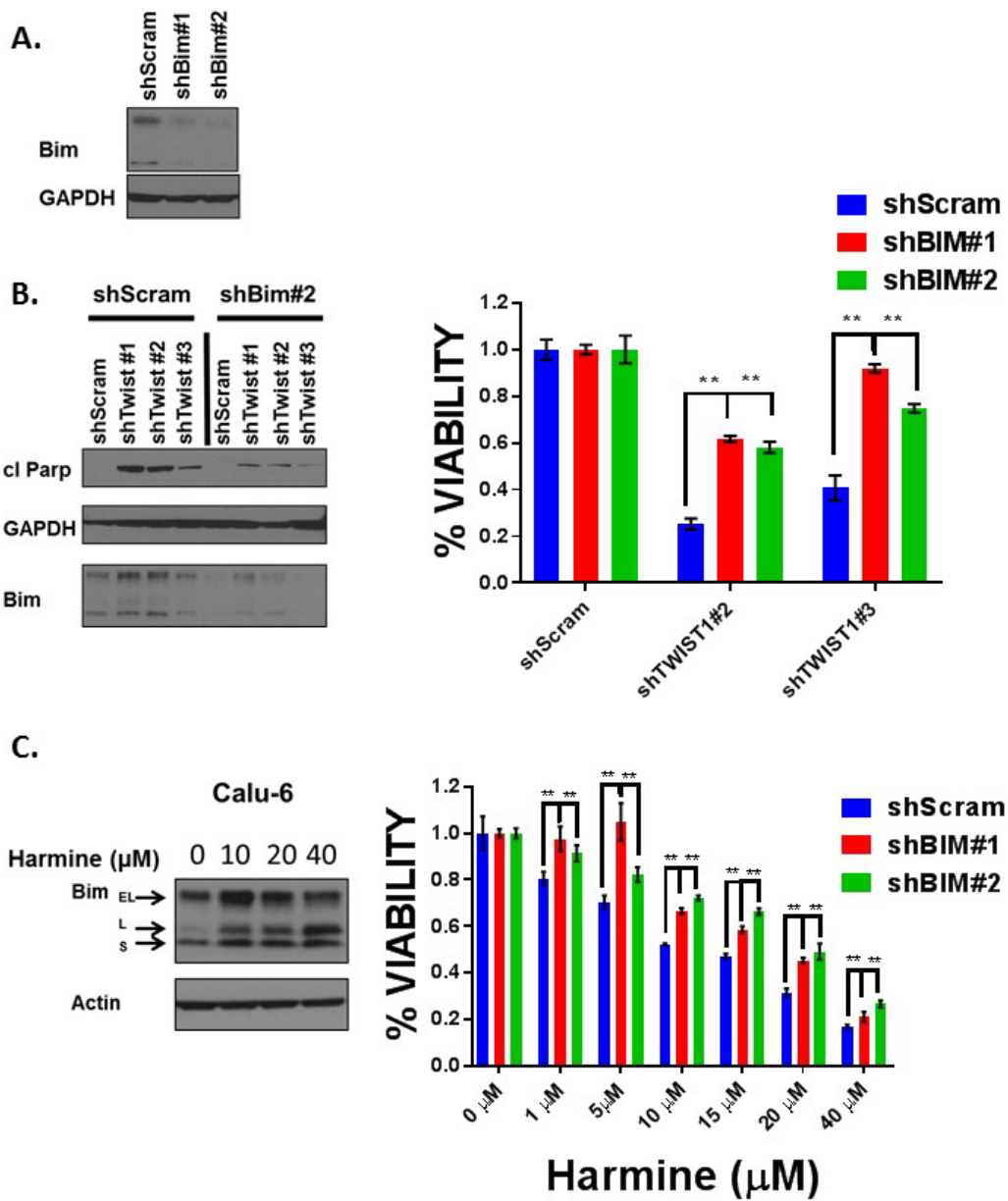


Figure 42: Knockdown of BIM partially rescues growth inhibition following pharmacologic and genetic inhibition of TWIST1

(A) Western blot demonstrating BIM knockdown following infection with two distinct shRNA targeting BIM. (B) LEFT: Western blot demonstrating that knockdown of BIM can partially prevent PARP cleavage following silencing of *TWIST1*. Calu-6 cells that stably express shScram or shBIM were infected with the indicated shRNA for 72 hours and then harvested for Western blot analysis. RIGHT: Cell-Titer Glo (CTG) proliferation assay demonstrating that knockdown can partially rescue growth inhibition following silencing of *TWIST1*. Calu-6 cells that stably express shScram or shBIM#1/2 were infected with the indicated shRNA for 96 hours. Data represent mean \pm SD (n=4 technical replicates). 2-tailed Student's t-test. **, p<.01 (C) LEFT: Western blot demonstrating that harmine treatment increases BIM expression. Calu-6 cells were treated with the indicated doses of harmine for 48 hours and then harvested for Western blot analysis. RIGHT: CTG proliferation assay demonstrating that BIM knockdown can partially rescue harmine-induced growth inhibition. Calu-6 cells stably expressing shBIM#1/2 or shScram were treated with harmine at the indicated μM concentrations (DMSO was used as control) for 96 hours. Data represent mean \pm SD (n=4 technical replicates). 2-tailed Student's t-test. **, p<.01

5.4.2 TWIST1 directly upregulates cFLIP

We have previously demonstrated that TWIST1 can modulate the intrinsic apoptotic protein, BIM (**Figure 29**). Given evidence that extrinsic pathway may be important for apoptosis following loss of TWIST1 expression (**Figure 41**), we explored whether TWIST1 modulates apoptotic proteins within the extrinsic pathway. Knockdown of TWIST1 in Calu-6 cells results in cleavage of caspase-3, -9, and -8 confirming that apoptosis following loss of TWIST1 involves both intrinsic and extrinsic apoptosis (**Figure 43A**). Additionally, TWIST1 knockdown resulted in increased levels of BID and decreased levels of both the short and long isoforms of cFLIP (cFLIP_S and cFLIP_L) (**Figure 43A**). Conversely, overexpression of TWIST1 results in increased levels of cFLIP_S, cFLIP_L and decreased levels of BID, suggesting that TWIST1 may regulate both apoptotic proteins (**Figure 43B**).

cFLIP can be regulated on the transcriptional and post-translational levels (338). Transcription factors like NF- κ B and androgen receptor have been shown to transcriptionally induce cFLIP and decrease sensitivity to TRAIL (338-340). Interestingly, other oncogenic transcription factors like cMYC have been shown to suppress cFLIP expression and confer sensitivity to TRAIL (338,341). We investigated the mechanism(s) by which TWIST1 regulates cFLIP expression in NSCLC cells. Initially, we explored whether TWIST1 could modulate *CFLAR* (gene encoding cFLIP) promoter activity, using a luciferase reporter construct containing the *CFLAR* promoter (341). We demonstrated that overexpression of TWIST1 increased *CFLAR* promoter activity, resulting in 3-fold increase in luciferase activity (**Figure 44A**). Of note, there are multiple E-box binding sites, the canonical binding site of TWIST1, within the *CFLAR*

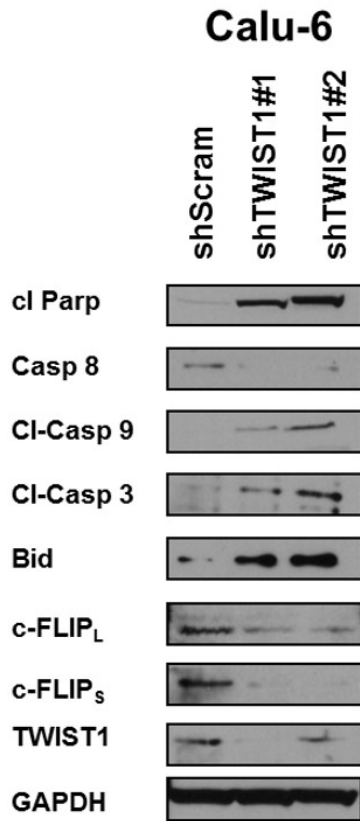
promoter. By removing regions of the putative *CFLAR* promoter, we created multiple luciferase promoter constructs that allowed for interrogation of the role of specific E-boxes in TWIST1-mediated transactivation of the *CFLAR* promoter (**Figure 44A**). Using these modified constructs, we demonstrated that TWIST1 transactivation was not affected by removal of the 5 E-boxes within a 676 base pair (bp) upstream region (-1179 to -503) in the *CFLAR* promoter (**Figure 44A**). However, TWIST1-mediated transactivation was markedly reduced in the PR4 and R281 constructs, suggesting that TWIST1 transactivation of the *CFLAR* promoter requires an E-box approximately 500 bp upstream of the transcriptional start site (TSS) and an E-box approximately 280 bp downstream of the TSS (**Figure 44A**).

Additionally, we and others have previously shown that TWIST1 homo- versus heterodimerization can influence the ability of TWIST to regulate target genes (248,265). We demonstrated that both the TWIST1-TWIST1 homodimer and TWIST1-E2A heterodimer were able to transactivate the *CFLAR* promoter (**Figure 44B**). Of note, the TWIST1-E2A heterodimers did demonstrate greater induction of luciferase activity than the TWIST1-TWIST1 homodimer (5-fold), suggesting that the TWIST1-E2A heterodimer may more effectively upregulate cFLIP (**Figure 44B**), which is consistent with our findings for other TWIST1 responsive promoters (**Figure 19B**). In order to determine if TWIST1 is directly regulating *CFLAR* transcription, we performed TWIST1-ChIP on multiple regions of the *CFLAR* promoter. We demonstrated that TWIST1 binds to two regions of the *CFLAR* promoter, a double E-box approximately 1000 bp upstream of the TSS (Primer#2) and the E-box approximately 500 bp upstream of the TSS (Primer#4) (**Figure 45**). Given the aforementioned luciferase reporter data, TWIST1 binding to the E-box in Primer#2 may not be required for TWIST1-mediated transactivation of the *CFLAR* promoter, given that removal of this double E-box did not affect

luciferase activity. TWIST1 binding to the E-box in Primer#4 seems to be required to be TWIST1-mediated transactivation, as its removal results in suppressed luciferase activity. Of note, TWIST1 did not directly bind to E-box downstream of the TSS (Primer#5) in our ChIP experiment, which was required TWIST1-mediated transactivation of the *CFLAR* promoter in our luciferase experiments. One potential explanation for the lack of TWIST1 binding to this downstream E-box may be that TWIST1 directly upregulates other EMT-transcription factors which can subsequently bind to this downstream E-box and regulate *CFLAR* expression. This phenomenon has been observed with other TWIST-regulated genes. For example, TWIST1-suppression of E-cadherin requires TWIST1 direct upregulation of the EMT-transcription factor, SNAI2 (236). However, TWIST1 upregulation of SNAI2 is unlikely to be important in *CFLAR* regulation, as overexpression of SNAI2 does not modulate *CFLAR* promoter activity (data not shown).

Another potential reason for the lack of binding of TWIST1 to this aforementioned downstream E-box (Primer#5) may be that the *CFLAR* promoter construct utilized may not recapitulate the chromatin structure of the endogenous *CFLAR* gene, as transiently transfected DNA does not recapitulate the chromatin structure of endogenous genes (342). Additionally, there are predicted binding sites for Retinoic X Receptor (RXR) and Aryl hydrocarbon receptor (AhR) exclusively found at sites flanking the E-boxes that TWIST1 binds (Primer#2 and Primer#4). Interestingly, RXR has previously been identified as a candidate co-factor for TWIST1 (343). TWIST1 binding specifically to these sites may be influenced by the presence of these other transcription factors.

A.



B.

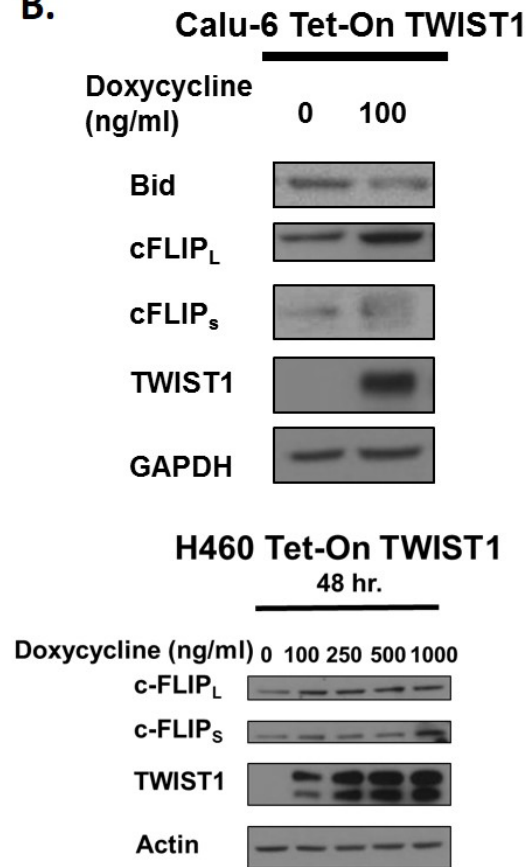


Figure 43: Modulation of TWIST1 expression results in altered expression of extrinsic apoptotic pathway members

(A) Western blot demonstrating that genetic silencing of *TWIST1* results in an increase in BID levels as well as cleaved PARP and caspase-3, -8, -9 and a decrease in cFLIP expression in *KRAS* mutant Calu-6 NSCLC cells, 4 days following shRNA infection. (B) Western blot demonstrating induction of cFLIP_S and cFLIP_L and repression of BID levels following exogenous TWIST1 protein expression in Calu-6 TRE3G-TWIST1 and H460 TRE3G-TWIST1 cells 72 hours (Calu-6) or 48 hours (H460) after treatment with the indicated doses of doxycycline.

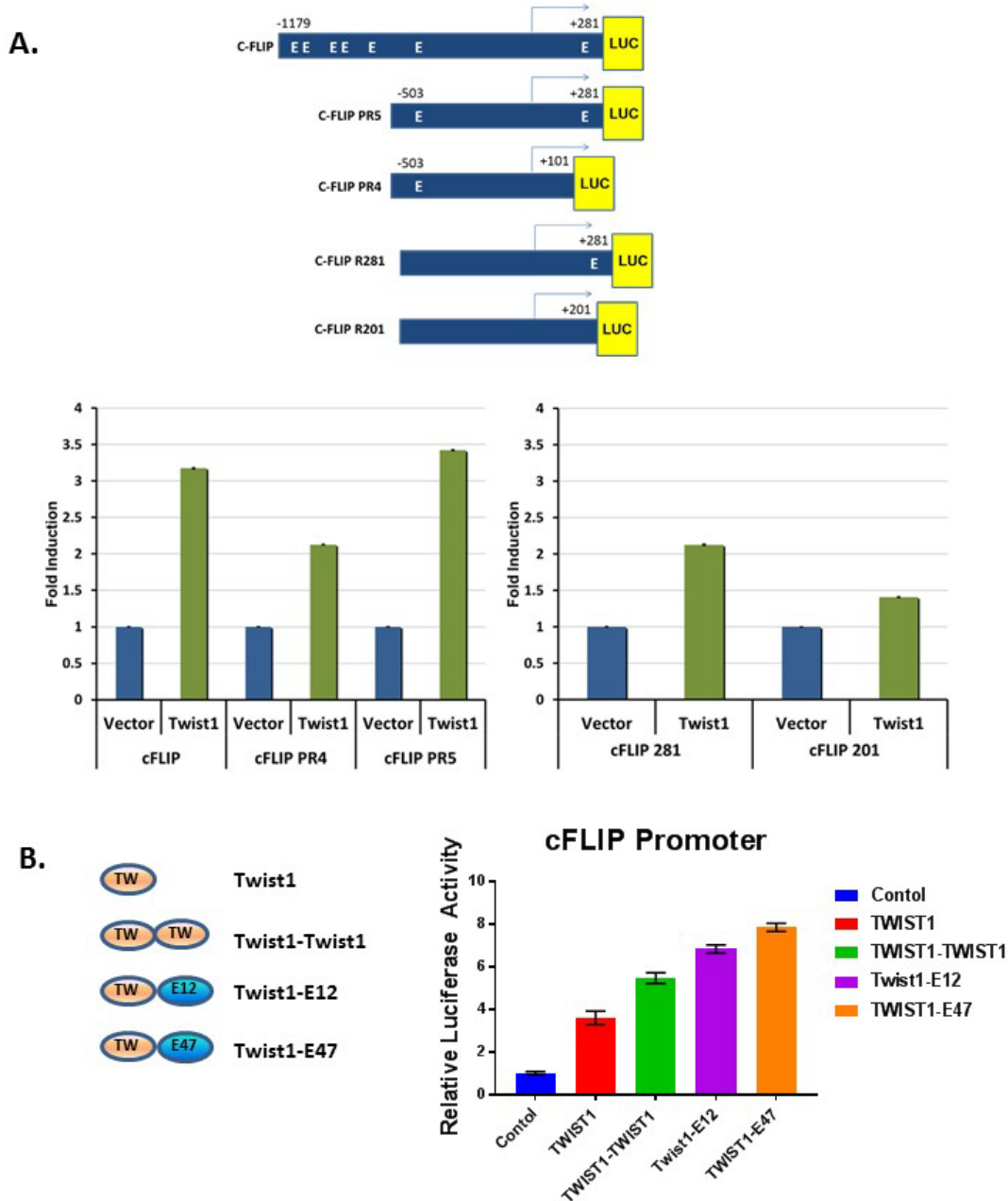


Figure 44: The TWIST1 homodimer and heterodimer transactivates the *CFLAR* promoter

(A) UPPER: A schematic representation of c-FLIP promoter constructs utilized in the current study. “E” marks denote the canonical E-box sequences (CANNTG) to which TWIST1 can potentially bind. LOWER: Luciferase assay showing increased *CFLAR* promoter activity in 293T cells transiently overexpressing TWIST1 compared to the reporter activity of the vector alone. 293T cells were co-transfected with 0.24 μ g of pGL4-cFLIP-Luc reporter plasmid, 0.48 μ g of either W118 empty plasmid or TWIST1 and 0.08 μ g pRL-TK. All values are normalized to the luciferase activity of pGL4-cFLIP-Luc alone that corresponds to 1. (B) Luciferase assay showing increased induction of *CFLAR* promoter activity in cells transiently overexpressing either TWIST1 alone, TWIST-TWIST homodimer, TWIST-E12 heterodimer, or TWIST-E47 heterodimer compared to the reporter activity with the vector alone (fold induction = 1) after 48 hours. 293T cells were co-transfected with 0.40 μ g of pGL4-cFLIP-Luc reporter plasmid, 0.40 μ g of either W118 empty plasmid, TWIST, TWIST-TWIST, TWIST-E12, or TWIST-E47 expression plasmids and 0.01 μ g pRL-TK after 48 hours. All luciferase values were normalized to the corresponding renilla luciferase value in each well.

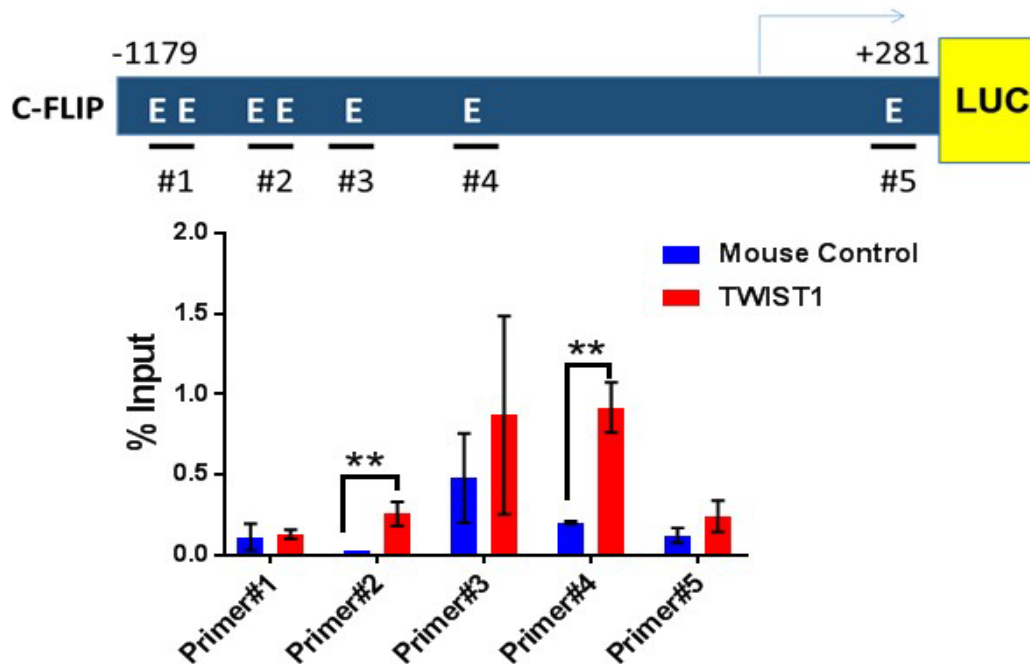


Figure 45: TWIST1 directly binds to the *CFLAR* promoter

ChIP assay demonstrating TWIST1 binding to the putative promoter of *CFLAR*. UPPER: Model demonstrating E-box sites within the *CFLAR* putative promoter that were interrogated for TWIST1 binding. LOWER: qRT-PCR demonstrating that TWIST1 is enriched at multiple sites within the *CFLAR* promoter. Data represent mean \pm SD (n=3 technical replicates). **, p<.01. 2-tailed Student's t-test.

5.4.3 TWIST1 mediates resistance to TRAIL-based therapies

Upregulation of cFLIP has been linked to TRAIL resistance (338). Additionally, previous studies have demonstrated that EMT may mediate resistance to TRAIL-based therapies (337). Given that TWIST1 can induce EMT and upregulate cFLIP, we investigated whether TWIST1 can mediate resistance to TRAIL. In order to this we created doxycycline inducible TWIST1 overexpressing H460 *KRAS* mutant NSCLC cells, which is a cell line sensitive to TRAIL. In this cell line, enforced expression of TWIST1 was sufficient to cause resistance to TRAIL (**Figure 46A**). Additionally, in Calu-6 cells, a TRAIL resistant NSCLC cell line, we demonstrated that

knockdown of TWIST1 increased TRAIL sensitivity (**Figure 46B**). These data suggested that TWIST1 is both sufficient and required for TRAIL resistance in a subset of NSCLC cell lines. Next, we explored whether TWIST1 mediates resistance to the novel TRAIL-inducing small molecule, TIC10. Previous studies have demonstrated that TIC10 has marked antitumor activity in solid tumors, including NSCLC (334,335). Additionally, previous studies have demonstrated that TIC10 cytotoxicity is primarily through induction of extrinsic apoptosis and that cFLIP overexpression can mediate resistance to TIC10 (344). Here, we investigated whether TWIST1 overexpression modulates response to TIC10 by generating doxycycline inducible TWIST1 overexpressing PC9 and H460 NSCLC cells, which are TIC10 sensitive NSCLC lines. We demonstrated that TWIST1 overexpression leads to suppression of TIC10-induced apoptosis in both H460 and PC9 NSCLC cell lines (**Figure 46C**). These data suggesting that TWIST1 can mediate resistance recombinant TRAIL and other TRAIL-based agents.

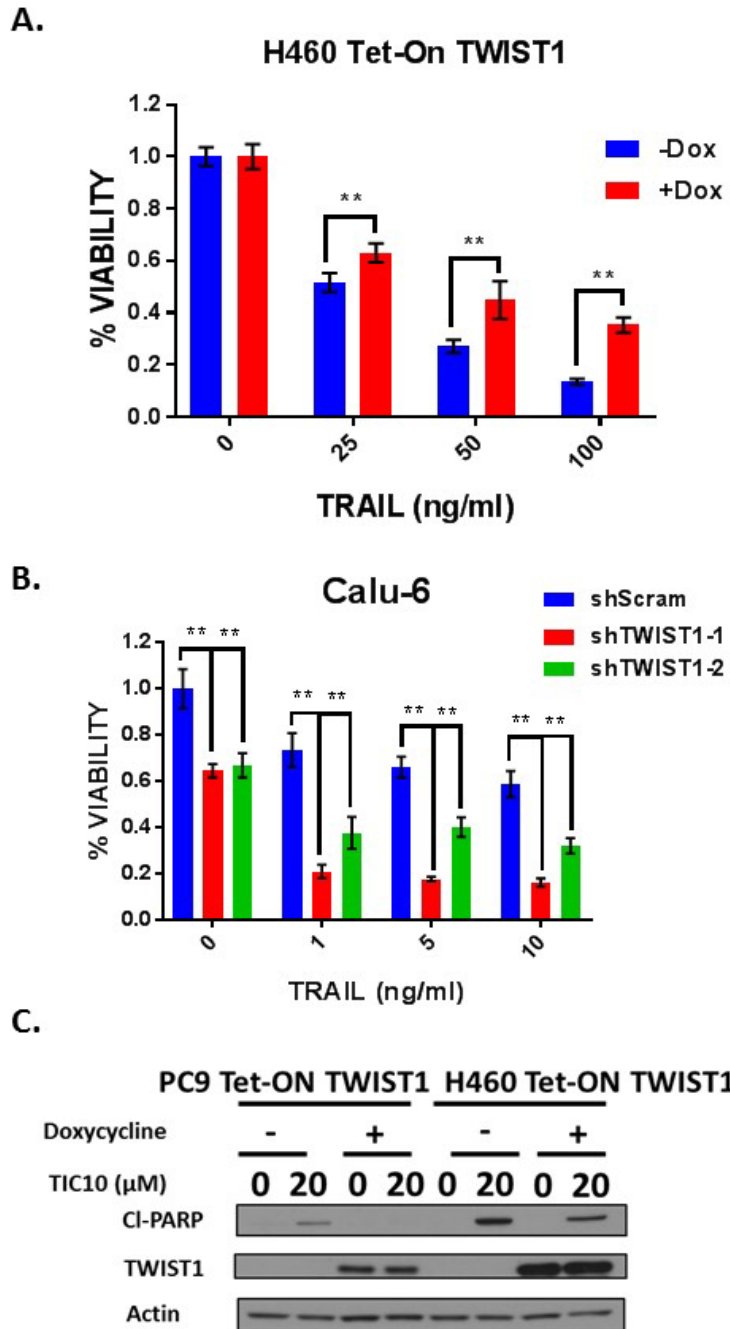


Figure 46: TWIST1 mediates resistance to TRAIL-based therapies

(A) Cell-Titer Glo (CTG) proliferation assay demonstrating decreased TRAIL sensitivity following TWIST1 overexpression. H460 doxycycline inducible TWIST1 cells were treated with doxycycline for 48 hours prior to TRAIL treatment and treated with TRAIL for 24 hours. Data represent mean \pm SD (n=4 technical replicates). **, p<.01, 2-tailed Student's t-test (B) CTG proliferation assay demonstrating increased TRAIL sensitivity following TWIST1 knockdown. Calu-6 cells were infected with the indicated shRNA for 48 hours and then treated with TRAIL for 48 hours. Data represent mean \pm SD (n=4 technical replicates). **, p<.01, 2-tailed Student's t-test (C) Western blot demonstrating TWIST1 overexpression suppresses TIC10-induced apoptosis in PC9 and H460 cells. PC9 and H460 doxycycline inducible TWIST1 cells were treated with doxycycline for 72 hours and subsequently treated with TIC10 for 24 hours.

5.5 DISCUSSION

We have previously shown that TWIST1 is required for oncogene-driven NSCLC and primarily functions to suppress OIS and apoptosis in NSCLC (232-234). In Chapter 3, we demonstrated that TWIST1 mediates resistance to EGFR tyrosine kinase inhibitors (TKIs) in *EGFR* mutant NSCLC by suppressing BIM-mediated apoptosis. Here, we demonstrated that growth inhibition following TWIST1 inhibition requires both intrinsic and extrinsic apoptosis. We establish that TWIST1 negative regulation of extrinsic apoptosis leads to resistance to both recombinant TRAIL and the novel TRAIL-inducing small molecule, TIC10. Our studies suggest that TWIST1 may be a viable therapeutic target to overcome both *de-novo* and acquired resistance to TRAIL-based therapies in NSCLC.

Our study is the first to demonstrate that the EMT-transcription factor (EMT-TF), TWIST1, mediates resistance to TRAIL and TIC10. Previous studies have implicated EMT in TRAIL resistance, however, the mechanism(s) by which an EMT phenotype promotes TRAIL resistance remain poorly elucidated (337,345). Our study suggests that EMT-TFs may mediate resistance to TRAIL-based therapies by suppressing extrinsic apoptotic signaling. Numerous studies have demonstrated that TWIST1 is a potent inducer of EMT (198), however, TWIST1-mediated TRAIL resistance may occur independently of EMT, as TWIST1 expression does not lead to an EMT phenotype in all NSCLC utilized in the current study. While we established that TWIST1 overexpression is sufficient for TRAIL and TIC10 resistance in NSCLC cell lines, we are currently exploring the role of TWIST1 in mediating resistance to TRAIL and TIC10 *in vivo*, using xenograft mouse models. Our studies also suggest that TWIST1 is a potential therapeutic target to overcome resistance to TRAIL-based therapies, as we demonstrated that knockdown of TWIST1 can resensitize TRAIL-resistant NSCLC cells to TRAIL. In Chapter 3, we

demonstrated resistance to EGFR TKIs can be overcome with our novel small molecule inhibitor of TWIST1, harmine. We are currently exploring whether harmine treatment is able to overcome TRAIL and TIC10 resistance both in NSCLC cell lines and *in vivo* using cell line and patient-derived xenograft mouse models.

Our study identified *CFLAR* (gene encoding cFLIP) as a novel target gene of TWIST1. Given that cFLIP has been previously identified as a mediator of resistance to TRAIL (181,330), it is likely that TWIST1 upregulation of cFLIP is a mechanism by which TWIST1 mediates resistance to TRAIL/TIC10. However, future studies will be aimed at determining if TWIST1 upregulation of cFLIP is the only mediator of TWIST1-mediated resistance or if TWIST1 regulation of other apoptotic proteins is important for TWIST1-mediated TRAIL resistance. Previous studies have demonstrated that downregulation of the pro-apoptotic proteins BIM or BID can cause resistance to TRAIL (346-348). Given that we have found that TWIST1 negatively regulates both proteins, future studies will be aimed at determining if TWIST1 regulation of either protein is important for TWIST1-mediated TRAIL resistance. Additionally, we are exploring the mechanism(s) by which TWIST1 negatively regulates BID expression. Previous studies have demonstrated that BID is regulated at both the transcriptional and post-translational levels (349). BID phosphorylation and ubiquitination play an important role in its post-translation stability (349,350). Few studies have investigated BID transcriptional regulation. However, BID has been identified as a p53 target gene that is important for p53-mediated apoptosis in response to chemotherapy (349,351). Given that we observed decreased BID protein levels with TWIST1 overexpression and conversely, increased expression with silencing of *TWIST1* in p53 mutant NSCLC cell lines, it is likely that TWIST1 regulation of BID is p53 independent. Alternatively, BID can be transcriptionally repressed by the transcription factor,

promyelocytic leukemia zinc finger (PLZF) protein (352). Currently, we are exploring if TWIST1 directly or indirectly regulates BID transcription and/or regulates BID expression by modulating its post-translational modification.

Initial studies investigating mechanisms of resistance to TIC10 have revealed that overexpression of cFLIP or BCL-2 leads to TIC10 resistance (344). Interestingly, a recent study demonstrated that TIC10 activity *in vivo* requires NK cells, as depletion of NK cells completely abrogated the antitumor activity of TIC10 (353). This study demonstrated that TIC10 increased NK cell TRAIL secretion, activation, and accumulation in tumors (353). While TWIST1 has not been implicated in NK cell biology, previous studies have demonstrated that TWIST1 can suppress NF- κ B signaling and suppress inflammation (198). Additionally, recent studies have demonstrated that an EMT phenotype is associated with an immunosuppressive tumor microenvironment (354-356). In our ongoing experiments investigating the role of TWIST1 in TIC10 resistance *in vivo*, we will investigate whether TWIST1 modulates NK cell activity and accumulation as a potential mechanism of resistance.

In summary, we demonstrated that TWIST1 suppresses both intrinsic and extrinsic apoptosis in NSCLC. We established that TWIST1 negatively regulates extrinsic apoptosis through upregulation of its novel target gene, *CFLAR*. Additionally, we demonstrated that TWIST1 expression is both sufficient and required for resistance to TRAIL-based therapies, such as recombinant TRAIL and TIC10. Given that most NSCLC is resistant to TRAIL and TWIST1 is frequently overexpressed in NSCLC, targeting TWIST1 with small molecules such as novel TWIST1 inhibitor, harmine, represents a therapeutic option to overcome resistance to TRAIL-based therapies in NSCLC.

6.0 CONCLUSIONS

Lung cancer remains the leading cause of cancer-related deaths in the United States and worldwide (2). There have been advances in the treatment of subsets of lung cancer patients, specifically those patients with non-small cell lung cancer (NSCLC). The current treatment paradigm in NSCLC revolves around classifying patients into subgroups based on histology and oncogenic drivers. The subgroups of NSCLC patients with targetable oncogenic drivers such as those patients with *EGFR* mutations or *ALK* translocations have benefitted significantly from the use of tyrosine kinase inhibitors (TKIs) targeting these oncogenes. However, the long-term efficacy of TKIs remains limited due to the fact that almost all patients that initially response to TKIs, inevitably develop acquired resistance. Additionally, a proportion of patients with targetable oncogenic drivers demonstrate *de-novo* resistance. Of note, there are no FDA approved targeted therapies for the 25% of NSCLC patients with the most frequent oncogenic driver, mutant *KRAS*. There is a clear clinical need to develop therapeutic strategies to durably target oncogene-driven NSCLC.

Epithelial-mesenchymal transition (EMT) has been associated with *de-novo* and acquired resistance to both chemotherapy and targeted therapies in NSCLC (160,186,278,357,358). However, the mechanisms by which EMT may promote therapeutic resistance remain poorly understood and currently no therapeutic strategies exist to overcome resistance associated with EMT. We have previously demonstrated that the EMT-transcription factor, TWIST1, is required

for oncogene-driven NSCLC both *in vitro* and *in vivo*. In this collection of studies, we identified and characterized a first-in-class small molecule inhibitor of TWIST1 and demonstrated that TWIST1 mediates resistance to targeted agents in NSCLC.

The first portion of our work focused on identifying potential small molecule inhibitors of TWIST1. Using a chemical-bioinformatic screen, we identified multiple potential inhibitors of TWIST1. Further characterization of the top hits from our screen, revealed that the harmala alkaloid, harmine, inhibited multiple TWIST1 functions including dissemination and suppression of mammary epithelial cell branching in 3D culture. We demonstrated that harmine promoted degradation of TWIST1 in NSCLC cells. Importantly, harmine had activity in oncogene-driven NSCLC cell lines including those with *EGFR* mutations, *MET* alterations, and *KRAS* mutations. Additionally, harmine had marked antitumor activity in both a patient-derived xenograft and transgenic mouse model of *KRAS* mutant NSCLC. Previous work has demonstrated that developing inhibitors of transcription factors is challenging (267). Our work is one of the first studies identifying and characterizing a small molecule inhibitor of an EMT-transcription factor.

Future studies will focus on the identifying the mechanism(s) by which harmine promotes TWIST1 degradation. Through our ongoing studies, we have demonstrated that harmine treatment increases TWIST1 ubiquitination and proteasomal degradation (data not shown). We are currently exploring if harmine promotes degradation of TWIST1 through upregulation of F-box proteins, specifically the F-box and leucine-rich repeat protein 14 (FBXL-14) which has been previously demonstrated to polyubiquitinate TWIST1 (224). Additionally, harmine has neurotoxicity in humans (269). The 7-methoxy moiety on harmine is associated with its neurotoxicity and we demonstrated that this structural moiety is not required for harmine

cytotoxicity in NSCLC (268-270). We are currently attempting to identify analogues of TWIST1 that potentially inhibit TWIST1 without the neurotoxicity associated with harmine.

Targeting TWIST1 is an exciting therapeutic option for oncogene-driven NSCLC. As previously mentioned TWIST1 is frequently overexpressed in NSCLC (233). Given that TWIST1 is required for *KRAS* mutant NSCLC, targeting TWIST1 may be a viable strategy to treat the 25% patients with *KRAS*-driven NSCLC, which currently has no approved targeted therapies (233,234). Additionally, TWIST1 is overexpressed in NSCLC with squamous histology (233). There are few efficacious therapies for patients with metastatic squamous NSCLC. Future studies aimed at characterizing the role of TWIST1 in squamous NSCLC tumorigenesis may provide insight into the potential efficacy of targeting TWIST1 in this subset of NSCLC patients. Furthermore, we have data suggesting that TWIST1 is enriched in lung brain metastases compared to matched primary lung tumors (personal communication). As brain metastases occur in 40% of lung cancer patients and often recur following radiation, targeting TWIST1 may also be effective for lung cancer patients with central nervous system involvement.

Targeting TWIST1 may also be a therapeutic option in other tumor types as it frequently overexpressed in solid tumors, such as breast, colon, and prostate cancer (198,213). In solid tumors, such as breast cancer, TWIST1 is an important mediator of cancer cell invasion, metastasis, and cancer cell stemness (198,213,359,360). Targeting TWIST1 in these settings represents a novel therapeutic strategy to prevent metastasis and/or eliminate cancer stem cells. Additionally, TWIST1 is amplified in approximately 20% patients with rhabdomyosarcoma (211,212,241). TWIST1 has been implicated in rhabdomyosarcoma tumorigenesis by preventing differentiation of myogenic precursors and promoting cell survival (241). Pharmacologic

inhibition of TWIST1 may have important clinical implications in the treatment of TWIST1-driven sarcomas.

TWIST1 overexpression is also associated with chemoresistance in solid tumors (198,213). For example, in breast cancer, TWIST1 mediates chemoresistance and resistance to endocrine therapy (252,361). Being able to directly target an EMT-transcription factor such as TWIST1 has vast therapeutic implications given that EMT is associated with *de-novo* and acquired resistance to chemotherapies, targeted therapies, and immunotherapies (160,161,295,362,363).

In the second portion of our work we focused on investigating the role of TWIST1 in therapeutic resistance to targeted therapies in NSCLC. In Chapter 3, we demonstrated that TWIST1 was both sufficient and required for resistance to both 1st and 3rd generation EGFR TKIs in *EGFR* mutant NSCLC. We also demonstrated in a mouse model of *EGFR* mutant lung cancer that *Twist1* expression led to erlotinib resistance. TWIST1 promoted resistance by suppressing EGFR TKI-induced apoptosis, specifically by repressing transcription of its novel pro-apoptotic target gene, *BCL2L11* (gene encoding BIM). Consistent with our data that TWIST1 suppresses apoptosis following EGFR TKI treatment, use of a BCL-2/BCL-xL inhibitor was able to overcome TWIST1-mediated resistance *in vitro*. Currently, we are investigating whether TWIST1 mediates resistance to EGFR TKIs through other mechanisms such as suppressing senescence or growth arrest in response to EGFR TKIs. Future studies will be aimed at determining if targeting TWIST1 with harmine or use of BCL-2/BCL-xL inhibitors can overcome *Twist1*-mediated resistance in our mouse model of *EGFR* mutant lung cancer.

An important unanswered question is whether TWIST1 is overexpressed in NSCLC patients with *de-novo* or acquired resistance to EGFR TKIs. We are currently assembling the

necessary tissues to try to answer this question. We also aim to determine if TWIST1 overexpression in EGFR TKI resistant patients occurs in patients with an EMT phenotype. Given that the frequency of *T790M* resistance mutations will likely decrease following first-line osimertinib treatment, EGFR-independent mechanisms of acquired resistance will likely increase in frequency. Initial studies have already demonstrated that previously uncommon mechanisms of resistance, such as EMT, *MET* amplification, and histological transformation are more frequently observed in the osimertinib resistant population (83,130,132,136,143,309-312). The increase in frequency of EGFR-independent resistance mechanisms to osimertinib suggests that TWIST1 may be a more frequent mediator of resistance in the setting of osimertinib resistance. Specifically validating TWIST1 as a mechanism of *de-novo* and/or acquired resistance to osimertinib will provide the clinical rationale for targeting TWIST1 directly or indirectly as a means to overcome or prevent osimertinib resistance.

In a parallel study to our work investigating the role of TWIST1 in resistance to EGFR inhibitors, we examined the role of TWIST1 in mediating *de-novo* and acquired resistance to MET TKIs as well as acquired resistance to EGFR and MET TKIs in the setting of HGF overexpression. We demonstrated that TWIST1 overexpression led to MET TKI resistance in MET-driven NSCLC cells. Targeting TWIST1 with harmine increased MET TKI sensitivity in *MET* altered cell lines. Given that we demonstrated that TWIST1 mediates resistance to EGFR TKIs by suppressing BIM-mediated apoptosis, we are currently determining if TWIST1 suppression of BIM is a mechanism by which TWIST1 mediates resistance to MET TKIs. Additionally, in our mouse model of Hgf-driven lung cancer, we are exploring if *Twist1* overexpression *in vivo* is sufficient to cause MET TKI resistance. Future studies will also be aimed at validating TWIST1 as a mediator of resistance to MET TKIs in patients with *MET*

amplified and *MET* mutant NSCLC. Given that mechanisms of resistance MET TKIs in MET-driven NSCLC are poorly described, validating TWIST1 as a mechanism of resistance to MET TKIs in patients will provide the rationale for targeting TWIST1 as a means to overcome MET TKI resistance in MET-driven NSCLC.

Additionally, in our initial studies investigating the role of TWIST1 in HGF-mediated resistance to TKIs, we demonstrated that HGF induces both EMT and TWIST1 expression in NSCLC cells. TWIST1 expression appears to be required for HGF-mediated resistance to MET and EGFR TKIs in MET- and EGFR-driven NSCLC as targeting TWIST1 with harmine overcame HGF-mediated resistance. Currently, we are exploring the mechanism(s) by which HGF induces TWIST1 expression in lung cancer. Additionally, we aim to determine if TWIST1 is upregulated in EGFR TKI resistant patients with *MET* amplification or HGF overexpression (tumor and/or blood). As previously mentioned, HGF is an important mediator of *de-novo* resistance to EGFR TKIs (149,151), while *MET* amplification is a well-validated mechanisms of resistance to 1st generation EGFR TKIs and importantly osimertinib (142,311). Our studies suggest that targeting TWIST1 in these patients may be a viable therapeutic strategy to combat MET-mediated resistance to EGFR TKIs. Importantly, we demonstrated that TWIST1-mediated EGFR TKI resistance can be overcome with a BCL-2/BCL-xL inhibitor. Targeting TWIST1-mediated resistance indirectly through use of navitoclax, a BCL-2/BCL-xL inhibitor, may represent another strategy to overcome TWIST1-mediated resistance to EGFR TKIs in the setting of *MET* amplification or HGF overexpression.

In Chapter 5, we demonstrate that apoptosis following loss of TWIST1 expression requires both the intrinsic and extrinsic apoptotic pathways. Investigation into the mechanisms by which TWIST1 suppresses extrinsic apoptosis revealed that TWIST1 modulates multiple

proteins in the extrinsic apoptotic pathway, specifically cFLIP and BID. We demonstrated that *CFLAR* (gene encoding cFLIP) is a direct target gene of TWIST1, as TWIST1 binds to the *CFLAR* promoter and increases *CFLAR* promoter activity. Of note, we are currently investigating the mechanisms by which TWIST1 regulates BID expression. Additionally, we demonstrated that TWIST1 suppression of extrinsic apoptosis signaling has therapeutic significance, as TWIST1 expression can mediate resistance to both recombinant TRAIL and the TRAIL-inducing small molecule, TIC10. Currently, we are examining if TWIST1 regulation of other apoptotic proteins, specifically BID, is required for TWIST1-mediated resistance to TRAIL-based therapies. Future studies will be aimed at determining if TWIST1 overexpression leads to TRAIL and TIC10 resistance *in vivo* and if targeting TWIST1 with harmine can overcome TWIST1-mediated resistance TRAIL and TIC10. Additionally, given that TRAIL has been implicated in T-cell and NK mediated killing of tumor cells (337,364), future studies will aim to determine if TWIST1 can mediate resistance to immunotherapies by negatively regulating death receptor signaling in cancer cells. Interestingly, we have evidence that TIC10 can degrade TWIST1 (data not shown). Given that TIC10 inhibits both AKT and ERK (334), both of which regulate TWIST1 stability and activity (203,222,246), we are exploring if TIC10 inhibition of AKT and ERK mediates TIC10-mediated degradation of TWIST1. Additionally, given that TWIST1 expression is required for survival of oncogene-driven NSCLC cells (232-234), we are also exploring if TIC10 degradation of TWIST1 is a mechanism by which TIC10 leads to cell death in NSCLC cells.

In summary, we have demonstrated that the EMT-transcription factor TWIST1 mediates resistance to both TKIs and TRAIL-based therapies in NSCLC. Our work provides insight into the mechanisms by which reactivation of TWIST1 expression in cancer leads to therapeutic

resistance. This collection of studies suggests that expression of the EMT-transcription factor, TWIST1, increases the apoptotic threshold in lung cancer cells by transcriptionally suppressing pro-apoptotic genes such as *BCL2L11* and inducing anti-apoptotic genes such as *CFLAR*. Overcoming TWIST1-suppression of apoptosis through use of BCL-2 or BCL-2/BCL-xL inhibitors may be a viable therapeutic strategy to overcome resistance associated with TWIST1 reactivation in cancers. Additionally, direct targeting of TWIST1 with small molecules, such as our novel TWIST1 inhibitor, harmine, represent an exciting therapeutic option to treat oncogene-driven NSCLC both in the primary and resistant setting.

APPENDIX A

SUPPLEMENTAL TABLES

Table 1. List of primers used for SYBR Green qRT-PCR

Primer	Primer Sequence (5'→ 3')
18s Forward	AAC GAA CGA GAC TCT GGC AT
18s Reverse	CAA GCT TAT GAC CCG CAC TT
TWIST1 Forward	GCT TGA GGG TCT GAA TCT TGC T
TWIST1 Reverse	GTC CGC AGT CTT ACG AGG AG
TCF3 Forward	GCA GCC TAG ACA CGC AGC CC
TCF3 Reverse	GCA GCC TAG ACA CGC AGC CC
BCL2L11 Forward	GGC CCC TAC CTC CCT ACA
BCL2L11 Reverse	GGG GTT TGT GTT GAT TTG TCA

Table 2. List of Primers used for Taqman qRT-PCR

Primer	Catalogue#
Eukaryotic 18S rRNA Endogenous Control	4333760T
Human TWIST1	4331182

Table 3. List of antibodies used for western blotting and immunohistochemistry

Antibody	Company	Product number
p21	Calbiochem	OP64
p27	Santa Cruz	sc-1641
cleaved PARP	Cell Signaling	5625
BIM	Cell Signaling	2933
E-Cadherin	Cell Signaling	3195
Vimentin	Cell Signaling	5741
E2A	Santa Cruz	sc-763
TWIST1	Abcam	ab50887
TWIST1 (used for immunohistochemistry)	Santa Cruz	sc- 81417
GAPDH	Santa Cruz	sc-25778
Actin	Millipore	MAB1501
Bcl-2	Cell Signaling	2870P
FLIP	Cell Signaling	8510
BID	Cell Signaling	2002S
Cleaved Caspase-3	Cell Signaling	9661
Cleaved Caspase-9	Cell Signaling	7237S
Caspase-8	Cell Signaling	9496S
Claudin	Cell Signaling	4933P
B-catenin	Cell Signaling	8480
Ki-67	Leica Biosystems	ACK02
Anti-Rabbit IgG HRP linked Secondary Ab	GE Healthcare, UK	NA934V
Anti-Mouse IgG HRP linked Secondary Ab	GE Healthcare, UK	NA931V
PowerVision Poly-HRP anti-rabbit IgG	Leica Biosystems	PV6118

Table 4. Sequences for TWIST1/BCL2L11/TCF3 shRNA (5'-3') in pKLO.1

shRNA Target	Clone ID	Target sequence	shRNA sequence
shTWIST1-1	TRCN0000020539	GCATTCTGA TAGAAGTCT GAA	CCGGGCATTCTGATAGA AGTCTGAACTCGAGTTCA GACTTCTATCAGAATGCT TTTT
shTWIST1-2	TRCN0000020543	GCTGGACTC CAAGATGGC AAG	CCGGGCTGGACTCCAAG ATGGCAAG- CTCGAGCTTGCCATCTTG GAGTCCAGCTTTTT
shTWIST1-3	TRCN0000020543	GCTGGACTC CAAGATGGC AAG	CCGGGCTGGACTCCAAG ATGGCAAG- CTCGAGCTTGCCATCTTG GAGTCCAGCTTTTT
shBIM-1	TRCN0000355973	TACGACTGT TACGTTACA TTG	CCGGTACGACTGTTACGT TACATTGCTCGAGCAATG TAACGTAACAGTCGTATT TTTG
shBIM-2	TRCN0000001051	ATGGTTATC TTACGACTG TTA	CCGGATGGTTATCTTACG ACTGTTACTCGAGTAACA GTCGTAAGATAACCATTT TTT
shBIM-5	TRCN0000001054	AGCCGAAGA CCACCCACG AAT	CCGGAGCCGAAGACCAC CCACGAATCTCGAGATTC GTGGGTGGTCTTCGGCTT TTTT
shTCF3-1	TRCN0000274216	ACGGCCTGC AGAGTAAGA TAG	CCGGACGGCCTGCAGAG TAAGATAG- CTCGAGCTATCTTACTCT GCAGGCCGTTTTTTG
shTCF3-3	TRCN0000274218	CCCGGATCA CTCAAGCAA TAA	CCGGCCCGGATCACTCA AGCAATAACTCGAGTTA TTGCTTGAGTGATCCGGG TTTTTG
shTCF3-4	TRCN0000017535	CAGCCTCTC TTCATCCAC ATT	CCGGCAGCCTCTCTTCAT CCACATTCTCGAGAATGT GGATGAAGAGAGGCTGT TTTT
shScram	Addgene (plasmid 1864) obtained from Dr. David Sabatini (365)	CAGCCTCTC TTCATCCAC ATT	CCTAAGGTTAAGTCGCCC TCGCTCGAGCGAGGGCG ACTTAACCTTAGG

Table 5. ORFs obtained from Johns Hopkins University HiT Center

ORF	CLONE ID	Catalogue#
BCL2	IOH10622	pENTR
TWIST1	IOH22915	pENTR

Table 6. Source of plasmids utilized

Plasmid	Ref
pLenti6/V5-DEST Gateway Vector (Invitrogen)	NA
pLVX-Tet3G (Clontech)	NA
pLVX-TRE3G-IRES (Clontech)	NA
pLenti CMV Puro DEST (w118-1) (Addgene (plasmid 17452))	(366)
pLenti CMV/TO NEO (Addgene (plasmid 17482))	(366)
pGL4-YBX1-Luc	(265)
pGL4-SNAI2-Luc	(265)
pGL3-FLIP1500 (Addgene plasmid 16016)	341)
pGL3-FLIP pr5 (Addgene plasmid 19130)	341)
pGL3-FLIP pr4 (Addgene plasmid 19129)	341)
pRL-RT	NA
pLenti CMV Pur W118 Twist1	(234)
pLenti CMV Pur W118 Twist1-Twist1	(265)
pLenti CMV Pur W118 Twist1-E12	(265)
pLenti CMV Pur W118 Twist1-E47	(232)

Table 7: ChIP Primers for *BCL2L1* Promoter

Primer	Primer Sequence (5' → 3')
BS1 Forward	AAA CTG TGG TGC CGA GTG AAA G
BS1 Reverse	GTC CGT GCG TTT CCT TGC AGA G
BS2 Forward	TGT CCC ACT GAC GTT ACA GAA G
BS2 Reverse	GAA ACT CTG TAA AGG GAC CAC CCT A
BS3 Forward	GGG TCC TAG CCA AAT GCA GTG
BS3 Reverse	CTA AGA GAC AGA GGC CGT GG
BS4 Forward	AGC TGA GGA CCT GCT CGT AG
BS4 Reverse	GAA ACA CCC TCA CAC TGC GC
BS5 Forward	TCA CAG TCA GGT TGT CCA G
BS5 Reverse	CAT GCC CAG GTC ACA GTT AGC C

Table 8: ChIP Primers for *CFLAR* Promoter

Primer	Primer Sequence (5' → 3')
#1 Forward	GCT GAA CAA AGG GAG AGG TTT GG
#1 Reverse	GAC TAA CAG CAG GAC GGC ATG AA
#2 Forward	TTC TTC ACC TTT CCT GTG AG
#2 Reverse	CCA CCA TGC CCG ACT AAT TT
#3 Forward	AGA CCA GCC TTG CCA ACA TG
#3 Reverse	CAA ACC ATC CAG CCC TCA GC
#4 Forward	TGT GTT CAC GTT TGC TAT GAC TCC
#4 Reverse	CAA AGT GCT GGG ATT ACA GGC G
#5 Forward	AAA GGG ACT CCC GGA GCT AG
#5 Reverse	GCT TCT CTC CTA CAC CTC CTC C

BIBLIOGRAPHY

1. Ridge CA, McErlean AM, Ginsberg MS. Epidemiology of lung cancer. *Semin Intervent Radiol.* 2013;30(2):93-98.
2. Society AC. Cancer Facts & Figures 2018. *Atlanta: American Cancer Society.* 2018.
3. Pfeifer GP, Denissenko MF, Olivier M, Tretyakova N, Hecht SS, Hainaut P. Tobacco smoke carcinogens, DNA damage and p53 mutations in smoking-associated cancers. *Oncogene.* 2002;21(48):7435-7451.
4. Vineis P, Alavanja M, Buffler P, Fontham E, Franceschi S, Gao YT, et al. Tobacco and cancer: recent epidemiological evidence. *J Natl Cancer Inst.* 2004;96(2):99-106.
5. Pawel DJ, Puskin JS. The U.S. Environmental Protection Agency's assessment of risks from indoor radon. *Health Phys.* 2004;87(1):68-74.
6. Rubin SA. Lung cancer: past, present, and future. *J Thorac Imaging.* 1991;7(1):1-8.
7. Pershagen G, Akerblom G, Axelson O, Clavensjo B, Damberg L, Desai G, et al. Residential radon exposure and lung cancer in Sweden. *N Engl J Med.* 1994;330(3):159-164.
8. Schoenberg JB, Klotz JB, Wilcox HB, Nicholls GP, Gil-del-Real MT, Stemhagen A, et al. Case-control study of residential radon and lung cancer among New Jersey women. *Cancer Res.* 1990;50(20):6520-6524.
9. Carbone M, Yang H. Molecular pathways: targeting mechanisms of asbestos and erionite carcinogenesis in mesothelioma. *Clin Cancer Res.* 2012;18(3):598-604.
10. Villaruz LC, Burns TF, Ramfidis VS, Socinski MA. Personalizing therapy in advanced non-small cell lung cancer. *Semin Respir Crit Care Med.* 2013;34(6):822-836.
11. Koinis F, Kotsakis A, Georgoulas V. Small cell lung cancer (SCLC): no treatment advances in recent years. *Translational Lung Cancer Research.* 2016;5(1):39-50.

12. Rosell R, Karachaliou N. Large-scale screening for somatic mutations in lung cancer. *Lancet*. 2016;387(10026):1354-1356.
13. Rosell R, Bivona TG, Karachaliou N. Genetics and biomarkers in personalisation of lung cancer treatment. *Lancet*. 2013;382(9893):720-731.
14. Cancer Genome Atlas Research N. Comprehensive molecular profiling of lung adenocarcinoma. *Nature*. 2014;511(7511):543-550.
15. Ferrara R, Mezquita L, Besse B. Progress in the Management of Advanced Thoracic Malignancies in 2017. *J Thorac Oncol*. 2018;13(3):301-322.
16. Roman M, Baraibar I, Lopez I, Nadal E, Rolfo C, Vicent S, et al. KRAS oncogene in non-small cell lung cancer: clinical perspectives on the treatment of an old target. *Mol Cancer*. 2018;17(1):33.
17. Tomasini P, Walia P, Labbe C, Jao K, Leighl NB. Targeting the KRAS Pathway in Non-Small Cell Lung Cancer. *Oncologist*. 2016;21(12):1450-1460.
18. Janes MR, Zhang J, Li LS, Hansen R, Peters U, Guo X, et al. Targeting KRAS Mutant Cancers with a Covalent G12C-Specific Inhibitor. *Cell*. 2018;172(3):578-589 e517.
19. Lito P, Solomon M, Li LS, Hansen R, Rosen N. Allele-specific inhibitors inactivate mutant KRAS G12C by a trapping mechanism. *Science*. 2016;351(6273):604-608.
20. Riely GJ, Johnson ML, Medina C, Rizvi NA, Miller VA, Kris MG, et al. A phase II trial of Salirasib in patients with lung adenocarcinomas with KRAS mutations. *J Thorac Oncol*. 2011;6(8):1435-1437.
21. Baines AT, Xu D, Der CJ. Inhibition of Ras for cancer treatment: the search continues. *Future Med Chem*. 2011;3(14):1787-1808.
22. Cancer Genome Atlas Research N. Comprehensive genomic characterization of squamous cell lung cancers. *Nature*. 2012;489(7417):519-525.
23. Gandara DR, Hammerman PS, Sos ML, Lara PN, Jr., Hirsch FR. Squamous cell lung cancer: from tumor genomics to cancer therapeutics. *Clin Cancer Res*. 2015;21(10):2236-2243.
24. Herbst RS, Gandara DR, Hirsch FR, Redman MW, LeBlanc M, Mack PC, et al. Lung Master Protocol (Lung-MAP)—A Biomarker-Driven Protocol for Accelerating Development of Therapies for Squamous Cell Lung Cancer: SWOG S1400. *Clinical Cancer Research*. 2015;21(7):1514.
25. Postmus PE, Kerr KM, Oudkerk M, Senan S, Waller DA, Vansteenkiste J, et al. Early and locally advanced non-small-cell lung cancer (NSCLC): ESMO Clinical Practice

- Guidelines for diagnosis, treatment and follow-up. *Ann Oncol.* 2017;28(suppl_4):iv1-iv21.
26. Rosen JE, Keshava HB, Yao X, Kim AW, Detterbeck FC, Boffa DJ. The Natural History of Operable Non-Small Cell Lung Cancer in the National Cancer Database. *Ann Thorac Surg.* 2016;101(5):1850-1855.
 27. Artal Cortes A, Calera Urquizu L, Hernando Cubero J. Adjuvant chemotherapy in non-small cell lung cancer: state-of-the-art. *Transl Lung Cancer Res.* 2015;4(2):191-197.
 28. McElnay P, Lim E. Adjuvant or neoadjuvant chemotherapy for NSCLC. *J Thorac Dis.* 2014;6 Suppl 2:S224-227.
 29. Lindberg K, Nyman J, Riesenfeld Kallskog V, Hoyer M, Lund JA, Lax I, et al. Long-term results of a prospective phase II trial of medically inoperable stage I NSCLC treated with SBRT - the Nordic experience. *Acta Oncol.* 2015;54(8):1096-1104.
 30. Versteegen NE, Lagerwaard FJ, Hashemi SM, Dahele M, Slotman BJ, Senan S. Patterns of Disease Recurrence after SABR for Early Stage Non-Small-Cell Lung Cancer: Optimizing Follow-Up Schedules for Salvage Therapy. *J Thorac Oncol.* 2015;10(8):1195-1200.
 31. Timmerman R, Paulus R, Galvin J, Michalski J, Straube W, Bradley J, et al. Stereotactic body radiation therapy for inoperable early stage lung cancer. *JAMA.* 2010;303(11):1070-1076.
 32. Fakiris AJ, McGarry RC, Yiannoutsos CT, Papiez L, Williams M, Henderson MA, et al. Stereotactic body radiation therapy for early-stage non-small-cell lung carcinoma: four-year results of a prospective phase II study. *Int J Radiat Oncol Biol Phys.* 2009;75(3):677-682.
 33. Hirsch FR, Scagliotti GV, Mulshine JL, Kwon R, Curran WJ, Jr., Wu YL, et al. Lung cancer: current therapies and new targeted treatments. *Lancet.* 2017;389(10066):299-311.
 34. Kim CS, Jeter MD. Radiation Therapy, Early Stage Non-Small Cell Lung Cancer. *StatPearls.* Treasure Island (FL)2018.
 35. Calikusi Z AP. Treatment of locally advanced, unresectable or medically inoperable stage III non-small-cell lung cancer: the past, present, and future of chemoradiotherapy. *Journal of Oncological Sciences.* 2018.
 36. Dillman RO, Seagren SL, Propert KJ, Guerra J, Eaton WL, Perry MC, et al. A randomized trial of induction chemotherapy plus high-dose radiation versus radiation alone in stage III non-small-cell lung cancer. *N Engl J Med.* 1990;323(14):940-945.

37. Curran WJ, Jr., Paulus R, Langer CJ, Komaki R, Lee JS, Hauser S, et al. Sequential vs. concurrent chemoradiation for stage III non-small cell lung cancer: randomized phase III trial RTOG 9410. *J Natl Cancer Inst.* 2011;103(19):1452-1460.
38. Liang J, Bi N, Wu S, Chen M, Lv C, Zhao L, et al. Etoposide and cisplatin versus paclitaxel and carboplatin with concurrent thoracic radiotherapy in unresectable stage III non-small cell lung cancer: a multicenter randomized phase III trial. *Ann Oncol.* 2017;28(4):777-783.
39. Ardizzoni A, Boni L, Tiseo M, Fossella FV, Schiller JH, Paesmans M, et al. Cisplatin-versus carboplatin-based chemotherapy in first-line treatment of advanced non-small-cell lung cancer: an individual patient data meta-analysis. *J Natl Cancer Inst.* 2007;99(11):847-857.
40. Dovedi SJ, Adlard AL, Lipowska-Bhalla G, McKenna C, Jones S, Cheadle EJ, et al. Acquired resistance to fractionated radiotherapy can be overcome by concurrent PD-L1 blockade. *Cancer Res.* 2014;74(19):5458-5468.
41. Zhang P, Su DM, Liang M, Fu J. Chemopreventive agents induce programmed death-1-ligand 1 (PD-L1) surface expression in breast cancer cells and promote PD-L1-mediated T cell apoptosis. *Mol Immunol.* 2008;45(5):1470-1476.
42. Antonia SJ, Villegas A, Daniel D, Vicente D, Murakami S, Hui R, et al. Durvalumab after Chemoradiotherapy in Stage III Non-Small-Cell Lung Cancer. *N Engl J Med.* 2017;377(20):1919-1929.
43. Hui R, Özgüroğlu M, Daniel D, Baz D, Murakami S, Yokoi T, et al. PL 02.02 Patient-Reported Outcomes with Durvalumab after Chemoradiation in Locally Advanced, Unresectable NSCLC: Data from PACIFIC. *Journal of Thoracic Oncology.* 2017;12(11):S1604.
44. Melosky B. Current Treatment Algorithms for Patients with Metastatic Non-Small Cell, Non-Squamous Lung Cancer. *Front Oncol.* 2017;7:38.
45. Schiller JH, Harrington D, Belani CP, Langer C, Sandler A, Krook J, et al. Comparison of four chemotherapy regimens for advanced non-small-cell lung cancer. *N Engl J Med.* 2002;346(2):92-98.
46. Scagliotti G, Hanna N, Fossella F, Sugarman K, Blatter J, Peterson P, et al. The differential efficacy of pemetrexed according to NSCLC histology: a review of two Phase III studies. *Oncologist.* 2009;14(3):253-263.
47. Soria JC, Mauguén A, Reck M, Sandler AB, Saijo N, Johnson DH, et al. Systematic review and meta-analysis of randomised, phase II/III trials adding bevacizumab to platinum-based chemotherapy as first-line treatment in patients with advanced non-small-cell lung cancer. *Ann Oncol.* 2013;24(1):20-30.

48. Langer CJ, Gadgeel SM, Borghaei H, Papadimitrakopoulou VA, Patnaik A, Powell SF, et al. Carboplatin and pemetrexed with or without pembrolizumab for advanced, non-squamous non-small-cell lung cancer: a randomised, phase 2 cohort of the open-label KEYNOTE-021 study. *Lancet Oncol.* 2016;17(11):1497-1508.
49. Socinski MA, Bondarenko I, Karaseva NA, Makhson AM, Vynnychenko I, Okamoto I, et al. Weekly nab-paclitaxel in combination with carboplatin versus solvent-based paclitaxel plus carboplatin as first-line therapy in patients with advanced non-small-cell lung cancer: final results of a phase III trial. *J Clin Oncol.* 2012;30(17):2055-2062.
50. Scagliotti GV, Parikh P, von Pawel J, Biesma B, Vansteenkiste J, Manegold C, et al. Phase III study comparing cisplatin plus gemcitabine with cisplatin plus pemetrexed in chemotherapy-naïve patients with advanced-stage non-small-cell lung cancer. *J Clin Oncol.* 2008;26(21):3543-3551.
51. Ernani V, Ganti AK. Immunotherapy in treatment naïve advanced non-small cell lung cancer. *J Thorac Dis.* 2018;10(Suppl 3):S412-S421.
52. Brahmer JR. Harnessing the immune system for the treatment of non-small-cell lung cancer. *J Clin Oncol.* 2013;31(8):1021-1028.
53. Dasanu CA, Sethi N, Ahmed N. Immune alterations and emerging immunotherapeutic approaches in lung cancer. *Expert Opin Biol Ther.* 2012;12(7):923-937.
54. Marincola FM, Jaffee EM, Hicklin DJ, Ferrone S. Escape of human solid tumors from T-cell recognition: molecular mechanisms and functional significance. *Adv Immunol.* 2000;74:181-273.
55. Sato Y, Mukai K, Watanabe S, Gotoh M, Matsuno Y, Furuya S, et al. Lymphocyte subsets in pulmonary venous and arterial blood of lung cancer patients. *Jpn J Clin Oncol.* 1989;19(3):229-236.
56. Wesselius LJ, Wheaton DL, Manahan-Wahl LJ, Sherard SL, Taylor SA, Abdou NA. Lymphocyte subsets in lung cancer. *Chest.* 1987;91(5):725-729.
57. Buchbinder EI, Desai A. CTLA-4 and PD-1 Pathways: Similarities, Differences, and Implications of Their Inhibition. *Am J Clin Oncol.* 2016;39(1):98-106.
58. Govindan R, Szczesna A, Ahn MJ, Schneider CP, Gonzalez Mella PF, Barlesi F, et al. Phase III Trial of Ipilimumab Combined With Paclitaxel and Carboplatin in Advanced Squamous Non-Small-Cell Lung Cancer. *J Clin Oncol.* 2017;35(30):3449-3457.
59. Lynch TJ, Bondarenko I, Luft A, Serwatowski P, Barlesi F, Chacko R, et al. Ipilimumab in Combination With Paclitaxel and Carboplatin As First-Line Treatment in Stage IIIB/IV Non-Small-Cell Lung Cancer: Results From a Randomized, Double-Blind, Multicenter Phase II Study. *Journal of Clinical Oncology.* 2012;30(17):2046-2054.

60. Reck M, Rodríguez-Abreu D, Robinson AG, Hui R, Csőszi T, Fülöp A, et al. Pembrolizumab versus Chemotherapy for PD-L1–Positive Non–Small-Cell Lung Cancer. *New England Journal of Medicine*. 2016;375(19):1823-1833.
61. Gandhi L, Rodriguez-Abreu D, Gadgeel S, Esteban E, Felip E, De Angelis F, et al. Pembrolizumab plus Chemotherapy in Metastatic Non-Small-Cell Lung Cancer. *N Engl J Med*. 2018.
62. Rittmeyer A, Barlesi F, Waterkamp D, Park K, Ciardiello F, von Pawel J, et al. Atezolizumab versus docetaxel in patients with previously treated non-small-cell lung cancer (OAK): a phase 3, open-label, multicentre randomised controlled trial. *Lancet*. 2017;389(10066):255-265.
63. Hellmann MD, Rizvi NA, Goldman JW, Gettinger SN, Borghaei H, Brahmer JR, et al. Nivolumab plus ipilimumab as first-line treatment for advanced non-small-cell lung cancer (CheckMate 012): results of an open-label, phase 1, multicohort study. *Lancet Oncol*. 2017;18(1):31-41.
64. Hellmann MD, Ciuleanu TE, Pluzanski A, Lee JS, Otterson GA, Audigier-Valette C, et al. Nivolumab plus Ipilimumab in Lung Cancer with a High Tumor Mutational Burden. *N Engl J Med*. 2018.
65. Gazdar AF, Shigematsu H, Herz J, Minna JD. Mutations and addiction to EGFR: the Achilles 'heal' of lung cancers? *Trends Mol Med*. 2004;10(10):481-486.
66. Wee P, Wang Z. Epidermal Growth Factor Receptor Cell Proliferation Signaling Pathways. *Cancers (Basel)*. 2017;9(5).
67. Yun CH, Boggon TJ, Li Y, Woo MS, Greulich H, Meyerson M, et al. Structures of lung cancer-derived EGFR mutants and inhibitor complexes: mechanism of activation and insights into differential inhibitor sensitivity. *Cancer Cell*. 2007;11(3):217-227.
68. Siegelin MD, Borczuk AC. Epidermal growth factor receptor mutations in lung adenocarcinoma. *Lab Invest*. 2014;94(2):129-137.
69. Carey KD, Garton AJ, Romero MS, Kahler J, Thomson S, Ross S, et al. Kinetic analysis of epidermal growth factor receptor somatic mutant proteins shows increased sensitivity to the epidermal growth factor receptor tyrosine kinase inhibitor, erlotinib. *Cancer Res*. 2006;66(16):8163-8171.
70. Mok TS, Wu YL, Thongprasert S, Yang CH, Chu DT, Saijo N, et al. Gefitinib or carboplatin-paclitaxel in pulmonary adenocarcinoma. *N Engl J Med*. 2009;361(10):947-957.
71. Rosell R, Carcereny E, Gervais R, Vergnenegre A, Massuti B, Felip E, et al. Erlotinib versus standard chemotherapy as first-line treatment for European patients with advanced

- EGFR mutation-positive non-small-cell lung cancer (EURTAC): a multicentre, open-label, randomised phase 3 trial. *Lancet Oncol.* 2012;13(3):239-246.
72. Mitsudomi T, Morita S, Yatabe Y, Negoro S, Okamoto I, Tsurutani J, et al. Gefitinib versus cisplatin plus docetaxel in patients with non-small-cell lung cancer harbouring mutations of the epidermal growth factor receptor (WJTOG3405): an open label, randomised phase 3 trial. *Lancet Oncol.* 2010;11(2):121-128.
 73. Sequist LV, Yang JC, Yamamoto N, O'Byrne K, Hirsh V, Mok T, et al. Phase III study of afatinib or cisplatin plus pemetrexed in patients with metastatic lung adenocarcinoma with EGFR mutations. *J Clin Oncol.* 2013;31(27):3327-3334.
 74. Wu YL, Zhou C, Liang CK, Wu G, Liu X, Zhong Z, et al. First-line erlotinib versus gemcitabine/cisplatin in patients with advanced EGFR mutation-positive non-small-cell lung cancer: analyses from the phase III, randomized, open-label, ENSURE study. *Ann Oncol.* 2015;26(9):1883-1889.
 75. Sequist LV, Waltman BA, Dias-Santagata D, Digumarthy S, Turke AB, Fidias P, et al. Genotypic and Histological Evolution of Lung Cancers Acquiring Resistance to EGFR Inhibitors. *Sci Transl Med.* 2011;3(75):75ra26.
 76. Yun CH, Mengwasser KE, Toms AV, Woo MS, Greulich H, Wong KK, et al. The T790M mutation in EGFR kinase causes drug resistance by increasing the affinity for ATP. *Proc Natl Acad Sci U S A.* 2008;105(6):2070-2075.
 77. Passaro A, Guerini-Rocco E, Pochesci A, Vacirca D, Spitaleri G, Catania CM, et al. Targeting EGFR T790M mutation in NSCLC: From biology to evaluation and treatment. *Pharmacol Res.* 2017;117:406-415.
 78. Cross DA, Ashton SE, Ghiorghiu S, Eberlein C, Nebhan CA, Spitzler PJ, et al. AZD9291, an irreversible EGFR TKI, overcomes T790M-mediated resistance to EGFR inhibitors in lung cancer. *Cancer Discov.* 2014;4(9):1046-1061.
 79. Janne PA, Yang JC, Kim DW, Planchard D, Ohe Y, Ramalingam SS, et al. AZD9291 in EGFR inhibitor-resistant non-small-cell lung cancer. *N Engl J Med.* 2015;372(18):1689-1699.
 80. Goss G, Tsai CM, Shepherd FA, Bazhenova L, Lee JS, Chang GC, et al. Osimertinib for pretreated EGFR Thr790Met-positive advanced non-small-cell lung cancer (AURA2): a multicentre, open-label, single-arm, phase 2 study. *Lancet Oncol.* 2016;17(12):1643-1652.
 81. Mok TS, Wu YL, Ahn MJ, Garassino MC, Kim HR, Ramalingam SS, et al. Osimertinib or Platinum-Pemetrexed in EGFR T790M-Positive Lung Cancer. *N Engl J Med.* 2017;376(7):629-640.

82. Soria JC, Ohe Y, Vansteenkiste J, Reungwetwattana T, Chewaskulyong B, Lee KH, et al. Osimertinib in Untreated EGFR-Mutated Advanced Non-Small-Cell Lung Cancer. *N Engl J Med*. 2018;378(2):113-125.
83. Thress KS, Paweletz CP, Felip E, Cho BC, Stetson D, Dougherty B, et al. Acquired EGFR C797S mutation mediates resistance to AZD9291 in non-small cell lung cancer harboring EGFR T790M. *Nat Med*. 2015;21(6):560-562.
84. Yang Z, Yang N, Ou Q, Xiang Y, Jiang T, Wu X, et al. Investigating Novel Resistance Mechanisms to Third-Generation EGFR Tyrosine Kinase Inhibitor Osimertinib in Non-Small Cell Lung Cancer Patients. *Clin Cancer Res*. 2018.
85. Chen L, Fu W, Zheng L, Liu Z, Liang G. Recent Progress of Small-Molecule Epidermal Growth Factor Receptor (EGFR) Inhibitors against C797S Resistance in Non-Small-Cell Lung Cancer. *J Med Chem*. 2017.
86. Lu X, Yu L, Zhang Z, Ren X, Smaill JB, Ding K. Targeting EGFR(L858R/T790M) and EGFR(L858R/T790M/C797S) resistance mutations in NSCLC: Current developments in medicinal chemistry. *Med Res Rev*. 2018.
87. Golding B, Luu A, Jones R, Vilorio-Petit AM. The function and therapeutic targeting of anaplastic lymphoma kinase (ALK) in non-small cell lung cancer (NSCLC). *Mol Cancer*. 2018;17(1):52.
88. Yao S, Cheng M, Zhang Q, Wasik M, Kelsh R, Winkler C. Anaplastic Lymphoma Kinase Is Required for Neurogenesis in the Developing Central Nervous System of Zebrafish. *PLOS ONE*. 2013;8(5):e63757.
89. de Pontual L, Kettaneh D, Gordon CT, Oufadem M, Boddaert N, Lees M, et al. Germline gain-of-function mutations of ALK disrupt central nervous system development. *Hum Mutat*. 2011;32(3):272-276.
90. Katayama R, Lovly CM, Shaw AT. Therapeutic targeting of anaplastic lymphoma kinase in lung cancer: a paradigm for precision cancer medicine. *Clin Cancer Res*. 2015;21(10):2227-2235.
91. Takeuchi K, Choi YL, Soda M, Inamura K, Togashi Y, Hatano S, et al. Multiplex reverse transcription-PCR screening for EML4-ALK fusion transcripts. *Clin Cancer Res*. 2008;14(20):6618-6624.
92. Gainor JF, Varghese AM, Ou SH, Kabraji S, Awad MM, Katayama R, et al. ALK rearrangements are mutually exclusive with mutations in EGFR or KRAS: an analysis of 1,683 patients with non-small cell lung cancer. *Clin Cancer Res*. 2013;19(15):4273-4281.

93. Solomon BJ, Mok T, Kim DW, Wu YL, Nakagawa K, Mekhail T, et al. First-line crizotinib versus chemotherapy in ALK-positive lung cancer. *N Engl J Med.* 2014;371(23):2167-2177.
94. Katayama R, Shaw AT, Khan TM, Mino-Kenudson M, Solomon BJ, Halmos B, et al. Mechanisms of acquired crizotinib resistance in ALK-rearranged lung Cancers. *Sci Transl Med.* 2012;4(120):120ra117.
95. Doebele RC, Pilling AB, Aisner DL, Kutateladze TG, Le AT, Weickhardt AJ, et al. Mechanisms of resistance to crizotinib in patients with ALK gene rearranged non-small cell lung cancer. *Clin Cancer Res.* 2012;18(5):1472-1482.
96. Azam M, Seeliger MA, Gray NS, Kuriyan J, Daley GQ. Activation of tyrosine kinases by mutation of the gatekeeper threonine. *Nat Struct Mol Biol.* 2008;15(10):1109-1118.
97. Friboulet L, Li N, Katayama R, Lee CC, Gainor JF, Crystal AS, et al. The ALK inhibitor ceritinib overcomes crizotinib resistance in non-small cell lung cancer. *Cancer Discov.* 2014;4(6):662-673.
98. Gadgeel SM, Gandhi L, Riely GJ, Chiappori AA, West HL, Azada MC, et al. Safety and activity of alectinib against systemic disease and brain metastases in patients with crizotinib-resistant ALK-rearranged non-small-cell lung cancer (AF-002JG): results from the dose-finding portion of a phase 1/2 study. *Lancet Oncol.* 2014;15(10):1119-1128.
99. Peters S, Camidge DR, Shaw AT, Gadgeel S, Ahn JS, Kim DW, et al. Alectinib versus Crizotinib in Untreated ALK-Positive Non-Small-Cell Lung Cancer. *N Engl J Med.* 2017;377(9):829-838.
100. Gainor JF, Dardaei L, Yoda S, Friboulet L, Leshchiner I, Katayama R, et al. Molecular Mechanisms of Resistance to First- and Second-Generation ALK Inhibitors in ALK-Rearranged Lung Cancer. *Cancer Discov.* 2016;6(10):1118-1133.
101. Shaw AT, Felip E, Bauer TM, Besse B, Navarro A, Postel-Vinay S, et al. Lorlatinib in non-small-cell lung cancer with ALK or ROS1 rearrangement: an international, multicentre, open-label, single-arm first-in-man phase 1 trial. *Lancet Oncol.* 2017;18(12):1590-1599.
102. Graveel CR, Tolbert D, Vande Woude GF. MET: a critical player in tumorigenesis and therapeutic target. *Cold Spring Harbor perspectives in biology.* 2013;5(7).
103. Sadiq AA, Salgia R. Inhibition of MET receptor tyrosine kinase and its ligand hepatocyte growth factor. *J Thorac Oncol.* 2012;7(16 Suppl 5):S372-374.
104. Ma PC, Jagadeeswaran R, Jagadeesh S, Tretiakova MS, Nallasura V, Fox EA, et al. Functional expression and mutations of c-Met and its therapeutic inhibition with

- SU11274 and small interfering RNA in non-small cell lung cancer. *Cancer Res.* 2005;65(4):1479-1488.
105. Park S, Choi YL, Sung CO, An J, Seo J, Ahn MJ, et al. High MET copy number and MET overexpression: poor outcome in non-small cell lung cancer patients. *Histology and histopathology.* 2012;27(2):197-207.
 106. Siegfried JM, Luketich JD, Stabile LP, Christie N, Land SR. Elevated hepatocyte growth factor level correlates with poor outcome in early-stage and late-stage adenocarcinoma of the lung. *Chest.* 2004;125(5 Suppl):116S-119S.
 107. Kris MG JB, Berry LD, Kwiatkowski DJ, Iafrate AJ, Wistuba II, Varella-Garcia M, Franklin WA, Aronson SL, Su P, Shyr Y, Camidge DR, Sequist LV, Glisson BS, Khuri FR, Garon EB, Pao W, Rudin C, Schiller J, Haura EB, Socinski M, Shirai K, Chen H, Giaccone G, Ladanyi M, Kugler K, Minna JD, Bunn PA. Using Multiplexed Assays of Oncogenic Drivers in Lung Cancers to Select Targeted Drugs. . *JAMA.* 2014;311(19):1998-2006.
 108. Tachibana K, Minami Y, Shiba-Ishii A, Kano J, Nakazato Y, Sato Y, et al. Abnormality of the hepatocyte growth factor/MET pathway in pulmonary adenocarcinogenesis. *Lung cancer (Amsterdam, Netherlands).* 2012;75(2):181-188.
 109. Tanizaki J, Okamoto I, Okamoto K, Takezawa K, Kuwata K, Yamaguchi H, et al. MET tyrosine kinase inhibitor crizotinib (PF-02341066) shows differential antitumor effects in non-small cell lung cancer according to MET alterations. *J Thorac Oncol.* 2011;6(10):1624-1631.
 110. Okamoto W, Okamoto I, Arai T, Kuwata K, Hatashita E, Yamaguchi H, et al. Antitumor action of the MET tyrosine kinase inhibitor crizotinib (PF-02341066) in gastric cancer positive for MET amplification. *Mol Cancer Ther.* 2012;11(7):1557-1564.
 111. Salgia R. MET in Lung Cancer: Biomarker Selection Based on Scientific Rationale. *Mol Cancer Ther.* 2017;16(4):555-565.
 112. Camidge D, Ou S, Shapiro G, Otterson G, Villaruz L, Villalona-Calero M, et al. Efficacy and safety of crizotinib in patients with advanced c-MET-amplified non-small cell lung cancer (NSCLC). *J Clin Oncol.* 2014;32(5).
 113. Bauer TM, Schuler M, Berardi R, Lim WT, Van Geel R, De Jonge M, et al. MINI01.03: Phase (Ph) I Study of the Safety and Efficacy of the cMET Inhibitor Capmatinib (INC280) in Patients with Advanced cMET+ NSCLC: Topic: Medical Oncology. *J Thorac Oncol.* 2016;11(11S):S257-S258.
 114. The Cancer Genome Atlas Research N. Comprehensive molecular profiling of lung adenocarcinoma. *Nature.* 2014;511(7511):543-550.

115. Kong-Beltran M, Seshagiri S, Zha J, Zhu W, Bhawe K, Mendoza N, et al. Somatic mutations lead to an oncogenic deletion of met in lung cancer. *Cancer Res.* 2006;66(1):283-289.
116. Ma PC, Tretiakova MS, MacKinnon AC, Ramnath N, Johnson C, Dietrich S, et al. Expression and mutational analysis of MET in human solid cancers. *Genes, chromosomes & cancer.* 2008;47(12):1025-1037.
117. Lu X, Peled N, Greer J, Wu W, Choi P, Berger AH, et al. MET Exon 14 Mutation Encodes an Actionable Therapeutic Target in Lung Adenocarcinoma. *Cancer Res.* 2017;77(16):4498-4505.
118. Frampton GM, Ali SM, Rosenzweig M, Chmielecki J, Lu X, Bauer TM, et al. Activation of MET via Diverse Exon 14 Splicing Alterations Occurs in Multiple Tumor Types and Confers Clinical Sensitivity to MET Inhibitors. *Cancer Discov.* 2015;5(8):850-859.
119. Awad MM, Oxnard GR, Jackman DM, Savukoski DO, Hall D, Shivdasani P, et al. MET Exon 14 Mutations in Non-Small-Cell Lung Cancer Are Associated With Advanced Age and Stage-Dependent MET Genomic Amplification and c-Met Overexpression. *J Clin Oncol.* 2016;34(7):721-730.
120. Paik PK, Drilon A, Fan P-D, Yu H, Rekhtman N, Ginsberg MS, et al. Response to MET Inhibitors in Patients with Stage IV Lung Adenocarcinomas Harboring MET Mutations Causing Exon 14 Skipping. *Cancer Discovery.* 2015;5(8):842-849.
121. Li A, Yang JJ, Zhang XC, Zhang Z, Su J, Gou LY, et al. Acquired MET Y1248H and D1246N Mutations Mediate Resistance to MET Inhibitors in Non-Small Cell Lung Cancer. *Clin Cancer Res.* 2017;23(16):4929-4937.
122. Bahcall M, Sim T, Paweletz CP, Patel JD, Alden RS, Kuang Y, et al. Acquired METD1228V Mutation and Resistance to MET Inhibition in Lung Cancer. *Cancer Discov.* 2016;6(12):1334-1341.
123. Niederst MJ, Engelman JA. Bypass mechanisms of resistance to receptor tyrosine kinase inhibition in lung cancer. *Sci Signal.* 2013;6(294):re6.
124. Liu Q, Yu S, Zhao W, Qin S, Chu Q, Wu K. EGFR-TKIs resistance via EGFR-independent signaling pathways. *Mol Cancer.* 2018;17(1):53.
125. Lin JJ, Riely GJ, Shaw AT. Targeting ALK: Precision Medicine Takes on Drug Resistance. *Cancer Discov.* 2017;7(2):137-155.
126. Dagogo-Jack I, Shaw AT. Crizotinib resistance: implications for therapeutic strategies. *Annals of Oncology.* 2016;27(suppl_3):iii42-iii50.

127. Xia B, Wurtz A, Gettinger SN, Herbst RS, Chiang AC, Wan M, et al. HER2 amplification in EGFR mutant NSCLC after acquired resistance (AR) to EGFR-directed therapies. *Journal of Clinical Oncology*. 2016;34(15_suppl):9049-9049.
128. Wilson FH, Johannessen CM, Piccioni F, Tamayo P, Kim JW, Van Allen EM, et al. A functional landscape of resistance to ALK inhibition in lung cancer. *Cancer Cell*. 2015;27(3):397-408.
129. Ortiz-Cuaran S, Scheffler M, Plenker D, Dahmen L, Scheel AH, Fernandez-Cuesta L, et al. Heterogeneous Mechanisms of Primary and Acquired Resistance to Third-Generation EGFR Inhibitors. *Clin Cancer Res*. 2016;22(19):4837-4847.
130. Ramalingam SS, Yang JC, Lee CK, Kurata T, Kim DW, John T, et al. Osimertinib As First-Line Treatment of EGFR Mutation-Positive Advanced Non-Small-Cell Lung Cancer. *J Clin Oncol*. 2017;JCO2017747576.
131. Bhattacharya S, Socinski MA, Burns TF. KRAS mutant lung cancer: progress thus far on an elusive therapeutic target. *Clinical and Translational Medicine*. 2015;4:35.
132. Eberlein CA, Stetson D, Markovets AA, Al-Kadhimi KJ, Lai Z, Fisher PR, et al. Acquired Resistance to the Mutant-Selective EGFR Inhibitor AZD9291 Is Associated with Increased Dependence on RAS Signaling in Preclinical Models. *Cancer Res*. 2015;75(12):2489-2500.
133. Stewart EL, Tan SZ, Liu G, Tsao MS. Known and putative mechanisms of resistance to EGFR targeted therapies in NSCLC patients with EGFR mutations-a review. *Transl Lung Cancer Res*. 2015;4(1):67-81.
134. Engelman JA, Mukohara T, Zejnullahu K, Lifshits E, Borrás AM, Gale C-M, et al. Allelic dilution obscures detection of a biologically significant resistance mutation in EGFR-amplified lung cancer. *Journal of Clinical Investigation*. 2006;116(10):2695-2706.
135. Kang J, Chen H, Zhou Q, Tu H-Y, Zhang X-C, Jian S, et al. Primary resistance to ALK inhibitor in ALK-positive non-small-cell lung cancer. *Journal of Clinical Oncology*. 2017;35(15_suppl):9063-9063.
136. Kim TM, Song A, Kim DW, Kim S, Ahn YO, Keam B, et al. Mechanisms of Acquired Resistance to AZD9291: A Mutation-Selective, Irreversible EGFR Inhibitor. *J Thorac Oncol*. 2015;10(12):1736-1744.
137. Sos ML, Koker M, Weir BA, Heynck S, Rabinovsky R, Zander T, et al. PTEN loss contributes to erlotinib resistance in EGFR-mutant lung cancer by activation of Akt and EGFR. *Cancer Res*. 2009;69(8):3256-3261.

138. Crystal AS, Shaw AT, Sequist LV, Friboulet L, Niederst MJ, Lockerman EL, et al. Patient-derived models of acquired resistance can identify effective drug combinations for cancer. *Science*. 2014;346(6216):1480.
139. Ohashi K, Sequist LV, Arcila ME, Moran T, Chmielecki J, Lin YL, et al. Lung cancers with acquired resistance to EGFR inhibitors occasionally harbor BRAF gene mutations but lack mutations in KRAS, NRAS, or MEK1. *Proc Natl Acad Sci U S A*. 2012;109(31):E2127-2133.
140. Husain H, Scur M, Murtuza A, Bui N, Woodward B, Kurzrock R. Strategies to Overcome Bypass Mechanisms Mediating Clinical Resistance to EGFR Tyrosine Kinase Inhibition in Lung Cancer. *Mol Cancer Ther*. 2017;16(2):265-272.
141. Rotow J, Bivona TG. Understanding and targeting resistance mechanisms in NSCLC. *Nat Rev Cancer*. 2017;17(11):637-658.
142. Engelman JA, Zejnullahu K, Mitsudomi T, Song Y, Hyland C, Park JO, et al. MET amplification leads to gefitinib resistance in lung cancer by activating ERBB3 signaling. *Science*. 2007;316(5827):1039-1043.
143. Planchard D, Loriot Y, Andre F, Gobert A, Auger N, Lacroix L, et al. EGFR-independent mechanisms of acquired resistance to AZD9291 in EGFR T790M-positive NSCLC patients. *Ann Oncol*. 2015;26(10):2073-2078.
144. Gouji T, Takashi S, Mitsuhiro T, Yukito I. Crizotinib Can Overcome Acquired Resistance to CH5424802: Is Amplification of the MET Gene a Key Factor? *Journal of Thoracic Oncology*. 9(3):e27-e28.
145. Tan DS-W, Kim D-W, Thomas M, Pantano S, Wang Y, Szpakowski SL, et al. Genetic landscape of ALK+ non-small cell lung cancer (NSCLC) patients (pts) and response to ceritinib in ASCEND-1. *Journal of Clinical Oncology*. 2016;34(15_suppl):9064-9064.
146. Koeppen H, Yu W, Zha J, Pandita A, Penuel E, Rangell L, et al. Biomarker analyses from a placebo-controlled phase II study evaluating erlotinib+/-onartuzumab in advanced non-small cell lung cancer: MET expression levels are predictive of patient benefit. *Clin Cancer Res*. 2014;20(17):4488-4498.
147. Ko B, He T, Gadgeel S, Halmos B. MET/HGF pathway activation as a paradigm of resistance to targeted therapies. *Annals of Translational Medicine*. 2017;5(1):4.
148. Donev IS, Wang W, Yamada T, Li Q, Takeuchi S, Matsumoto K, et al. Transient PI3K inhibition induces apoptosis and overcomes HGF-mediated resistance to EGFR-TKIs in EGFR mutant lung cancer. *Clin Cancer Res*. 2011;17(8):2260-2269.
149. Yano S, Yamada T, Takeuchi S, Tachibana K, Minami Y, Yatabe Y, et al. Hepatocyte growth factor expression in EGFR mutant lung cancer with intrinsic and acquired

- resistance to tyrosine kinase inhibitors in a Japanese cohort. *J Thorac Oncol*. 2011;6(12):2011-2017.
150. Isozaki H, Ichihara E, Takigawa N, Ohashi K, Ochi N, Yasugi M, et al. Non-Small Cell Lung Cancer Cells Acquire Resistance to the ALK Inhibitor Alectinib by Activating Alternative Receptor Tyrosine Kinases. *Cancer Res*. 2016;76(6):1506-1516.
 151. Yano S, Wang W, Li Q, Matsumoto K, Sakurama H, Nakamura T, et al. Hepatocyte growth factor induces gefitinib resistance of lung adenocarcinoma with epidermal growth factor receptor-activating mutations. *Cancer Res*. 2008;68(22):9479-9487.
 152. Niederst MJ, Sequist LV, Poirier JT, Mermel CH, Lockerman EL, Garcia AR, et al. RB loss in resistant EGFR mutant lung adenocarcinomas that transform to small-cell lung cancer. *Nat Commun*. 2015;6:6377.
 153. Kobayashi Y, Sakao Y, Ito S, Park J, Kuroda H, Sakakura N, et al. Transformation to Sarcomatoid Carcinoma in ALK-Rearranged Adenocarcinoma, Which Developed Acquired Resistance to Crizotinib and Received Subsequent Chemotherapies. *Journal of Thoracic Oncology*.8(8):e75-e78.
 154. Cha YJ, Cho BC, Kim HR, Lee HJ, Shim HS. A Case of ALK-Rearranged Adenocarcinoma with Small Cell Carcinoma-Like Transformation and Resistance to Crizotinib. *J Thorac Oncol*. 2016;11(5):e55-58.
 155. Lochmann TL, Floros KV, Naseri M, Powell KM, Cook W, March RJ, et al. Venetoclax Is Effective in Small-Cell Lung Cancers with High BCL-2 Expression. *Clinical Cancer Research*. 2018;24(2):360.
 156. Thiery JP, Acloque H, Huang RY, Nieto MA. Epithelial-mesenchymal transitions in development and disease. *Cell*. 2009;139(5):871-890.
 157. Kalluri R, Weinberg RA. The basics of epithelial-mesenchymal transition. *J Clin Invest*. 2009;119(6):1420-1428.
 158. Gower A, Hsu W-H, Hsu S-T, Wang Y, Giaccone G. EMT is associated with, but does not drive resistance to ALK inhibitors among EML4-ALK non-small cell lung cancer. *Molecular Oncology*. 2016;10(4):601-609.
 159. Kim HR, Kim WS, Choi YJ, Choi CM, Rho JK, Lee JC. Epithelial-mesenchymal transition leads to crizotinib resistance in H2228 lung cancer cells with EML4-ALK translocation. *Mol Oncol*. 2013;7(6):1093-1102.
 160. Song KA, Niederst MJ, Lochmann TL, Hata AN, Kitai H, Ham J, et al. Epithelial-to-Mesenchymal Transition Antagonizes Response to Targeted Therapies in Lung Cancer by Suppressing BIM. *Clin Cancer Res*. 2018;24(1):197-208.

161. Zhang Z, Lee JC, Lin L, Olivás V, Au V, LaFramboise T, et al. Activation of the AXL kinase causes resistance to EGFR-targeted therapy in lung cancer. *Nat Genet.* 2012;44(8):852-860.
162. Chang TH, Tsai MF, Su KY, Wu SG, Huang CP, Yu SL, et al. Slug confers resistance to the epidermal growth factor receptor tyrosine kinase inhibitor. *Am J Respir Crit Care Med.* 2011;183(8):1071-1079.
163. Yochum ZA, Socinski MA, Burns TF. Paradoxical functions of ZEB1 in EGFR-mutant lung cancer: tumor suppressor and driver of therapeutic resistance. *J Thorac Dis.* 2016;8(11):E1528-E1531.
164. Zhang T, Guo L, Creighton CJ, Lu Q, Gibbons DL, Yi ES, et al. A genetic cell context-dependent role for ZEB1 in lung cancer. *Nat Commun.* 2016;7:12231.
165. Izumchenko E, Chang X, Michailidi C, Kagohara L, Ravi R, Paz K, et al. The TGF β -miR200-MIG6 Pathway Orchestrates the EMT-Associated Kinase Switch That Induces Resistance to EGFR Inhibitors. *Cancer Research.* 2014;74(14):3995-4005.
166. Vazquez-Martin A, Cufi S, Oliveras-Ferraro C, Torres-Garcia VZ, Corominas-Faja B, Cuyas E, et al. IGF-1R/epithelial-to-mesenchymal transition (EMT) crosstalk suppresses the erlotinib-sensitizing effect of EGFR exon 19 deletion mutations. *Sci Rep.* 2013;3:2560.
167. Jakobsen KR, Demuth C, Sorensen BS, Nielsen AL. The role of epithelial to mesenchymal transition in resistance to epidermal growth factor receptor tyrosine kinase inhibitors in non-small cell lung cancer. *Transl Lung Cancer Res.* 2016;5(2):172-182.
168. Adams JM, Cory S. The BCL-2 arbiters of apoptosis and their growing role as cancer targets. *Cell Death And Differentiation.* 2017;25:27.
169. Galluzzi L, Vitale I, Aaronson SA, Abrams JM, Adam D, Agostinis P, et al. Molecular mechanisms of cell death: recommendations of the Nomenclature Committee on Cell Death 2018. *Cell Death Differ.* 2018;25(3):486-541.
170. Pfeffer CM, Singh ATK. Apoptosis: A Target for Anticancer Therapy. *Int J Mol Sci.* 2018;19(2).
171. Hanahan D, Weinberg RA. Hallmarks of cancer: the next generation. *Cell.* 2011;144(5):646-674.
172. Fernald K, Kurokawa M. Evading apoptosis in cancer. *Trends Cell Biol.* 2013;23(12):620-633.
173. Tummers B, Green DR. Caspase-8: regulating life and death. *Immunol Rev.* 2017;277(1):76-89.

174. Fu TM, Li Y, Lu A, Li Z, Vajjhala PR, Cruz AC, et al. Cryo-EM Structure of Caspase-8 Tandem DED Filament Reveals Assembly and Regulation Mechanisms of the Death-Inducing Signaling Complex. *Mol Cell*. 2016;64(2):236-250.
175. Hughes MA, Powley IR, Jukes-Jones R, Horn S, Feoktistova M, Fairall L, et al. Cooperative and Hierarchical Binding of c-FLIP and Caspase-8: A Unified Model Defines How c-FLIP Isoforms Differentially Control Cell Fate. *Mol Cell*. 2016;61(6):834-849.
176. Yip KW, Reed JC. Bcl-2 family proteins and cancer. *Oncogene*. 2008;27(50):6398-6406.
177. Hubner A, Barrett T, Flavell RA, Davis RJ. Multisite phosphorylation regulates Bim stability and apoptotic activity. *Mol Cell*. 2008;30(4):415-425.
178. Koff JL, Ramachandiran S, Bernal-Mizrachi L. A time to kill: targeting apoptosis in cancer. *Int J Mol Sci*. 2015;16(2):2942-2955.
179. Fulda S. Targeting extrinsic apoptosis in cancer: Challenges and opportunities. *Semin Cell Dev Biol*. 2015;39:20-25.
180. LeBlanc HN, Ashkenazi A. Apo2L/TRAIL and its death and decoy receptors. *Cell Death Differ*. 2003;10(1):66-75.
181. Thome M, Schneider P, Hofmann K, Fickenscher H, Meinel E, Neipel F, et al. Viral FLICE-inhibitory proteins (FLIPs) prevent apoptosis induced by death receptors. *Nature*. 1997;386(6624):517-521.
182. Longley DB, Wilson TR, McEwan M, Allen WL, McDermott U, Galligan L, et al. c-FLIP inhibits chemotherapy-induced colorectal cancer cell death. *Oncogene*. 2006;25(6):838-848.
183. Wilson TR, McLaughlin KM, McEwan M, Sakai H, Rogers KM, Redmond KM, et al. c-FLIP: a key regulator of colorectal cancer cell death. *Cancer Res*. 2007;67(12):5754-5762.
184. Riley JS, Hutchinson R, McArt DG, Crawford N, Holohan C, Paul I, et al. Prognostic and therapeutic relevance of FLIP and procaspase-8 overexpression in non-small cell lung cancer. *Cell Death Dis*. 2013;4:e951.
185. Li C, Egloff AM, Sen M, Grandis JR, Johnson DE. Caspase-8 mutations in head and neck cancer confer resistance to death receptor-mediated apoptosis and enhance migration, invasion, and tumor growth. *Mol Oncol*. 2014;8(7):1220-1230.
186. Faber AC, Corcoran RB, Ebi H, Sequist LV, Waltman BA, Chung E, et al. BIM expression in treatment-naive cancers predicts responsiveness to kinase inhibitors. *Cancer Discov*. 2011;1(4):352-365.

187. Tanizaki J, Okamoto I, Okamoto K, Takezawa K, Kuwata K, Yamaguchi H, et al. MET Tyrosine Kinase Inhibitor Crizotinib (PF-02341066) Shows Differential Antitumor Effects in Non-small Cell Lung Cancer According to MET Alterations. *Journal of Thoracic Oncology*. 2011;6(10):1624-1631.
188. Cragg MS, Jansen ES, Cook M, Harris C, Strasser A, Scott CL. Treatment of B-RAF mutant human tumor cells with a MEK inhibitor requires Bim and is enhanced by a BH3 mimetic. *J Clin Invest*. 2008;118(11):3651-3659.
189. Zhang W, Konopleva M, Ruvolo VR, McQueen T, Evans RL, Bornmann WG, et al. Sorafenib induces apoptosis of AML cells via Bim-mediated activation of the intrinsic apoptotic pathway. *Leukemia*. 2008;22(4):808-818.
190. Costa DB, Halmos B, Kumar A, Schumer ST, Huberman MS, Boggon TJ, et al. BIM mediates EGFR tyrosine kinase inhibitor-induced apoptosis in lung cancers with oncogenic EGFR mutations. *PLoS Med*. 2007;4(10):1669-1679; discussion 1680.
191. Shi P, Oh YT, Deng L, Zhang G, Qian G, Zhang S, et al. Overcoming acquired resistance to AZD9291, a third generation EGFR inhibitor, through modulation of MEK/ERK-dependent Bim and Mcl-1 degradation. *Clin Cancer Res*. 2017.
192. Tanimoto A, Takeuchi S, Arai S, Fukuda K, Yamada T, Roca X, et al. Histone Deacetylase 3 Inhibition Overcomes BIM Deletion Polymorphism-Mediated Osimertinib Resistance in EGFR-Mutant Lung Cancer. *Clin Cancer Res*. 2017;23(12):3139-3149.
193. Nie W, Tao X, Wei H, Chen W-s, Li B. The BIM deletion polymorphism is a prognostic biomarker of EGFR-TKIs response in NSCLC: A systematic review and meta-analysis. *Oncotarget*. 2015;6(28):25696-25700.
194. Bean GR, Ganesan YT, Dong Y, Takeda S, Liu H, Chan PM, et al. PUMA and BIM are required for oncogene inactivation-induced apoptosis. *Sci Signal*. 2013;6(268):ra20.
195. Wu DW, Chen CY, Chu CL, Lee H. Paxillin confers resistance to tyrosine kinase inhibitors in EGFR-mutant lung cancers via modulating BIM and Mcl-1 protein stability. *Oncogene*. 2016;35(5):621-630.
196. Yin Z, Xu XL, Frasch M. Regulation of the twist target gene tinman by modular cis-regulatory elements during early mesoderm development. *Development*. 1997;124(24):4971-4982.
197. Lee YM, Park T, Schulz RA, Kim Y. Twist-mediated activation of the NK-4 homeobox gene in the visceral mesoderm of Drosophila requires two distinct clusters of E-box regulatory elements. *J Biol Chem*. 1997;272(28):17531-17541.
198. Ansieau S, Morel AP, Hinkal G, Bastid J, Puisieux A. TWISTing an embryonic transcription factor into an oncoprotein. *Oncogene*. 2010;29:3173.

199. Qian J, Luo Y, Gu X, Zhan W, Wang X. Twist1 promotes gastric cancer cell proliferation through up-regulation of FoxM1. *PLoS One*. 2013;8(10):e77625.
200. Pan D, Fujimoto M, Lopes A, Wang Y-X. Twist-1 Is a PPAR δ -Inducible, Negative-Feedback Regulator of PGC-1 α in Brown Fat Metabolism. *Cell*. 2009;137(1):73-86.
201. Chen YT, Akinwunmi PO, Deng JM, Tam OH, Behringer RR. Generation of a Twist1 conditional null allele in the mouse. *Genesis*. 2007;45(9):588-592.
202. Thisse B, el Messal M, Perrin-Schmitt F. The twist gene: isolation of a Drosophila zygotic gene necessary for the establishment of dorsoventral pattern. *Nucleic Acids Res*. 1987;15(8):3439-3453.
203. Hong J, Zhou J, Fu J, He T, Qin J, Wang L, et al. Phosphorylation of serine 68 of Twist1 by MAPKs stabilizes Twist1 protein and promotes breast cancer cell invasiveness. *Cancer Res*. 2011;71(11):3980-3990.
204. Simpson P. Maternal-Zygotic Gene Interactions during Formation of the Dorsoventral Pattern in Drosophila Embryos. *Genetics*. 1983;105(3):615-632.
205. Xu Y, Xu Y, Liao L, Zhou N, Theissen SM, Liao XH, et al. Inducible knockout of Twist1 in young and adult mice prolongs hair growth cycle and has mild effects on general health, supporting Twist1 as a preferential cancer target. *Am J Pathol*. 2013;183(4):1281-1292.
206. Connerney J, Andreeva V, Leshem Y, Muentener C, Mercado MA, Spicer DB. Twist1 dimer selection regulates cranial suture patterning and fusion. *Dev Dyn*. 2006;235(5):1345-1357.
207. Connerney J, Andreeva V, Leshem Y, Mercado MA, Dowell K, Yang X, et al. Twist1 homodimers enhance FGF responsiveness of the cranial sutures and promote suture closure. *Dev Biol*. 2008;318(2):323-334.
208. Franco HL, Casasnovas J, Rodriguez-Medina JR, Cadilla CL. Redundant or separate entities?--roles of Twist1 and Twist2 as molecular switches during gene transcription. *Nucleic Acids Res*. 2011;39(4):1177-1186.
209. Firulli BA, Krawchuk D, Centonze VE, Vargesson N, Virshup DM, Conway SJ, et al. Altered Twist1 and Hand2 dimerization is associated with Saethre-Chotzen syndrome and limb abnormalities. *Nat Genet*. 2005;37(4):373-381.
210. Wang SM, Coljee VW, Pignolo RJ, Rotenberg MO, Cristofalo VJ, Sierra F. Cloning of the human twist gene: its expression is retained in adult mesodermally-derived tissues. *Gene*. 1997;187(1):83-92.

211. Entz-Werlé N, Stoetzel, C. , Berard-Marec, P. , Kalifa, C. , Brugiere, L. , Pacquement, H. , Schmitt, C. , Tabone, M. , Gentet, J. , Quillet, R. , Oudet, P. , Lutz, P. , Babin-Boilletot, A. , Gaub, M. and Perrin-Schmitt, F. . Frequent genomic abnormalities at TWIST in human pediatric osteosarcomas. . *Int. J. Cancer*. 2005;117: :349-355.
212. Bastid J CC, Puisieux A, Ansieau S. Role of TWIST proteins in cancer progression. *Atlas Genet Cytogenet Oncol Haematol*. 2010;14(9):898-907.
213. Zhao Z, Rahman MA, Chen ZG, Shin DM. Multiple biological functions of Twist1 in various cancers. *Oncotarget*. 2017;8(12):20380-20393.
214. Cheng GZ ZW, Sun M, Wang Q, Coppola D, Mansour M, et al. . Twist is transcriptionally induced by activation of STAT3 and mediates STAT3 oncogenic function. . *J Biol Chem*. 2008(283):14665-14673.
215. Cho KH, Jeong KJ, Shin SC, Kang J, Park CG, Lee HY. STAT3 mediates TGF-beta1-induced TWIST1 expression and prostate cancer invasion. *Cancer Lett*. 2013;336(1):167-173.
216. Li CW, Xia W, Huo L, Lim SO, Wu Y, Hsu JL, et al. Epithelial-mesenchymal transition induced by TNF-alpha requires NF-kappaB-mediated transcriptional upregulation of Twist1. *Cancer Res*. 2012;72(5):1290-1300.
217. Šošić D, Richardson JA, Yu K, Ornitz DM, Olson EN. Twist Regulates Cytokine Gene Expression through a Negative Feedback Loop that Represses NF-κB Activity. *Cell*. 2003;112(2):169-180.
218. Satoh K, Hamada S, Kimura K, Kanno A, Hirota M, Umino J, et al. Up-regulation of MSX2 enhances the malignant phenotype and is associated with twist 1 expression in human pancreatic cancer cells. *Am J Pathol*. 2008;172(4):926-939.
219. Thuault S, Valcourt U, Petersen M, Manfioletti G, Heldin CH, Moustakas A. Transforming growth factor-beta employs HMGA2 to elicit epithelial-mesenchymal transition. *J Cell Biol*. 2006;174(2):175-183.
220. Ruppenthal RD, Nicolini C, Filho AF, Meurer R, Damin AP, Rohe A, et al. TWIST1 promoter methylation in primary colorectal carcinoma. *Pathol Oncol Res*. 2011;17(4):867-872.
221. Gort EH, Suijkerbuijk KP, Roothaan SM, Raman V, Vooijs M, van der Wall E, et al. Methylation of the TWIST1 promoter, TWIST1 mRNA levels, and immunohistochemical expression of TWIST1 in breast cancer. *Cancer Epidemiol Biomarkers Prev*. 2008;17(12):3325-3330.

222. Xue G, Restuccia DF, Lan Q, Hynx D, Dirnhofer S, Hess D, et al. Akt/PKB-mediated phosphorylation of Twist1 promotes tumor metastasis via mediating cross-talk between PI3K/Akt and TGF-beta signaling axes. *Cancer Discov.* 2012;2(3):248-259.
223. Li C-W, Xia W, Lim S-O, Hsu JL, Huo L, Wu Y, et al. AKT1 Inhibits Epithelial-to-Mesenchymal Transition in Breast Cancer through Phosphorylation-Dependent Twist1 Degradation. *Cancer Research.* 2016;76(6):1451.
224. Yang WH, Su YH, Hsu WH, Wang CC, Arbiser JL, Yang MH. Imipramine blue halts head and neck cancer invasion through promoting F-box and leucine-rich repeat protein 14-mediated Twist1 degradation. *Oncogene.* 2016;35(18):2287-2298.
225. Bialek P, Kern B, Yang X, Schrock M, Sosic D, Hong N, et al. A twist code determines the onset of osteoblast differentiation. *Dev Cell.* 2004;6(3):423-435.
226. Gajula RP, Chettiar ST, Williams RD, Thiyagarajan S, Kato Y, Aziz K, et al. The twist box domain is required for Twist1-induced prostate cancer metastasis. *Mol Cancer Res.* 2013;11(11):1387-1400.
227. Piccinin S, Tonin E, Sessa S, Demontis S, Rossi S, Pecciarini L, et al. A "twist box" code of p53 inactivation: twist box: p53 interaction promotes p53 degradation. *Cancer Cell.* 2012;22(3):404-415.
228. Qiang L, Zhao B, Ming M, Wang N, He TC, Hwang S, et al. Regulation of cell proliferation and migration by p62 through stabilization of Twist1. *Proc Natl Acad Sci U S A.* 2014;111(25):9241-9246.
229. Lander R, Nordin K, LaBonne C. The F-box protein Ppa is a common regulator of core EMT factors Twist, Snail, Slug, and Sip1. *J Cell Biol.* 2011;194(1):17-25.
230. Shi J, Wang Y, Zeng L, Wu Y, Deng J, Zhang Q, et al. Disrupting the Interaction of BRD4 with Diacetylated Twist Suppresses Tumorigenesis in Basal-like Breast Cancer. *Cancer Cell.* 2014;25(2):210-225.
231. Hayashi M, Nimura K, Kashiwagi K, Harada T, Takaoka K, Kato H, et al. Comparative roles of Twist-1 and Id1 in transcriptional regulation by BMP signaling. *J Cell Sci.* 2007;120(Pt 8):1350-1357.
232. Yochum ZA, Cades J, Mazzacurati L, Neumann NM, Khetarpal SK, Chatterjee S, et al. A First-in-Class TWIST1 Inhibitor with Activity in Oncogene-driven Lung Cancer. *Mol Cancer Res.* 2017.
233. Tran PT, Shroff EH, Burns TF, Thiyagarajan S, Das ST, Zabuawala T, et al. Twist1 suppresses senescence programs and thereby accelerates and maintains mutant Kras-induced lung tumorigenesis. *PLoS Genet.* 2012;8(5):e1002650.

234. Burns TF, Dobromilskaya I, Murphy SC, Gajula RP, Thiyagarajan S, Chatley SN, et al. Inhibition of TWIST1 leads to activation of oncogene-induced senescence in oncogene-driven non-small cell lung cancer. *Mol Cancer Res.* 2013;11(4):329-338.
235. Vesuna F, van Diest P, Chen JH, Raman V. Twist is a transcriptional repressor of E-cadherin gene expression in breast cancer. *Biochemical and Biophysical Research Communications.* 2008;367(2):235-241.
236. Casas E, Kim J, Bendesky A, Ohno-Machado L, Wolfe CJ, Yang J. Snail2 is an Essential Mediator of Twist1-Induced Epithelial Mesenchymal Transition and Metastasis. *Cancer Research.* 2011;71(1):245.
237. Alexander NR, Tran NL, Rekapally H, Summers CE, Glackin C, Heimark RL. N-cadherin gene expression in prostate carcinoma is modulated by integrin-dependent nuclear translocation of Twist1. *Cancer Res.* 2006;66(7):3365-3369.
238. Yang J, Mani SA, Donaher JL, Ramaswamy S, Itzykson RA, Come C, et al. Twist, a master regulator of morphogenesis, plays an essential role in tumor metastasis. *Cell.* 2004;117(7):927-939.
239. Yang MH, Wu MZ, Chiou SH, Chen PM, Chang SY, Liu CJ, et al. Direct regulation of TWIST by HIF-1 α promotes metastasis. *Nature cell biology.* 2008;10(3):295-305.
240. Yang M-H, Hsu DS-S, Wang H-W, Wang H-J, Lan H-Y, Yang W-H, et al. Bmi1 is essential in Twist1-induced epithelial–mesenchymal transition. *Nature cell biology.* 2010;12:982.
241. Maestro R, Dei Tos AP, Hamamori Y, Krasnokutsky S, Sartorelli V, Kedes L, et al. Twist is a potential oncogene that inhibits apoptosis. *Genes Dev.* 1999;13(17):2207-2217.
242. Shiota M, Izumi H, Onitsuka T, Miyamoto N, Kashiwagi E, Kidani A, et al. Twist and p53 reciprocally regulate target genes via direct interaction. *Oncogene.* 2008;27(42):5543-5553.
243. Stasinopoulos IA, Mironchik Y, Raman A, Wildes F, Winnard P, Jr., Raman V. HOXA5-twist interaction alters p53 homeostasis in breast cancer cells. *J Biol Chem.* 2005;280(3):2294-2299.
244. Kwok WK, Ling MT, Yuen HF, Wong YC, Wang X. Role of p14ARF in TWIST-mediated senescence in prostate epithelial cells. *Carcinogenesis.* 2007;28(12):2467-2475.
245. Hamamori Y, Sartorelli V, Ogryzko V, Puri PL, Wu HY, Wang JY, et al. Regulation of histone acetyltransferases p300 and PCAF by the bHLH protein twist and adenoviral oncoprotein E1A. *Cell.* 1999;96(3):405-413.

246. Vichalkovski A, Gresko E, Hess D, Restuccia DF, Hemmings BA. PKB/AKT phosphorylation of the transcription factor Twist-1 at Ser42 inhibits p53 activity in response to DNA damage. *Oncogene*. 2010;29(24):3554-3565.
247. Jin HO, Hong SE, Woo SH, Lee JH, Choe TB, Kim EK, et al. Silencing of Twist1 sensitizes NSCLC cells to cisplatin via AMPK-activated mTOR inhibition. *Cell Death Dis*. 2012;3:e319.
248. Jacqueroud L, Bouard C, Richard G, Payen L, Devouassoux-Shisheboran M, Spicer DB, et al. The Heterodimeric TWIST1-E12 Complex Drives the Oncogenic Potential of TWIST1 in Human Mammary Epithelial Cells. *Neoplasia*. 2016;18(5):317-327.
249. Ansieau S, Bastid J, Doreau A, Morel AP, Bouchet BP, Thomas C, et al. Induction of EMT by twist proteins as a collateral effect of tumor-promoting inactivation of premature senescence. *Cancer Cell*. 2008;14(1):79-89.
250. Saxena M, Stephens MA, Pathak H, Rangarajan A. Transcription factors that mediate epithelial–mesenchymal transition lead to multidrug resistance by upregulating ABC transporters. *Cell Death & Disease*. 2011;2:e179.
251. Liu YR, Liang L, Zhao JM, Zhang Y, Zhang M, Zhong WL, et al. Twist1 confers multidrug resistance in colon cancer through upregulation of ATP-binding cassette transporters. *Oncotarget*. 2017;8(32):52901-52912.
252. Cheng GZ, Chan J, Wang Q, Zhang W, Sun CD, Wang LH. Twist transcriptionally up-regulates AKT2 in breast cancer cells leading to increased migration, invasion, and resistance to paclitaxel. *Cancer Res*. 2007;67(5):1979-1987.
253. Chen HF, Huang CH, Liu CJ, Hung JJ, Hsu CC, Teng SC, et al. Twist1 induces endothelial differentiation of tumour cells through the Jagged1-KLF4 axis. *Nat Commun*. 2014;5:4697.
254. Pham CG, Bubici C, Zazzeroni F, Knabb JR, Papa S, Kuntzen C, et al. Upregulation of Twist-1 by NF-kappaB blocks cytotoxicity induced by chemotherapeutic drugs. *Molecular and cellular biology*. 2007;27(11):3920-3935.
255. Gardner EE, Lok BH, Schneeberger VE, Desmeules P, Miles LA, Arnold PK, et al. Chemosensitive Relapse in Small Cell Lung Cancer Proceeds through an EZH2-SLFN11 Axis. *Cancer Cell*. 2017;31(2):286-299.
256. Yu HA, Riely GJ, Lovly CM. Therapeutic strategies utilized in the setting of acquired resistance to EGFR tyrosine kinase inhibitors. *Clin Cancer Res*. 2014;20(23):5898-5907.
257. Cox AD, Fesik SW, Kimmelman AC, Luo J, Der CJ. Drugging the undruggable RAS: Mission possible? *Nat Rev Drug Discov*. 2014;13(11):828-851.

258. Puisieux A, Brabletz T, Caramel J. Oncogenic roles of EMT-inducing transcription factors. *Nature cell biology*. 2014;16(6):488-494.
259. Davis FM, Stewart TA, Thompson EW, Monteith GR. Targeting EMT in cancer: opportunities for pharmacological intervention. *Trends Pharmacol Sci*. 2014;35(9):479-488.
260. Ansieau S, Collin G, Hill L. EMT or EMT-Promoting Transcription Factors, Where to Focus the Light? *Front Oncol*. 2014;4:353.
261. Zhuo WL, Wang Y, Zhuo XL, Zhang YS, Chen ZT. Short interfering RNA directed against TWIST, a novel zinc finger transcription factor, increases A549 cell sensitivity to cisplatin via MAPK/mitochondrial pathway. *Biochem Biophys Res Commun*. 2008;369(4):1098-1102.
262. Lamb J CE, Peck D, Modell JW, Blat IC, Wrobel MJ, et al. The Connectivity Map: using gene-expression signatures to connect small molecules, genes, and disease. *Science*. 2006 313(5795):1929-1935.
263. Shamir ER, Pappalardo E, Jorgens DM, Coutinho K, Tsai WT, Aziz K, et al. Twist1-induced dissemination preserves epithelial identity and requires E-cadherin. *J Cell Biol*. 2014;204(5):839-856.
264. Moffat J, Grueneberg DA, Yang X, Kim SY, Kloepfer AM, Hinkle G, et al. A lentiviral RNAi library for human and mouse genes applied to an arrayed viral high-content screen. *Cell*. 2006;124(6):1283-1298.
265. Gajula RP, Chettiar ST, Williams RD, Nugent K, Kato Y, Wang H, et al. Structure-function studies of the bHLH phosphorylation domain of TWIST1 in prostate cancer cells. *Neoplasia*. 2015;17(1):16-31.
266. Tran PT, Bendapudi PK, Lin HJ, Choi P, Koh S, Chen J, et al. Survival and Death Signals Can Predict Tumor Response to Therapy After Oncogene Inactivation. *Science Translational Medicine*. 2011;3(103):103ra199-103ra199.
267. Hagenbuchner J AM. Targeting transcription factors by small compounds--Current strategies and future implications. *Biochem Pharmacol*. 2016;107:1-13.
268. Cao R, Fan W, Guo L, Ma Q, Zhang G, Li J, et al. Synthesis and structure-activity relationships of harmine derivatives as potential antitumor agents. *Eur J Med Chem*. 2013;60:135-143.
269. Chen Q, Chao R, Chen H, Hou X, Yan H, Zhou S, et al. Antitumor and neurotoxic effects of novel harmine derivatives and structure-activity relationship analysis. *Int J Cancer*. 2005;114(5):675-682.

270. Ishida J, Wang HK, Bastow KF, Hu CQ, Lee KH. Antitumor agents 201. Cytotoxicity of harmine and beta-carboline analogs. *Bioorg Med Chem Lett*. 1999;9(23):3319-3324.
271. Moloudizargari M, Mikaili P, Aghajanshakeri S, Asghari MH, Shayegh J. Pharmacological and therapeutic effects of Peganum harmala and its main alkaloids. *Pharmacogn Rev*. 2013;7(14):199-212.
272. Cao R, Peng W, Chen H, Ma Y, Liu X, Hou X, et al. DNA binding properties of 9-substituted harmine derivatives. *Biochem Biophys Res Commun*. 2005;338(3):1557-1563.
273. Radhakrishnan A, Nanjappa V, Raja R, Sathe G, Puttamallesh VN, Jain AP, et al. A dual specificity kinase, DYRK1A, as a potential therapeutic target for head and neck squamous cell carcinoma. *Scientific Reports*. 2016;6:36132.
274. Sobhani AM, Ebrahimi SA, Mahmoudian M. An in vitro evaluation of human DNA topoisomerase I inhibition by Peganum harmala L. seeds extract and its beta-carboline alkaloids. *J Pharm Pharm Sci*. 2002;5(1):19-23.
275. Zhang L, Zhang F, Zhang W, Chen L, Gao N, Men Y, et al. Harmine suppresses homologous recombination repair and inhibits proliferation of hepatoma cells. *Cancer Biol Ther*. 2015;16(11):1585-1592.
276. Zhang XF, Sun RQ, Jia YF, Chen Q, Tu RF, Li KK, et al. Synthesis and mechanisms of action of novel harmine derivatives as potential antitumor agents. *Sci Rep*. 2016;6:33204.
277. Pallier K, Cessot A, Cote JF, Just PA, Cazes A, Fabre E, et al. TWIST1 a new determinant of epithelial to mesenchymal transition in EGFR mutated lung adenocarcinoma. *PLoS One*. 2012;7(1):e29954.
278. Kitai H, Ebi H, Tomida S, Floros KV, Kotani H, Adachi Y, et al. Epithelial-to-Mesenchymal Transition Defines Feedback Activation of Receptor Tyrosine Kinase Signaling Induced by MEK Inhibition in KRAS-Mutant Lung Cancer. *Cancer Discov*. 2016;6(7):754-769.
279. Matsubara D, Ishikawa S, Oguni S, Aburatani H, Fukayama M, Niki T. Molecular predictors of sensitivity to the MET inhibitor PHA665752 in lung carcinoma cells. *J Thorac Oncol*. 2010;5(9):1317-1324.
280. Demontis S, Rigo C, Piccinin S, Mizzau M, Sonogo M, Fabris M, et al. Twist is substrate for caspase cleavage and proteasome-mediated degradation. *Cell Death and Differentiation*. 2006;13(2):335-345.
281. Su YW, Xie TX, Sano D, Myers JN. IL-6 stabilizes Twist and enhances tumor cell motility in head and neck cancer cells through activation of casein kinase 2. *PLoS One*. 2011;6(4):e19412.

282. Weiss MB, Abel EV, Mayberry MM, Basile KJ, Berger AC, Aplin AE. TWIST1 Is an ERK1/2 Effector That Promotes Invasion and Regulates MMP-1 Expression in Human Melanoma Cells. *Cancer Res.* 2012;72(24):6382-6392.
283. Takahashi E, Funato N, Higashihori N, Hata Y, Gridley T, Nakamura M. Snail regulates p21(WAF/CIP1) expression in cooperation with E2A and Twist. *Biochem Biophys Res Commun.* 2004;325(4):1136-1144.
284. Cao R, Chen Q, Hou X, Chen H, Guan H, Ma Y, et al. Synthesis, acute toxicities, and antitumor effects of novel 9-substituted beta-carboline derivatives. *Bioorg Med Chem.* 2004;12(17):4613-4623.
285. Chang AT, Liu Y, Ayyanathan K, Benner C, Jiang Y, Prokop JW, et al. An evolutionarily conserved DNA architecture determines target specificity of the TWIST family bHLH transcription factors. *Genes Dev.* 2015;29(6):603-616.
286. Casas E, Kim J, Bendesky A, Ohno-Machado L, Wolfe CJ, Yang J. Snail2 is an essential mediator of Twist1-induced epithelial mesenchymal transition and metastasis. *Cancer research.* 2011;71(1):245-254.
287. Shiota M, Izumi H, Onitsuka T, Miyamoto N, Kashiwagi E, Kidani A, et al. Twist promotes tumor cell growth through YB-1 expression. *Cancer Res.* 2008;68(1):98-105.
288. Castanon I, Von Stetina S, Kass J, Baylies MK. Dimerization partners determine the activity of the Twist bHLH protein during Drosophila mesoderm development. *Development.* 2001;128(16):3145-3159.
289. Firulli BA, Redick BA, Conway SJ, Firulli AB. Mutations within helix I of Twist1 result in distinct limb defects and variation of DNA binding affinities. *J Biol Chem.* 2007;282(37):27536-27546.
290. Ansieau S, Morel AP, Hinkal G, Bastid J, Puisieux A. TWISTing an embryonic transcription factor into an oncoprotein. *Oncogene.* 2010;29(22):3173-3184.
291. Xu Y, Qin L, Sun T, Wu H, He T, Yang Z, et al. Twist1 promotes breast cancer invasion and metastasis by silencing Foxa1 expression. *Oncogene.* 2016.
292. Rosell R, Molina MA, Costa C, Simonetti S, Gimenez-Capitan A, Bertran-Alamillo J, et al. Pretreatment EGFR T790M mutation and BRCA1 mRNA expression in erlotinib-treated advanced non-small-cell lung cancer patients with EGFR mutations. *Clin Cancer Res.* 2011;17(5):1160-1168.
293. Rosell R, Carcereny E, Gervais R, Vergnenegre A, Massuti B, Felip E, et al. Erlotinib versus standard chemotherapy as first-line treatment for European patients with advanced EGFR mutation-positive non-small-cell lung cancer (EURTAC): a multicentre, open-label, randomised phase 3 trial. *Lancet Oncol.* 2012;13(3):239-246.

294. McGowan M, Kleinberg L, Halvorsen AR, Helland A, Brustugun OT. NSCLC depend upon YAP expression and nuclear localization after acquiring resistance to EGFR inhibitors. *Genes Cancer*. 2017;8(3-4):497-504.
295. Byers LA, Diao L, Wang J, Saintigny P, Girard L, Peyton M, et al. An epithelial-mesenchymal transition gene signature predicts resistance to EGFR and PI3K inhibitors and identifies Axl as a therapeutic target for overcoming EGFR inhibitor resistance. *Clin Cancer Res*. 2013;19(1):279-290.
296. Suda K, Tomizawa K, Fujii M, Murakami H, Osada H, Maehara Y, et al. Epithelial to mesenchymal transition in an epidermal growth factor receptor-mutant lung cancer cell line with acquired resistance to erlotinib. *J Thorac Oncol*. 2011;6(7):1152-1161.
297. Witta SE, Gemmill RM, Hirsch FR, Coldren CD, Hedman K, Ravdel L, et al. Restoring E-cadherin expression increases sensitivity to epidermal growth factor receptor inhibitors in lung cancer cell lines. *Cancer Res*. 2006;66(2):944-950.
298. Yoshida T, Song L, Bai Y, Kinose F, Li J, Ohaegbulam KC, et al. ZEB1 Mediates Acquired Resistance to the Epidermal Growth Factor Receptor-Tyrosine Kinase Inhibitors in Non-Small Cell Lung Cancer. *PLoS One*. 2016;11(1):e0147344.
299. Tran PT, Shroff EH, Burns TF, Thiyagarajan S, Das ST, Zabuawala T, et al. Twist1 suppresses senescence programs and thereby accelerates and maintains mutant Kras-induced lung tumorigenesis. *PLoS Genet*. 2012;8(5):e1002650.
300. Politi K, Zakowski MF, Fan PD, Schonfeld EA, Pao W, Varmus HE. Lung adenocarcinomas induced in mice by mutant EGF receptors found in human lung cancers respond to a tyrosine kinase inhibitor or to down-regulation of the receptors. *Genes Dev*. 2006;20(11):1496-1510.
301. Tran PT, Bendapudi PK, Lin HJ, Choi P, Koh S, Chen J, et al. Survival and Death Signals Can Predict Tumor Response to Therapy After Oncogene Inactivation. *Science Translational Medicine*. 2011;3(103).
302. Hwang W, Chiu YF, Kuo MH, Lee KL, Lee AC, Yu CC, et al. Expression of Neuroendocrine Factor VGF in Lung Cancer Cells Confers Resistance to EGFR Kinase Inhibitors and Triggers Epithelial-to-Mesenchymal Transition. *Cancer Res*. 2017;77(11):3013-3026.
303. Roberts CM, Tran MA, Pitruzzello MC, Wen W, Loeza J, Dellinger TH, et al. TWIST1 drives cisplatin resistance and cell survival in an ovarian cancer model, via upregulation of GAS6, L1CAM, and Akt signalling. *Sci Rep*. 2016;6:37652.
304. Zhuo WL, Wang Y, Zhuo XL, Zhang YS, Chen ZT. Short interfering RNA directed against TWIST, a novel zinc finger transcription factor, increases A549 cell sensitivity to

- cisplatin via MAPK/mitochondrial pathway. *Biochem Bioph Res Co.* 2008;369(4):1098-1102.
305. Deng J, Shimamura T, Perera S, Carlson NE, Cai D, Shapiro GI, et al. Proapoptotic BH3-only BCL-2 family protein BIM connects death signaling from epidermal growth factor receptor inhibition to the mitochondrion. *Cancer Res.* 2007;67(24):11867-11875.
306. Sionov RV, Vlahopoulos SA, Granot Z. Regulation of Bim in Health and Disease. *Oncotarget.* 2015;6(27):23058-23134.
307. Fane M, Harris L, Smith Aaron G, Piper M. Nuclear factor one transcription factors as epigenetic regulators in cancer. *International Journal of Cancer.* 2017;140(12):2634-2641.
308. Zheng H, Kang Y. Multilayer control of the EMT master regulators. *Oncogene.* 2014;33(14):1755-1763.
309. Chen K, Zhou F, Shen W, Jiang T, Wu X, Tong X, et al. Novel Mutations on EGFR Leu792 Potentially Correlate to Acquired Resistance to Osimertinib in Advanced NSCLC. *J Thorac Oncol.* 2017;12(6):e65-e68.
310. Ricordel C, Llamas-Gutierrez F, Chiforeanu D, Lena H, Corre R. Large Cell Neuroendocrine Lung Carcinoma Transformation as an Acquired Resistance Mechanism to Osimertinib. *J Thorac Oncol.* 2017;12(11):e184-e186.
311. Ou SI, Agarwal N, Ali SM. High MET amplification level as a resistance mechanism to osimertinib (AZD9291) in a patient that symptomatically responded to crizotinib treatment post-osimertinib progression. *Lung cancer (Amsterdam, Netherlands).* 2016;98:59-61.
312. Li L, Wang H, Li C, Wang Z, Zhang P, Yan X. Transformation to small-cell carcinoma as an acquired resistance mechanism to AZD9291: A case report. *Oncotarget.* 2017;8(11):18609-18614.
313. Borghaei H, Paz-Ares L, Horn L, Spigel DR, Steins M, Ready NE, et al. Nivolumab versus Docetaxel in Advanced Nonsquamous Non-Small-Cell Lung Cancer. *N Engl J Med.* 2015;373(17):1627-1639.
314. Soh SX, Siddiqui FJ, Allen JC, Kim GW, Lee JC, Yatabe Y, et al. A systematic review and meta-analysis of individual patient data on the impact of the BIM deletion polymorphism on treatment outcomes in epidermal growth factor receptor mutant lung cancer. *Oncotarget.* 2017;8(25):41474-41486.
315. Pennacchietti S, Cazzanti M, Bertotti A, Rideout WM, 3rd, Han M, Gyuris J, et al. Microenvironment-derived HGF overcomes genetically determined sensitivity to anti-MET drugs. *Cancer Res.* 2014;74(22):6598-6609.

316. Hui L, Zhang S, Dong X, Tian D, Cui Z, Qiu X. Prognostic significance of twist and N-cadherin expression in NSCLC. *PLoS One*. 2013;8(4):e62171.
317. Schneeberger VE, Allaj V, Gardner EE, Poirier JT, Rudin CM. Quantitation of Murine Stroma and Selective Purification of the Human Tumor Component of Patient-Derived Xenografts for Genomic Analysis. *PLOS ONE*. 2016;11(9):e0160587.
318. Liu F, Song S, Yi Z, Zhang M, Li J, Yang F, et al. HGF induces EMT in non-small-cell lung cancer through the hBVR pathway. *European Journal of Pharmacology*. 2017;811:180-190.
319. Ogunwobi OO, Liu C. Hepatocyte growth factor upregulation promotes carcinogenesis and epithelial-mesenchymal transition in hepatocellular carcinoma via Akt and COX-2 pathways. *Clin Exp Metastasis*. 2011;28(8):721-731.
320. Hu HJ, Lin XL, Liu MH, Fan XJ, Zou WW. Curcumin mediates reversion of HGF-induced epithelial-mesenchymal transition via inhibition of c-Met expression in DU145 cells. *Oncol Lett*. 2016;11(2):1499-1505.
321. Bendinelli P, Maroni P, Matteucci E, Desiderio MA. HGF and TGF β 1 differently influenced Wwox regulatory function on Twist program for mesenchymal-epithelial transition in bone metastatic versus parental breast carcinoma cells. *Molecular Cancer*. 2015;14(1):112.
322. Koefinger P, Wels C, Joshi S, Damm S, Steinbauer E, Beham-Schmid C, et al. The cadherin switch in melanoma instigated by HGF is mediated through epithelial-mesenchymal transition regulators. *Pigment Cell & Melanoma Research*. 2010;24(2):382-385.
323. Yoshida K, Choisunirachon N, Saito T, Matsumoto K, Saeki K, Mochizuki M, et al. Hepatocyte growth factor-induced up-regulation of Twist drives epithelial-mesenchymal transition in a canine mammary tumour cell line. *Res Vet Sci*. 2014;97(3):521-526.
324. Stabile LP, Lyker JS, Land SR, Dacic S, Zamboni BA, Siegfried JM. Transgenic mice overexpressing hepatocyte growth factor in the airways show increased susceptibility to lung cancer. *Carcinogenesis*. 2006;27(8):1547-1555.
325. Stabile LP, Rothstein ME, Gubish CT, Cunningham DE, Lee N, Siegfried JM. Co-targeting c-Met and COX-2 leads to enhanced inhibition of lung tumorigenesis in a murine model with heightened airway HGF. *J Thorac Oncol*. 2014;9(9):1285-1293.
326. Rohrbeck L, Gong JN, Lee EF, Kueh AJ, Behren A, Tai L, et al. Hepatocyte growth factor renders BRAF mutant human melanoma cell lines resistant to PLX4032 by downregulating the pro-apoptotic BH3-only proteins PUMA and BIM. *Cell Death Differ*. 2016;23(12):2054-2062.

327. Crowder RN, Dicker DT, El-Deiry WS. The Deubiquitinase Inhibitor PR-619 Sensitizes Normal Human Fibroblasts to Tumor Necrosis Factor-related Apoptosis-inducing Ligand (TRAIL)-mediated Cell Death. *J Biol Chem*. 2016;291(11):5960-5970.
328. de Miguel D, Lemke J, Anel A, Walczak H, Martinez-Lostao L. Onto better TRAILs for cancer treatment. *Cell Death Differ*. 2016;23(5):733-747.
329. Lemke J, von Karstedt S, Abd El Hay M, Conti A, Arce F, Montinaro A, et al. Selective CDK9 inhibition overcomes TRAIL resistance by concomitant suppression of cFlip and Mcl-1. *Cell Death And Differentiation*. 2013;21:491.
330. Irmeler M, Thome M, Hahne M, Schneider P, Hofmann K, Steiner V, et al. Inhibition of death receptor signals by cellular FLIP. *Nature*. 1997;388(6638):190-195.
331. Grotzer MA, Eggert A, Zuzak TJ, Janss AJ, Marwaha S, Wiewrodt BR, et al. Resistance to TRAIL-induced apoptosis in primitive neuroectodermal brain tumor cells correlates with a loss of caspase-8 expression. *Oncogene*. 2000;19(40):4604-4610.
332. Jin Z, McDonald ER, 3rd, Dicker DT, El-Deiry WS. Deficient tumor necrosis factor-related apoptosis-inducing ligand (TRAIL) death receptor transport to the cell surface in human colon cancer cells selected for resistance to TRAIL-induced apoptosis. *J Biol Chem*. 2004;279(34):35829-35839.
333. Burns TF, El-Deiry WS. Identification of inhibitors of TRAIL-induced death (ITIDs) in the TRAIL-sensitive colon carcinoma cell line SW480 using a genetic approach. *J Biol Chem*. 2001;276(41):37879-37886.
334. Allen JE, Krigsfeld G, Mayes PA, Patel L, Dicker DT, Patel AS, et al. Dual inactivation of Akt and ERK by TIC10 signals Foxo3a nuclear translocation, TRAIL gene induction, and potent antitumor effects. *Sci Transl Med*. 2013;5(171):171ra117.
335. Feng Y, Zhou J, Li Z, Jiang Y, Zhou Y. Small Molecular TRAIL Inducer ONC201 Induces Death in Lung Cancer Cells: A Preclinical Study. *PLoS One*. 2016;11(9):e0162133.
336. Joshi P, Jeon YJ, Lagana A, Middleton J, Secchiero P, Garofalo M, et al. MicroRNA-148a reduces tumorigenesis and increases TRAIL-induced apoptosis in NSCLC. *Proc Natl Acad Sci U S A*. 2015;112(28):8650-8655.
337. Hamilton DH, Griner LM, Keller JM, Hu X, Southall N, Marugan J, et al. Targeting Estrogen Receptor Signaling with Fulvestrant Enhances Immune and Chemotherapy-Mediated Cytotoxicity of Human Lung Cancer. *Clin Cancer Res*. 2016;22(24):6204-6216.
338. Safa AR. Roles of c-FLIP in Apoptosis, Necroptosis, and Autophagy. *Journal of carcinogenesis & mutagenesis*. 2013;Suppl 6:003.

339. Gao S, Wang H, Lee P, Melamed J, Li CX, Zhang F, et al. Androgen receptor and prostate apoptosis response factor-4 target the c-FLIP gene to determine survival and apoptosis in the prostate gland. *J Mol Endocrinol*. 2006;36(3):463-483.
340. Micheau O, Lens S, Gaide O, Alevizopoulos K, Tschopp J. NF-kappaB signals induce the expression of c-FLIP. *Molecular and cellular biology*. 2001;21(16):5299-5305.
341. Ricci MS, Jin Z, Dews M, Yu D, Thomas-Tikhonenko A, Dicker DT, et al. Direct repression of FLIP expression by c-myc is a major determinant of TRAIL sensitivity. *Molecular and cellular biology*. 2004;24(19):8541-8555.
342. Smith CL, Hager GL. Transcriptional regulation of mammalian genes in vivo. A tale of two templates. *J Biol Chem*. 1997;272(44):27493-27496.
343. Lee MP, Ratner N, Yutzey KE. Genome-wide Twist1 occupancy in endocardial cushion cells, embryonic limb buds, and peripheral nerve sheath tumor cells. *BMC Genomics*. 2014;15:821.
344. Allen JE, Prabhu VV, Talekar M, van den Heuvel AP, Lim B, Dicker DT, et al. Genetic and Pharmacological Screens Converge in Identifying FLIP, BCL2, and IAP Proteins as Key Regulators of Sensitivity to the TRAIL-Inducing Anticancer Agent ONC201/TIC10. *Cancer Res*. 2015;75(8):1668-1674.
345. Padmanabhan C, Rellinger EJ, Zhu J, An H, Woodbury LG, Chung DH, et al. cFLIP critically modulates apoptotic resistance in epithelial-to-mesenchymal transition. *Oncotarget*. 2017;8(60):101072-101086.
346. Sivaprasad U, Shankar E, Basu A. Downregulation of Bid is associated with PKC ϵ -mediated TRAIL resistance. *Cell Death And Differentiation*. 2006;14:851.
347. Goncharenko-Khaider N, Lane D, Matte I, Rancourt C, Piche A. The inhibition of Bid expression by Akt leads to resistance to TRAIL-induced apoptosis in ovarian cancer cells. *Oncogene*. 2010;29(40):5523-5536.
348. Romano G, Acunzo M, Garofalo M, Di Leva G, Cascione L, Zanca C, et al. MiR-494 is regulated by ERK1/2 and modulates TRAIL-induced apoptosis in non-small-cell lung cancer through BIM down-regulation. *Proceedings of the National Academy of Sciences*. 2012;109(41):16570.
349. Yin X-M. Bid, a BH3-only multi-functional molecule, is at the cross road of life and death. *Gene*. 2006;369:7-19.
350. Prakasam A, Ghose S, Oleinik NV, Bethard JR, Peterson YK, Krupenko NI, et al. JNK1/2 regulate Bid by direct phosphorylation at Thr59 in response to ALDH1L1. *Cell Death Dis*. 2014;5:e1358.

351. Sax JK, Fei P, Murphy ME, Bernhard E, Korsmeyer SJ, El-Deiry WS. BID regulation by p53 contributes to chemosensitivity. *Nature cell biology*. 2002;4(11):842-849.
352. Parrado A, Robledo M, Moya-Quiles MR, Marin LA, Chomienne C, Padua RA, et al. The promyelocytic leukemia zinc finger protein down-regulates apoptosis and expression of the proapoptotic BID protein in lymphocytes. *Proc Natl Acad Sci U S A*. 2004;101(7):1898-1903.
353. Wagner J, Kline CL, Zhou L, Campbell KS, MacFarlane AW, Olszanski AJ, et al. Dose intensification of TRAIL-inducing ONC201 inhibits metastasis and promotes intratumoral NK cell recruitment. *J Clin Invest*. 2018.
354. Chae YK, Chang S, Ko T, Anker J, Agte S, Iams W, et al. Epithelial-mesenchymal transition (EMT) signature is inversely associated with T-cell infiltration in non-small cell lung cancer (NSCLC). *Scientific Reports*. 2018;8(1):2918.
355. Suarez-Carmona M, Lesage J, Cataldo D, Gilles C. EMT and inflammation: inseparable actors of cancer progression. *Mol Oncol*. 2017;11(7):805-823.
356. Dongre A, Rashidian M, Reinhardt F, Bagnato A, Keckesova Z, Ploegh HL, et al. Epithelial-to-Mesenchymal Transition Contributes to Immunosuppression in Breast Carcinomas. *Cancer Res*. 2017;77(15):3982-3989.
357. Shintani Y, Fujiwara A, Kimura T, Kawamura T, Funaki S, Minami M, et al. IL-6 Secreted from Cancer-Associated Fibroblasts Mediates Chemoresistance in NSCLC by Increasing Epithelial-Mesenchymal Transition Signaling. *J Thorac Oncol*. 2016;11(9):1482-1492.
358. Liang SQ, Marti TM, Dorn P, Froment L, Hall SR, Berezowska S, et al. Blocking the epithelial-to-mesenchymal transition pathway abrogates resistance to anti-folate chemotherapy in lung cancer. *Cell Death Dis*. 2015;6:e1824.
359. Vesuna F, Bergman Y, Raman V. Genomic pathways modulated by Twist in breast cancer. *BMC Cancer*. 2017;17(1):52.
360. Xu Y, Lee DK, Feng Z, Xu Y, Bu W, Li Y, et al. Breast tumor cell-specific knockout of Twist1 inhibits cancer cell plasticity, dissemination, and lung metastasis in mice. *Proc Natl Acad Sci U S A*. 2017;114(43):11494-11499.
361. Vesuna F, Lisok A, Kimble B, Domek J, Kato Y, van der Groep P, et al. Twist contributes to hormone resistance in breast cancer by downregulating estrogen receptor-alpha. *Oncogene*. 2012;31(27):3223-3234.
362. Hugo W, Zaretsky JM, Sun L, Song C, Moreno BH, Hu-Lieskovan S, et al. Genomic and Transcriptomic Features of Response to Anti-PD-1 Therapy in Metastatic Melanoma. *Cell*. 2017;168(3):542.

363. Singh A, Settleman J. EMT, cancer stem cells and drug resistance: an emerging axis of evil in the war on cancer. *Oncogene*. 2010;29(34):4741-4751.
364. Lehnert C, Weiswange M, Jeremias I, Bayer C, Grunert M, Debatin KM, et al. TRAIL-receptor costimulation inhibits proximal TCR signaling and suppresses human T cell activation and proliferation. *J Immunol*. 2014;193(8):4021-4031.
365. Sarbassov DD, Guertin DA, Ali SM, Sabatini DM. Phosphorylation and regulation of Akt/PKB by the rictor-mTOR complex. *Science*. 2005;307(5712):1098-1101.
366. Campeau E, Ruhl VE, Rodier F, Smith CL, Rahmberg BL, Fuss JO, et al. A versatile viral system for expression and depletion of proteins in mammalian cells. *PLoS One*. 2009;4(8):e6529.